XL International Moor Excursion

Western Switzerland

05.-10. September 2016

Excursion Guide

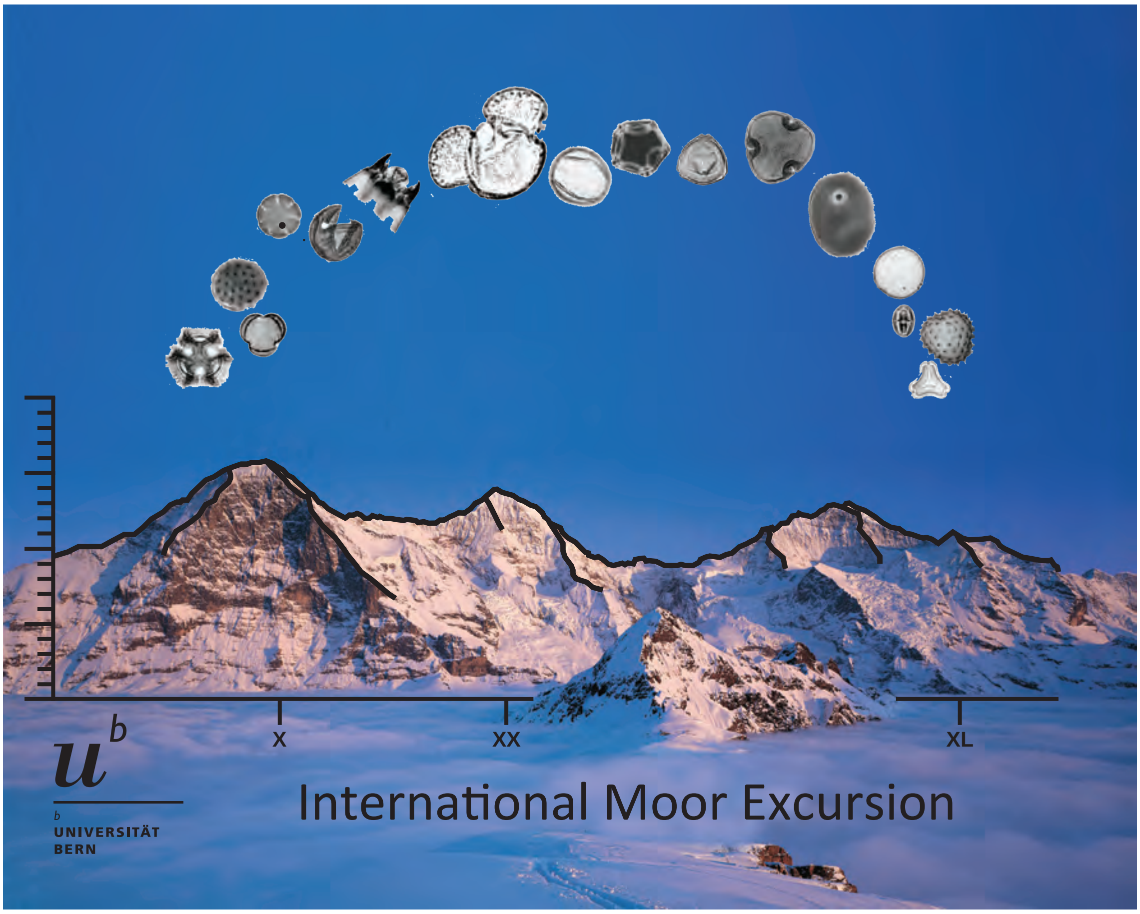

Organizers:

Fabian Rey, Christoph Schwörer, Erika Gobet

Institute of Plant Sciences and Oeschger Centre for Climate Change Research, University of Bern

UNIVERSITÄT BERN

OESCHGER CENTRE
CLIMATE CHANGE RESEARCH

Important Addresses

Institute of Plant Sciences
Altenbergrain 21
3013 Bern
www.ips.unibe.ch

Hotel Engel
Kasernenstrasse 10
4410 Liestal
Tel: +41 61 927 80 80
www.engel-liestal.ch

Hotel Al Ponte
Wangenstrasse 55
3380 Wangen an der Aare
Tel: +41 32 636 54 54
www.alponte.ch

Hotel Krone
Kronenplatz 1
3775 Lenk
Tel: +41 33 736 33 44
www.krone-lenk.ch

Hôtel Castel
Rue du Scex 38
1950 Sion
Tel: +41 27 527 21 00
www.hotelcastel.ch

Restaurant Cave de Tous-Vents
Rue des Châteaux 16
1950 Sion
Tel: +41 27 322 46 84
www.cave-tous-vents.ch

Hôtel de Gruyères
Rlle des Chevaliers 1
1663 Gruyères
Tel: +41 26 921 80 30
www.chevaliers-gruyeres.ch

Restaurant Chalet de Gruyères
Rue du Bourg 53
1663 Gruyères
Tel: +41 26 921 21 54
www.chalet-gruyeres.ch

Fabian: +41 79 741 96 78
Christoph: +41 76 407 95 84
Erika: +41 79 778 79 74

Index

Programme

Monday, 05.09.2016

Afternoon:	Arrival at the Institute of Plant Sciences and Botanical Garden Bern
17 h	Welcome at IPS
18.30 h	Dinner at the Botanical Garden
20.30 h	Departure to Liestal
21.30 h	Arrival at Hotel Engel (Liestal)

Tuesday, 06.09.2016

8:30 h	Departure to Rheinfelden
9.10 h	Commemoration
9:15 h	**Rheinfelden Häxeplatz**: Karstic hole, extirpation of *Abies alba*, forest history and land use since the end of the Neolithic (Lucia Wick)
10:15 h	Departure to Augusta Raurica
10:30 h	Augusta Raurica, visit of Roman town
11 h	Departure to Burgäschisee
12 h	Lunch at Restaurant Seeblick, Burgäschi
13 h	**Burgäschisee**: landscape, vegetation and fire history (Erika Gobet)
14 h	Introduction to lake dwellings (Othmar Wey, excavation leader)
15:30 h	Neolithic high resolution multiproxy (Fabian Rey)
16:30 h	Comparison to other Neolithic on-site studies (Erika Gobet, Oliver Heiri)
17:30 h	Departure to Wangen an der Aare
18 h	Arrival at Hotel al Ponte (Wangen an der Aare)
19 h	Dinner at Hotel al Ponte

Wednesday, 07.09.2016

8:30 h	Departure to Moossee
9 h	**Moossee**: Introduction to lake-settlement archaeology (Fabian Rey)
9:30 h	Landscape, vegetation and fire history of the Bern area. Neolithic high-resolution multiproxy (Fabian Rey)
11 h	Development of agriculture and dietary change in Switzerland from the Hallstatt to the High Middle Ages (Ryan Hughes)
11.45 h	Lunch at Restaurant Seerose, Moosseedorf
13 h	Departure to Gerzensee
13:30 h	**Gerzensee**: multiproxy evidence of rapid warming and cooling and ecosystem responses (Brigitta Ammann with contributions from Oliver Heiri, Daniele Colombaroli, Lucia Wick and John Birks)
15.15 h	Chitinous invertebrate remains as indicators of past methane availability in lakes (Oliver Heiri)
16 h	Departure to Faulenseemoos
16:30 h	**Faulenseemoos**: Threats to unique natural archives and restoration efforts, first influx calculations worldwide by Max Welten (Willy Tinner, Brigitta Ammann)
17 h	Departure to Lenk im Simmental
18 h	Arrival at Hotel Krone (Lenk im Simmental)
19 h	Dinner at Hotel Krone
21 h	Surprise

Thursday, 08.09.2016

8:30 h	Departure to Lauenensee
9:30 h	**Lauenensee**: Vegetation and fire history of mountain environments, early human impact during the Neolithic and Bronze Age, high resolution series (Fabian Rey)
10:30 h	Chironomids as a proxy for temperature changes in the Alps (Oliver Heiri)
11 h	Departure to Gsteig
11:45 h	Cable car to Sénin and hike to Col du Sanetsch (2.5 hours). Alternative: Bus to Col du Sanetsch. Lunch en route.
14:45 h	**Col du Sanetsch**: Vegetation and fire history (Christoph Schwörer)
15:15 h	Past, present and future of treeline environments, the **Iffigsee** study (Christoph Schwörer)
16:15 h	Prehistory of pass environments, ice patch archaeology of Schnidejoch (Christoph Schwörer)
16:45 h	Frozen fire: Monte Rosa ice core palynology (Sandra Brügger)
17:30 h	Departure to Sion
18:30 h	Arrival at Hôtel Castel (Sion)
19:30 h	Dinner at Restaurant Cave de Tous-Vents (Sion)

Friday, 09.09.2016

8:30 h	Walk to the Valais Museum of History
9:00 h	Archaeology of Central Alpine environments (Philippe Curdy)
10:00 h	Departure to Lac du Mont d'Orge
10:30 h	**Lac du Mont d'Orge**: 16'000 years of vegetation history, the Welten record. Human impact and diversity dynamics at the Mesolithic/Neolithic transition (Daniele Colombaroli)
11:30 h	Charcoal and pollen trap measurements: remote-sensing based fire and biodiversity estimates (Carole Adolf)
12:00 h	Ancient viticulture (Lucia Wick)
12:30 h	Lunch
13:30 h	Departure to Villars-sur-Ollon
15 h	Train to Col de Bretaye
15:45 h	**Lac de Bretaye**: vegetation, land use and fire history, extinct boreo-nemoral forests in the Alps (Lena Thöle and Christoph Schwörer)
17:30 h	Train back to Villars-sur-Ollon (last train!)
18 h	Departure to Gruyères
19 h	Arrival at Hôtel de Gruyères (Gruyères)
20 h	Farewell dinner at Chalet de Gruyères (Gruyères)

Saturday, 10.09.2016

8:30 h	Departure to Bern
9:30-10 h	Arrival at the Institute of Plant Sciences (Bern)

Participants

Carole Adolf
Oeschger Centre for Climate Change Research and Institute of Plant Sciences, University of Bern, Bern, Switzerland
carole.adolf@ips.unibe.ch

Brigitta Ammann
Oeschger Centre for Climate Change Research and Institute of Plant Sciences, University of Bern, Bern, Switzerland
brigitta.ammann@ips.unibe.ch

Karl-Ernst Behre
Niedersächsiches Institut für historische Küstenforschung (NIhK), Willhelmshaven, Germany
behre@nihk.de

John Birks
Department of Biology and Bjerknes Centre for Climate Research, University of Bergen, Bergen, Norway
john.birks@bio.uib.no

Hilary Birks
Department of Biology and Bjerknes Centre for Climate Research, University of Bergen, Bergen, Norway
hilary.birks@bio.uib.no

Felix Bittmann
Niedersächsiches Institut für historische Küstenforschung (NIhK), Willhelmshaven, Germany
bittmann@nihk.de

Tatiana Blyakharchuk
Institute of Monitoring of Climatic and Ecological Systems SB RAS, Tomsk, Russia
tarun5@rambler.ru

Sandra Brügger
Oeschger Centre for Climate Change Research and Institute of Plant Sciences, University of Bern, Bern, Switzerland
sandra.bruegger@ips.unibe.ch

Daniele Colombaroli
Oeschger Centre for Climate Change Research and Institute of Plant Sciences, University of Bern, Bern, Switzerland
daniele.colombaroli@ips.unibe.ch

Basil Davis
Institute of Earth Surface Dynamics, University of Lausanne, Lausanne, Switzerland
basil.davis@unil.ch

Benjamin Dietre
Institute of Botany, University of Innsbruck, Innsbruck, Austria
benjamin.dietre@univ-fcomte.fr

Ilse Draxler
Geological Survey of Austria, Vienna, Austria
pal.draxler@gmail.com

Sebastian Eggenberger
Oeschger Centre for Climate Change Research and Institute of Plant Sciences, University of Bern, Bern, Switzerland
s.eggenberger@students.unibe.ch

Erika Gobet
Oeschger Centre for Climate Change Research and Institute of Plant Sciences, University of Bern, Bern, Switzerland
erika.gobet@ips.unibe.ch

Moritz Gubler
Oeschger Centre for Climate Change Research and Institute of Plant Sciences, University of Bern, Bern, Switzerland
moritz.gubler@students.unibe.ch

Jean Nicolas Haas
Institute of Botany, University of Innsbruck, Innsbruck, Austria
jean-nicolas.haas@uibk.ac.at

Oliver Heiri
Oeschger Centre for Climate Change Research and Institute of Plant Sciences, University of Bern, Bern, Switzerland
oliver.heiri@ips.unibe.ch

Henry Hooghiemstra
Institute for Biodiversity and Ecosystem Dynamics, University of Amsterdam, Amsterdam, The Netherlands
H.Hooghiemstra@uva.nl

Ryan Hughes
Institute of Earth Surface Dynamics, University of Lausanne, Lausanne, Switzerland
ryan.hughes@unil.ch

Petra Boltshauser-Kaltenrieder
Oeschger Centre for Climate Change Research and Institute of Plant Sciences, University of Bern, Bern, Switzerland
petra.boltshauser@ips.unibe.ch

Jed Kaplan
Institute of Earth Surface Dynamics, University of Lausanne, Lausanne, Switzerland
jed.kaplan@unil.ch

Andrea Kay
Institute of Earth Surface Dynamics, University of Lausanne, Lausanne, Switzerland
andrea.kay@unil.ch

Angelika Kleinmann
a.kleinmann@gmx.de

Kerstin Kowarik
Institute of Prehistoric and Historic Archaeology, University of Vienna, Vienna, Austria
kerstin.kowarik@univie.ac.at

Josef Merkt
josefmerkt@gmx.de

Michael O'Connell
School of Geography and Archaeology, National University of Ireland Galway, Galway, Ireland
michael.oconnell@nuigalway.ie

Klaus Oeggl
Institute of Botany, University of Innsbruck, Innsbruck, Austria
klaus.oeggl@uibk.ac.at

Notburga Oeggl-Wahlmüller
Institute of Botany, University of Innsbruck, Innsbruck, Austria
notburga.oeggl-wahlmueller@uibk.ac.at

Tiziana Pedrotta
Oeschger Centre for Climate Change Research and Institute of Plant Sciences, University of Bern, Bern, Switzerland
tiziana.pedrotta@ips.unibe.ch

Leanne Phelps
Institute of Earth Surface Dynamics, University of Lausanne, Lausanne, Switzerland
lnphel@gmail.com

Anne-Marie Rachoud
annemarie.rachoud@gmail.com

Fabian Rey
Oeschger Centre for Climate Change Research and Institute of Plant Sciences, University of Bern, Bern, Switzerland
fabian.rey@ips.unibe.ch

Marie-Claire Ries
Institute of Prehistoric and Historic Archaeology, University of Vienna, Vienna, Austria
claire_r@gmx.at

Siegfried Schloss
Naturkundemuseum Karlsruhe, Karlsruhe, Germany
s.schloss@t-online.de

Christoph Schwörer
Oeschger Centre for Climate Change Research and Institute of Plant Sciences, University of Bern, Bern, Switzerland
christoph.schwoerer@ips.unibe.ch

Philipp Sommer
Institute of Earth Surface Dynamics, University of Lausanne, Lausanne, Switzerland
philipp.sommer@unil.ch

Astrid Stobbe
Institute of Archaeological Sciences, Goethe University Frankfurt, Frankfurt am Main, Germany
stobbe@em.uni-frankfurt.de

Willy Tinner
Oeschger Centre for Climate Change Research and Institute of Plant Sciences, University of Bern, Bern, Switzerland
willy.tinner@ips.unibe.ch

Pim van der Knaap
Oeschger Centre for Climate Change Research and Institute of Plant Sciences, University of Bern, Bern, Switzerland
pim.vanderknaap@ips.unibe.ch

Jacqueline van Leeuwen
Oeschger Centre for Climate Change Research and Institute of Plant Sciences, University of Bern, Bern, Switzerland
jacqueline.vanleeuwen@ips.unibe.ch

Richard Vogt
Landesdenkmalpflege Baden-Württemberg, Hemmenhofen, Germany
richard.vogt@rps.bwl.de

Lucia Wick
Institute of Integrative Biology, Prehistory and Archaeological Sciences (IPNA), University of Basel, Basel, Switzerland
lucia.wick@unibas.ch

Bernd Zolitschka
Institute of Geography, University of Bremen, Bremen, Germany
zoli@uni-bremen.de

Invited Speakers

Philippe Curdy
Historical Museum Valère, Sion, Switzerland
philippe.curdy@admin.vs.ch

Lena Thöle
Institute of Geology, University of Bern, Bern, Switzerland
lena.thoele@geo.unibe.ch

Othmar Wey
Institute of Archaeological Sciences, University of Bern, Switzerland
othmar.wey@iaw.unibe.ch

Introduction


Burgäschisee


Moossee


Gerzensee

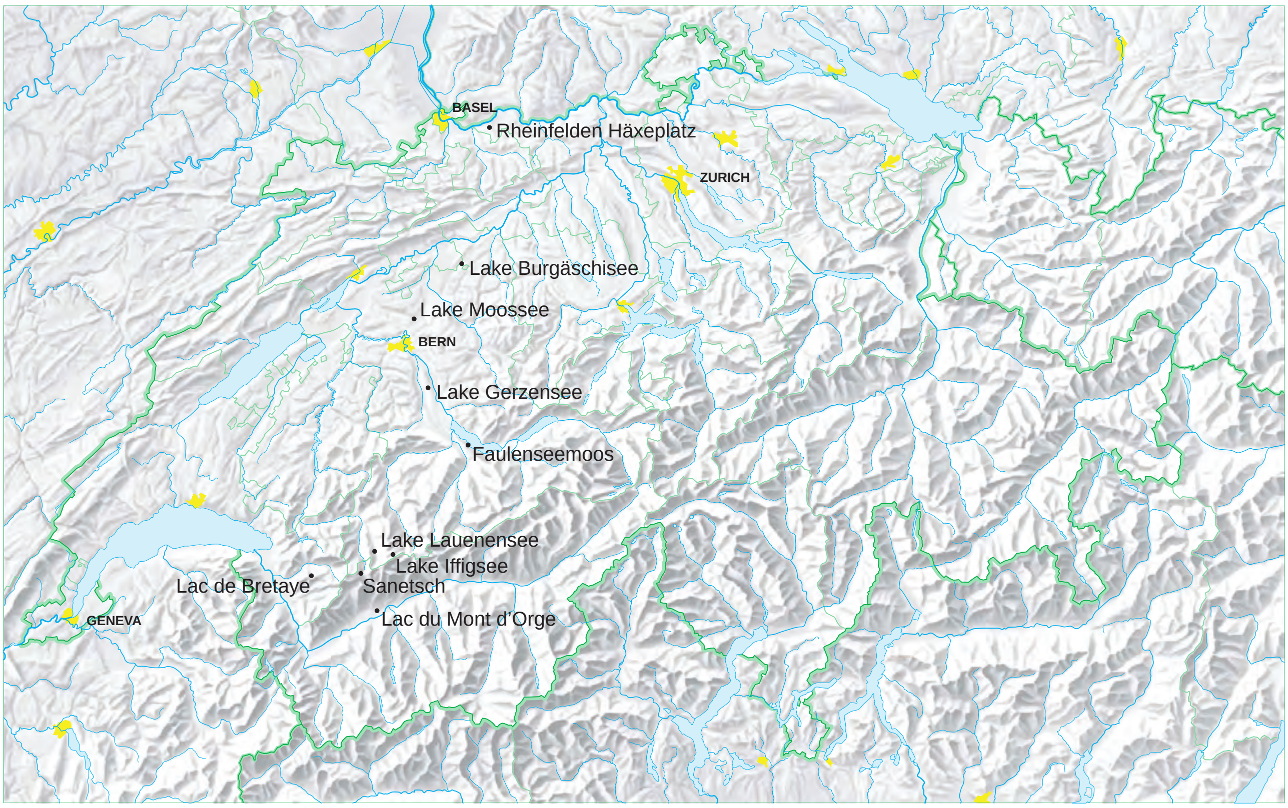


Faulenseemoos


Lauenensee

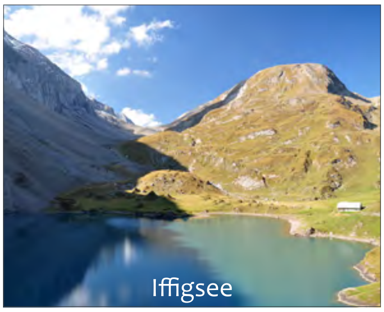
Iffigsee


Col du Sanetsch


Lac du Mont d'Orge


Lac de Bretaye

Geology

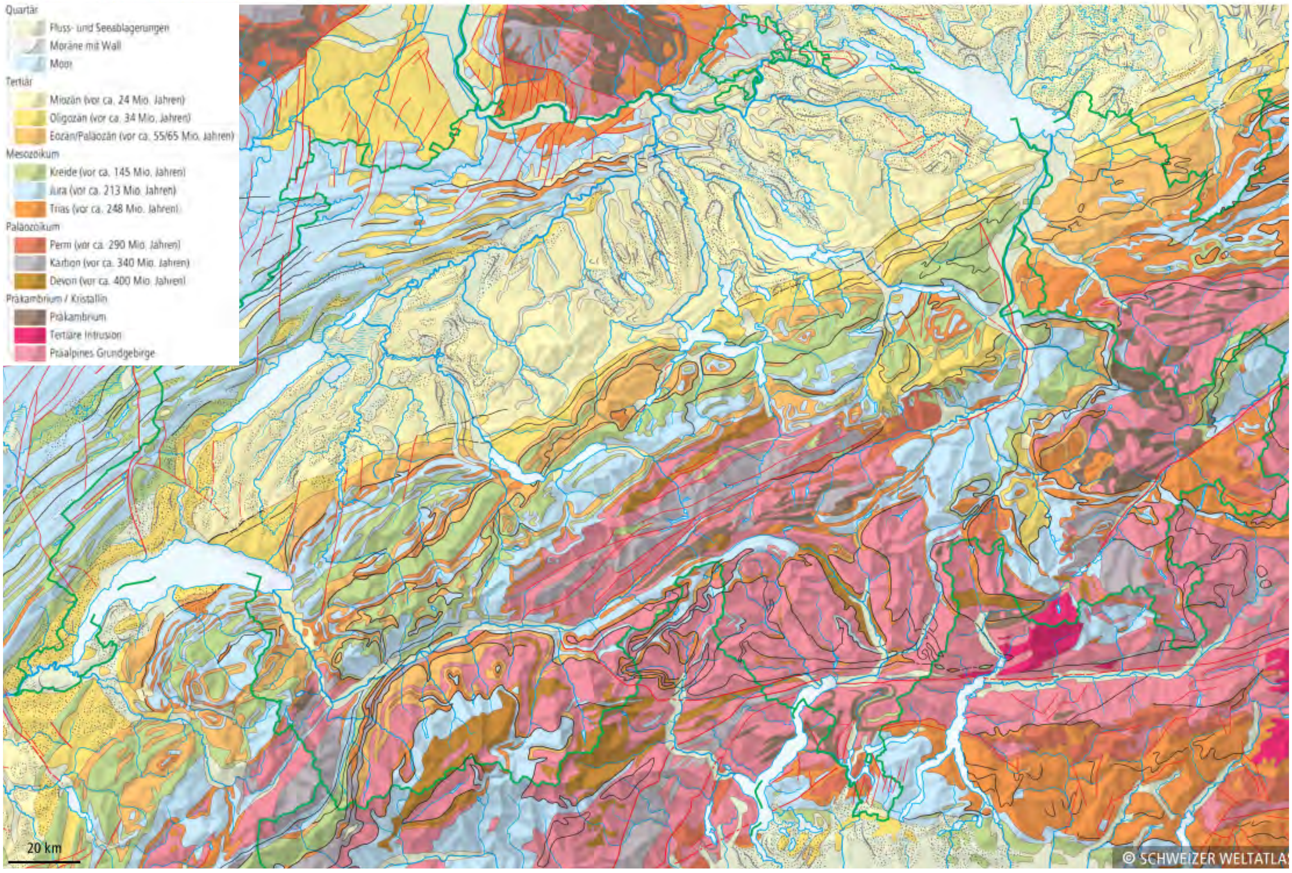

Figure 1: Geological map of Switzerland (Schweizer Weltatlas 2013)

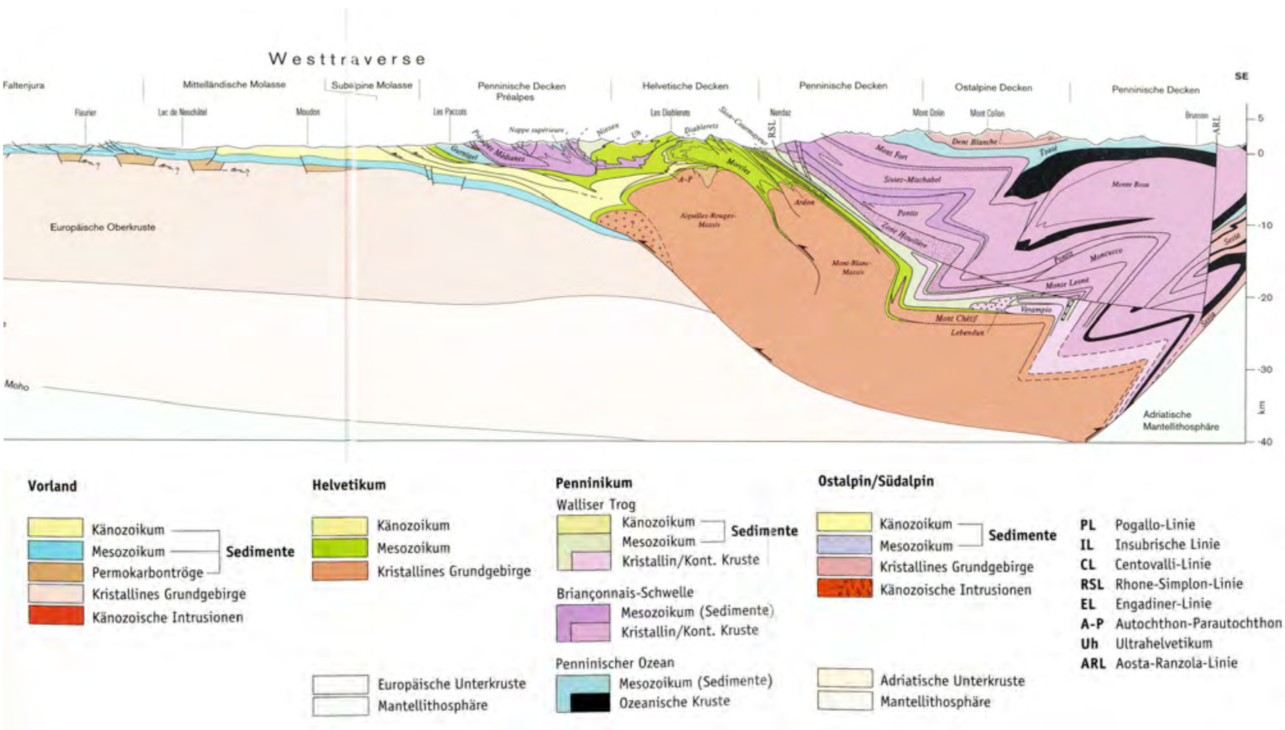

Figure 2: Geological profile through the Western Swiss Alps (Gnägi & Labhart 2015)

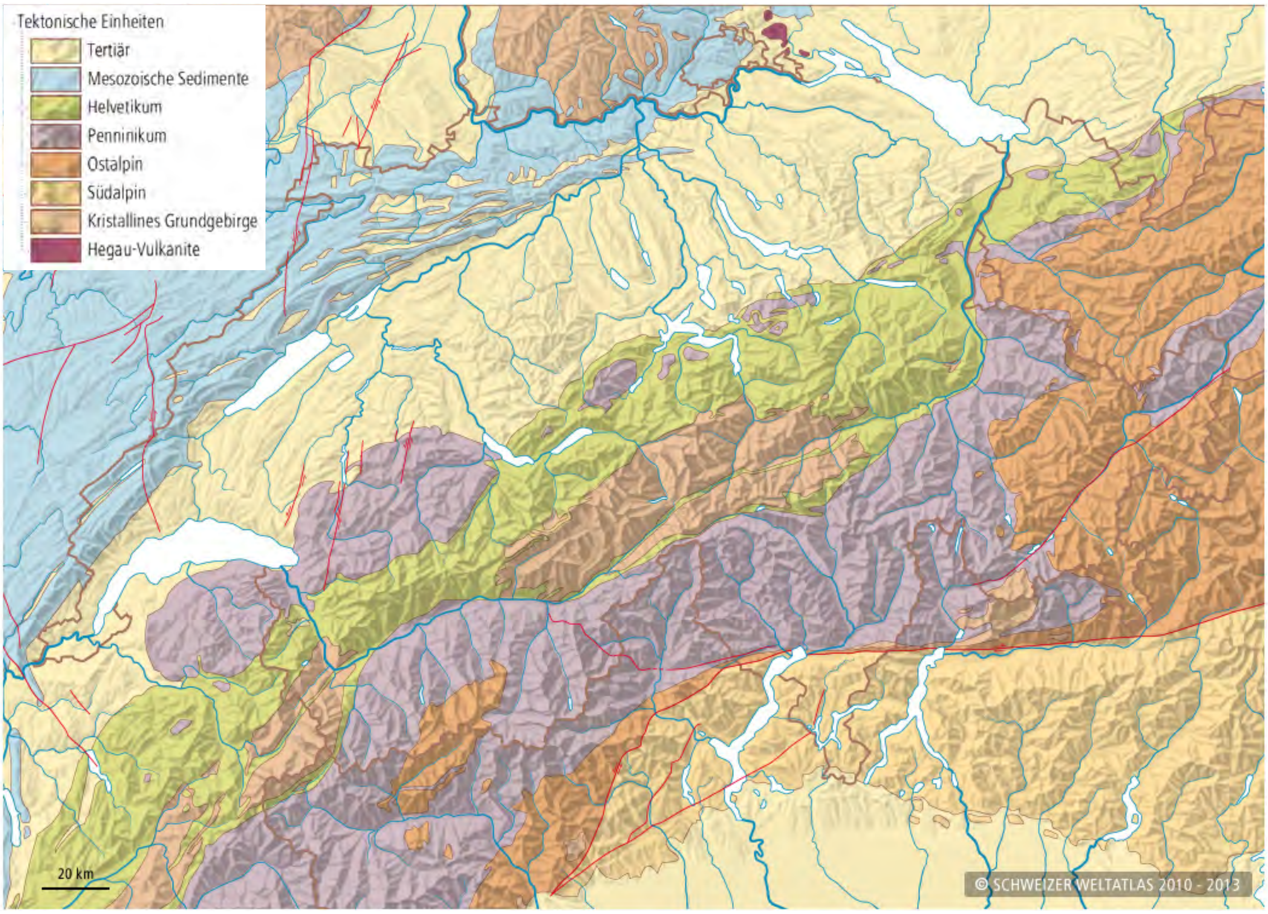

Figure 3: Tectonic map of Switzerland (Schweizer Weltatlas 2013)

Figure 4: Map of Switzerland during the Last Glacial Maximum (Bini et al. 2009)

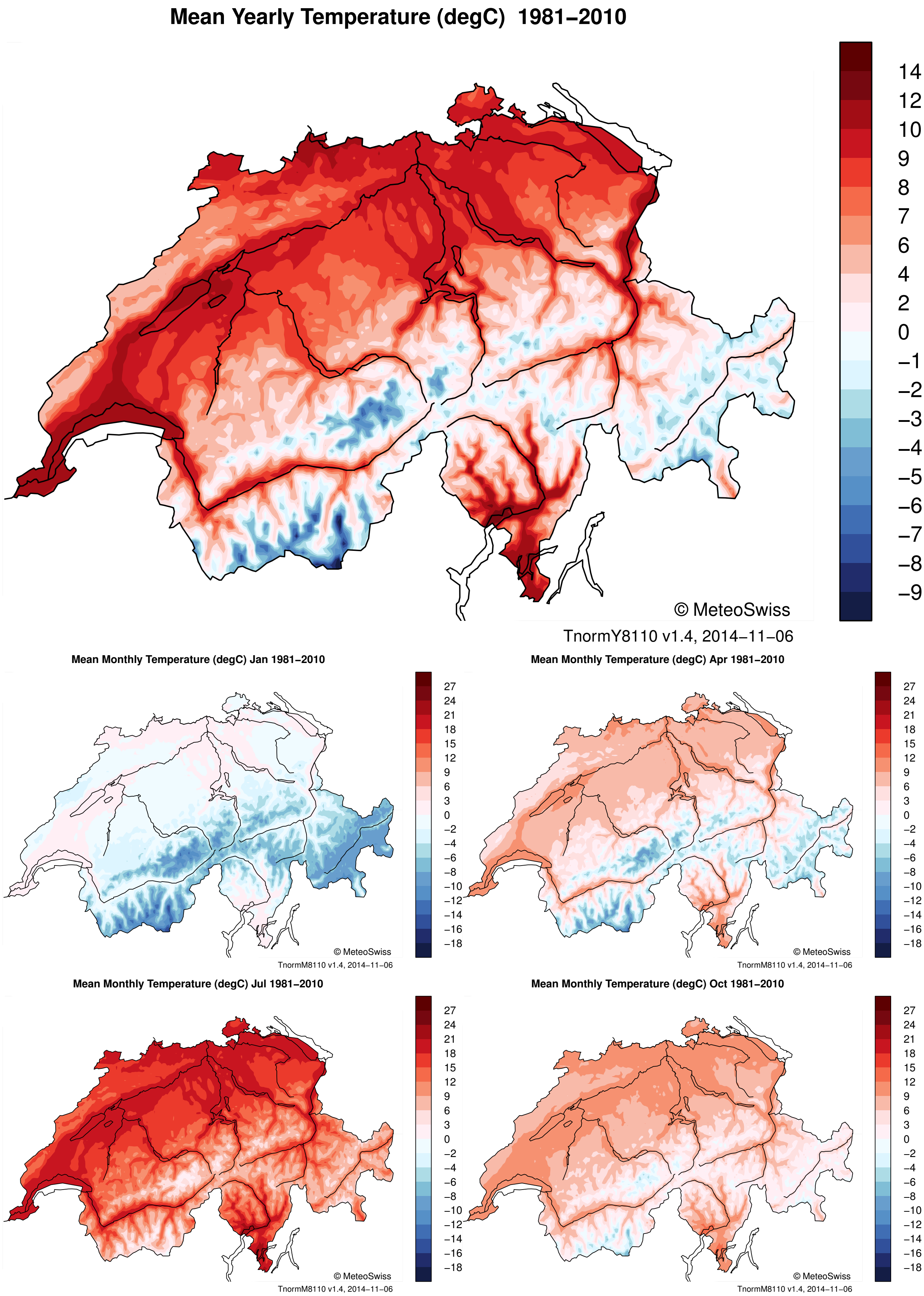

Figure 5: Mean annual (top) and monthly (below) temperature (°C) in Switzerland for the reference period 1981 - 2010

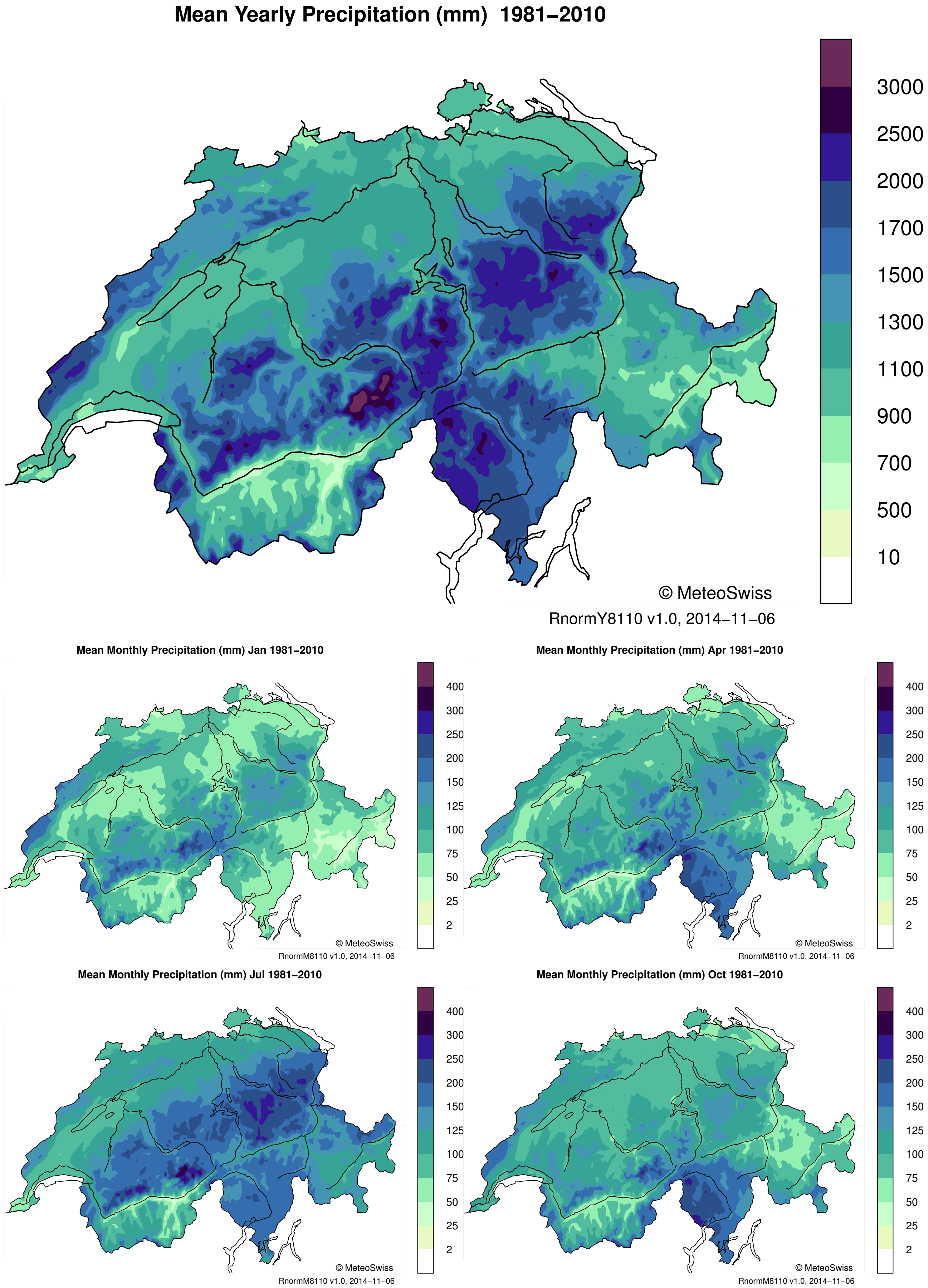

Figure 6: Mean annual (top) and monthly (below) precipitation (mm) in Switzerland for the reference period 1981 - 2010

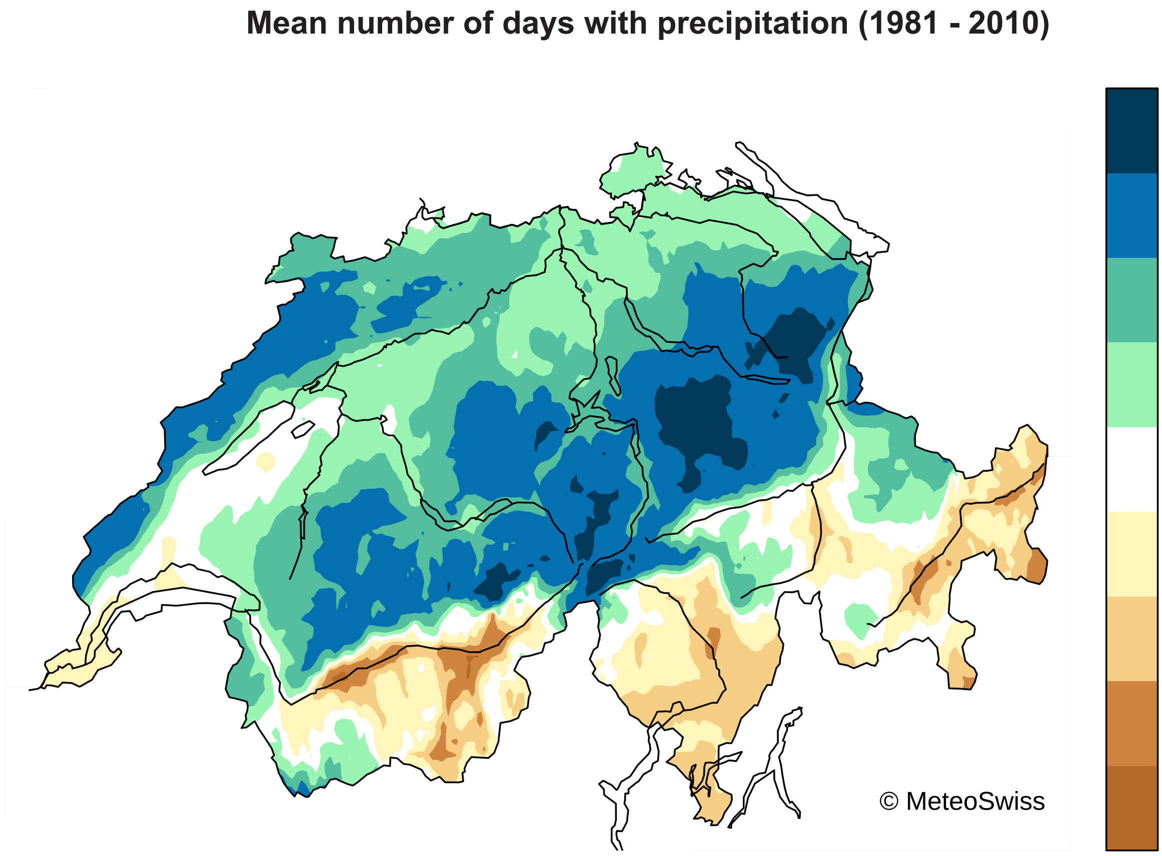

Figure 7: Mean annual number of days with precipitation in Switzerland for the reference period 1981 - 2010

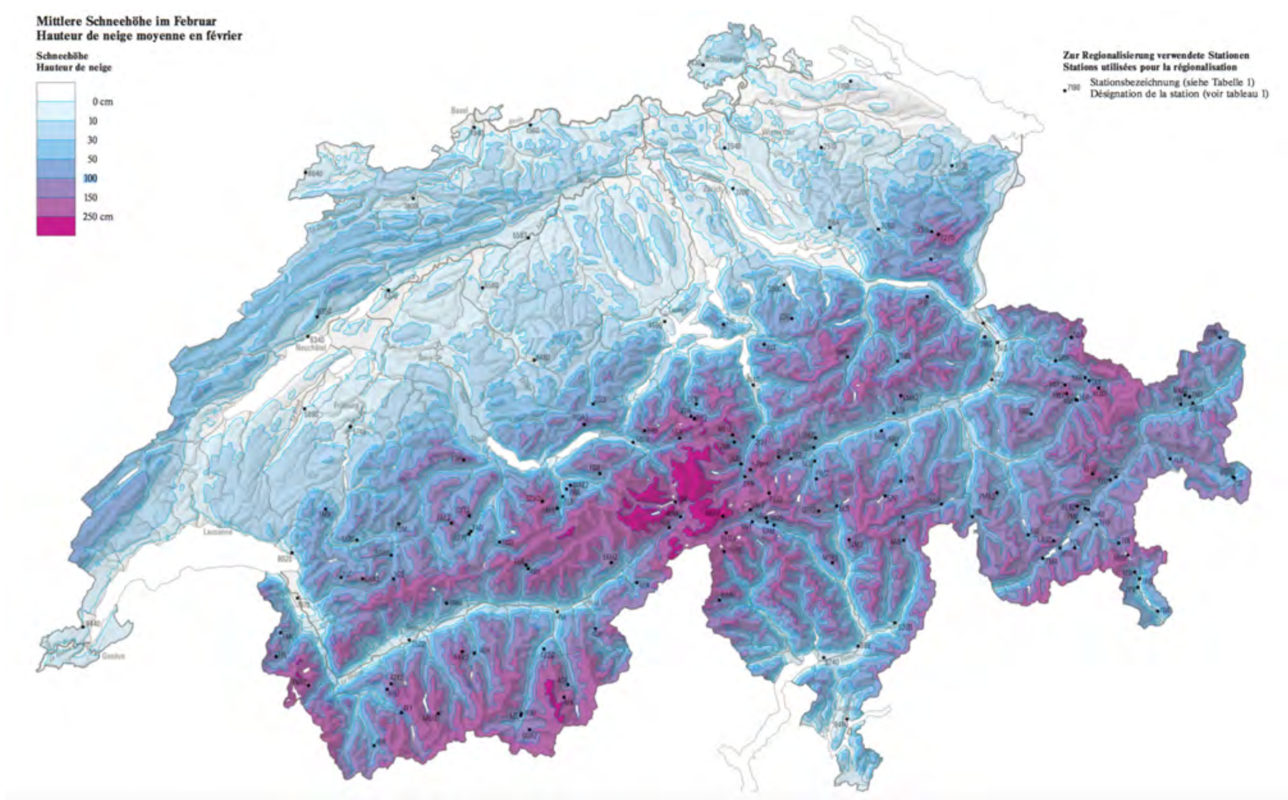

Figure 8: Mean snowdepth (cm) in February in Switzerland for the reference period 1983 - 2002 (Auer et al 2007)

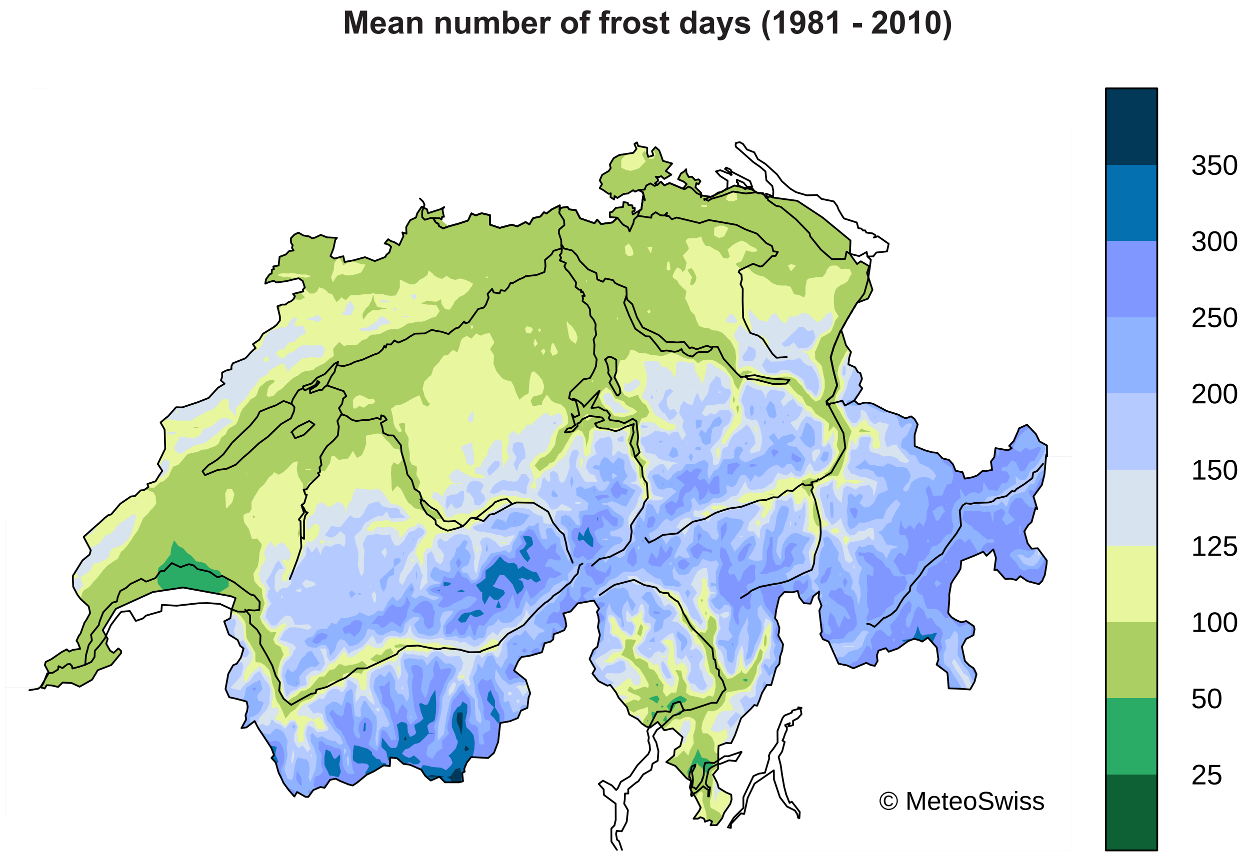

Figure 9: Mean annual number of frost days in Switzerland for the reference period 1981 - 2010

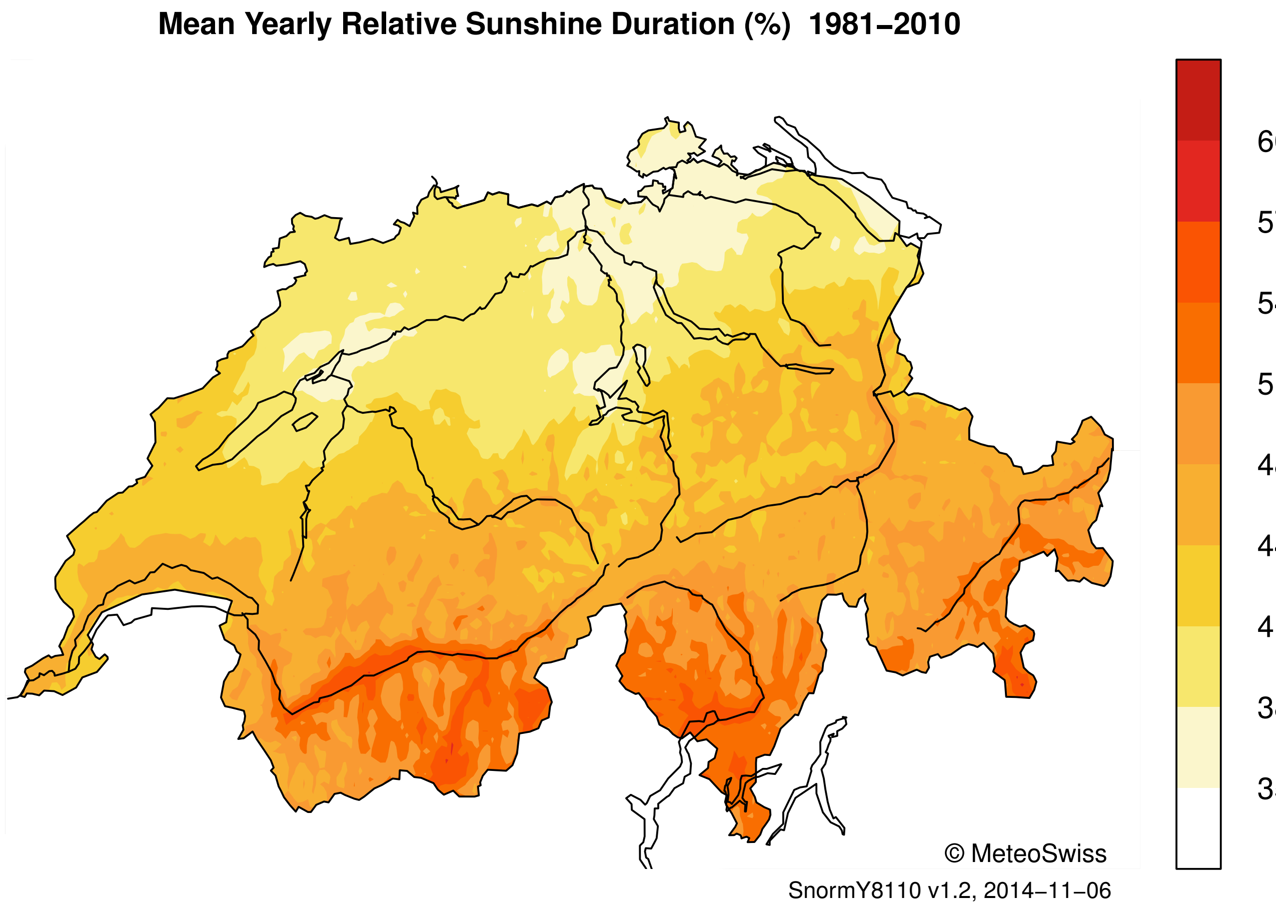

Figure 10: Mean annual relative sunshine duration in Switzerland for the reference period 1981 - 2010 as a percentage of the maximal possible sunshine duration at any given location.

Vegetation

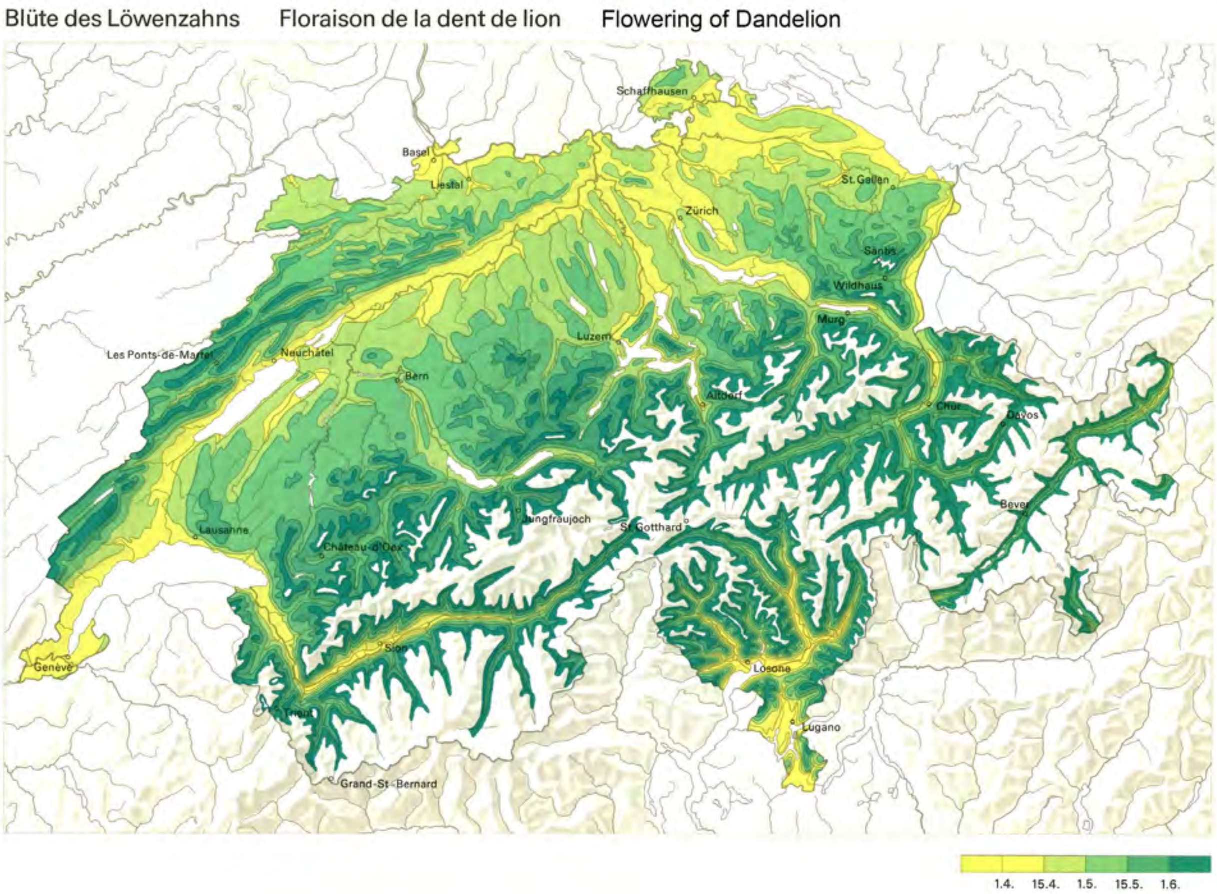

Figure 11: Phenological map of Switzerland showing the flowering of Dandelion (*Taraxacum officinale*) in spring based on the reference period 1951-1975 (Kirchhofer 2000)

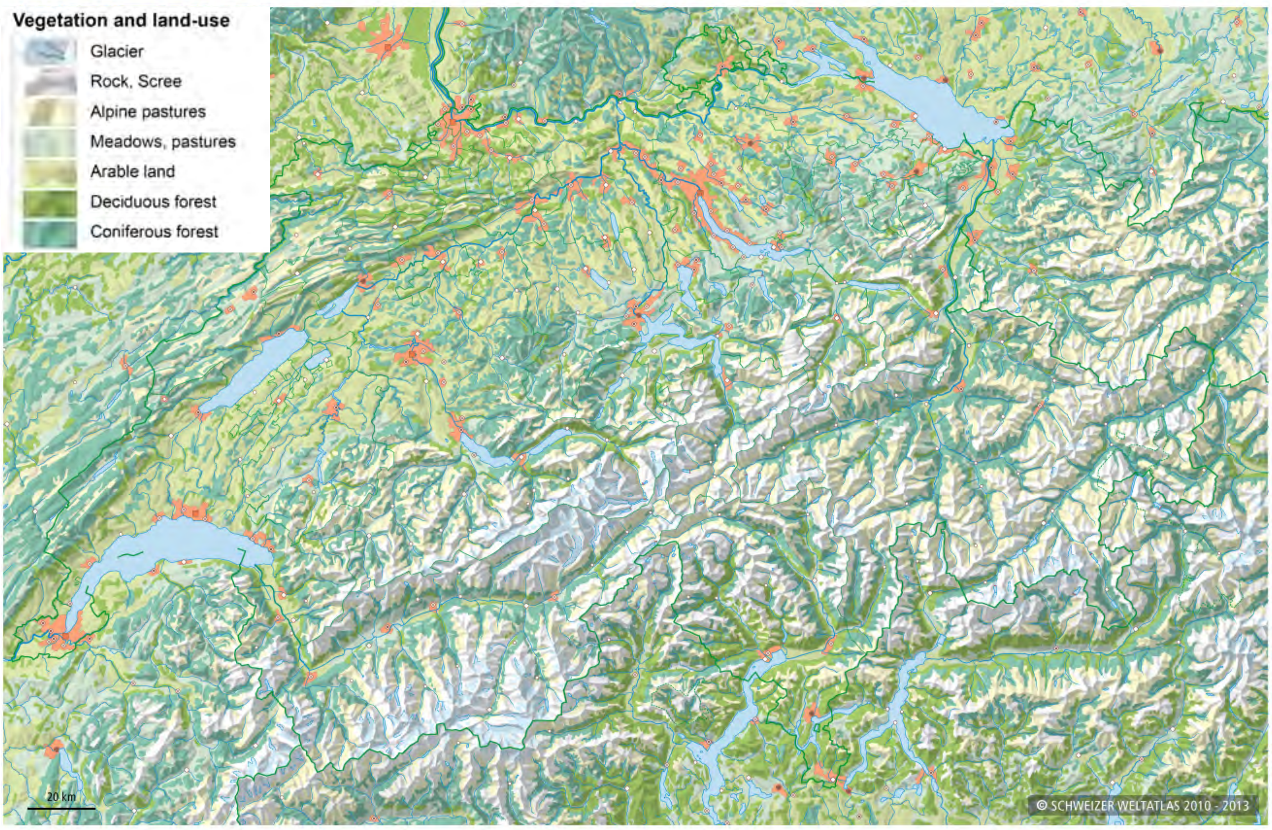

Figure 12: Vegetation and land-use in Switzerland. (Schweizer Weltatlas 2013)

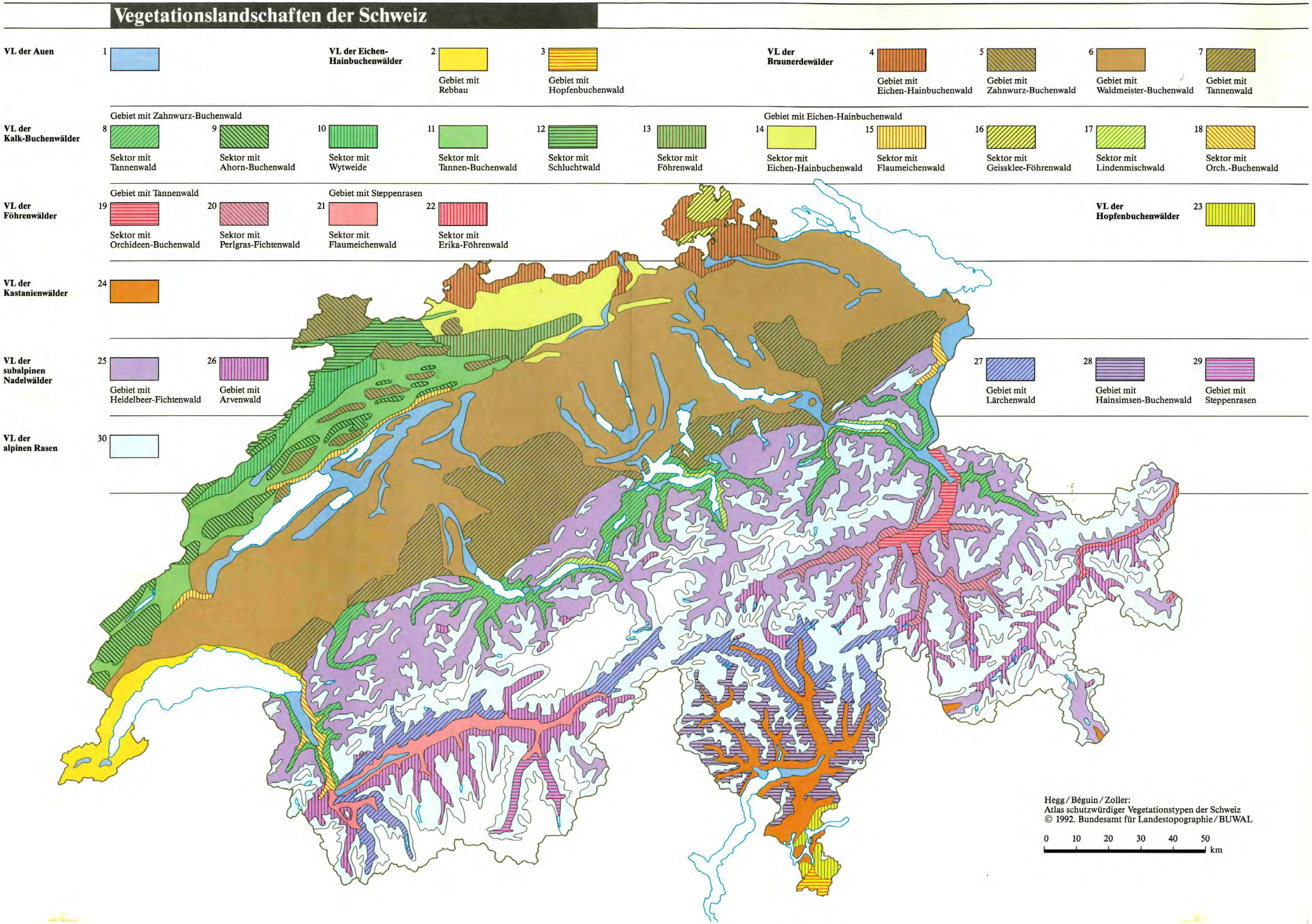

Figure 13: Vegetation types of Switzerland. (Hegg et al. 1993)

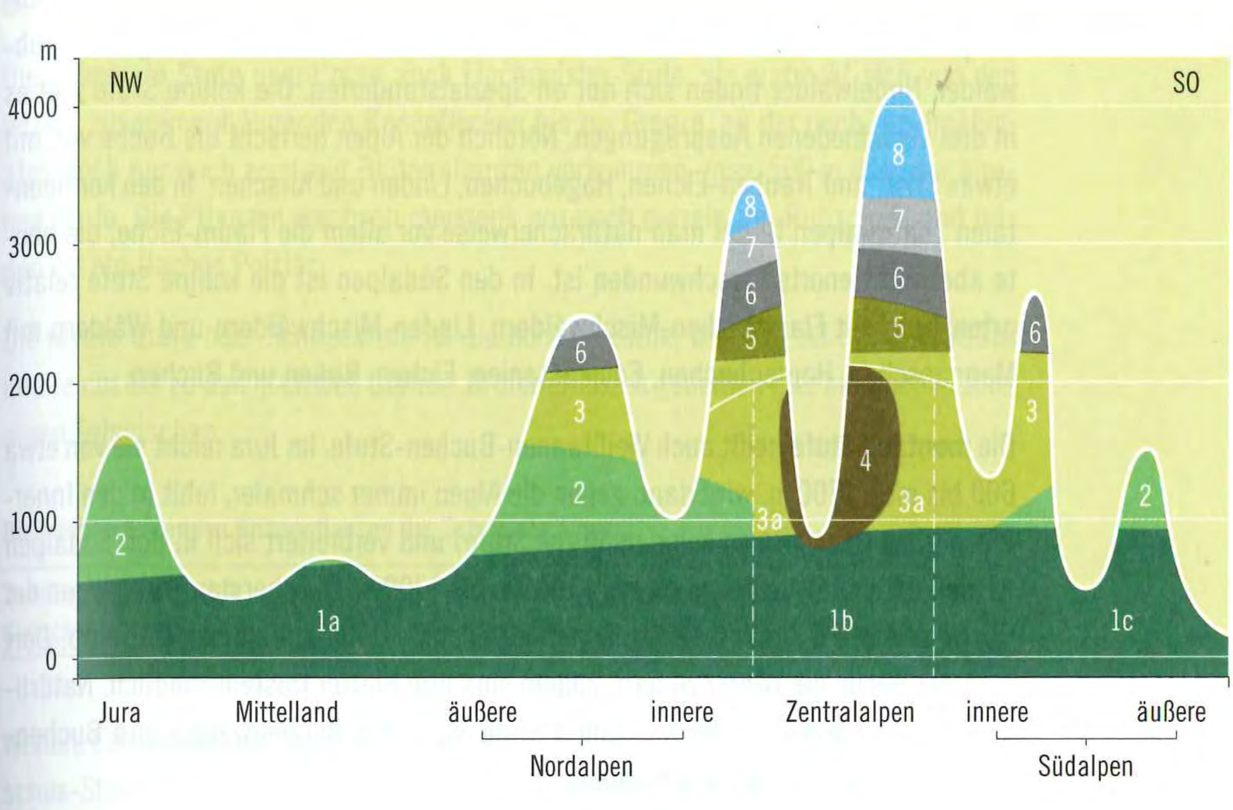

Figure 14: Vegetation belts in Switzerland on an elevational profile through the Swiss Alps (after Landolt 2003)

1 colline belt (oak-beech-belt)
  1a Northern Alps, dominated by *Qercus robur, Q. petreae* and *Fagus sylvatica*
  1b Central Alps, dominated by *Quercus pubescens*, beech is notably absent
  1c Southern Alps, dominated by *Quercus pubescens* and *Fagus sylvatica*
2 montane belt with *Fagus sylvatica* and *Abies alba*
3 subalpine belt, dominated by *Picea abies*
  3a Central Alps, dominated by *Picea abies* and *Pinus sylvestris*
4 continental belt with *Pinus sylvestris*
5 supra-subalpine belt with *Pinus cembra*
6 alpine belt with meadows
7 subnival belt with scree-vegetation
8 nival belt without flowering plants (only in favourable microsites)

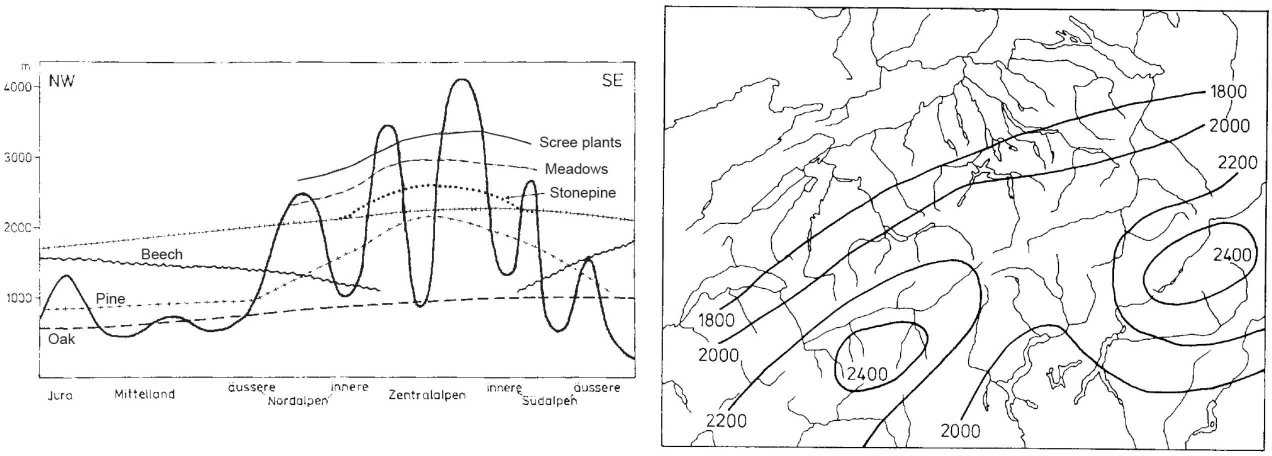

Figure 15: upper altitudinal range limits of select tree species and alpine plant groups (left) as well as average natural treeline elevation in m a.s.l. (right) (Landolt 2003)

Potential natural vegetation

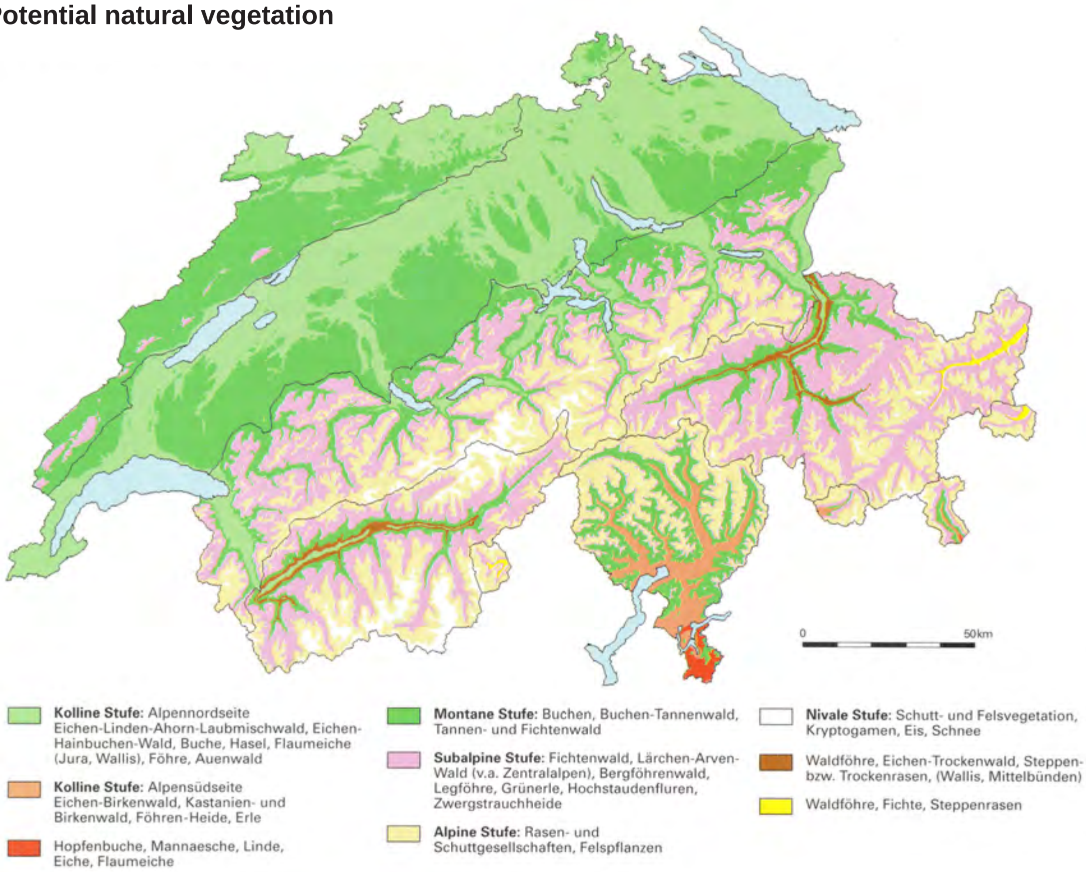

Figure 16: Present-day potential natural vegetation (Burga et al. 1998)

Atlas Welten & Sutter - Number of plants

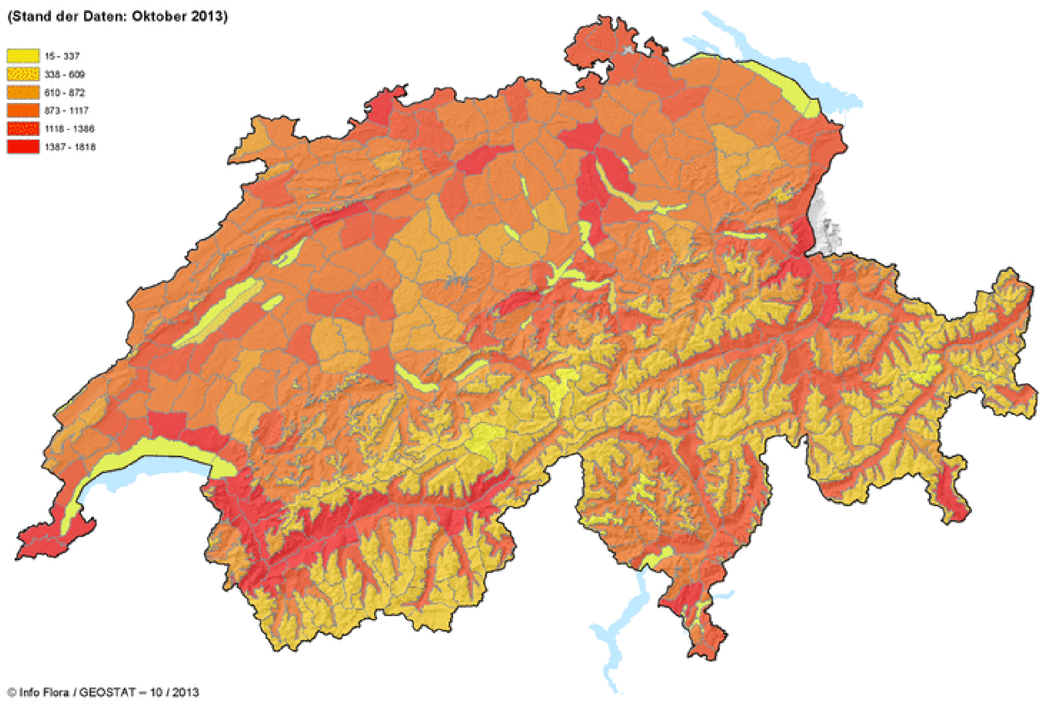

Figure 17: Plant biodiversity in Switzerland. (InfoFlora 2013)

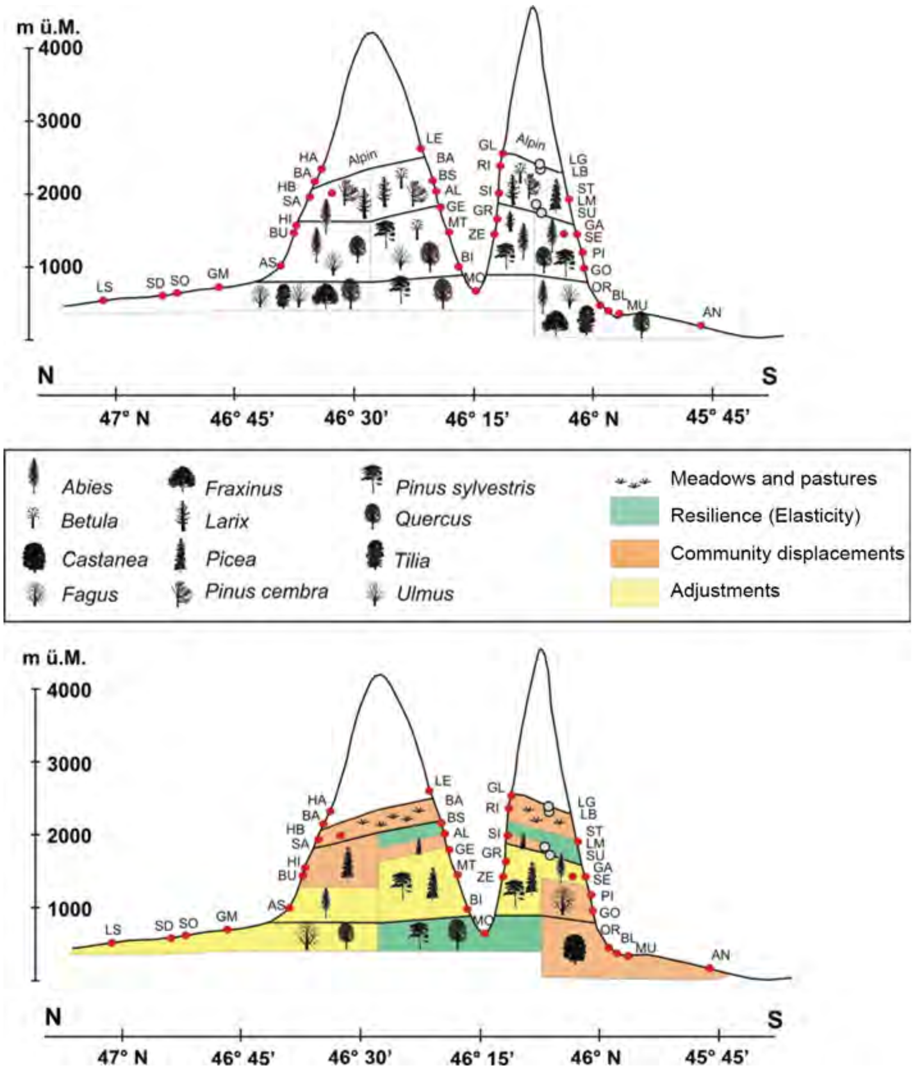

Figure 18: Altitudinal transect through the western Alps: top) Important forest trees at around 6500 cal. yr BP, when summer climate was about 1.5 °C warmer than today. bottom) Modern forest distribution in regard to forest changes during the past 6500 yr. Abbreviations of study sites: AL = Aletschwald (Welten 1982), AN = Annone (Wick Olatunbosi 1996), AS = Aegelsee (Wegmüller und Lotter 1990), BA = Bachalpsee (Lotter et al. 2006), BI = Bitsch (Welten 1982), BL = Balladrum (Hofstetter et al. 2006), BS = Böhnigsee (Markgraf 1969), BU= Untere Bunschleralp (Welten 1982), GA = Gondo-Alpjen (Welten 1982), GE = Greicheralp (Welten 1982), GL = Gouillé Loéré (Tinner und Theurillat 2003), GM = Gänsemoos (Welten 1982), GO = Gola di Lago (Zoller und Kleiber 1971), GR = Grächensee (Welten 1982), MT = Montana (Welten 1982), HA = Hagelseewli (Lotter et al. 2000), HB = Höhenbiel (Küttel 1990), HI = Hinterburgsee (Heiri et al. 2003a, b), LB = Lago Basso (Wick 1994b), LE = Lengi Egga (Tinner und Theurillat 2003), LG = Lago Grande (Wick 1994a), LM = Lej da San Murezzan (Gobet et al. 2005), LS = Lobsigensee (Ammann et al. 1985), MO = Mont d'Orge (Welten 1982), MU = Muzzano (Gobet et al. 2000), OR = Origlio (Tinner et al. 1999), PI = Piano (Valsecchi et al. 2010), RI = Gouillé Rion (Tinner et al. 1996), SA = Sägistalsee (Wick et al. 2003), SE = Segna (Valsecchi et al. 2010), SO = Soppensee (Lotter 1999), SD = Lac de Seedorf (Richoz 1998), SI = Simplon (Lang and Tobolski 1985), ST = Lago Starlarescio (Vescovi et al. in prep), SU = Suossa (Zoller and Kleiber 1971), ZE = Zeneggen (Welten 1982). The latitudinal position is only approximate. Three sites in the southern Alps (open circles) are not part of the north-south transect. These locations are shown according to their position within the different eco-regions. (Gobet et al. 2010)

Geography

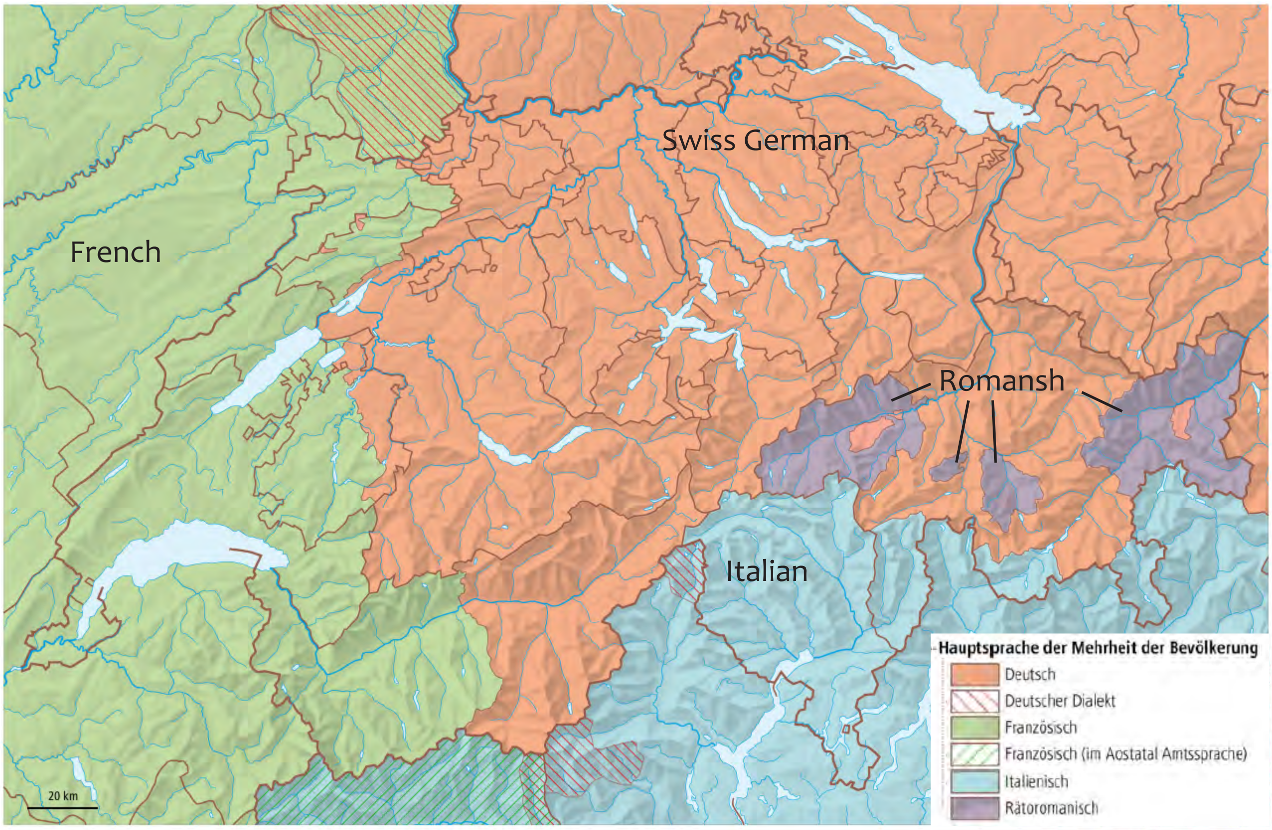

Figure 19: Main languages spoken in Switzerland. (Schweizer Weltatlas 2013)

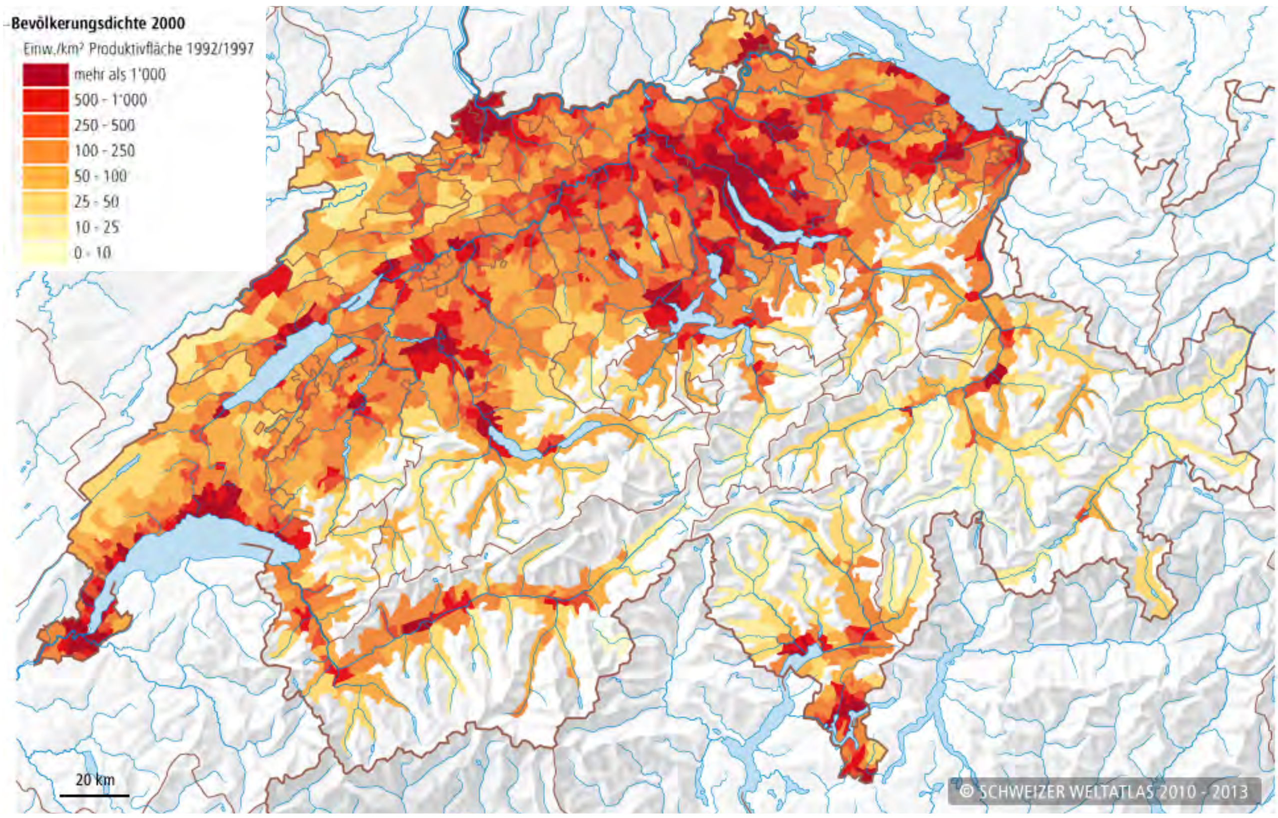

Figure 20: Population density of Switzerland as people/km^2 in 1992/1997 (Schweizer Weltatlas 2013)

Monday 05.09.2016

Afternoon:	Arrival at the Institute of Plant Sciences and Botanical Garden Bern
17 h	Welcome at IPS
18.30 h	Dinner at the Botanical Garden
20.30 h	Departure to Liestal
21.30 h	Arrival at Hotel Engel (Liestal)

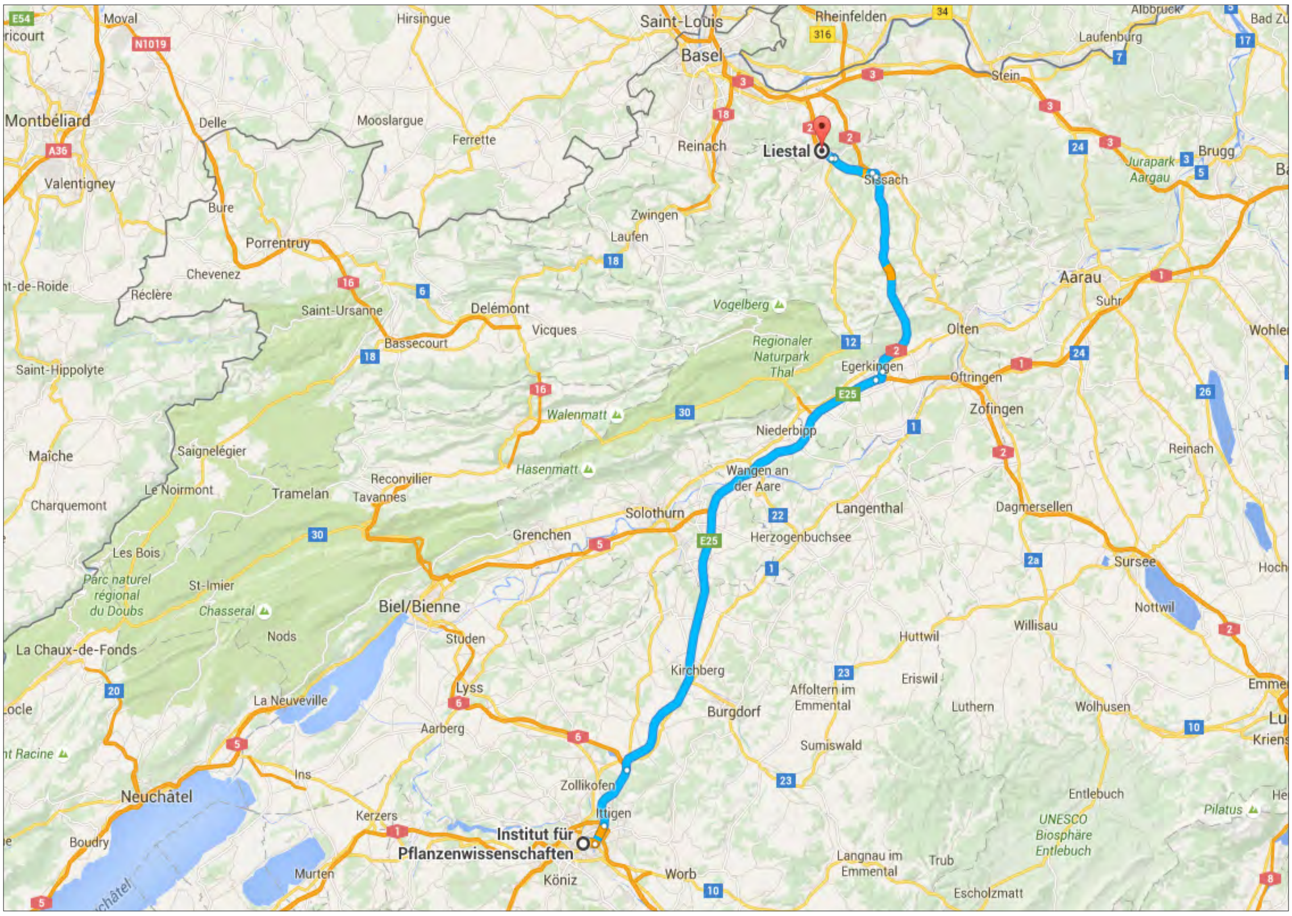

Tuesday 06.09.2016

8:30 h	Departure to Rheinfelden
9.10 h	Commemoration
9:15 h	**Rheinfelden Häxeplatz**: Karstic hole, extirpation of *Abies alba*, forest history and land use since the end of the Neolithic (Lucia Wick)
10:15 h	Departure to Augusta Raurica
10:30 h	Augusta Raurica, visit of Roman town
11 h	Departure to Burgäschisee
12 h	Lunch at Restaurant Seeblick, Burgäschi
13 h	**Burgäschisee**: landscape, vegetation and fire history (Erika Gobet)
14 h	Introduction to lake dwellings (Othmar Wey, excavation leader)
15:30 h	Neolithic high resolution multiproxy (Fabian Rey)
16:30 h	Comparison to other Neolithic on-site studies (Erika Gobet, Oliver Heiri)
17:30 h	Departure to Wangen an der Aare
18 h	Arrival at Hotel al Ponte (Wangen an der Aare)
19 h	Dinner at Hotel al Ponte

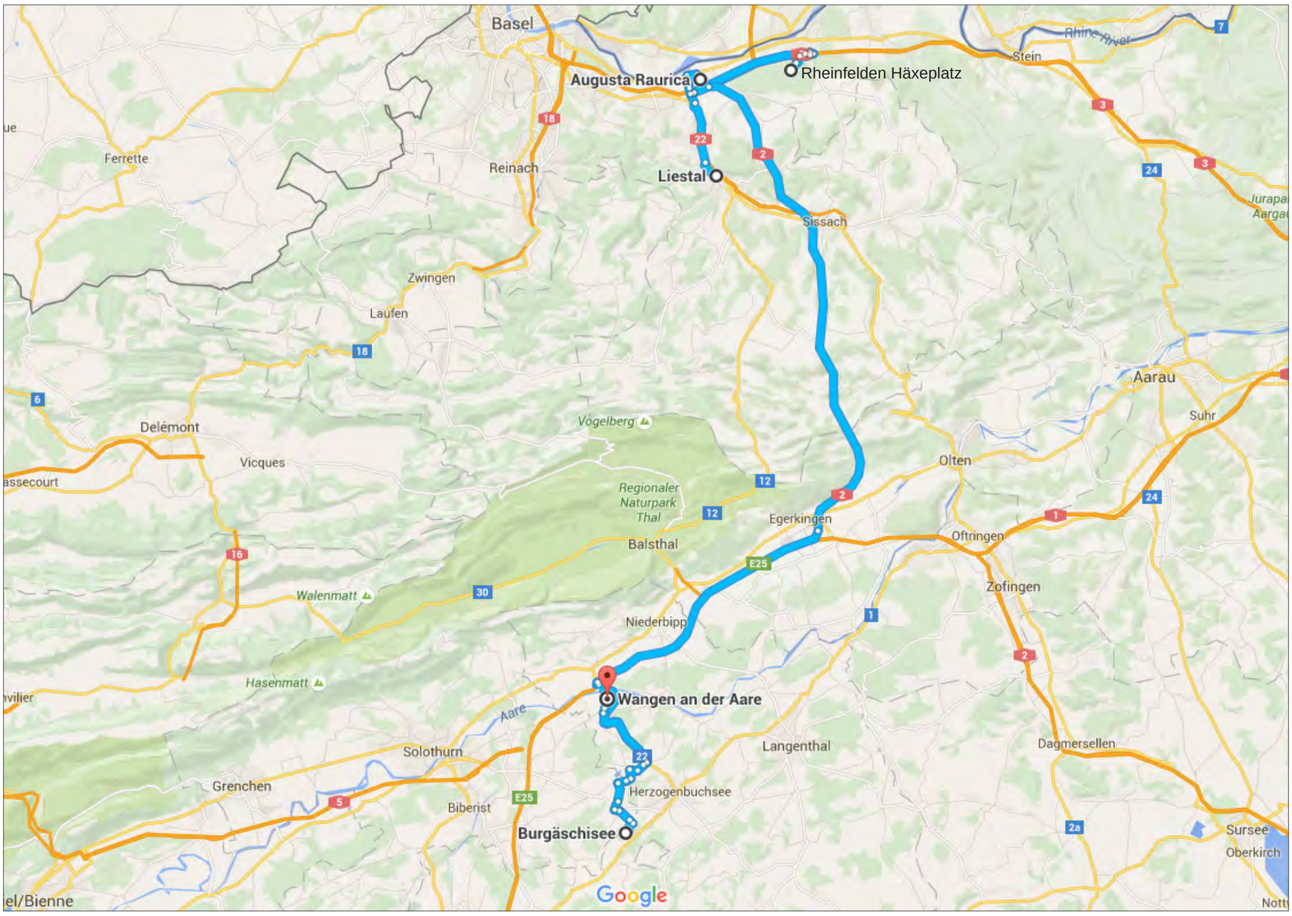

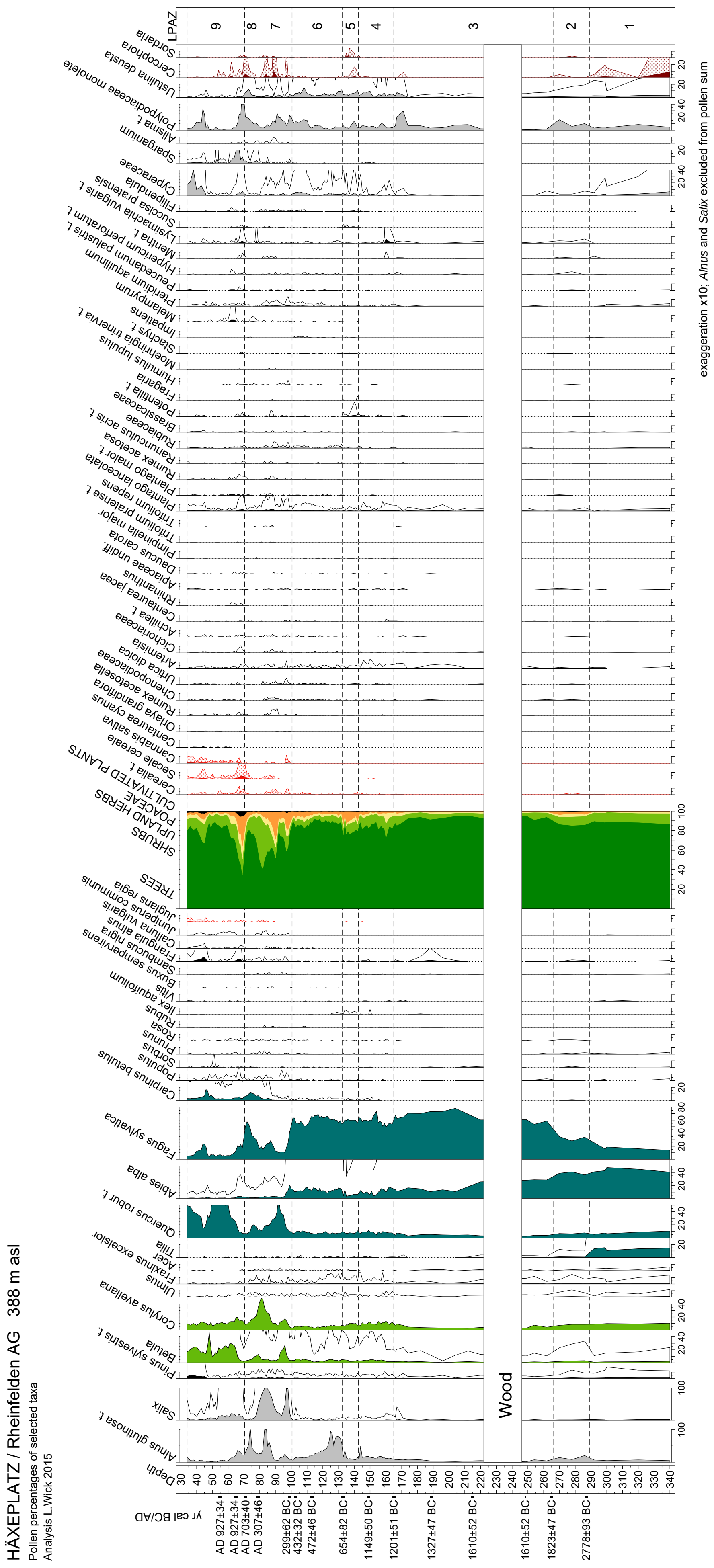
HÄXEPLATZ / Rheinfelden AG 388 m asl
Pollen percentages of selected taxa
Analysis L. Wick 2015
yr cal BC/AD
Depth
AD 927±34
AD 927±34
AD 703±40
AD 307±46
299±62 BC
432±32 BC
472±46 BC
654±82 BC
1149±50 BC
1201±51 BC
1327±47 BC
1610±52 BC
1610±52 BC
1823±47 BC
2778±93 BC
Alnus glutinosa t.
Salix
Wood
Pinus sylvestris t.
Betula
Corylus avellana
Ulmus
Fraxinus excelsior
Acer
Tilia
Quercus robur t.
Abies alba
Fagus sylvatica
Carpinus betulus
Populus
Sorbus
Prunus
Rosa
Rubus
Ilex aquifolium
Vitis
Buxus sempervirens
Sambucus nigra
Frangula alnus
Calluna vulgaris
Juniperus communis
Juglans regia
TREES
SHRUBS
UPLAND HERBS
POACEAE
CULTIVATED PLANTS
Cerealia t.
Secale cereale
Cannabis sativa
Centaurea cyanus
Orlaya grandiflora
Rumex acetosella
Chenopodiaceae
Urtica dioica
Artemisia
Cichoriaceae
Achillea t.
Centaurea jacea
Rhinanthus
Apiaceae undiff.
Daucus carota
Pimpinella major
Trifolium pratense t.
Trifolium repens
Plantago lanceolata
Plantago major t.
Rumex acetosa
Ranunculus acris t.
Rubiaceae
Brassicaceae
Potentilla t.
Fragaria
Humulus lupulus
Moehringia trinervia t.
Stachys t.
Impatiens
Melampyrum
Pteridium aquilinum
Peucedanum palustre t.
Hypericum perforatum t.
Mentha t.
Lysimachia vulgaris t.
Succisa pratensis
Filipendula
Cyperaceae
Sparganium
Alisma t.
Polypodiaceae monolete
Ustulina deusta
Cercophora
Sordaria
LPAZ
exaggeration x10; Alnus and Salix excluded from pollen sum

HÄXEPLATZ / Rheinfelden AG
selected macrofossil concentrations / 30 ml sediment

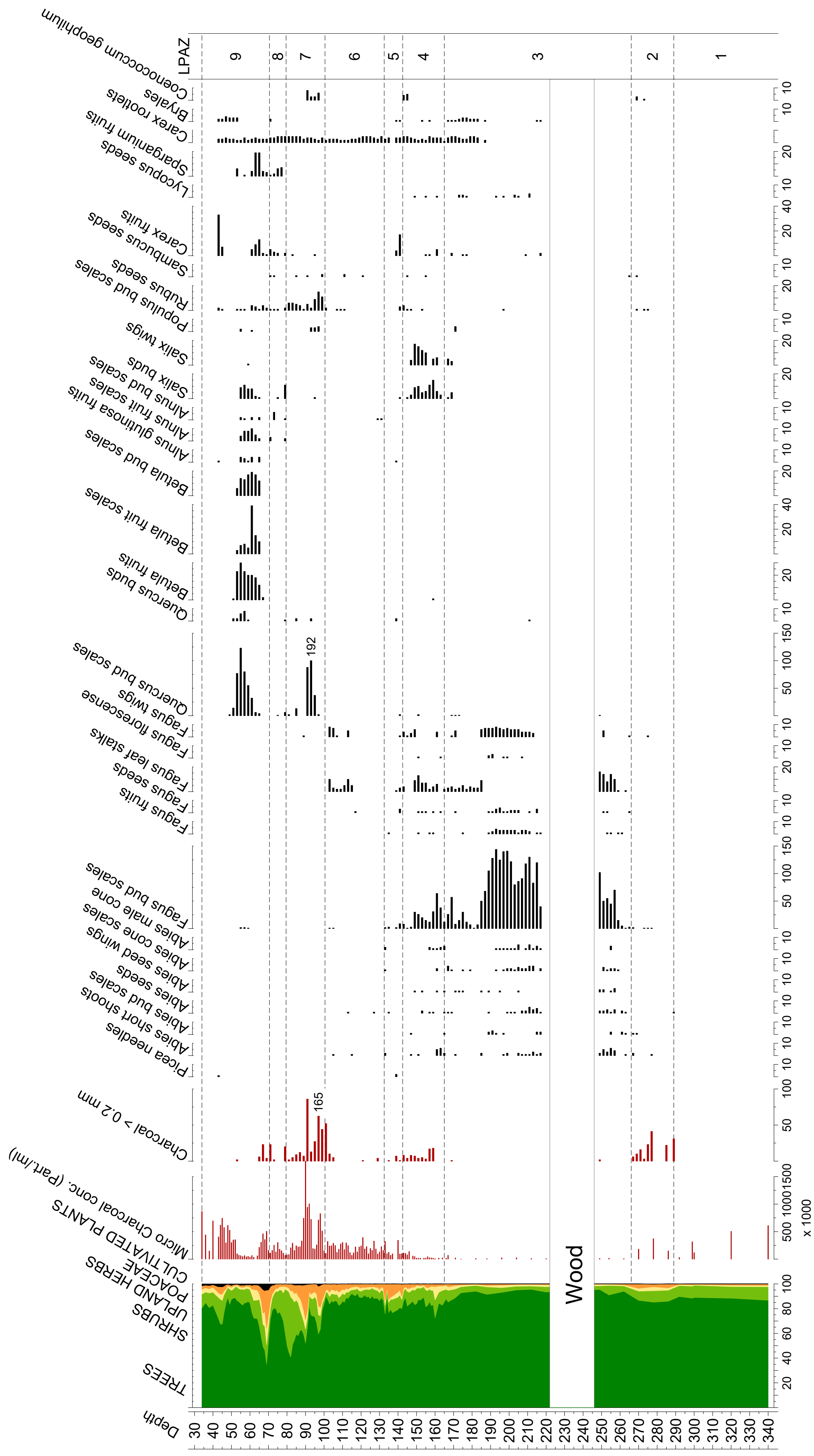

Augusta Raurica – a brief history

The capital of the Colonia Raurica was the largest Roman settlement in present-day Switzerland. Due to its favourable location at the Rhine, on the intersection between the north-south axis linking the Rhineland with Italy and the west-east route from Gaul to the Danube and Raetia, the town developed into an important trading centre. A large number of villae rusticae in the hinterland provided the population with agricultural products.

44 BC	establishment of the Colonia Raurica by Lucius Munatius Plancus under Julius Caesar
c. 15-10 BC	foundation of the town Augusta Raurica; timber constructions (the oldest dendrochronological date is 6 BC). From AD 20-50 military fort with foot soldiers and cavalry.
AD 40-70	rebuilding of the town in stone. First public buildings: theatre, temple, forum.
late 1st – early 3rd cent.	Boom years; around AD 200 construction of the thermae, the amphitheatre and luxurious private buildings. Development to a flourishing trading and handicraft centre with 15’000 – 20’000 inhabitants.
c. AD 250	the town was largely destroyed by an earthquake
around AD 260	first attacks of the Alemanni
AD 273/274	destruction of the civil city by Germanic tribes; construction of the military fort Kastelen; in the early 4th cent. the military fort Castrum Rauracense near the Rhine river was built and became an important military base.
	Wars and epidemics as well as crop failures caused by a deteriorating climate led to the abandonment of large parts of the town. Around AD 300 the settlement moved into the protection of the military fort.
c. AD 400	withdrawal of the Roman troops. The settlement, now called Rauraci, remained an administrative centre and important market place.
7th century AD	Basle began to flourish; Rauraci went into decline and reverted to a small fishing village

Rundgänge
Circuits
Walks
Percorsi

Im römischen Stadtzentrum
Le centre-ville romain
In the Roman town centre
Nel centro della città romana

Rund um den Tierpark
Autour du parc aux animaux
Round about the animal park
Nei dintorni del parco zoologico

Römisches Stadtgebiet
Extension de la cité romaine
Roman town area
Area della città romana

Picknickplatz
Pique-nique
Picnic area
Area picnic

Zeltplatz
Camping
Campsite
Campeggio

Information
Information
Information
Informazioni

Gladiatoren und Götter
Les gladiateurs et les dieux
Gods and gladiators
Gladiatori e dei

Im Kastell am Rhein
Le Castrum au bord du Rhin
In the fortress by the Rhine
Nel castrum sul Reno

Fussweg
Chemin de piétons
Pedestrian route
Percorso pedonale

Schwimmbad
Piscine
Pool
Piscina

Geldautomat
Guichet automatique bancaire
Automatic teller machine
Bancomat

Burgäschisee: landscape, vegetation, fire history and archaeology

Fabian Rey[1,2], Erika Gobet[1,2], Jacqueline F. N. van Leeuwen[1,2,] Adrian Gilli[3], Ulrike J. van Raden[3], Othmar Wey[2,4], Albert Hafner[2,4], Willy Tinner[1,2]

[1] Institute of Plant Sciences, University of Bern, Altenbergrain 21, 3013 Bern, Switzerland
[2] Oeschger Centre for Climate Change Research, University of Bern, Falkenplatz 16, 3012 Bern, Switzerland
[3] Geological Institute, ETH Zurich, Sonneggstrasse 5, 8092 Zurich, Switzerland
[4] Institute of Archaeological Sciences, University of Bern, Muesmattstrasse 27, 3012 Bern, Switzerland

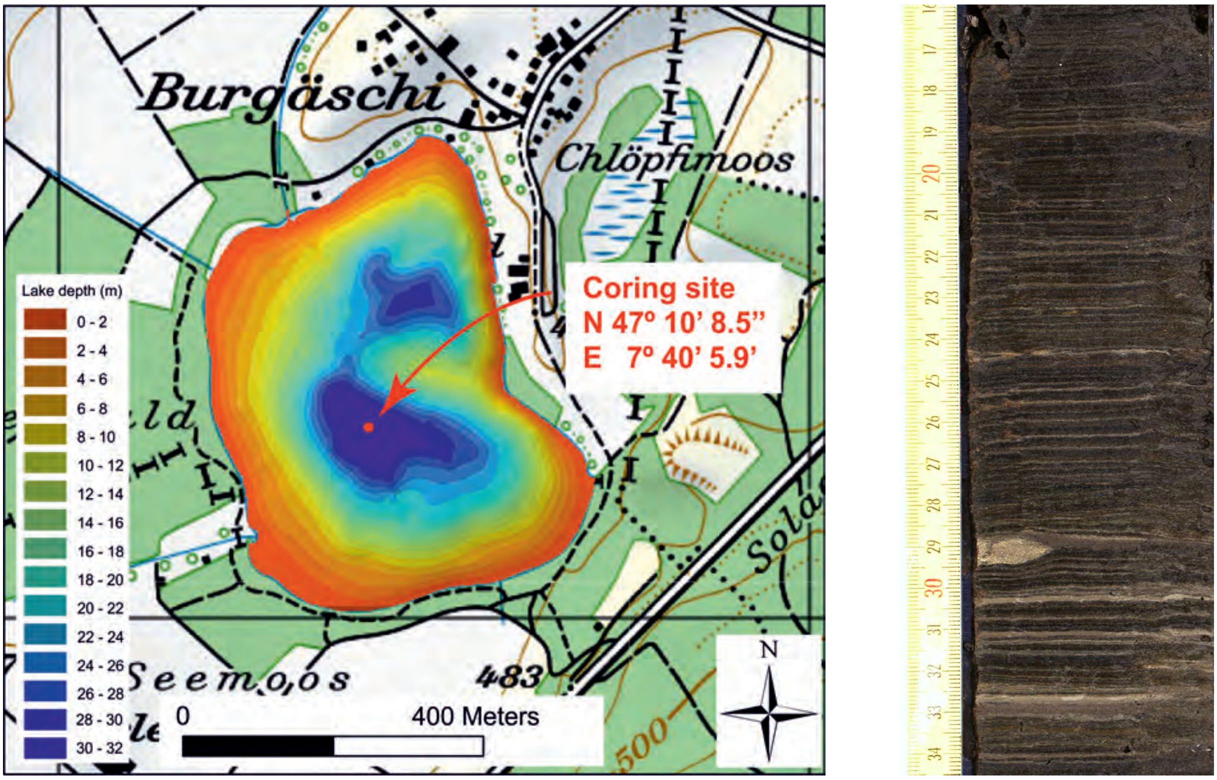

Fig. 1 Seismic map of Burgäschisee with the coring locality (left) (©swisstopo). Part of the laminated sediments of Burgäschisee (Roman Period, c. 2000 cal. B.P.) (right).

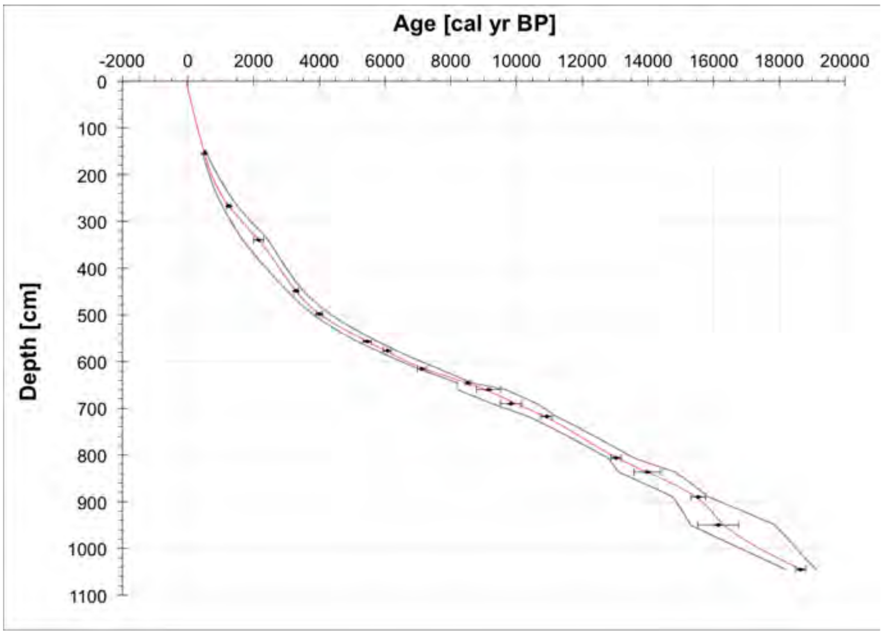

Fig. 2 Age-depth-model of Burgäschisee: Black dots show calibrated ages of terrestrial plant macrofossils with 2 sigma error bars (IntCal13, Reimer et al. 2013). The red line is the modelled chronology (Smooth spline 0.23 with the program clam 2.2, Blaauw 2010). The grey lines indicate the 95% confidence envelope of the generalized mixed effect regression (GAM, Heegaard et al. 2005).

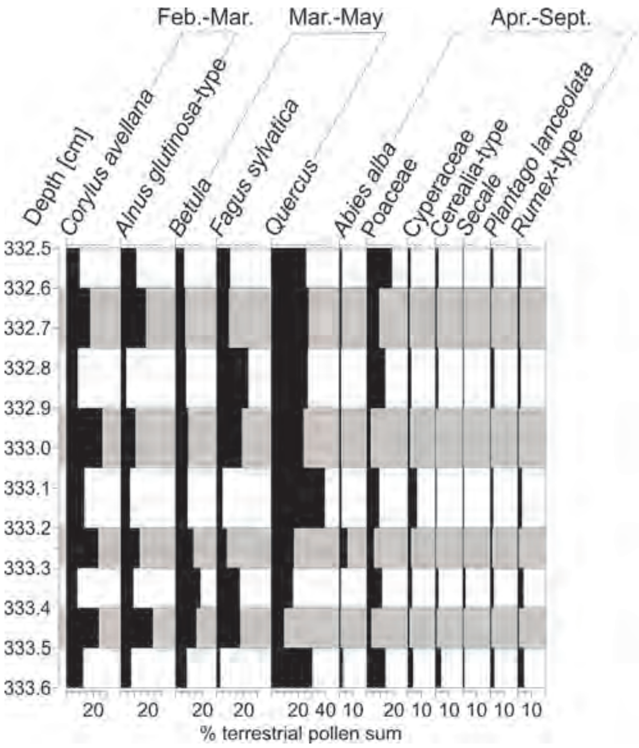

Fig. 3 Pollen analysis of seven consecutive sediment layers (5 light laminae and 4 dark laminae) from 333.6-332.5 cm (sum > 400 terrestrial pollen). The selected pollen types are ordered by the timing of their general blooming (Leuschner 1974; Leuschner 1991; Lauber et al. 2014).

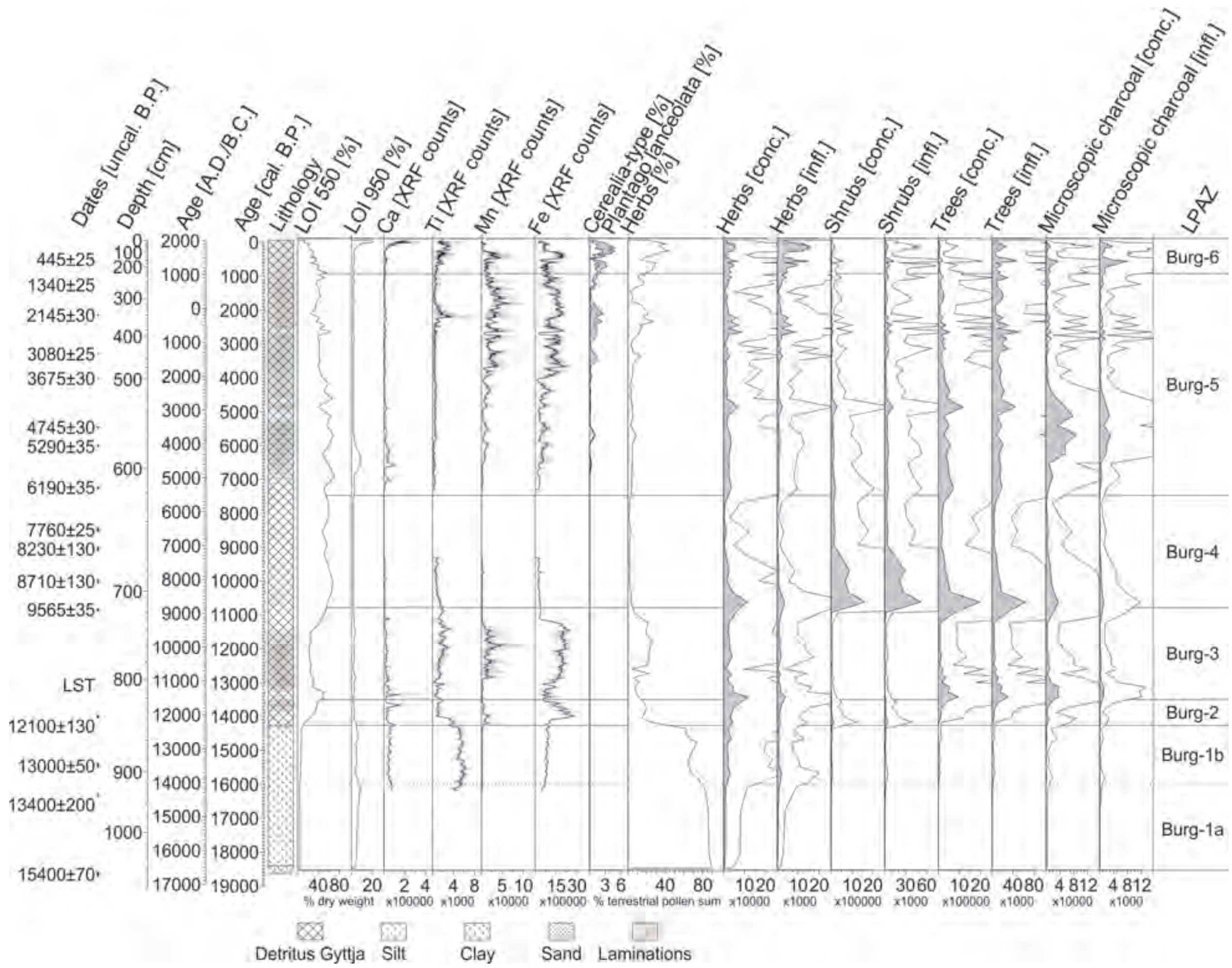

Fig. 4 Composite of loss on ignition at 550°C (LOI 550) and 950°C (LOI 950), XRF counts of selected elements, pollen percentages of selected pollen types, pollen concentrations of herbs, shrubs and trees, pollen influx of herbs, shrubs and trees, microscopic charcoal concentrations and microscopic charcoal influx. Empty curves are the 10x exaggerations. The grey lines of the XRF data show the original counts, the black lines are the moving averages (period = 19). LPAZ = local pollen assemblage zones. LST = Laacher See tephra.

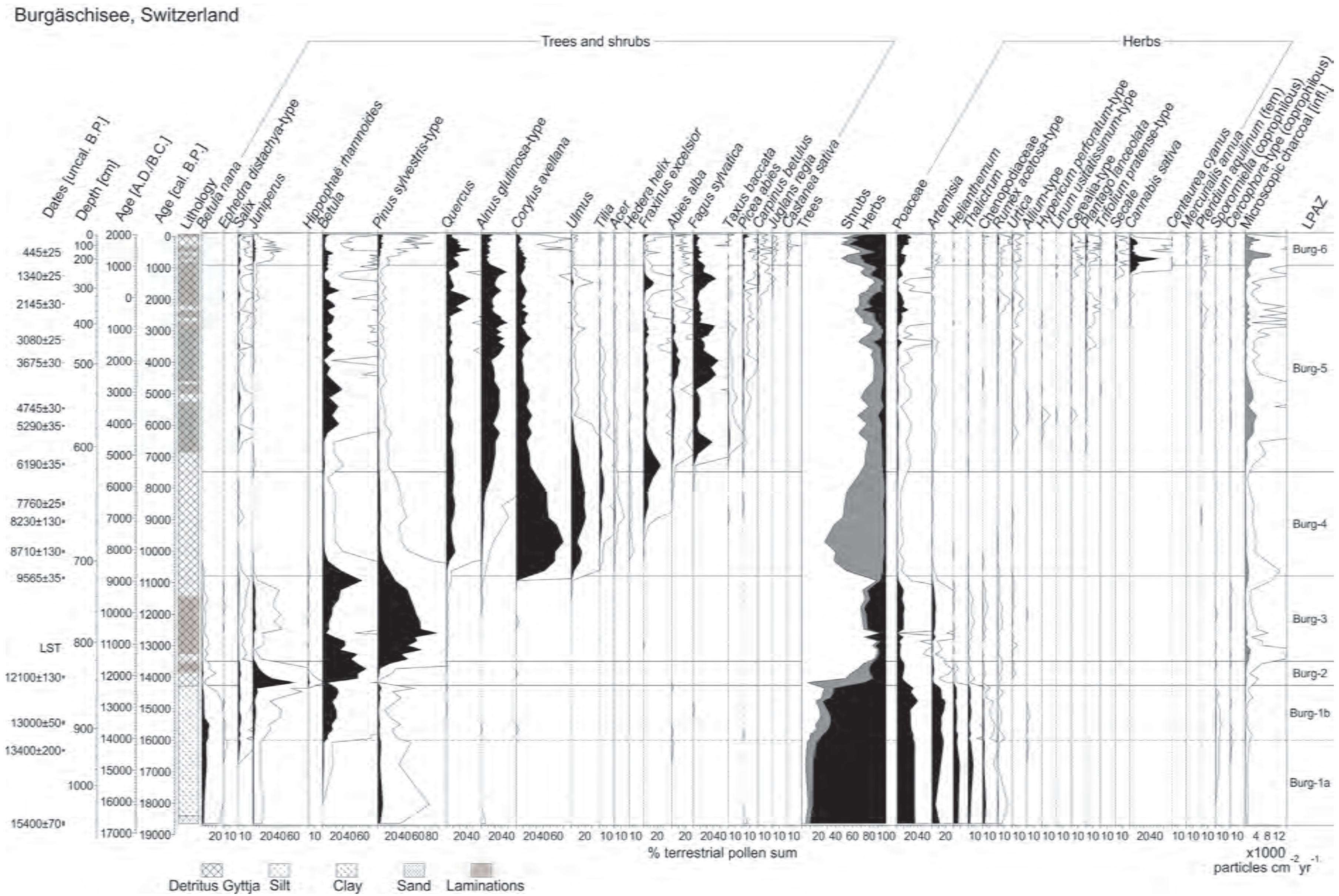

Fig. 5 Percentages of selected pollen types, fern spores and coprophilous fungi spores and charcoal influx values of Burgäschisee. Empty curves are the 10x exaggerations. LPAZ = local pollen assemblage zones. LST = Laacher See tephra.

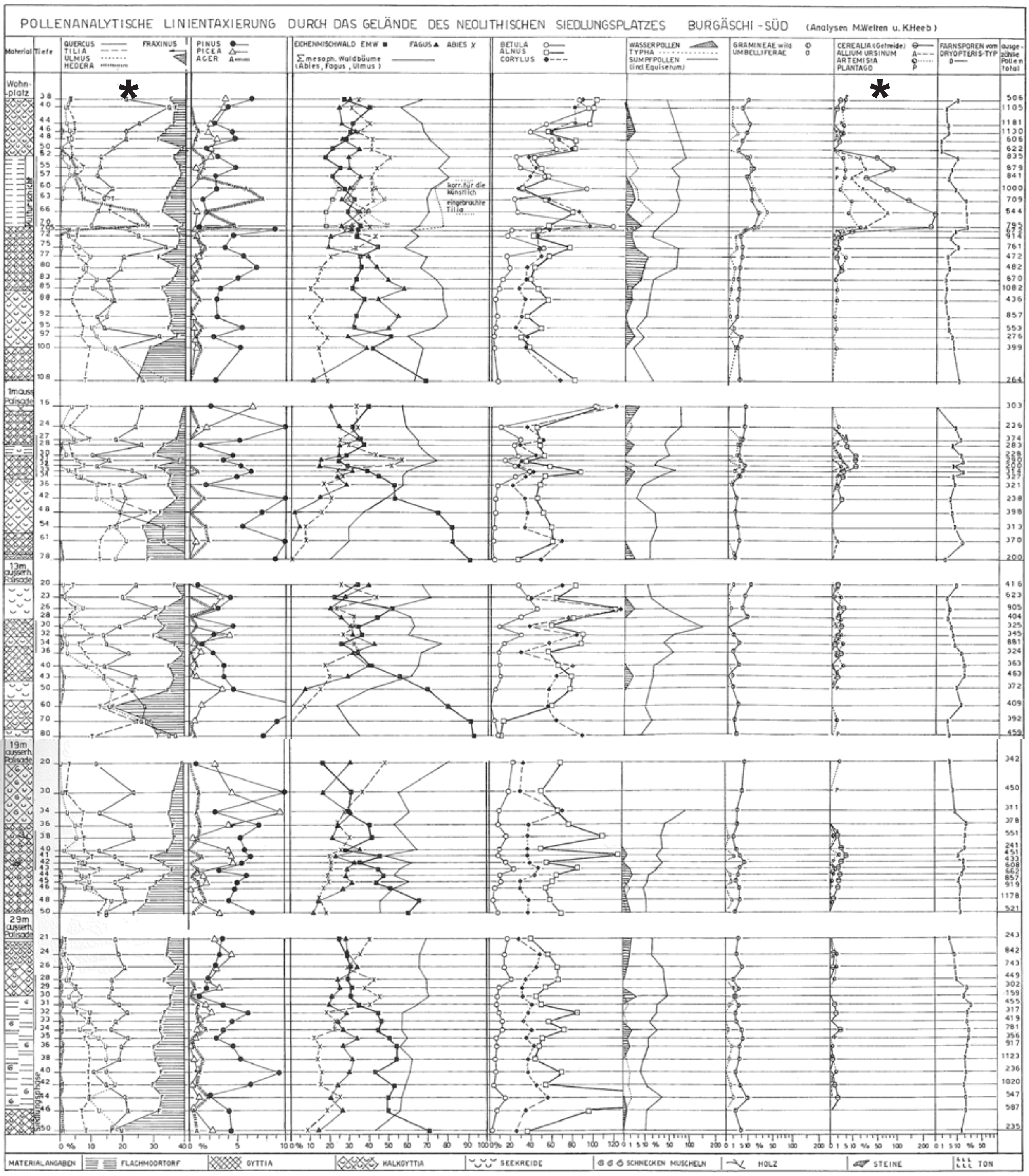

Fig. 6 On-site pollen diagrams along a transect from the 1952 excavation at Burgäschisee Süd, Cortaillod (Welten. 1967)

Figure 7. Excavations of Burgäschisee Nord (2011). The cultural layers are from the Cortaillod period.

Figure 8. Pot with scratched decorations unique for the Late Cortaillod, excavated at Burgäschisee Nord.

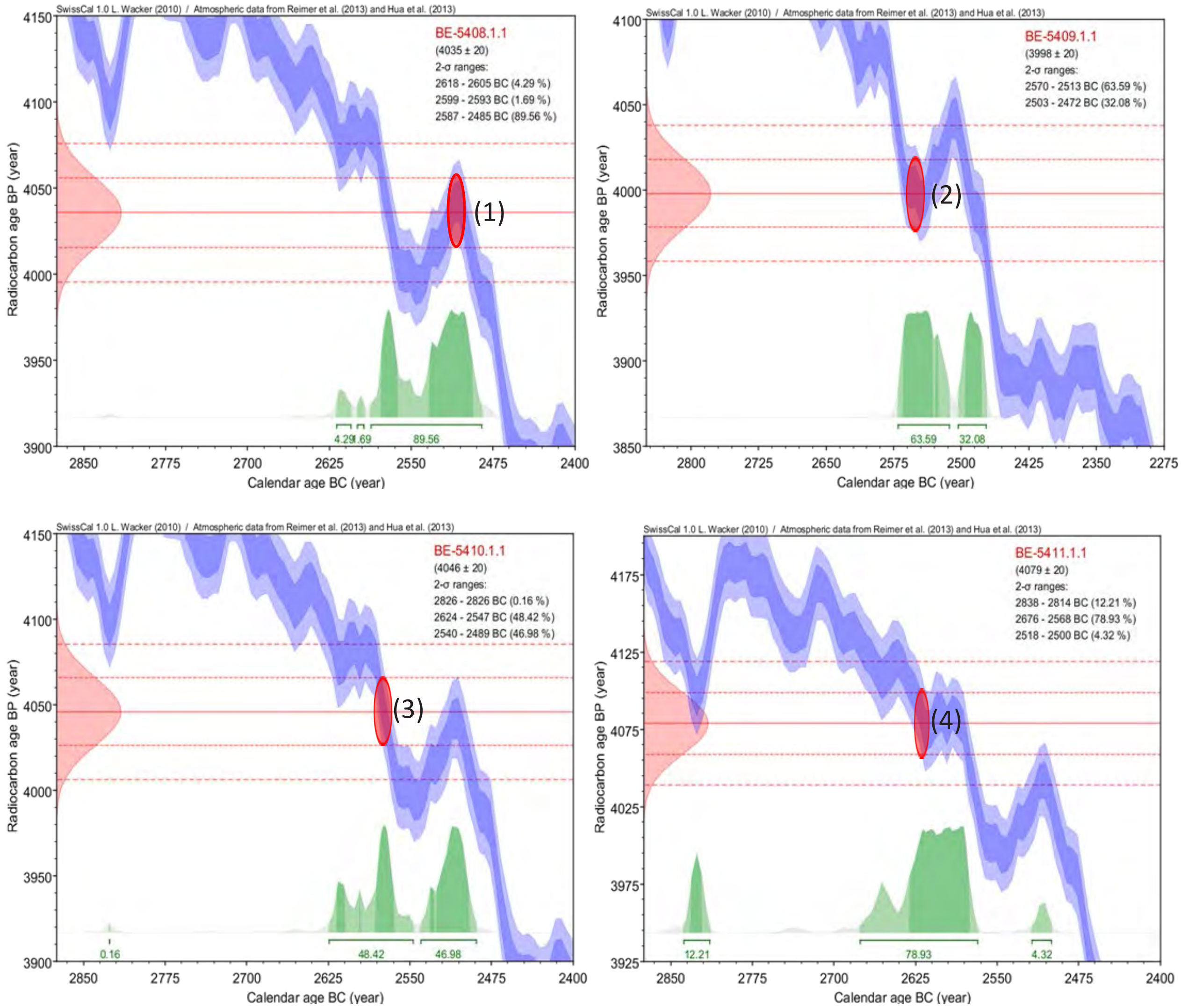

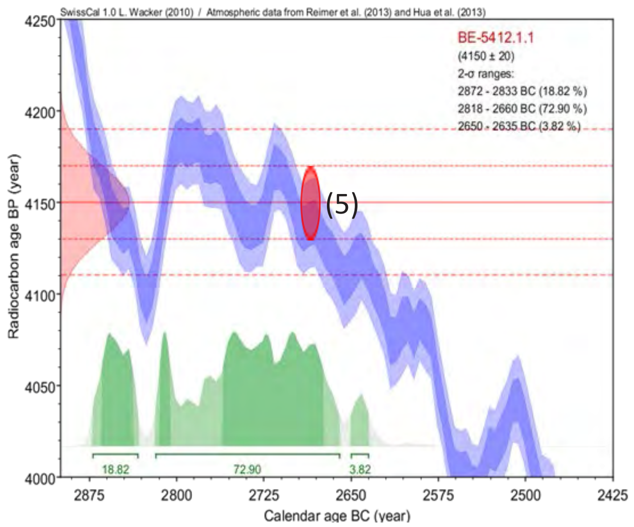

Fig. 9 Calibration plots for the five lake sediment radiocarbon dates BE-5408.1 (4'035±20 uncal. B.P., (1) top) to BE-5412.1.1 (4'150±20 uncal. B.P., (5) bottom). The highlighted (red) area is marking the most probable location of the dates on the calibration curve (visually). The radiocarbon dates fit well into the inversion of the calibration curve around 2'500 cal. B.C.

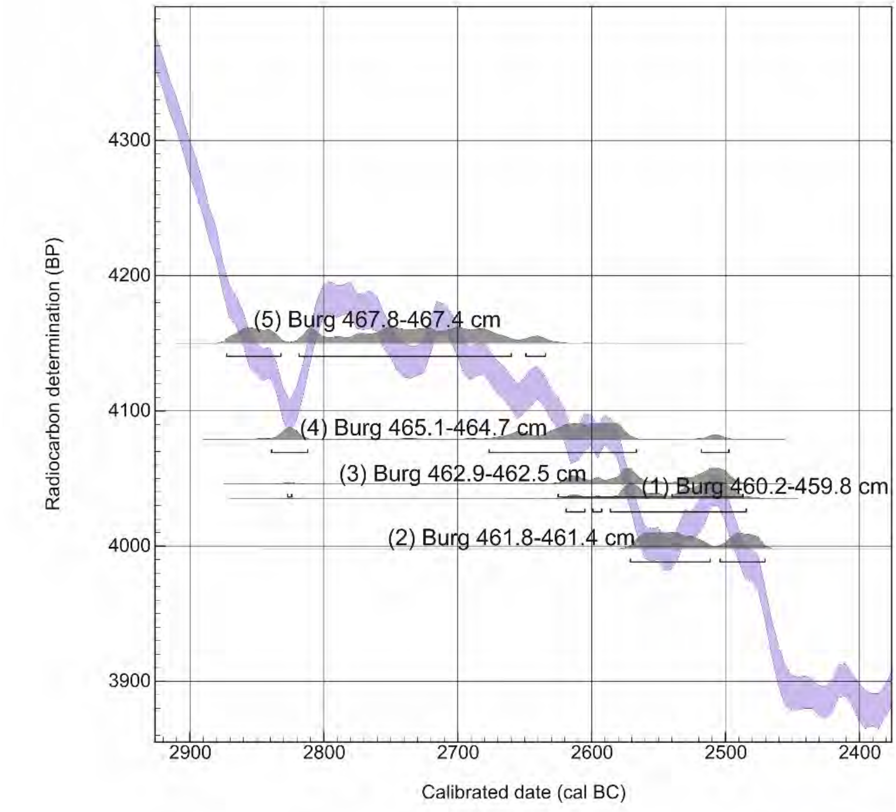

Fig. 10 Summary of the calibration plots (see Fig. 9) from top (1) Burg 460.2-459.8 cm to bottom (5) 467.8-467.4 cm using OxCal 4.2 (Bronk Ramsey 2009).

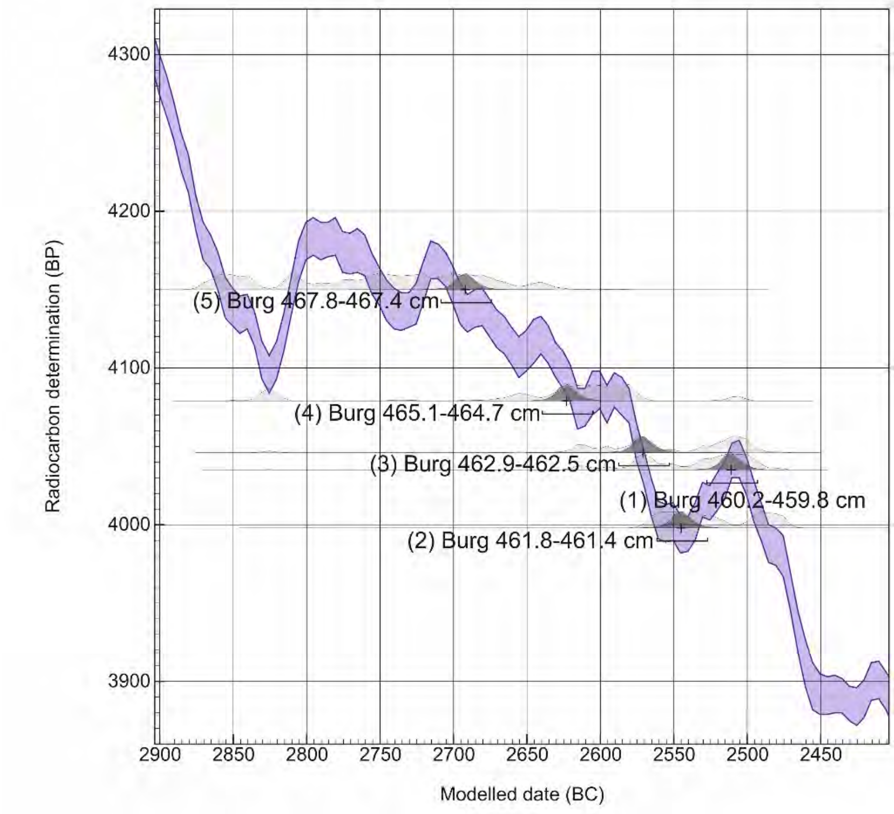

Fig. 11 Wiggle matching of the five dates from Fig. 9 and 10 using D-Sequence in OxCal 4.2 (Bronk Ramsey 2001). The light grey areas are the calibration plots used in Fig. 10 and the dark grey areas are the modelled dates with an error range of ±17 years.

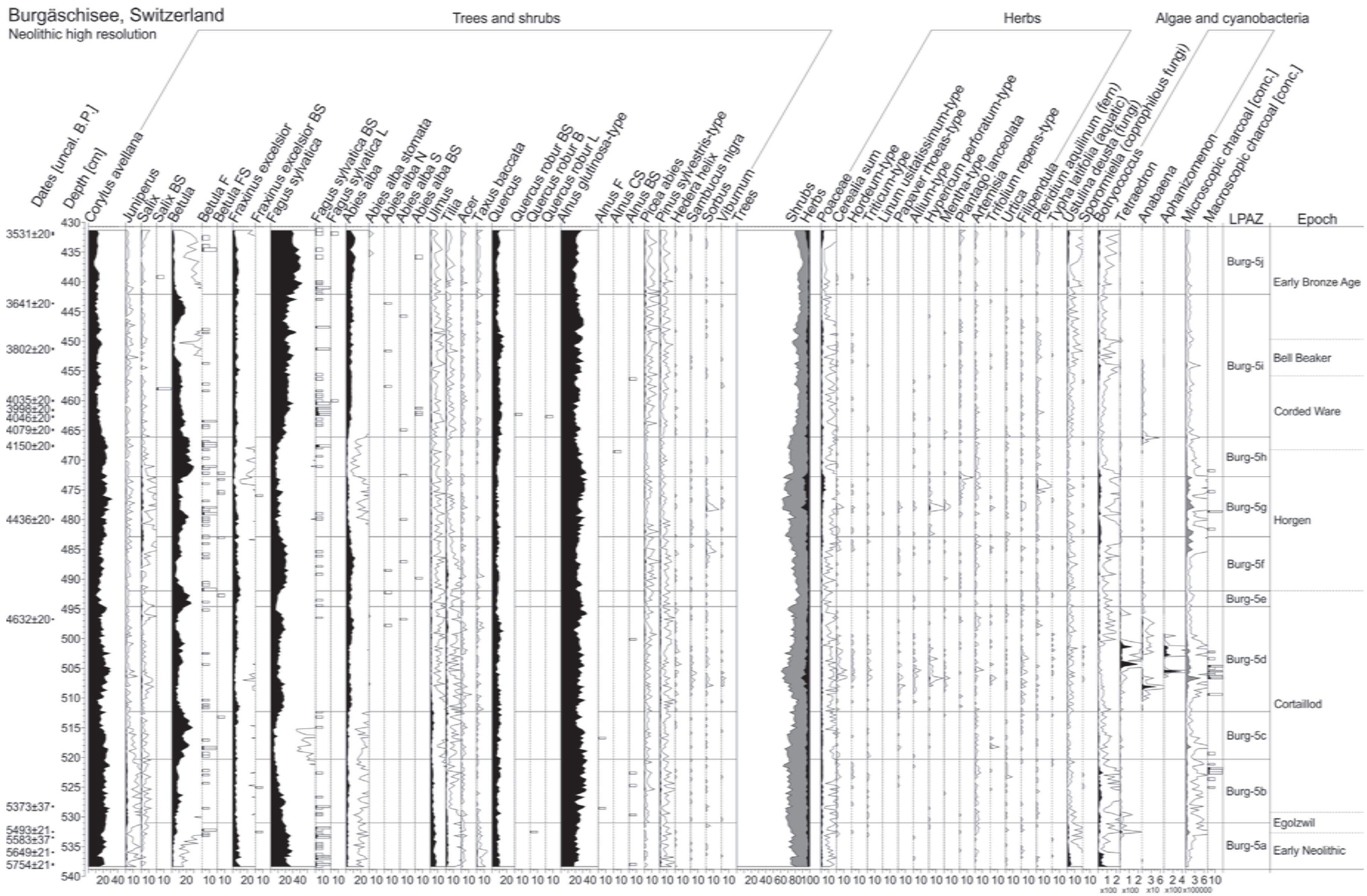

Fig. 11 Percentages of selected pollen types, fern spores, coprophilous fungi spores, fungi spores, green algae and cyanobacteria, microscopic charcoal concentrations, plant macrofossils concentrations as well as macroscopic charcoal concentrations (particles >200μm) of the Neolithic high resolution at Burgäschisee. Empty curves are the 10x exaggerations. LPAZ = local pollen assemblage zones. LST = Laacher See tephra. B = bud, BS = bud scale, CS = cone scale, F = fruit, FS = fruit scale, L = leaf, N = needle, S = seed.

References

Blaauw M (2010) Methods and code for 'classical' age-modelling of radiocarbon sequences. Quat Geochronol 5:512–518

Bronk Ramsey C (2009). Bayesian analysis of radiocarbon dates. Radiocarbon, 51:1 337-360

Heegaard E, Birks HJB, Telford RJ (2005) Relationships between calibrated ages and depth in stratigraphical sequences: an estimation procedure by mixed-effect regression. Holocene 15:4, 612-618

Lauber K, Wagner G, Gygax A (2014) Flora Helvetica, 5th edn. Haupt/Stuttgart, Bern/Wien

Leuschner R (1974) Pollen calendars for Switzerland. In: Charpin J, Surinyach R, Frankland AW (eds) Atlas of European allergenic pollens. Sandoz Editions, pp 193-199

Leuschner R (1991) Comparison of airborne pollen levels in Switzerland at 4 recording stations in Davos, Lucerne, Nyon and Basle during 1989. Int J Biometeorol 35:2, 71-75

Reimer P J, Bard E, Bayliss A, Beck JW, Blackwell PG, Bronk Ramsey C, Grootes PM, Guilderson TP, Haflidason H, Hajdas I, Hattž C, Heaton TJ, Hoffmann DL, Hogg AG, Hughen KA, Kaiser, KF, Kromer B, Manning SW, Niu M, Reimer RW, Richards DA, Scott EM, Southon JR, Staff RA, Turney CSM, van der Plicht J (2013) IntCal13 and Marine13 Radiocarbon Age Calibration Curves 0-50,000 Years cal BP. Radiocarbon 55:4, 1869-1887

Welten M (1967) Bemerkungen zur paläobotanischen Untersuchung von vorgeschichtlichen Feuchtbodenwohnplätzen und Ergänzungen zur pollenanalytischen Untersuchung von Burgäschisee-Süd. In: Brunnacker K, Heim R, Huber B, Klötzli F, Müller-Beck H, Oertli HJ, Oeschger H, Schmid E, Schweingruber F, Villaret M, Volkart HD, Welten M, Wuthrich M (eds.) Seeberg Burgäschisee-Süd, Teil 4: Chronologie und Umwelt, Verlag Stämpli, Bern

Zürich-Parkhaus Opéra: a Neolithic wetland site

Fig. 1 Zürich Opéra and other important neolithic settlements nearby

Zürich Opéra "off site"

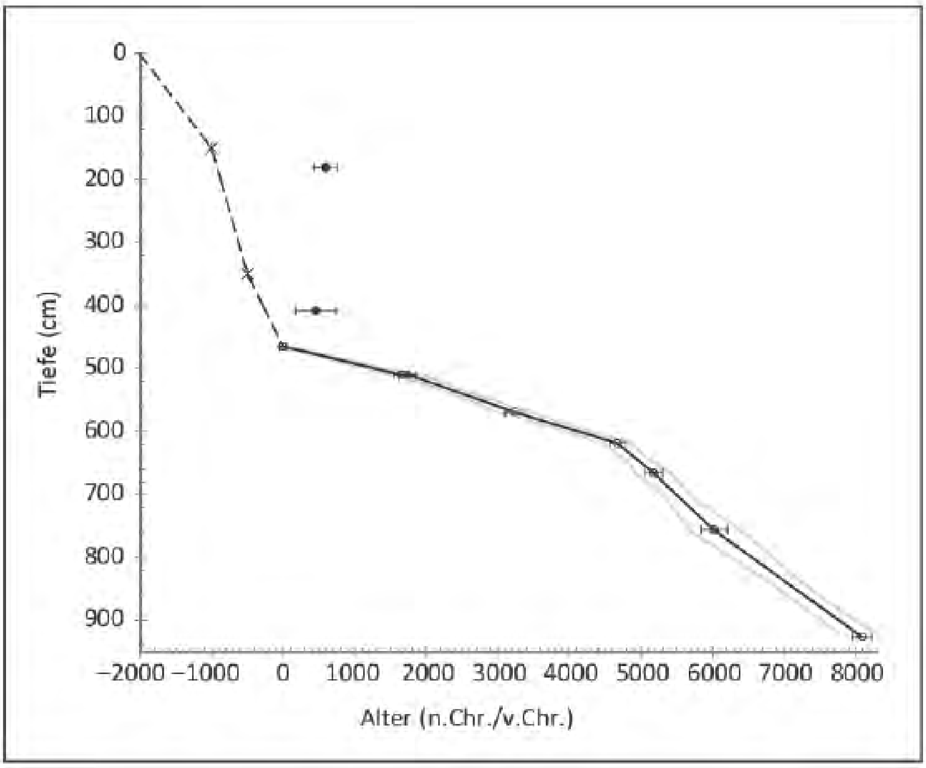

Fig. 2 Depth age model sediment core Zürich Opéra. X= biostratigraphic ages, circle = radiocarbon ages, dots= rejected ages. Dashed line: dating based only on biostratigraphy.

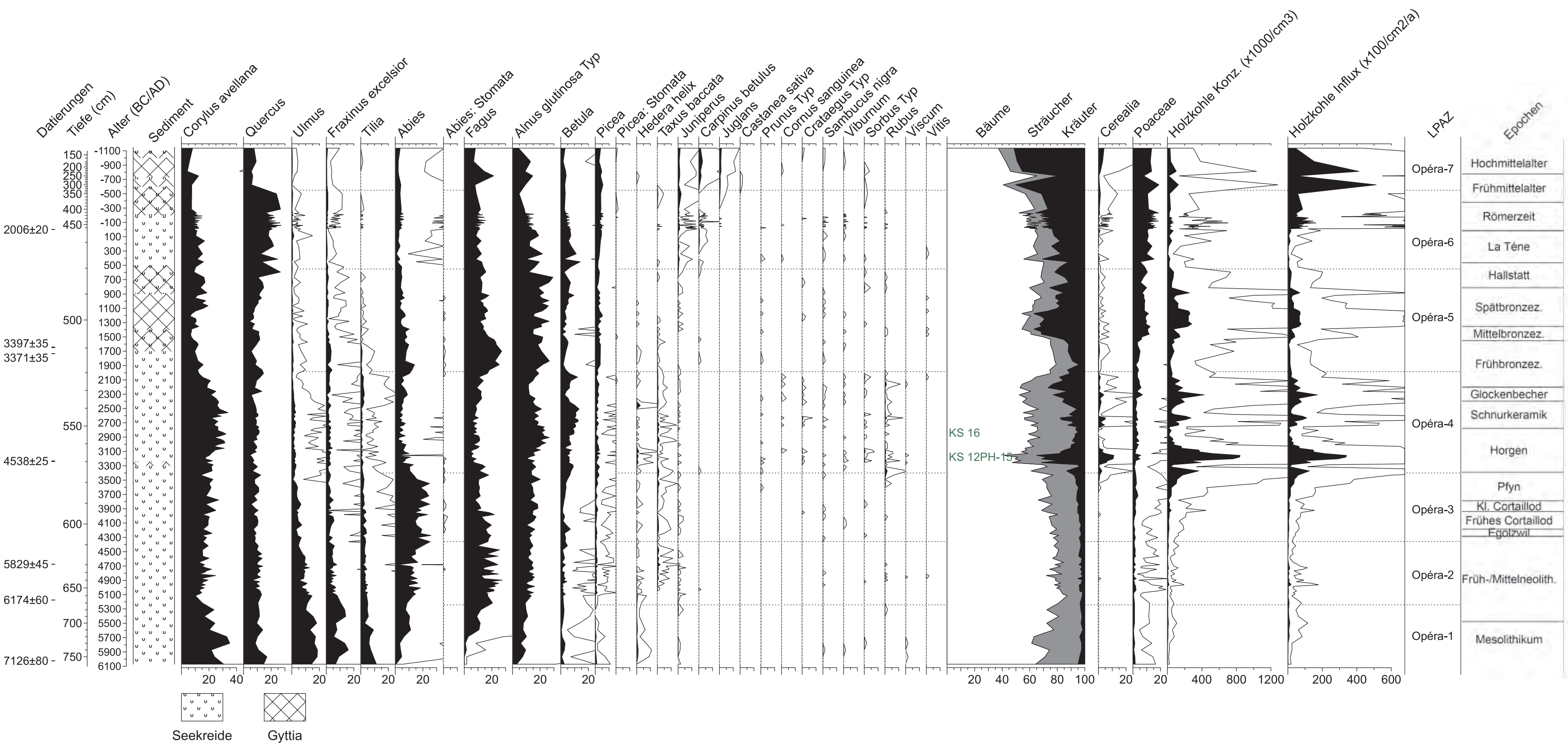

Fig. 3a Zürich Opéra sediment core "off site": pollen percentages of selected arboreal taxa, charcoal concentration and influx

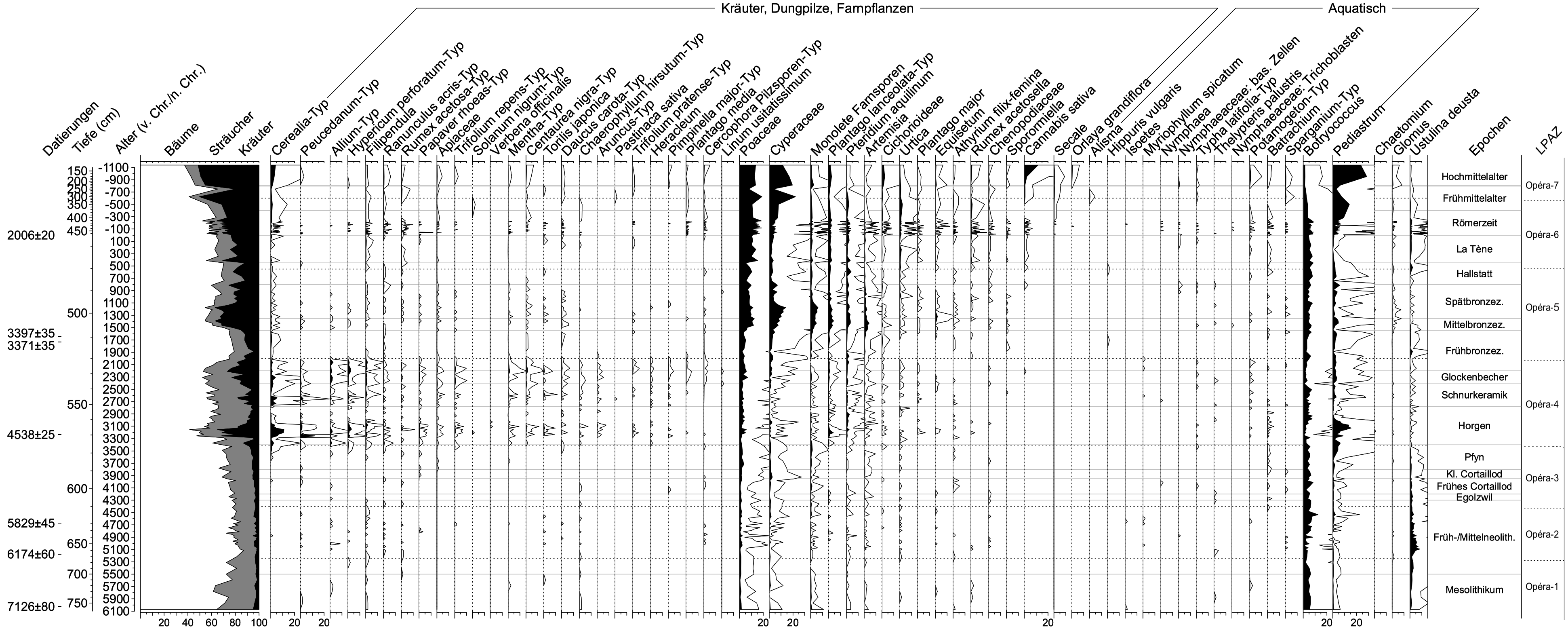

Fig. 3b Zürich Opéra sediment core “off site”: pollen and spore percentages of selected herbaceous and aquatic types, charcoal concentration and influx

Zürich Opéra "on site"

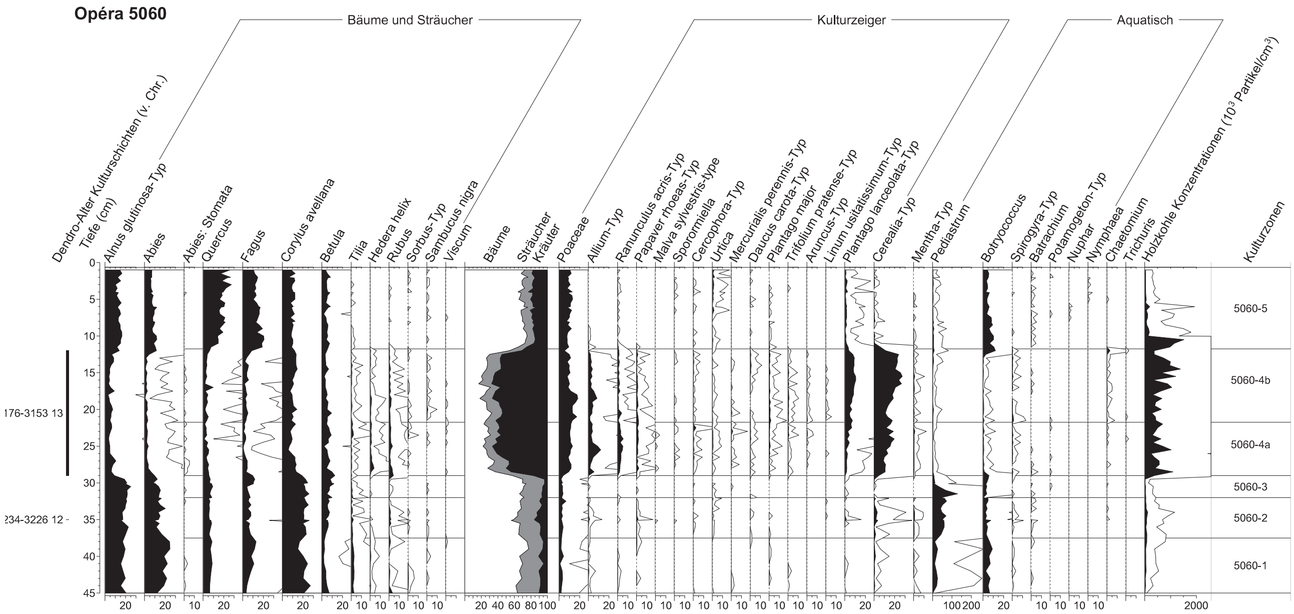

Fig. 4 Pollen and spore percentages and charcoal concentrations "on site", profile 5060

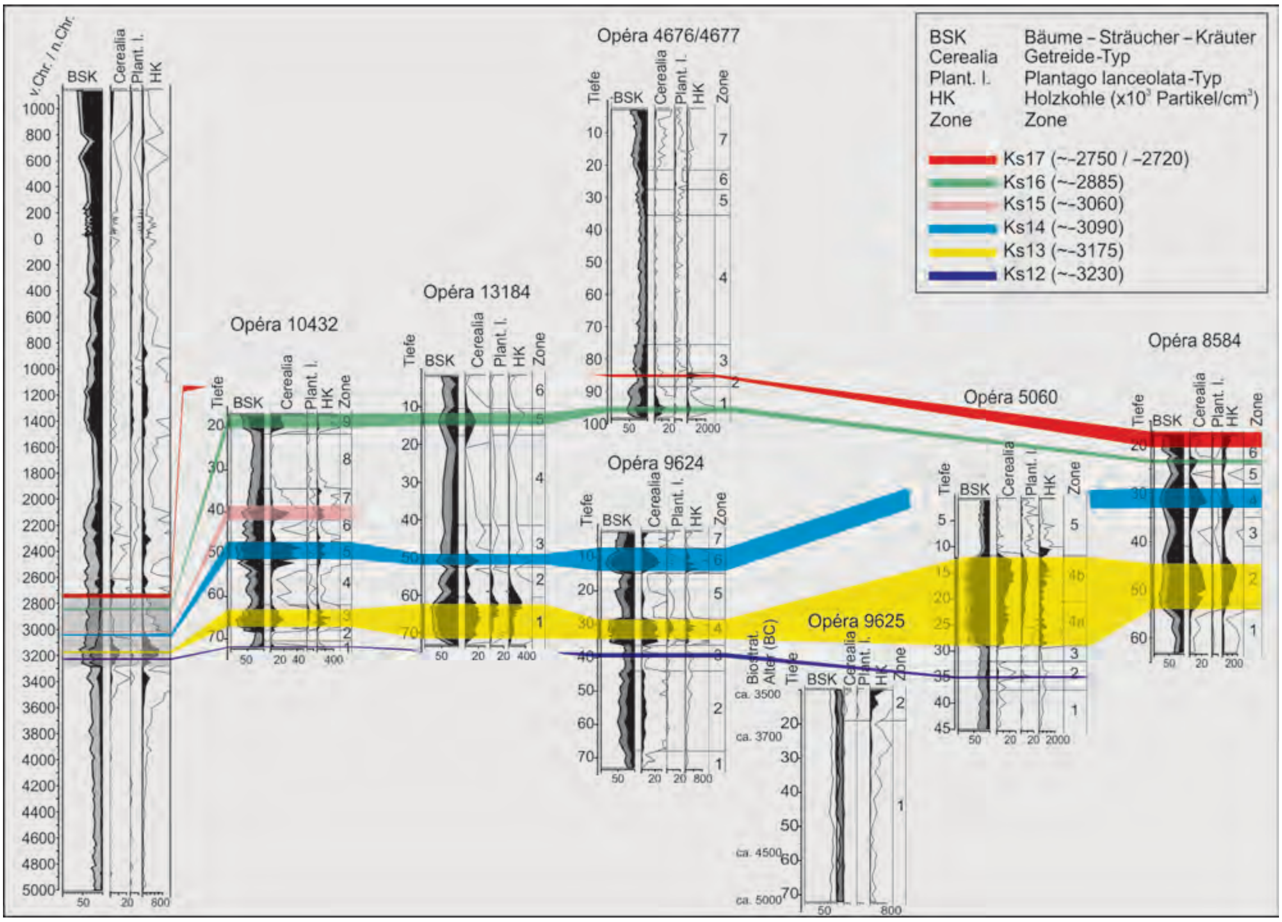

Fig. 5 Overview of pollen percentages and charcoal concentrations of the analysed "on site" profiles

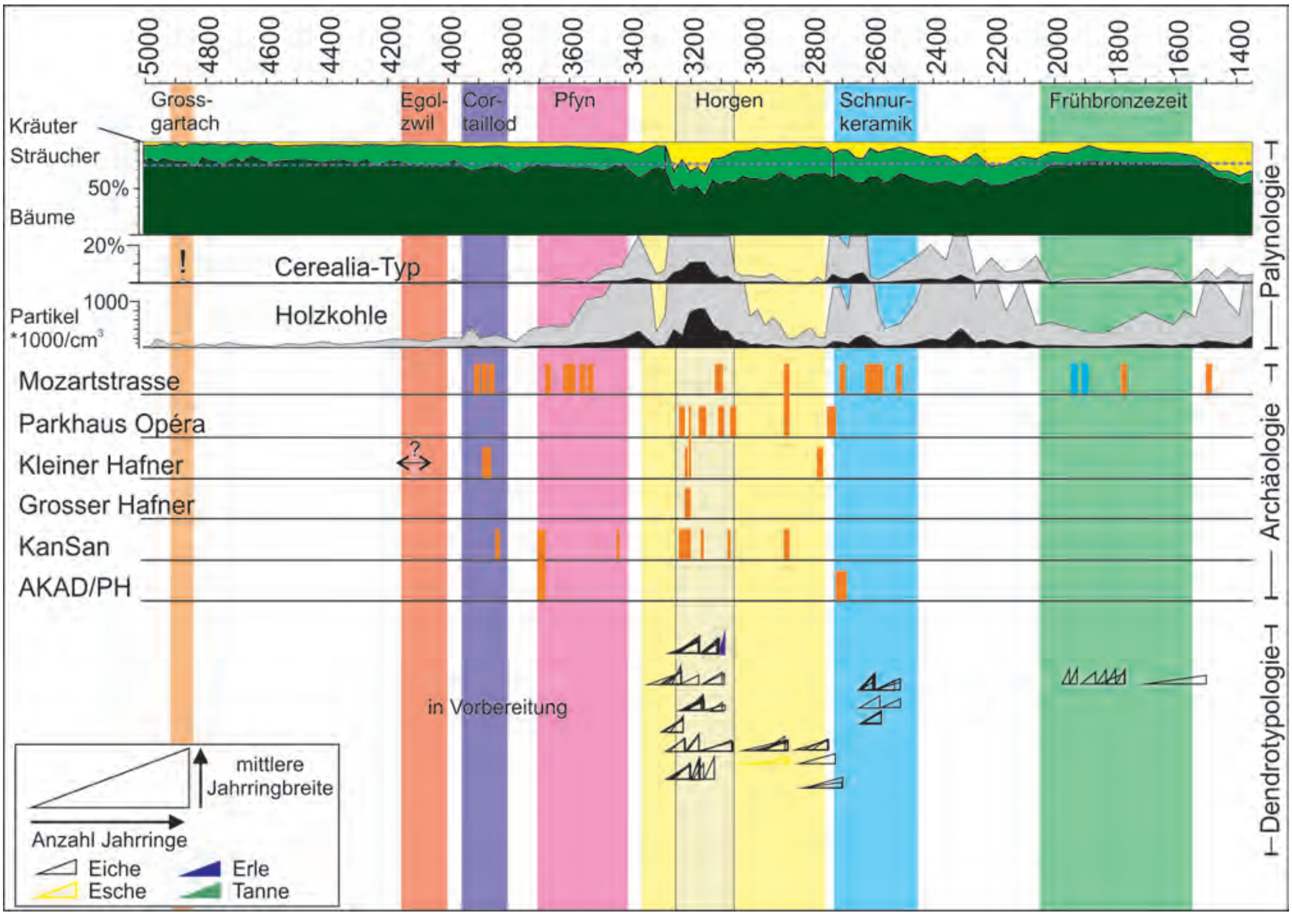

Fig. 6 Synthesis Zürich Opéra (Figure: N. Bleicher)

Chironomid and cladoceran assemblages in the Zürich Opéra sediments

Oliver Heiri, Institute of Plant Sciences and Oeschger Centre for Climate Change Research, University of Bern, oliver.heiri@ips.unibe.ch

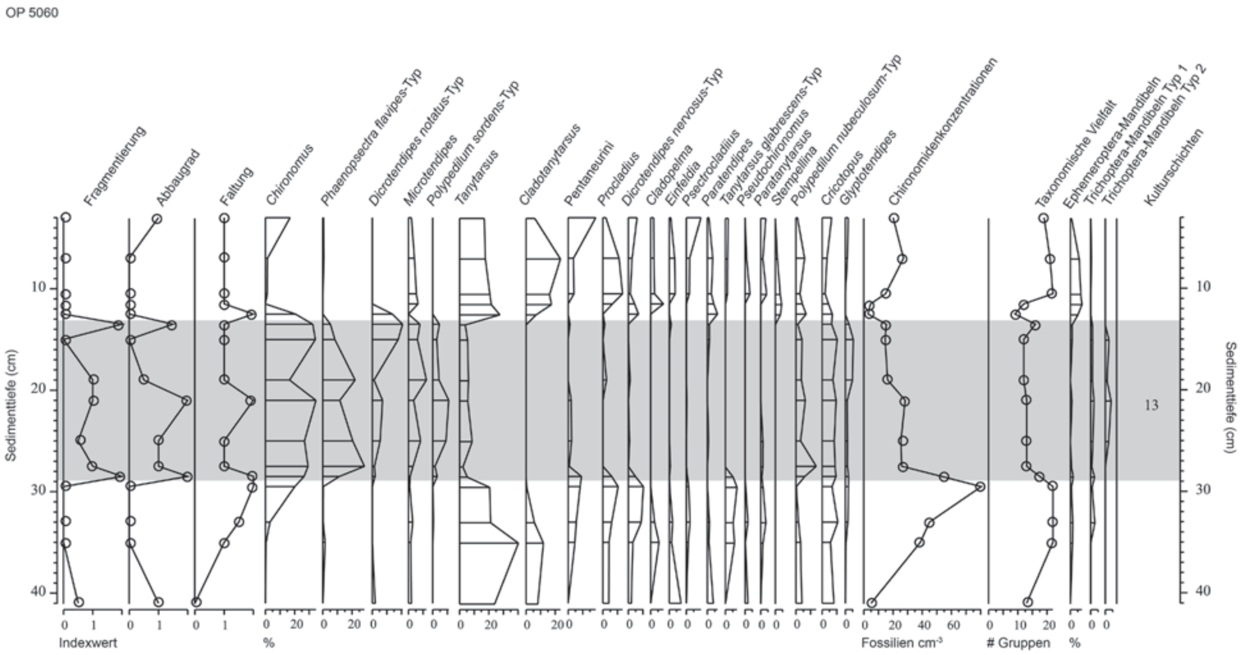

Figure 1. Chironomid assemblages in the sediment profile OP5060 (in percentages), together with chironomid concentrations, taxonomic diversity, relative abundances of ephemeropteran and trichopteran remains (as a percentage of the chironomid abundances). Fragmentation, degradation and folding of fossils is indicated in index scores at the left of the diagram on a semiquantitative scale from 0-5, with high values indicating poor preservation. The grey bar indicates the position of cultural layer 13 in the sequence.

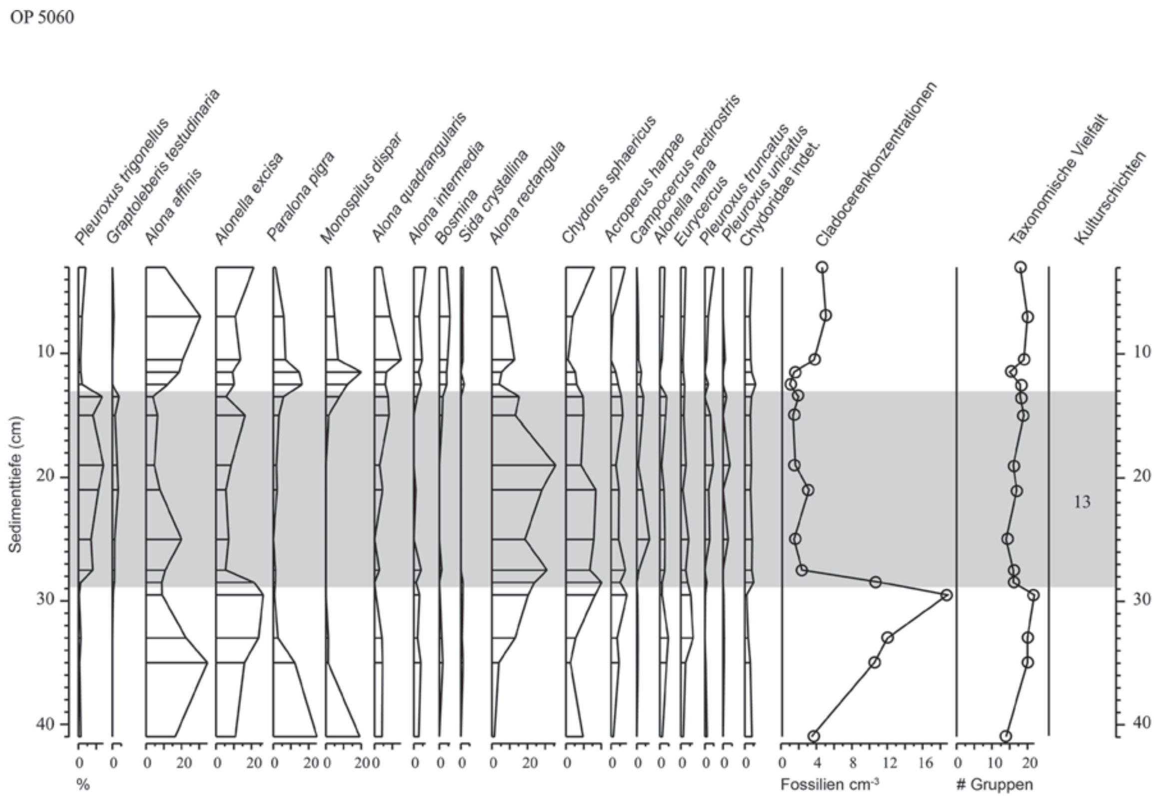

Figure 2. Cladoceran assemblages in the sediment profile OP5060 (in percentages), together with cladoceran concentrations and cladoceran diversity. The grey bar indicates the position of cultural layer 13 in the sequence.

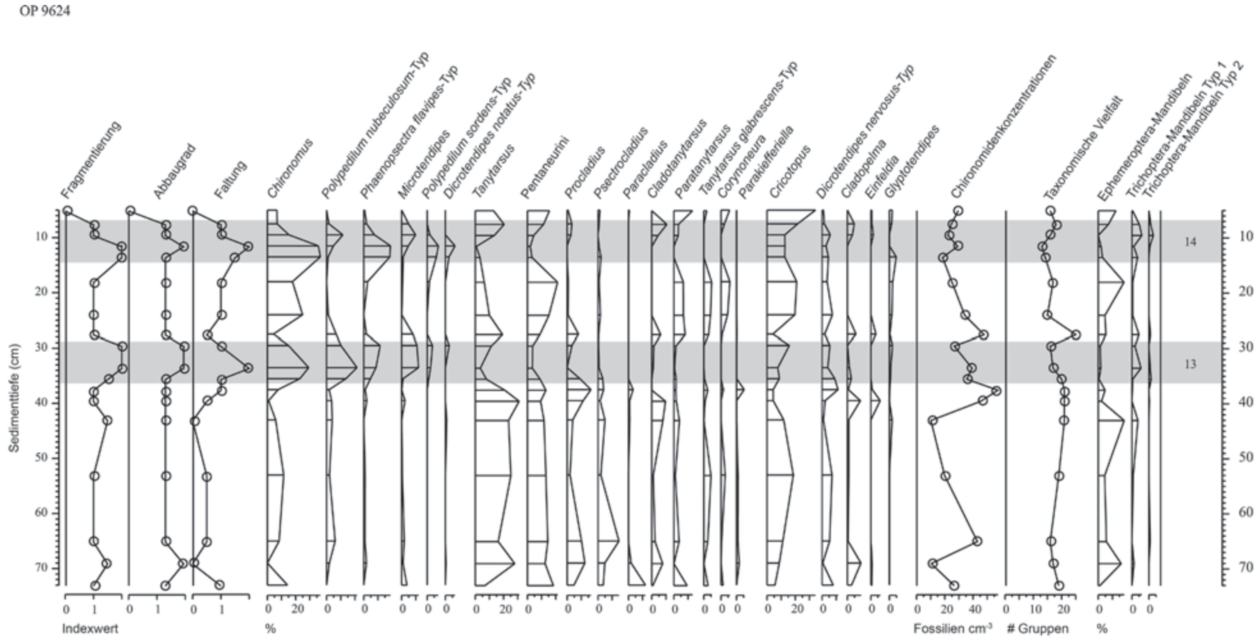

Figure 3. Chironomid assemblages in the sediment profile OP9624 (in percentages), together with chironomid concentrations, taxonomic diversity, relative abundances of ephemeropteran and trichopteran remains (as a percentage of the chironomid abundances). Fragmentation, degradation and folding of fossils is indicated in index scores at the left of the diagram on a semiquantitative scale from 0-5, with high values indicating poor preservation. The grey bars indicate the position of cultural layers 13 and 14 in the sequence.

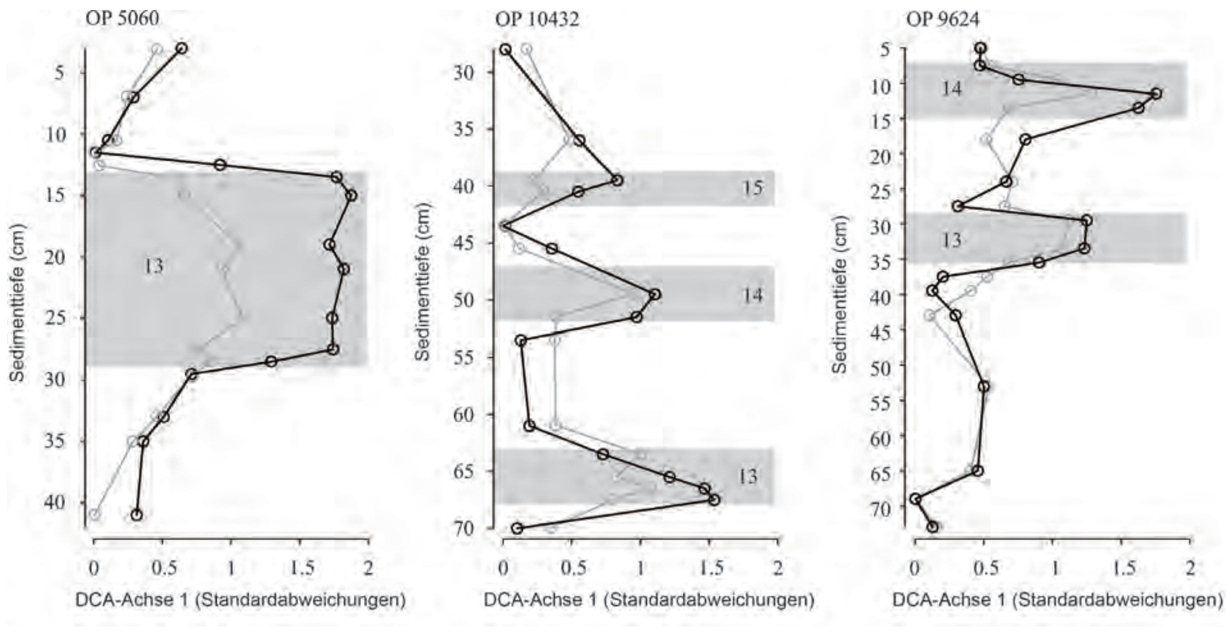

Figure 4. Changes along Detrended Correspondence Analysis (DCA) axis 1 calculated for cladoceran and chironomid assemblages in sediment columns OP5060, OP10432 and OP9624. Grey bars indicate the cultural layers and changes along DCA axis 1 summarize assemblage changes within the columns.

Reference

Heiri, O., Tóth, M., van Hardenbroek, M., Zweifel, N., 2016. Chironomiden- und Cladocerenfossilien. In: Niels Bleicher, Christian Harb, Zürich-Parkhaus Opéra. Eine neolithische Feuchtbodenfundstelle. Band 2. In press.

Wednesday 07.09.2016

8:30 h	Departure to Moossee
9 h	**Moossee**: Introduction to lake-settlement archaeology (Fabian Rey)
9:30 h	Landscape, vegetation and fire history of the Bern area. Neolithic high-resolution multiproxy (Fabian Rey)
11 h	Development of agriculture and dietary change in Switzerland from the Hallstatt to the High Middle Ages (Ryan Hughes)
11.45 h	Lunch at Restaurant Seerose, Moosseedorf
13 h	Departure to Gerzensee
13:30 h	**Gerzensee**: multiproxy evidence of rapid warming and cooling and ecosystem responses (Brigitta Ammann with contributions from Oliver Heiri, Daniele Colombaroli, Lucia Wick and John Birks)
15.15 h	Chitinous invertebrate remains as indicators of past methane availability in lakes (Oliver Heiri)
16 h	Departure to Faulenseemoos
16:30 h	**Faulenseemoos**: Threats to unique natural archives and restoration efforts, first influx calculations worldwide by Max Welten (Willy Tinner, Brigitta Ammann)
17 h	Departure to Lenk im Simmental
18 h	Arrival at Hotel Krone (Lenk im Simmental)
19 h	Dinner at Hotel Krone
21 h	Surprise

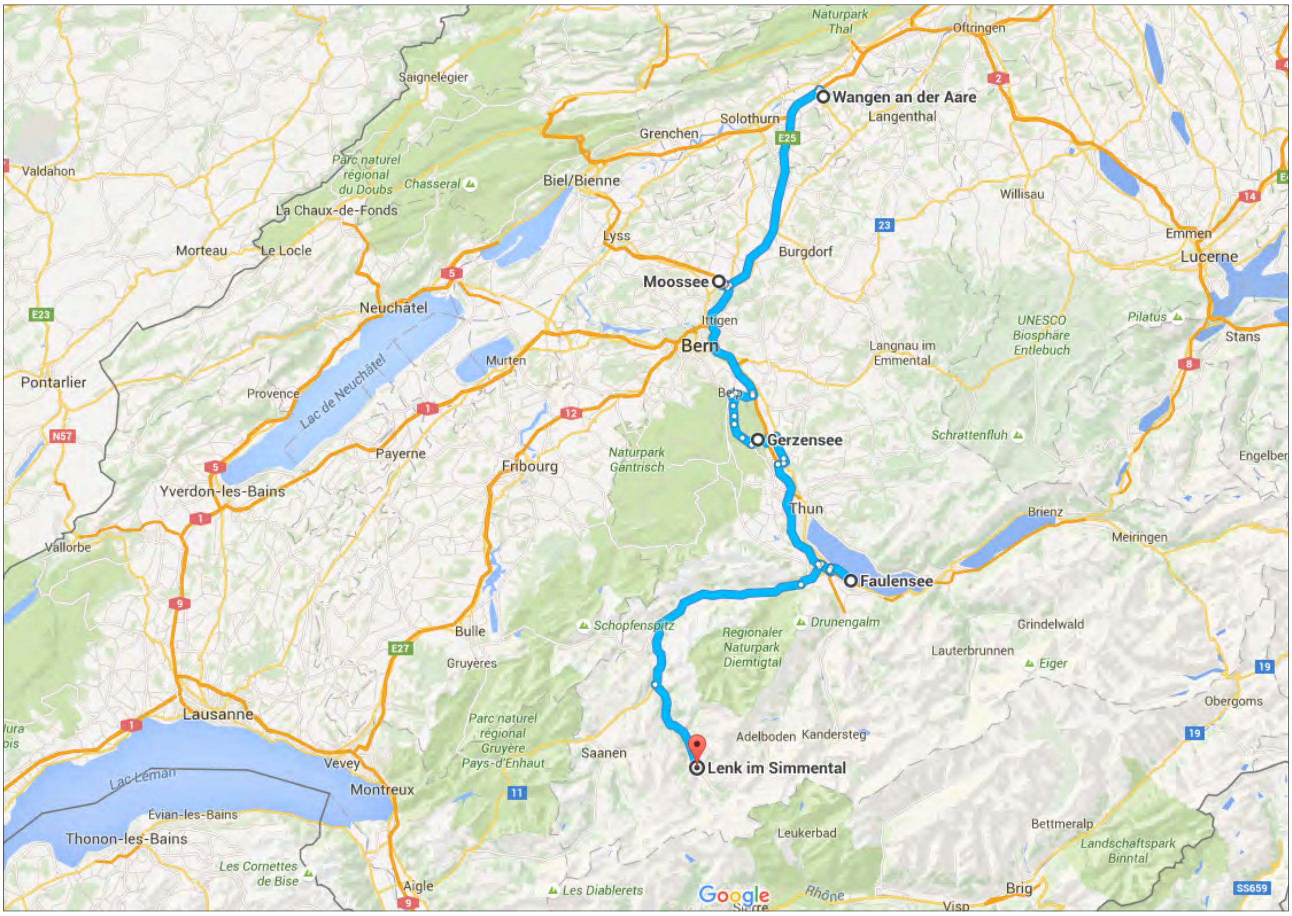

Moossee: local and regional archaeology

Fabian Rey[1,2], Albert Hafner[2,3]

[1] Institute of Plant Sciences, University of Bern, Altenbergrain 21, 3013 Bern, Switzerland

[2] Oeschger Centre for Climate Change Research, University of Bern, Falkenplatz 16, 3012 Bern, Switzerland

[3] Institute of Archaeological Sciences, University of Bern, Muesmattstrasse 27, 3012 Bern, Switzerland

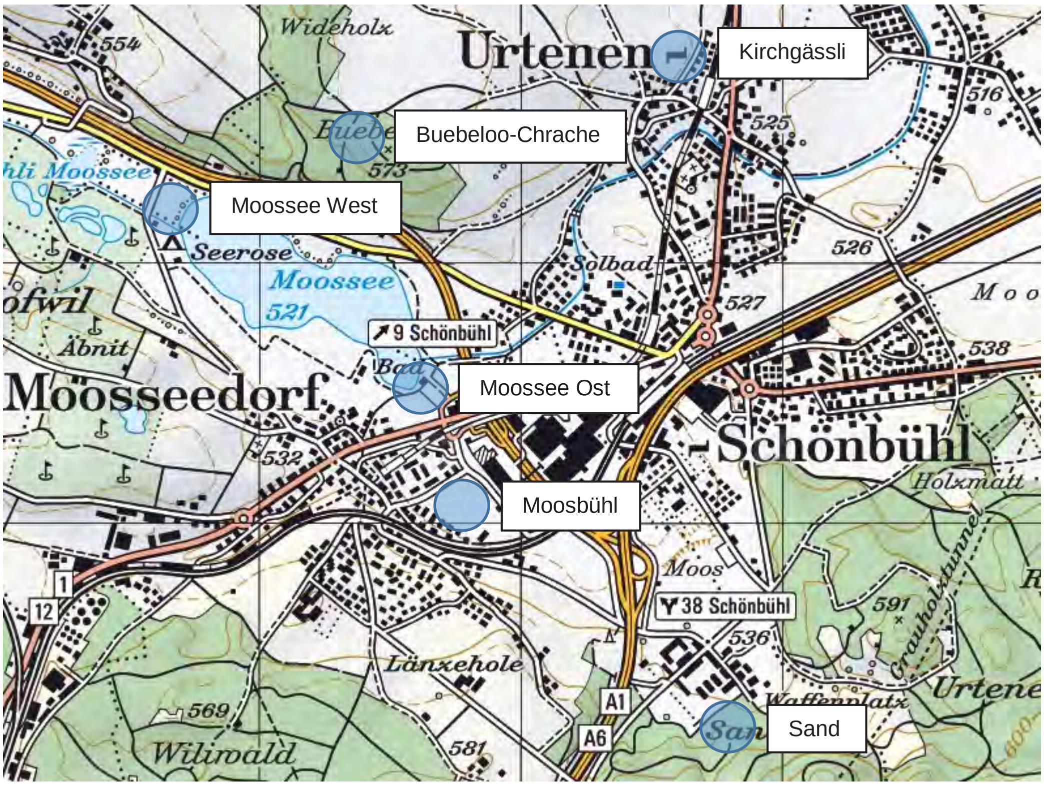

Fig. 1 Archaeological findings in the Moossee region (blue circles). Moosbühl: reindeer hunter camp (c. 13,500 B.C.); Moossee Ost: logboat (c. 4,600 B.C.), pile dwelling (c. 3,800 B.C.); Moossee West: pile dwelling (c. 3,800 B.C.); Kirchgässli: burning hole (probably around 1,300 B.C.); Buebeloo-Chrache/Sand: grave mounds (c. 1,000-500 B.C.) (©swisstopo).

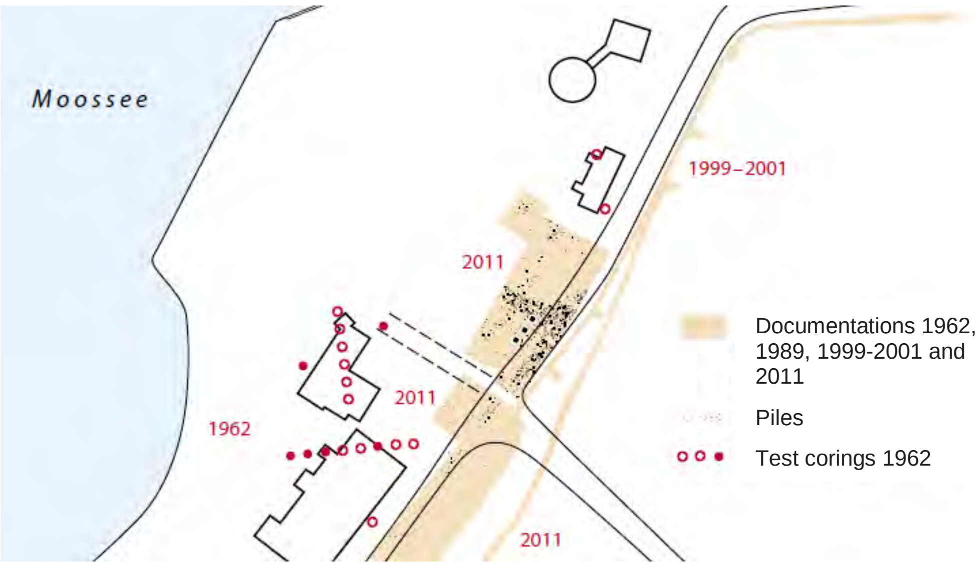

Fig. 2 Excavations and test corings at Moossee Ost (Hafner et al. 2012, modified).

Fig. 3 Logboat from c. 4,600 B.C. (left) and log path from the Corded ware culture (around 2,835 B.C.) (right) found at Moossee Ost during the 2011 excavations. The log path lies on top of a pile dwelling from the Cortaillod period (3,800 B.C.).

Fig. 4 Burning hole (1,300 B.C.?) excavated at Kirchgässli and gold jewellery (Hallstatt c. 1,000-500 B.C.) found in one of the grave mounds.

Reference

Hafner A, Harb C, Amstutz M, Francuz J, Moll-Dau F (2012) Moosseedorf, Moossee Oststation, Strandbad – Strandbadneubau, Pfahlbauten und das älteste Boot der Schweiz. Jahrbuch des Archäologischen Dienstes des Kantons Bern 71-77

Moossee: landscape, vegetation and fire history of Bern area, the capital of Switzerland

Fabian Rey[1,2], Erika Gobet[1,2,] Adrian Gilli[3], Albert Hafner[2,4], Willy Tinner[1,2]

[1] Institute of Plant Sciences, University of Bern, Altenbergrain 21, 3013 Bern, Switzerland

[2] Oeschger Centre for Climate Change Research, University of Bern, Falkenplatz 16, 3012 Bern, Switzerland

[3] Geological Institute, ETH Zurich, Sonneggstrasse 5, 8092 Zurich, Switzerland

[4] Institute of Archaeological Sciences, University of Bern, Muesmattstrasse 27, 3012 Bern, Switzerland

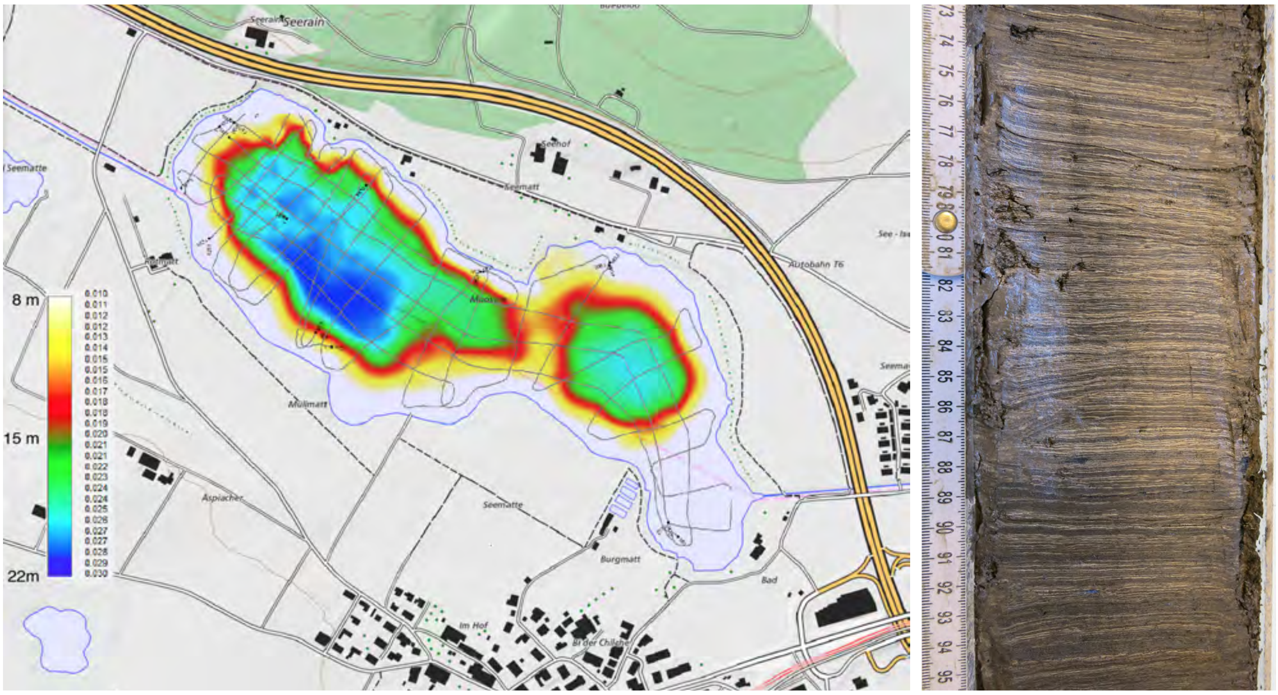

Fig. 1 Seismic map of Moossee (left) (©swisstopo). The coring took place in the smaller basin close to the village. Part of the laminated sediments of Moossee (Neolithic, c. 5800 cal. B.P.) (right).

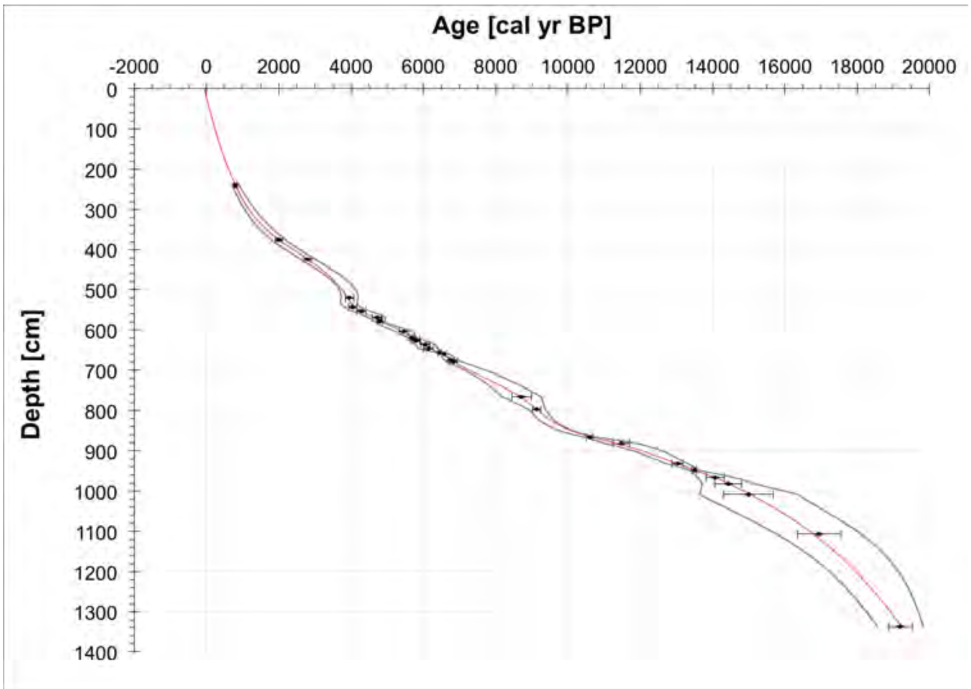

Fig. 2 Age-depth-model of Moossee: Black dots show calibrated ages of terrestrial plant macrofossils with 2 sigma error bars (IntCal13, Reimer et al. 2013). The uppermost three dots are biostratigraphically dated. The red line is the modelled chronology (Smooth spline 0.38 with the program clam 2.2, Blaauw 2010). The grey lines indicate the 95% confidence envelope of the generalized mixed effect regression (GAM, Heegaard et al. 2005).

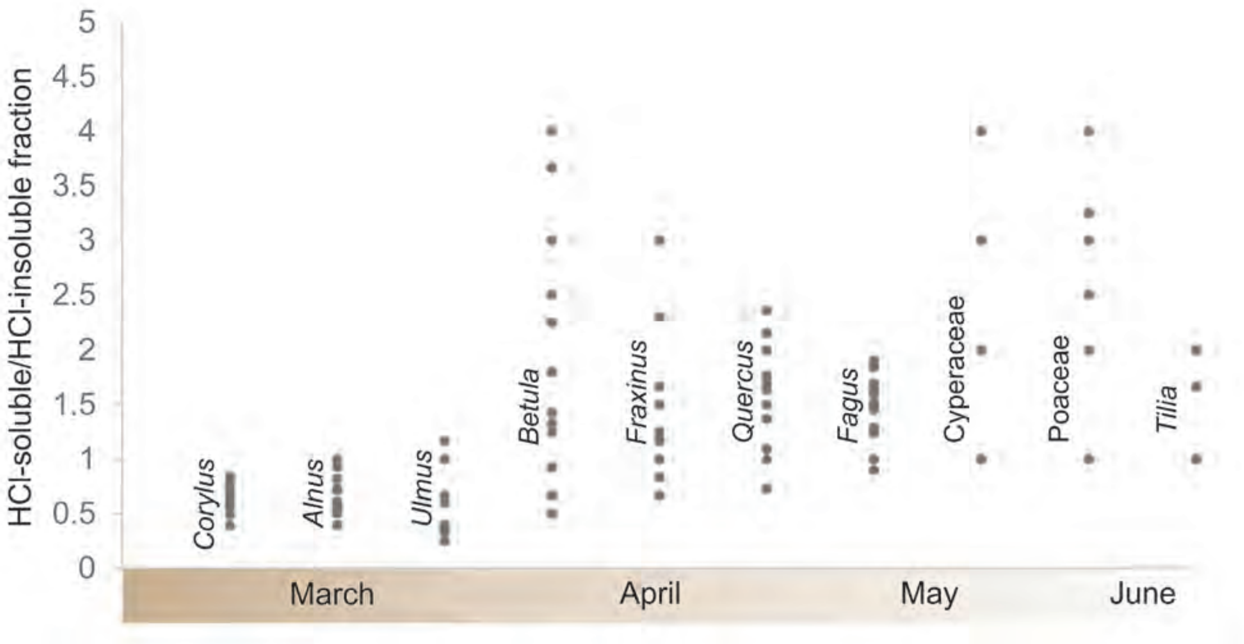

Fig. 3 Ratio of the HCl soluble (Ca-rich) to the HCl insoluble (organic-rich) sediment fraction of 13 laminated samples (pollen sum: 200 terrestrial pollen grains per fraction) along a transect (from 700 cm to 354.5 cm, approx. every 30 cm). The taxa are grouped according to the time of their flowering (Leuschner 1974; Leuschner 1991; Lauber et al. 2014).

References

Blaauw M (2010) Methods and code for 'classical' age-modelling of radiocarbon sequences. Quat Geochronol 5:512–518

Heegaard E, Birks HJB, Telford RJ (2005) Relationships between calibrated ages and depth in stratigraphical sequences: an estimation procedure by mixed-effect regression. Holocene 15:4, 612-618

Lauber K, Wagner G, Gygax A (2014) Flora Helvetica, 5th edn. Haupt/Stuttgart, Bern/Wien

Leuschner R (1974) Pollen calendars for Switzerland. In: Charpin J, Surinyach R, Frankland AW (eds) Atlas of European allergenic pollens. Sandoz Editions, pp 193-199

Leuschner R (1991) Comparison of airborne pollen levels in Switzerland at 4 recording stations in Davos, Lucerne, Nyon and Basle during 1989. Int J Biometeorol 35:2, 71-75

Reimer P J, Bard E, Bayliss A, Beck JW, Blackwell PG, Bronk Ramsey C, Grootes PM, Guilderson TP, Haflidason H, Hajdas I, Hattž C, Heaton TJ, Hoffmann DL, Hogg AG, Hughen KA, Kaiser, KF, Kromer B, Manning SW, Niu M, Reimer RW, Richards DA, Scott EM, Southon JR, Staff RA, Turney CSM, van der Plicht J (2013) IntCal13 and Marine13 Radiocarbon Age Calibration Curves 0-50,000 Years cal BP. Radiocarbon 55:4, 1869-1887

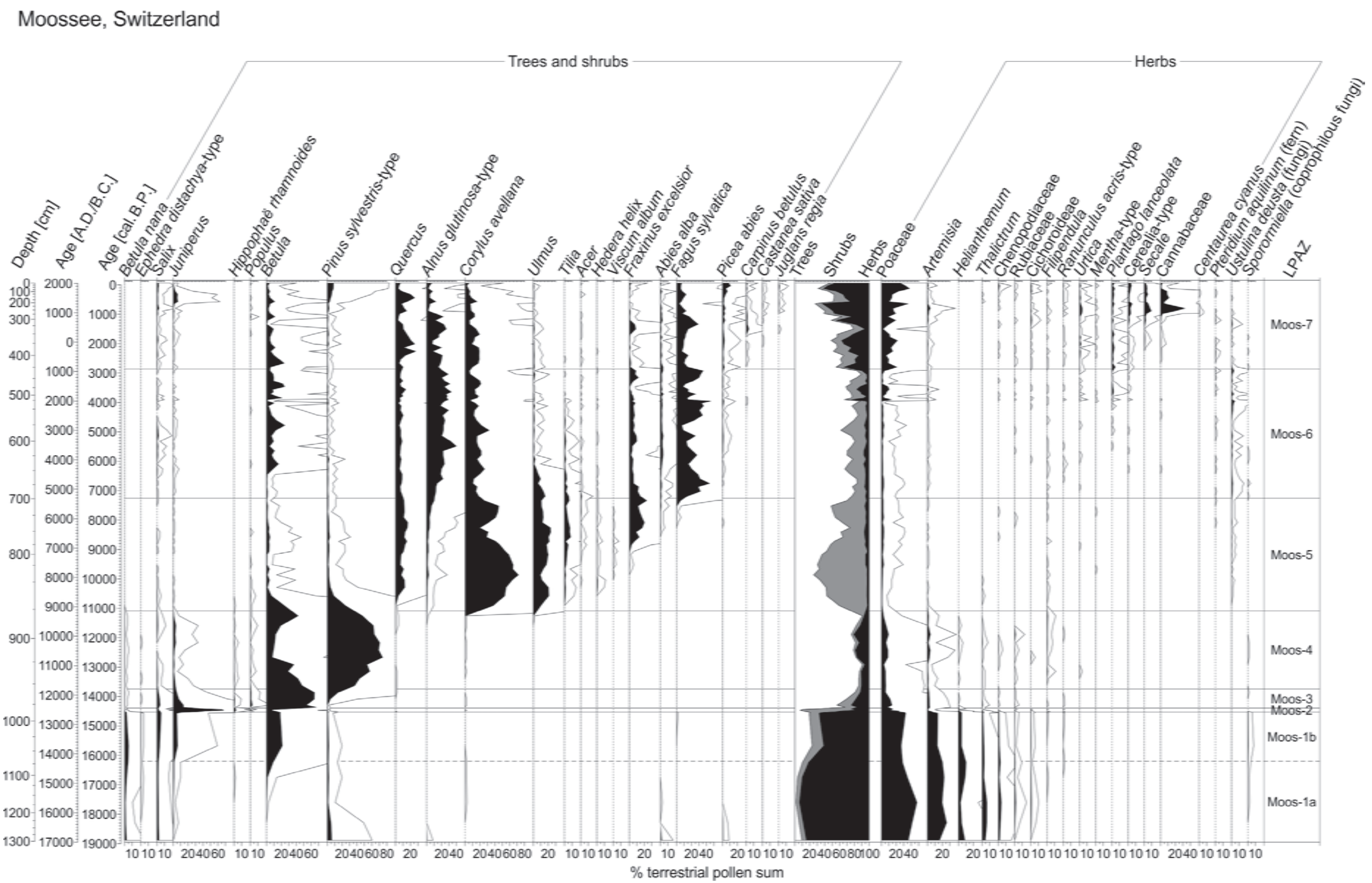

Fig. 4 Percentages of selected pollen types, fern spores, fungi spores and coprophilous fungi spores of Moossee. Empty curves are the 10x exaggerations. LPAZ = local pollen assemblage zones.

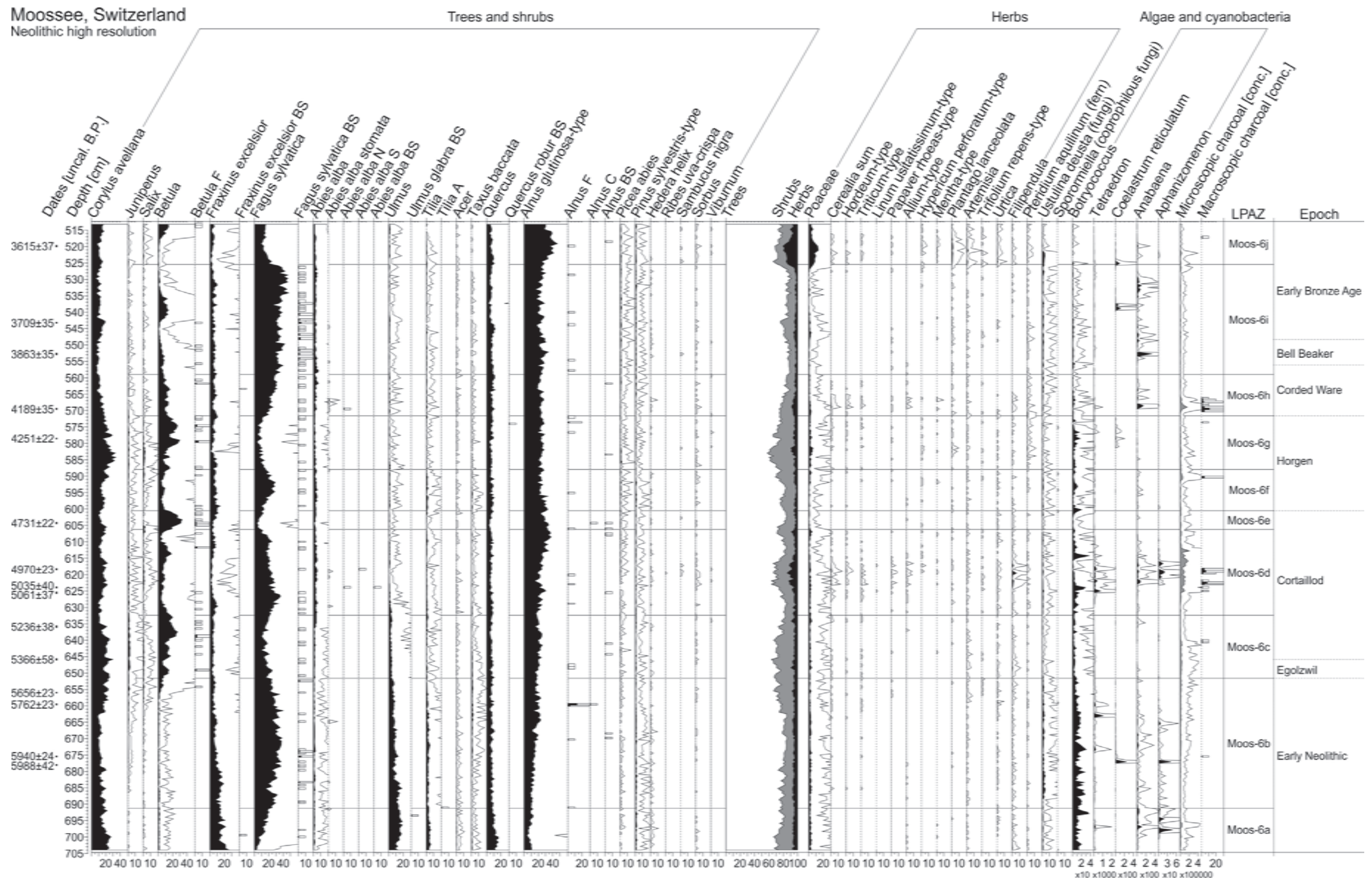

Fig. 5 Percentages of selected pollen types, fern spores, coprophilous fungi spores, fungi spores, green algae and cyanobacteria, microscopic charcoal concentrations, plant macrofossils concentrations as well as macroscopic charcoal concentrations (particles >200µm) of the Neolithic high resolution at Moossee. Empty curves are the 10x exaggerations. LPAZ = local pollen assemblage zones. LST = Laacher See tephra. A = anther, BS = bud scale, C = cone, CS = cone scale, F = fruit, FS = fruit scale, N = needle, S = seed.

Agricultural Development and Dietary Change in Switzerland from the Hallstatt (800 B.C./2750 BP) to the Rise of the Carolingian Dynasty (A.D. 754/1196 BP)

Ryan E. Hughes

ARVE Research Group, Institute of Earth Surface Dynamics, University of Lausanne, Switzerland

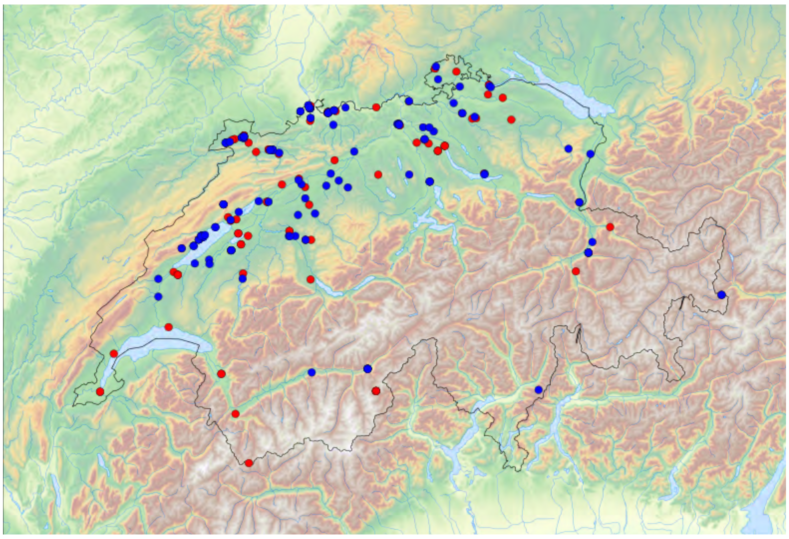

Figure 1. Sites studied. Blue = Botanical; Red = Faunal

The modern Swiss agricultural landscape has its roots buried deep in the ancient past. The phase of agricultural development spanning from the Iron Age, beginning with the Hallstatt period in 800 B.C. (2750 BP), to the last of the Merovingian dynasty in A.D. 754 (1196 BP), was one of the most vibrant and important periods in the evolution of the landscape and agriculture of Switzerland. This phase, which begins with independent Iron Age tribes, encompasses the first large-scale conquest of the land of Switzerland, the incorporation of the region into the Roman Empire and the transition of control to the Frankish Kings which laid the foundation in the Early Middle Ages for the modern agricultural landscape. This study explores these developments in the three topographical zones of Switzerland (the Jura Massif and northwestern Switzerland, the Plateau and the Alps) through the archaeological record by combining archaeobotanical and archaeozoological remains recovered from excavations with the results of pollen studies and climatological research to acquire a holistic view of ancient agriculture and dietary preference. During the Hallstatt period (800-480 B.C./2750-2430 BP), the three topographical zones had similar agricultural activities, however, beginning in the La Tène Period (480-13 B.C./2430-1963 BP) these show a significant divergence that further intensifies with the arrival of the Romans and persists after the transition of power to the Frankish Kings in the late 5th century A.D. (c. 1474 BP). The arrival of the Romans in the late 1st century B.C. had an immediate impact with the introduction of new crops into local cultivation alongside advanced horticulture, viticulture and animal husbandry practices, as well as a lasting presence in Swiss agriculture due to the persistence of many of these crops after the removal of Roman influence. Concurrently, the cultivation of Iron Age crops, primarily hardy hulled wheats and barley, continued throughout the Roman period, particularly at sites dominated by Celtic peoples, with Roman influence being most felt at higher status sites such as the capital at Avenches, the colony of Augst and the major military installation at Windisch. Roman influence on meat consumption is demonstrated by elevated levels of swine and chickens with a continuation of the dominance of cattle at predominately Celtic sites in the Jura and Plateau alongside elevated levels of sheep and goats at Alpine sites in the Rhône Valley. By combining archaeobotany, archaeozoology and palynology with climatological studies, this work shows that the arrival of the Romans had an immediate impact during the first centuries A.D., aided by favourable climatic conditions. After the removal of direct Roman influence and increasing climatic instability beginning in the mid-3rd century A.D., many of the crops, fruits and garden plants persisted with the arrival of Frankish and Germanic peoples into the region alongside a resurgence in the prevalence of cereal crops cultivated during the Iron Age.

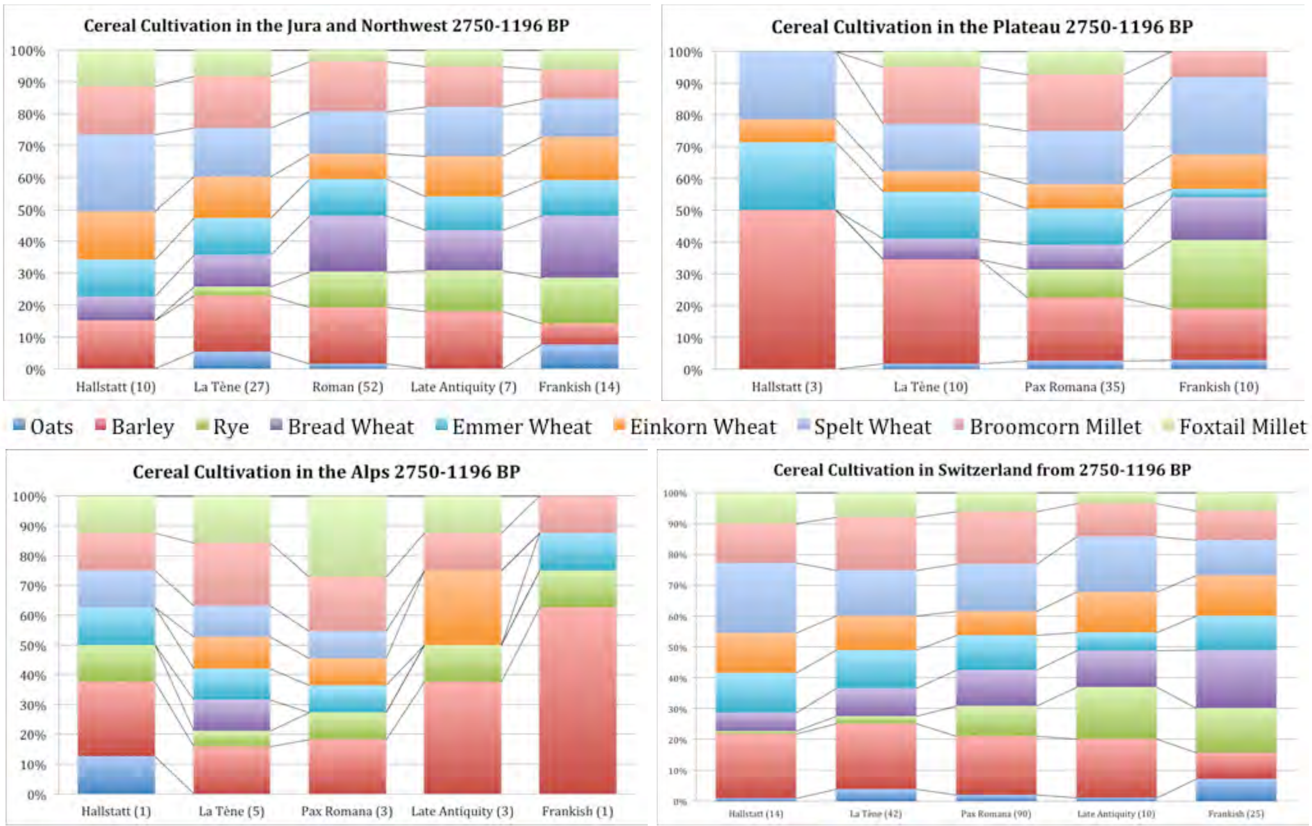

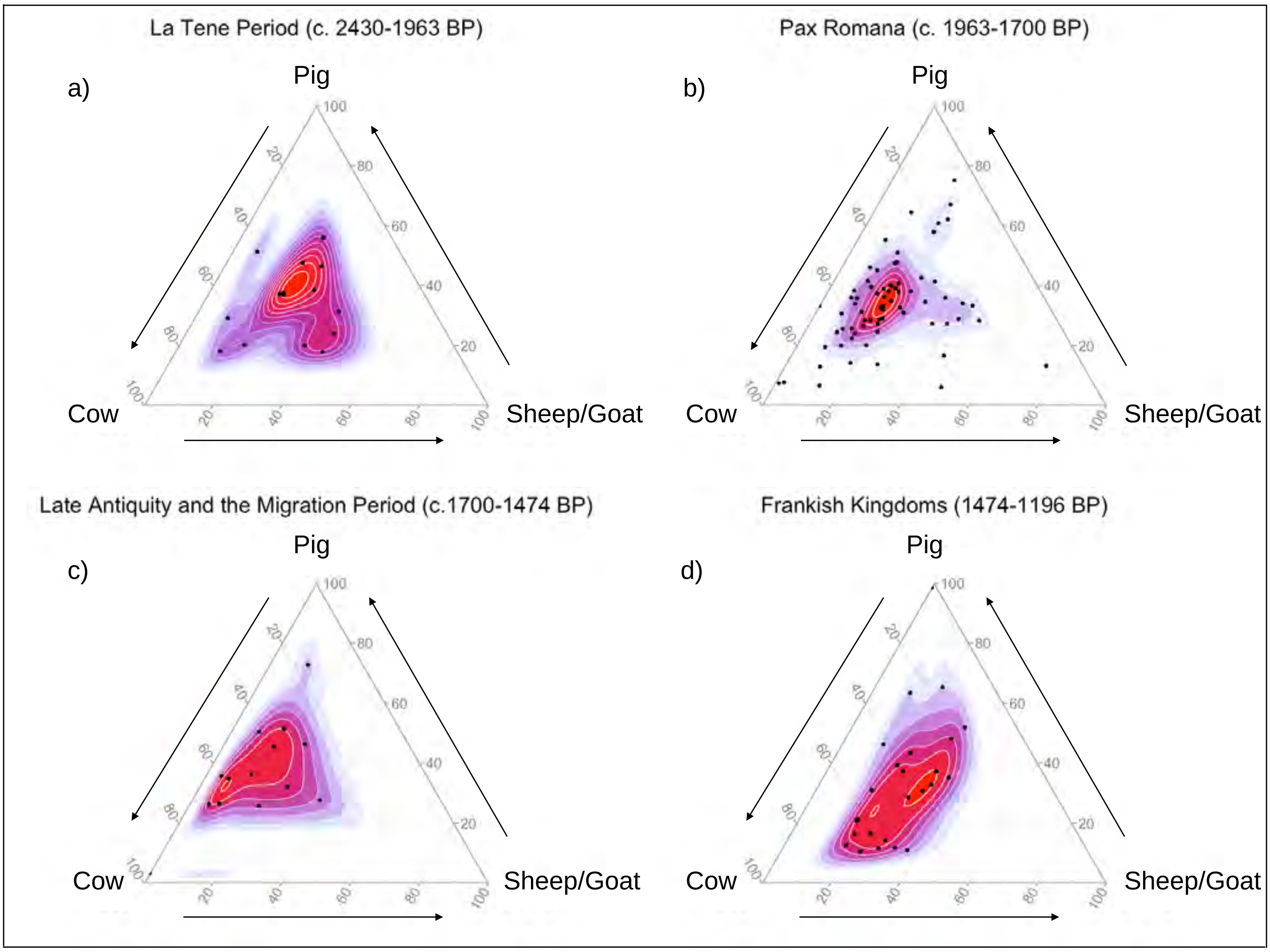

Figure 3. Faunal remains (Number of Identified Specimens) from the Jura, Switzerland.

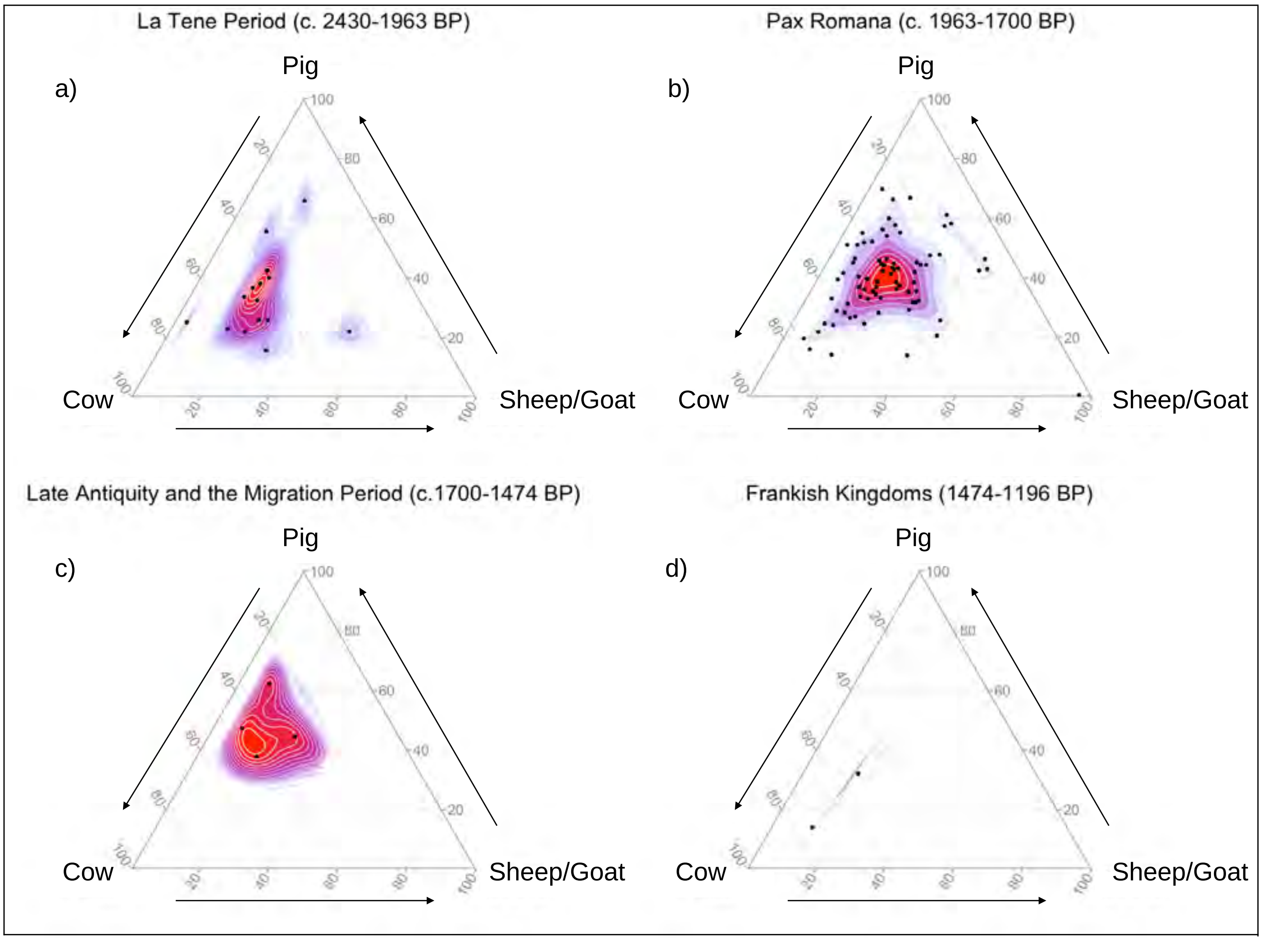

Figure 4. Faunal remains (Number of Identified Specimens) from the Plateau, Switzerland.

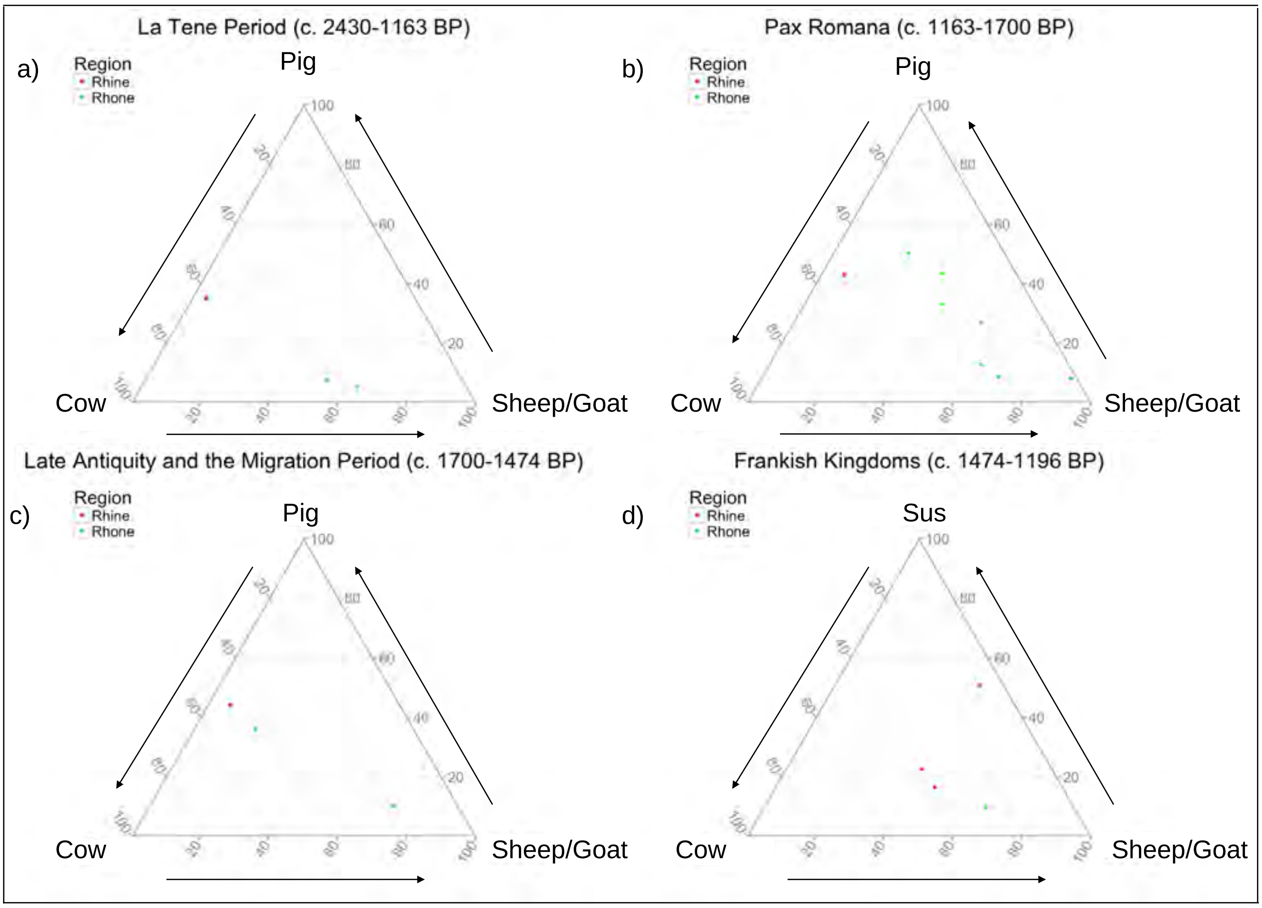

Figure 5. Faunal remains (Number of Identified Specimens) from the Alps, Switzerland.

Page 3 of 3

Rapid summer temperature changes during Termination 1a: high-resolution multi-proxy climate reconstructions from Gerzensee (Switzerland)

André F. Lotter [a,*], Oliver Heiri [a,c], Stephen Brooks [b], Jacqueline F.N. van Leeuwen [c], Ulrich Eicher [d], Brigitta Ammann [c]

[a] Institute of Environmental Biology, Palaeoecology, Laboratory of Palaeobotany and Palynology, Utrecht University, Budapestlaan 4, 3584 CD Utrecht, The Netherlands
[b] Dept. of Entomology, Natural History Museum, Cromwell Road, London SW7 5BD, UK
[c] Institute of Plant Sciences, University of Bern, Altenbergrain 21, CH-3013 Bern, Switzerland, and Oeschger Centre for Climate Change Research, Zähringerstrasse 25, CH-3012 Bern, Switzerland
[d] Zelgweg 10, CH-3132 Riggisberg, Switzerland

QSR 2012 36:103-113

ARTICLE INFO

Article history:
Received 5 February 2010
Received in revised form
1 June 2010
Accepted 10 June 2010
Available online 7 July 2010

ABSTRACT

Quantitative July temperature reconstructions using fossil chironomid and pollen data have been carried out with a high temporal resolution for the Termination 1a and the late-glacial Interstadial (ca 15 000–13 000 cal years BP) on a sediment core from Gerzensee (Switzerland). The biota-based July temperature reconstructions show a rapid warming of 4–5 °C (pollen) and 2–3 °C (chironomids) at Termination 1a (i.e. the onset of the late-glacial Interstadial, ca 14 650 cal. BP). These temperature changes go parallel with a shift of more than 3‰ in a high-resolution stable oxygen isotope record measured on bulk carbonates from the same core, also indicating a substantial and rapid warming.

Pollen-inferred July temperatures follow the shape of the oxygen-isotope record with a generally decreasing trend of ca 2 °C throughout the Interstadial, showing even minor cold oscillations of 0.5–1 °C in July temperature recorded in many central European sites (e.g. Aegelsee and Gerzensee Oscillations) and the Greenland ice cores (e.g. GI-1d and GI-1b). Chironomid-inferred summer temperatures, however, show a gradual increase of ca 2–3 °C throughout the Interstadial, interrupted by some cold oscillations (e.g. GI-1b) of 0.5–1 °C.

The reconstructions based on both proxies are in agreement with comparable studies in the Jura Mountains and the Alps. Given the close correlation between the oxygen isotope record and the pollen-inferred temperatures, the discrepancies between the two biota-specific July temperature inferences could be explained by the higher sensitivity of vegetation to changes in seasonality and precipitation, whereas aquatic organisms such as chironomids are more responsive to summer season conditions.

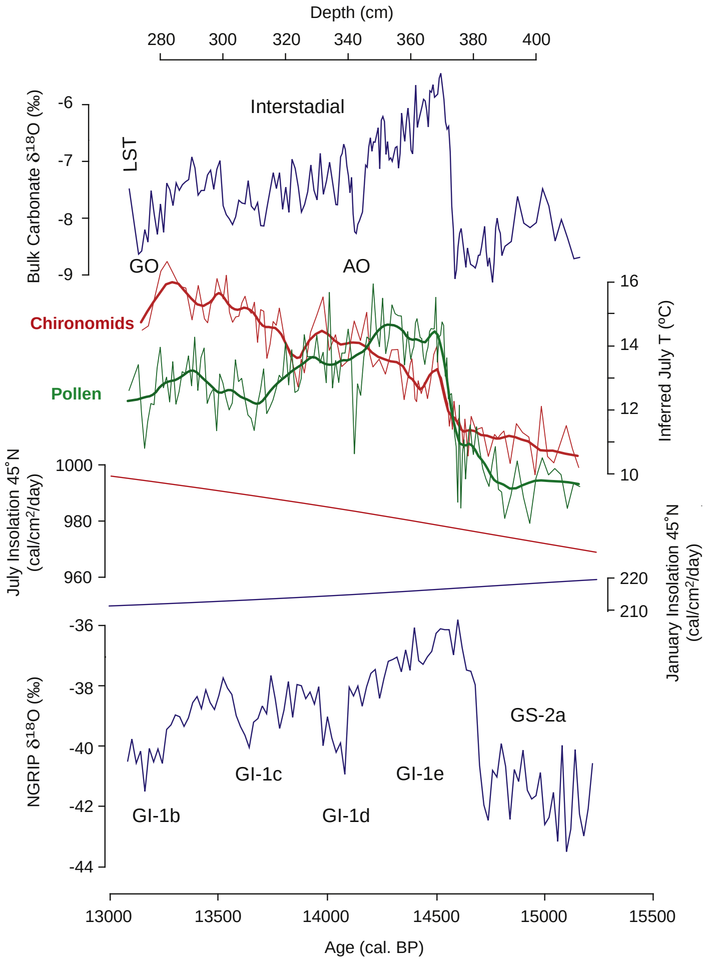

Fig. 4. Comparison of Gerzensee bulk carbonate stable oxygen isotopes (LST: Laacher See Tephra; AO: Aegelsee Oscillation; GO: Gerzensee Oscillation, Lotter et al., 1992), chironomid- and pollen-inferred July air temperatures (all on a depth scale), with January and July insolation at 45° N (Laskar et al., 1993), and the Greenland NGRIP stable oxygen isotope curve (Rasmussen et al., 2006) using the INTIMATE terminology (Björck et al., 1998) for the different phases (the latter three on an age scale).

High-resolution late-glacial chronology for the Gerzensee lake record (Switzerland): δ^{18}O correlation between a Gerzensee-stack and NGRIP

Ulrike J. van Raden [a,*], Daniele Colombaroli [b], Adrian Gilli [a], Jakob Schwander [c], Stefano M. Bernasconi [a], Jacqueline van Leeuwen [d], Markus Leuenberger [c], Ueli Eicher [c]

[a] Geological Institute, ETH Zurich, Sonneggstrasse 5, 8092 Zürich, Switzerland
[b] Oeschger Centre for Climate Change Research & Institute of Plant Sciences, University of Bern, Altenbergrain 21, 3013 Bern, Switzerland
[c] Physics Institute, University of Bern, Sidlerstrasse 5, 3012 Bern, Switzerland
[d] Institute of Plant Sciences, University of Bern, Altenbergrain 21, 3013 Bern, Switzerland

PPP 2013 391: 13-24

ARTICLE INFO

Article history:
Received 23 January 2012
Received in revised form 17 May 2012
Accepted 19 May 2012
Available online 29 May 2012

Keywords:
Climate oscillations
Bølling/Allerød
Stable isotopes
Authigenic calcite
Monte Carlo simulation

ABSTRACT

Oxygen-isotope variations were analyzed on bulk samples of shallow-water lake marl from Gerzensee, Switzerland, in order to evaluate major and minor climatic oscillations during the late-glacial. To highlight the overall signature of the Gerzensee δ^{18}O record, δ^{18}O records of four parallel sediment cores were first correlated by synchronizing major isotope shifts and pollen abundances. Then the records were stacked with a weighting depending on the differing sampling resolution. To develop a precise chronology, the δ^{18}O-stack was then correlated with the NGRIP δ^{18}O record applying a Monte Carlo simulation, relying on the assumption that the shifts in δ^{18}O were climate-driven and synchronous in both archives. The established chronology on the GICC05 time scale is the basis for (1) comparing the δ^{18}O changes recorded in Gerzensee with observed climatic and environmental fluctuations over the whole North Atlantic region, and (2) comparing sedimentological and biological changes during the rapid warming with smaller climatic variations during the Bølling/Allerød period. The δ^{18}O record of Gerzensee is characterized by two major isotope shifts at the onset and at the termination of the Bølling/Allerød warm period, as well as four intervening negative shifts labeled GI-1e2, d, c2, and b, which show a shift of one third to one fourth of the major δ^{18}O shifts at the beginning and end of the Bølling/Allerød. Despite some inconsistency in terminology, these oscillations can be observed in various climatic proxies over wide regions in the North Atlantic region, especially in reconstructed colder temperatures, and they seem to be caused by hemispheric climatic variations.

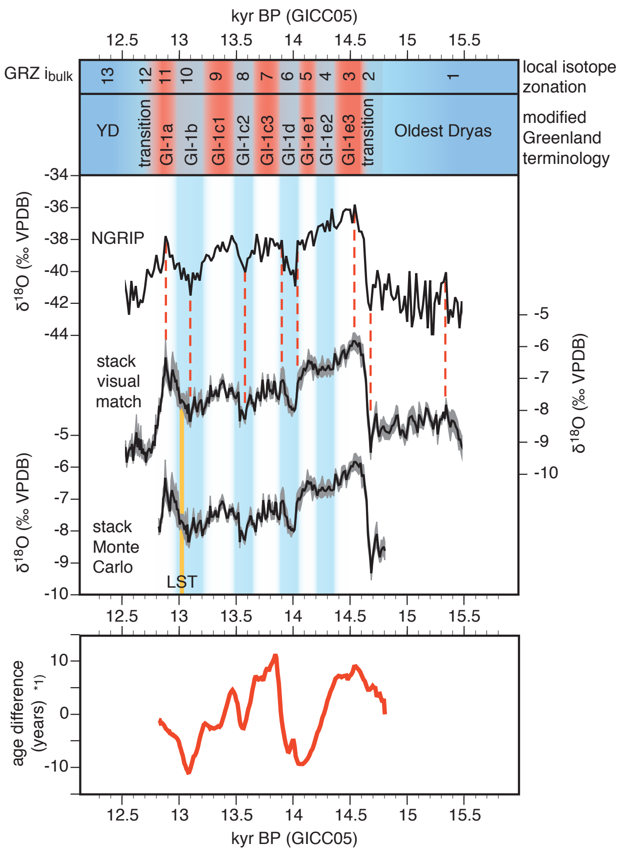

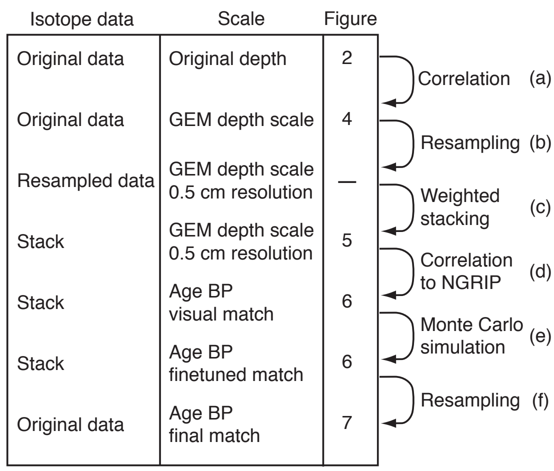

Fig. 3. Schematic workflow for establishing the age-depth model for the Gerzensee sediments. For details see Section 3. "Method for establishing a high-resolution core chronology".

Fig. 6. Correlation between the NGRIP and stacked Gerzensee d18O records on GICC05- timescale (converted to years before 1950 AD). A) Local isotope zonation (GRZ ibulk = Gerzensee oxygen isotope of bulk sediment without shell debris) and detailed modified Greenland terminology (GI = Greenland Interstadial, YD = Younger Dryas) divide the records into periods of higher and lower d18O values. Dashed lines mark the visually assigned tie points between the NGRIP and the stacked Gerzensee record. The result of the fine-tuning of the visual match by applying a modified Monte Carlo method is shown for the period of 12.8–14.8 kyr BP. The age difference between the visual correlation and the correlation by the Monte Carlo method is shown in B).

Table 2

Terminology and timing of events during the late-glacial period for the oxygen isotope records from Gerzensee lake marl and Greenland ice cores. Ages are presented on GICC05 time-scale (converted to years before 1950 AD).

isotope zones GRZ ibulk	classical terminology used in Swiss lakes		refined Greenland terminology	Gerz stack age (yr BP)	Gerz stack depth (cm)	GEJK depth (cm)	Lowe et al. 2008, GICC05 (yr BP)	INTIMATE Greenland terminology
13	Younger Dryas							GS-1
				12710	273.75			
12	transition*1						12846	
				12877	262.75			
11			GI-1a *2					GI-1a
				12989	269.25		13049	
10	Gerzensee Oscillation*3	LST*4	GI-1b	13034	272	272		GI-1b
				13274	282.75	285	13261	
9	Allerød		GI-1c1					GI-1c
				13522	293.25	299		
8			GI-1c2*5					
				13624	298.25	308		
7			GI-1c3					
				13908	315.25	338.5	13904	
6	Aegelsee Oscillation	Older Dryas	GI-1d					GI-1d
				14044	322.25	345.5	14025	
5	Bølling		GI-1e1					GI-1e
				14183	326.25	351.5		
4			GI-1e2*6					
				14439	336.25	361.5		
3			GI-1e3*2					
				14590	341.75	369.5		
2	transition*1						14604	
				14685	345.25	374		
1	Oldest Dryas							GS-2

*1: High sampling resolution enables definition of transitions as separate zones.
*2: Differs from Greenland terminology, since transitions (GRZ ibulk 2 and 12) were added as separate zones.
*3: Also known as IACP (Lehmann and Keigwin, 1992), parallel to Killarney Oscillation in North America (Levesque et al., 1993).
*4: Laacher See Tephra.
*5: Term adopted from Brauer et al., 2000.
*6: GI-1e was separated into sub-zones (this study), term "Inter Bølling Cold Period" (IBCP) was avoided since it has been used inconsistently (e.g. Karpuz and Jansen, 1992; Hughen et al., 1996).

Table 3

Overview of different terminologies used for synchronous intervals in various records of different areas in the North Atlantic region. GI = Greenland Interstadial, GS = Greenland Stadial, IACP = Inter Allerød Cold Period, IBCP = Inter Bølling Cold Period, BCP = Bølling Cold Period.

Local isotope zonation GRZi bulk	Modified Greenland terminology	Swiss Plateau, S-Germany *1)	Eifel region, N-Germany *2) *3)	N-America, Cariaco basin *4) *5)	N-America *6)	Norwegian Sea *7)	N-Atlantic *8)	Greenland *9)
13	Younger Dryas	Younger Dryas	Younger Dryas	Younger Dryas	Younger Dryas	Younger Dryas	Younger Dryas	GS-1
12	transition							
11	GI-1a							GI-1a
10	GI-1b	Gerzensee Oscillation	Gerzensee Oscillation	IACP	Killarney Oscillation	Older Dryas II	IACP II	GI-1b
9	GI-1c1	Allerød	Allerød	Allerød	Allerød	Allerød	Allerød	GI-1c
8	GI-1c2		Older Dryas	Older Dryas		Older Dryas I	IACP I	
7	GI-1c3		Bølling	Bølling				
6	GI-1d	Aegelsee Oscillation	Oldest Dryas	IBCP	Older Dryas	BCP II	Older Dryas	GI-1d
5	GI-1e1	Bølling	Meiendorf	Bølling	Bølling	Bølling	Bølling	GI-1e
4	GI-1e2					BCP I		
3	GI-1e3							
2	transition							
1	Oldest Dryas	Oldest Dryas	Pleniglacial	Oldest Dryas	Oldest Dryas	Oldest Dryas	Oldest Dryas	GS-2

*1: (Lotter et al., 1992).
*2: (Merkt and Müller, 1999).
*3: (Litt and Stebich, 1999).
*4: (Yu, 2007).
*5: (Hughen et al., 1996).
*6: (Yu and Eicher, 1998)
*7: (Karpuz and Jansen, 1992).
*8: (Thornalley et al., 2010).
*9: (Lowe et al., 2008).

The oxygen and carbon isotopic signatures of biogenic carbonates in Gerzensee, Switzerland, during the rapid warming around 14,685 years BP and the following interstadial

Ulrich von Grafenstein [a,*], Soumaya Belmecheri [a], Ueli Eicher [b], Ulrike J. van Raden [c], Helmut Erlenkeuser [d], Nils Andersen [d], Brigitta Ammann [e]

[a] Laboratoire des Sciences du Climat et de l'Environnement (CNRS, CEA, UVSQ), Bat 701, Orme des Merisiers, 91191 Gif-sur-Yvette, France
[b] Physics Institute, University of Bern, Sidlerstrasse 5, 3012 Bern, Switzerland
[c] Geological Institute, ETH Zürich, Switzerland
[d] Leibniz-Labor für Altersbestimmung und Isotopenforschung, Universität Kiel, Max-Eyth Strasse 11-13, 24118 Kiel, Germany
[e] Oeschger Centre for Climate Change Research, Zaehringerstrasse 25, 3012 Bern, Switzerland

PPP 2013 391: 25-32

A R T I C L E I N F O

Article history:
Received 22 August 2012
Received in revised form 17 July 2013
Accepted 22 August 2013
Available online xxxx

Keywords:
Stable isotopes
Late-glacial
Ostracods
Temperature
Termination 1a

A B S T R A C T

The stable isotope signature of ostracods, molluscs, and charophyte remains from the late glacial section of a shallow core from lake Gerzensee, Switzerland, is analyzed along with the bulk carbonate isotope composition in a multi-proxy study aiming to document the biotic responses to the first strong warming ca. 14.6 ka ago after full glacial conditions. The main goal of our contribution is to understand the climatic significance of the oxygen-isotope variations in and between the different carbonate species and ideally provide a quantitative estimate of the oxygen isotopic composition of meteoric precipitation, which then could be translated to mean temperature estimates. Corrected for the respective vital offsets, the different carbonates show almost identical oxygen-isotope ratios for the time preceding and after the rapid transition from Greenland climate stages GS2 to GI1, indicating low and seasonally constant water temperatures at the sediment–water interface for this period. In the following the difference between cold season and warm-season carbonates increases gradually, pointing to a summer–winter temperature difference of roughly 10 K at the end of GI1. We conclude that this gradual water-temperature increase is independent of climate and is mainly due to sedimentation, shallowing the sediment–water interface, eventually accentuated by a gradual decrease of Gerzensee's water level during GI1. Corrected for the isotope fractionation induced by the long term trend of such water temperature change, the higher resolved $\delta^{18}O$ record from the bulk carbonates allows calculation of the presumed oxygen–isotope ratio of former lake water ($\delta^{18}O_L$), which shows striking similarity to the record from Ammersee. Introducing a tentative hydrological correction close to the present day offset between $\delta^{18}O_L$ and the oxygen–isotopes in meteoric precipitation ($\delta^{18}O_P$), we propose a quantitative $\delta^{18}O_P$ and mean air temperature record for the Gerzensee region.

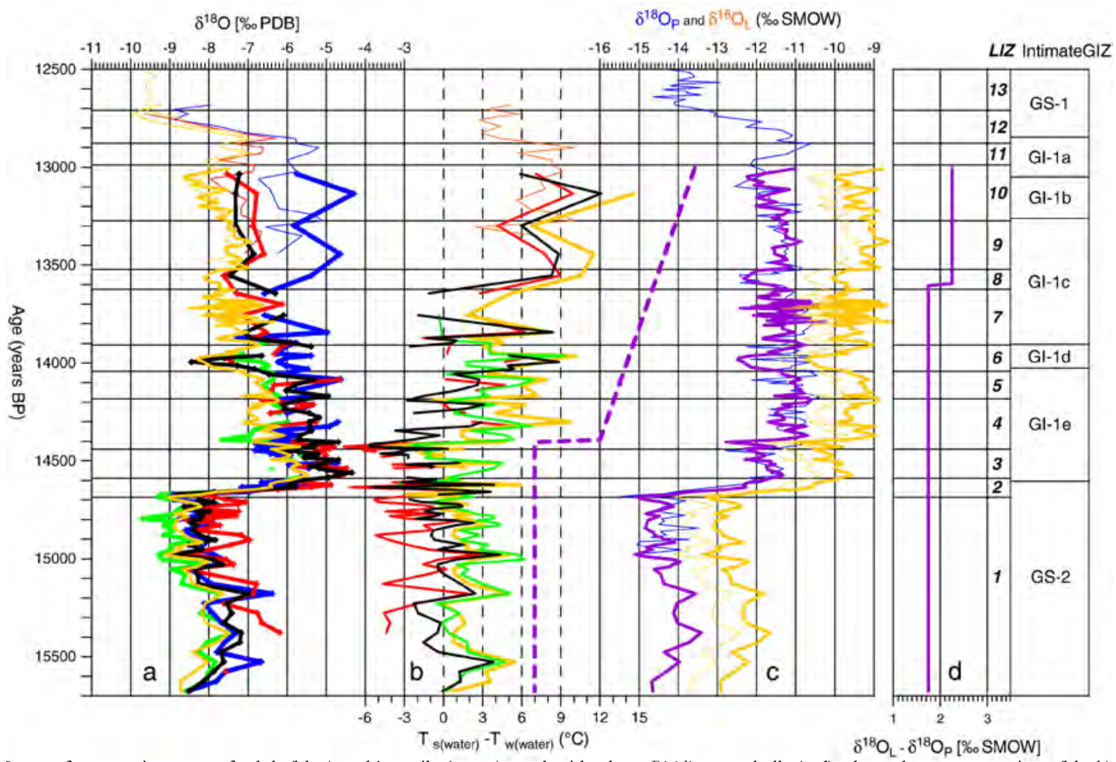

Fig. 2. a) Means of oxygen isotopes of adult (blue) and juvenile (green) candonid valves, *Pisidium* sp. shells (red), charophyte encrustations (black), and bulk carbonate (yellow) against age. Ostracod and mollusc values are corrected for their respective "vital offsets". b) Differences of the formation temperatures between the warm-season carbonates (colors as in a) and the cold season adult candonids using $\Delta t = (d^{18}Oadult–d^{18}Owarm\text{-}season) * (-0.25)$. The stippled violet line gives the simplified warm-season temperatures deduced from those differences. c) Yellow solid line: estimation of the oxygen–isotope ratio of Gerzensee lake water ($d^{18}OL$) calculated from $d^{18}Obulk$ and the simplified warm-season temperatures using (Friedman and O'Neil, 1977). The pointed yellow line gives the same estimation but using 3 °C lower warm-season temperatures. The violet line shows an estimation of the oxygen–isotopic composition of past atmospheric precipitation ($d^{18}OP$) calculated from d18OL by subtracting the evaporative enrichment given in graph d. The thin blue line gives the $d^{18}OP$ estimations for the Ammersee region (von Grafenstein et al., 1999a). d) Estimated evaporative enrichment ($d^{18}OP–d^{18}OL$) used to calculate $d^{18}OP$ for the Gerzensee region in graph c. The italic numbers above graph d give the local isotope zones (LIZ). The Greenland isotope zones (IntimateGIZ) are shown at the top (both LIZ and IntimateGIZ) according to van Raden et al., in this issue.

Palaeogeography, Palaeoclimatology, Palaeoecology 391 (2013) 33–39

Contents lists available at ScienceDirect

Palaeogeography, Palaeoclimatology, Palaeoecology

journal homepage: www.elsevier.com/locate/palaeo

Climatic and environmental changes reflected by lake-level fluctuations at Gerzensee from 14,850 to 13,050 yr BP

Michel Magny *

CNRS-UMR 6249, Laboratoire de Chrono-Environnement, Faculté des Sciences et Techniques, 16 route de Gray, 25 030 Besançon, France

A R T I C L E   I N F O

Article history:
Received 6 February 2012
Received in revised form 3 May 2012
Accepted 6 May 2012
Available online 17 May 2012

Keywords:
lake-level fluctuations
water budget
sediment analysis
Lateglacial
Swiss Plateau

A B S T R A C T

High-resolution sediment analysis at Gerzensee, Swiss Plateau, focused on the reconstruction of lake-level changes during the last glaciation Greenland Stadial 2a (GS-2a) and a large portion of Lateglacial including the Gerzensee oscillation. The chronology is derived from a comparison of the oxygen-isotope stratigraphy established at Gerzensee with that of the NGRIP ice core. On a multi-millennial scale differences between the lake-level and oxygen-isotope records established from cores GEJ–GEK reflect a complex interplay among climate, vegetation and lake level during retreat of the ice sheet. But on a multi-centennial scale both the lake-level and oxygen-isotope records show a general agreement, i.e. cool periods such as Greenland Stadial GS-2a and Greenland Interstadials-1d and -1b, which coincided with more positive water budgets and, conversely, warm periods (Greenland Interstadials-1e and -1c) with more negative water budget. This is in agreement with the regional pattern of palaeohydrological changes reconstructed from previous studies. Despite possible reduced annual precipitation during GS-2a, the maintenance of relatively high lake-level conditions at Gerzensee at this time could have resulted from reduced evaporation and stronger runoff on bare slopes, whereas during the Lateglacial Interstadial the phases of lake-level lowering may have been associated with summer dryness linked to increasing summer insolation.

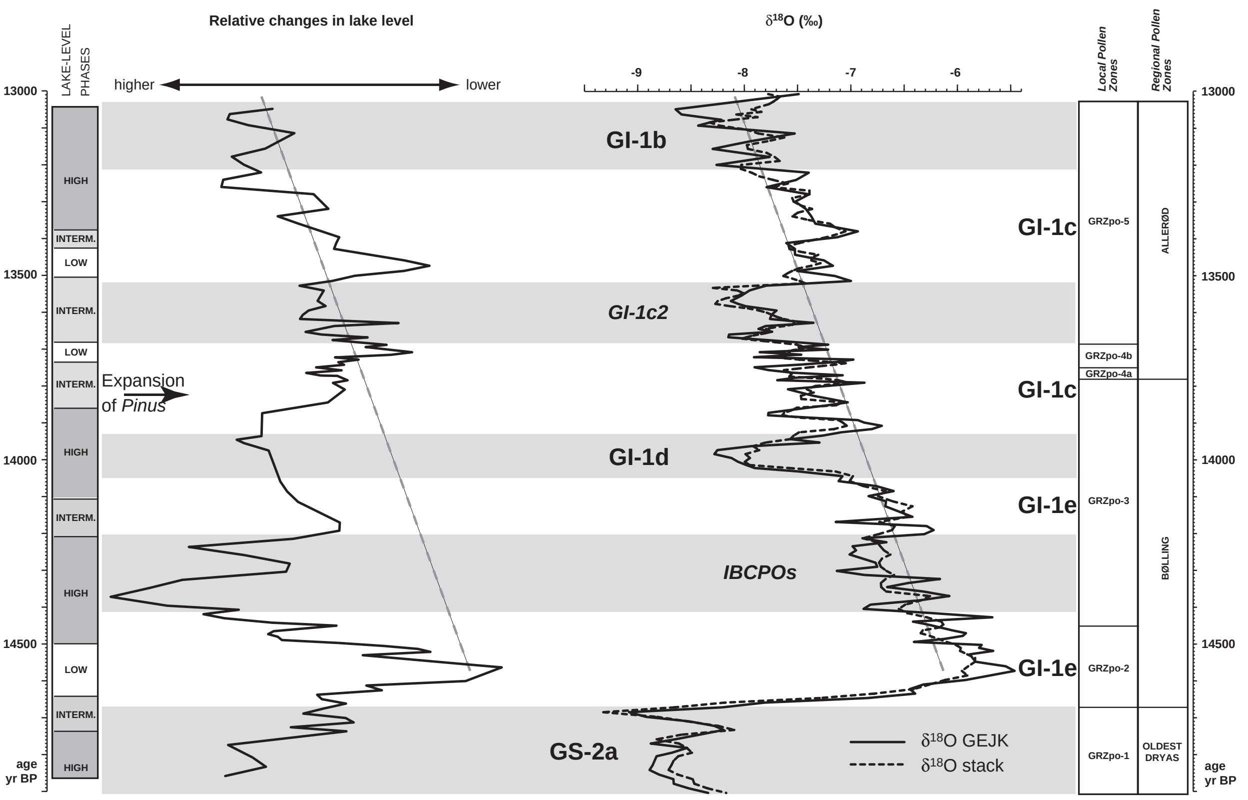

Fig. 3. Comparison between the lake-level (this study) and oxygen-isotope records (van Raden et al., 2013–this volume) at Gerzensee. The oxygen-isotope record GEJK has been established from cores GEJ and GEK, and the stack record from cores GEJ, GEK, GEA–GEA, GEM, and GEW. The grey bands point to periods of negative anomalies in the oxygen-isotope records. The pollen zones refer to B. Ammann et al. (2013–this volume-a, 2013–this volume-b).

Vegetation responses to rapid warming and to minor climatic fluctuations during the Late-Glacial Interstadial (GI-1) at Gerzensee (Switzerland)

Brigitta Ammann [a,*], Jacqueline F.N. van Leeuwen [a], Willem O. van der Knaap [a], Heike Lischke [b], Oliver Heiri [a], Willy Tinner [a]

[a] Institute of Plant Sciences and Oeschger Centre for Climate Change Research, University of Bern, Altenbergrain 21, CH-3013 Bern, Switzerland
[b] Swiss Federal Research Institute WSL, Zürcherstr. 111, CH-8903 Birmensdorf, Switzerland

PPP 2013 391: 40-59

ARTICLE INFO

Article history:
Received 18 March 2012
Received in revised form 11 July 2012
Accepted 15 July 2012
Available online 25 July 2012

Keywords:
Biotic responses to climatic change
Vegetation
Pollen
Late-Glacial
Oldest Dryas
Bølling
Allerød
Afforestation
Plant–population dynamics
Primary succession

ABSTRACT

High-resolution pollen analyses made on the same samples on which the ratios of oxygen isotopes were measured that provided the time scale and a temperature proxy after correlation to NorthGRIP.

(1) A primary succession: The vegetation responded to the rapid rise of temperatures around 14,685 yr BP, with a primary succession on a decadal to centennial time scale. The succession between ca 15,600 and 13,000 yr BP included:

(1.1.) The replacement of shrub-tundra by woodland of *Juniperus* and tree birch (around 14,665 yr BP)
(1.2.) The response of *Juniperus* pollen to the shift in oxygen isotopes in less than 20 yr,
(1.3.) A sequence of population increases of *Hippophaë rhamnoides* (ca 14,600 yr BP), *Salix* spp. (ca 14,600 yr BP), *Betula* trees (ca.14,480 yr BP), *Populus* cf. *tremula* (ca. 14,300 yr BP), and *Pinus* cf. *sylvestris* (ca. 13,830 yr BP).

(2) Biological processes: Plants responded to the rapid increase of summer temperatures on all organisational levels:

(2.1) Individuals may have produced more pollen (e.g. *Juniperus*);
(2.2) Populations increased or decreased (e.g. *Juniperus*, *Betula*, later *Pinus*), and
(2.3) Populations changed their biogeographical range and may show migrational lags.
(2.4) Plant communities changed in their composition because the species pools changed through immigration and (local) extinction. Some plant communities may have been without modern analogue. These mechanisms require increasing amounts of time.
(2.5) Processes on the level of ecosystems, with species interactions, may involve various time scales. Besides competition and facilitation, nitrogen fixation is discussed.

(3) The minor fluctuations of temperature during the Late-Glacial Interstadial, which are recorded in $\delta^{18}O$, resulted in only very minor changes in pollen during the Aegelsee Oscillation (Older Dryas biozone, GI-1d) and the Gerzensee Oscillation (GI-1b).
(4) Biodiversity: The afforestation at the onset of Bølling coincided with a gradual increase of taxonomic diversity up to the time of the major *Pinus* expansion.

Conclusions

1. Some of the vegetational changes were responses to the early rapid warming (as recorded in the oxygen-isotope ratios between 14,830 and 14,400 yr BP) within the sampling resolution (which was about 8.4 yr in this section) or up to 20 yr before and after. In other cases, recorded vegetational changes were probably triggered by the rapid warming but then took centuries to develop (e.g. migrations).
2. Afforestation (shift from shrub-tundra to a juniper–birch-woodland) was at Gerzensee the main response of regional vegetation to the rapid warming after 14,685 yr BP, as was the case at numerous sites on the Swiss Plateau and several sites in southern Central Europe.
3. The characteristic sequence of immigration and expansion of woody taxa is confirmed for southern Central Europe: *Juniperus* – *Hippophaë* – *Betula* (trees) – *Salix* – *Pinus*.
4. Population growth was hyperexponential in some cases, i.e. with positive and increasing intrinsic growth rate α, e.g. in *Juniperus*.
5. In *Pinus*, four steps and four levels can be distinguished as phases of population build-up (each lasting about 35–100 yr).
6. Vegetation responded to the very rapid warming after 14,850 yr BP on all organisational levels

(a) Level of the individual organism, here pollen production (e.g. *Juniperus*); this is the fastest response, as it can occur within a year or two.
(b) Level of the population: intermediate response times, especially the building-up of populations, a process that depends heavily on generation times (e.g. annuals vs trees).
(c) Level of biogeography: migration can be fast or slow depending on the vectors, life-history traits such as generation times, as well as on geographical barriers.
(d) Level of plant communities: the species pool changed rapidly, the unvegetated surfaces decreased, or with afforestation the distribution of plant-functional types changed.
(e) Level of the ecosystem: response times vary, depending on species competition (e.g. for light) or facilitation (e.g. by enhanced pedogenesis), and on changing types and abundances of nitrogen-fixers.

7. The minor cool phases recorded in the oxygen-isotope record during the Late Glacial Interstadial were no more than weakly reflected in pollen stratigraphy at this altitude of 600 m asl. Even the relatively marked cool phase about 14,044–13,908 yr BP (GI-1d; Aegelsee Oscillation; Older Dryas biozone) resulted in no more than very minor peaks in a few herb taxa, which were, all the same, picked up in the reconstruction of July temperatures by Lotter et al. (2012). Sites at higher altitudes may have been ecotonal and therefore more sensitive.
8. The estimates of palynological diversity based on pollen influx which is independent of pollen abundances) indicate that floristic diversity gradually increased during afforrestation up to the time of major *Pinus* expansion.

Table 2
Relationships between the isotopic zones GRZi$_{bulk}$-1 to GRZi$_{bulk}$-7 and the population dynamics of the six major woody taxa during the early Late-Glacial at Gerzensee: *Juniperus*, *Hippophaë*, *Salix*, *Betula* (tree taxa), *Populus*, and Pinus. Relationship between isotopic zones GRZibulk and populations of woody taxa during the millennium of the first forests of Bølling & Allerød.

Relationship between isotopic zones GRZi$_{bulk}$ and populations of woody taxa during the millennium of the first forests of Bølling & Allerød

Isotope zones	GEJK Depth	GICC05 BP Greenland	Depth (of biotic events)	Age (of biotic events)	*Juniperus*	*Salix* spp.	*Hippophaë*	*Betula*	*Populus*	*Pinus*, see also Tab. 3	PAZ GRZ$_{po}$	
Limit ↑	cm	yr before 1950	314.5	13677				Plateau, sub–dominance	Continuous curve ends	**Level d**		**Allerød**
GRZi$_{bulk}$–7		**GI–1c3**	315.5	13684						313 cm **Step 4 ↑** 319 cm	**4b**	
			319	13708				Co–dominant with pine	Several minor Fluctuations	**Level c** Co–dominant with birch		
			323	13734								
			325	13749				Step ↓		323 cm **Step 3 ↑** 325.5	**13753** 325.5	
					Very low values		Very low values	Third dominance		**Level b**	**4a**	
			329	13777						329 cm **Step 2 ↑** 337 cm		
			336	13872	Rel. low values		Low values				**13835** 333.5	
Limit	338.5	**13908**	339	13916				Recovery		**Level a**	**GRZ$_{pol}$–3**	**OD**
GRZi$_{bulk}$–6		**GI–1d Aegelsee osc**	342	13974	Step ↓	Step ↓	Step ↓	Step ↓	Step ↓	342 cm **Step 1 ↑** 347 cm		
Limit	345.5	**14044**		14085				Second dominance	Slope ↓			**Bølling**
GRZi$_{bulk}$–5		**GI–1e1**	347 348.5									
Limit	351.5	**14183**	351.5	14202	plateau	Peak		Minor dip	Peak			
GRZi$_{bulk}$–4		**GI–1e–2 IBCP**	353	14235				First dominance				
						Increase			shoulder			
			356	14302		Plateau			**Onset ↑**			
Limit	361.5	**14 439**	361	14416		↑ % & PAR	Step ↓				**14443** 362.25	
GRZi$_{bulk}$–3		**GI–1e3**										
			364	14470	Rapid ↓	Several minor fluctuations	Shoulder					
			365.5	14494			Onset of ↓	**Strong ↑**	1st grains		**GRZ$_{pol}$–2**	
			367	14519	Onset of ↓		Peak	**Slight ↑**				
			368.5	14548	Peak							
Limit	369.5	**14 573**	370	14585			**Strong onset ↑**					
GRZi$_{bulk}$–2	**Rapid ↑↑↑ Transition**		373.25	14672	**Strong ↑, in % & PAR**	**%↓, PAR↓**	**Slight ↑**				**14665**	
Limit	374	**14 685**										
GRZi$_{bulk}$–1					1. plateau	fluctuation					**GRZ$_{pol}$–1**	**Oldest Dryas**
			376	14742	1. stoma							
			396	15088	Slight ↑							
			398	15104			Continous					

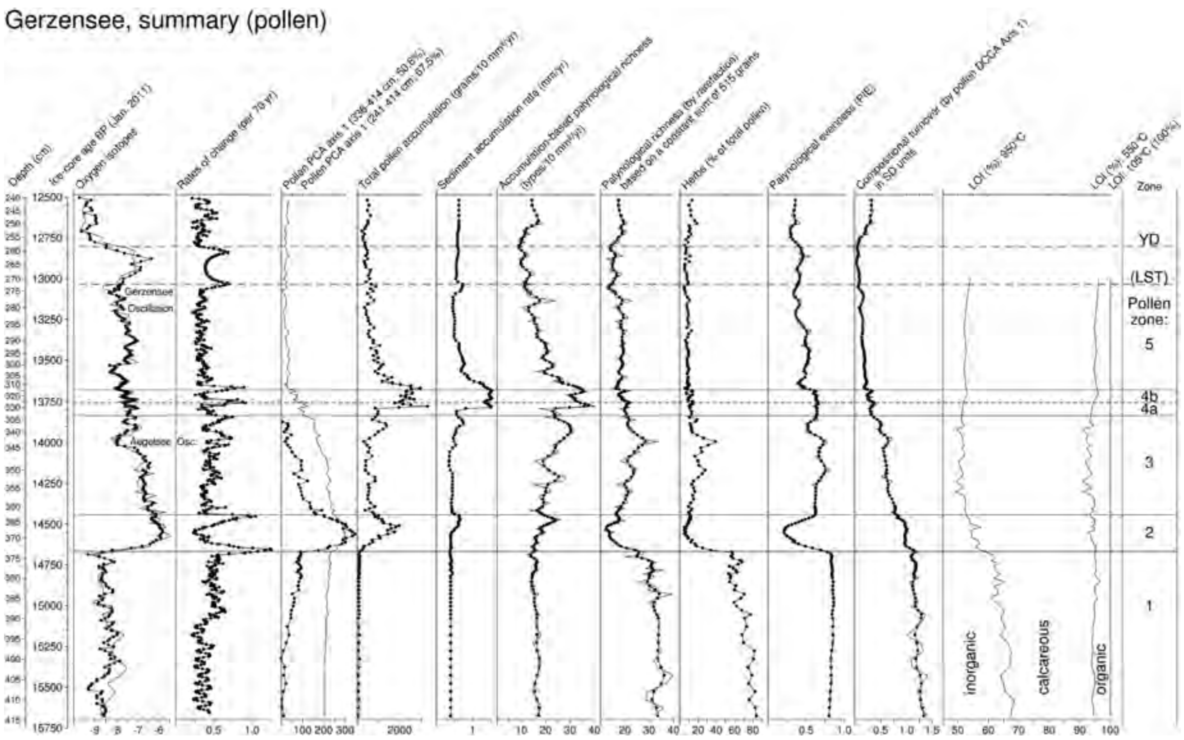

Fig. 4. Quantitative estimates of palynological change from the late Oldest Dryas to the onset of the Younger Dryas. Changes in the pollen record are summarized in four ways and compared to changes in the oxygen-isotopes. From left to right: Oxygen isotopes, diamonds before 12,970 BP for stacked values, dots after 12,970 BP for measured values (see van Raden et al., this issue). Palynological changes as (1) rates of change (smoothed); as (2) scores on the first axis of a PCA (calculated separately for the whole period and for the older period of the afforestation, about 15,300 to 14,000 BP); as (3) the estimate of pollen diversity presented in two ways, i.e. as percentages and as PAR (or influx) (based on rarefaction analysis, according to Birks and Line, 1992); and finally (4) as compositional turnover estimated by DCCA and expressed in units of standard deviation. Interpretations are given in the text (Section 4).

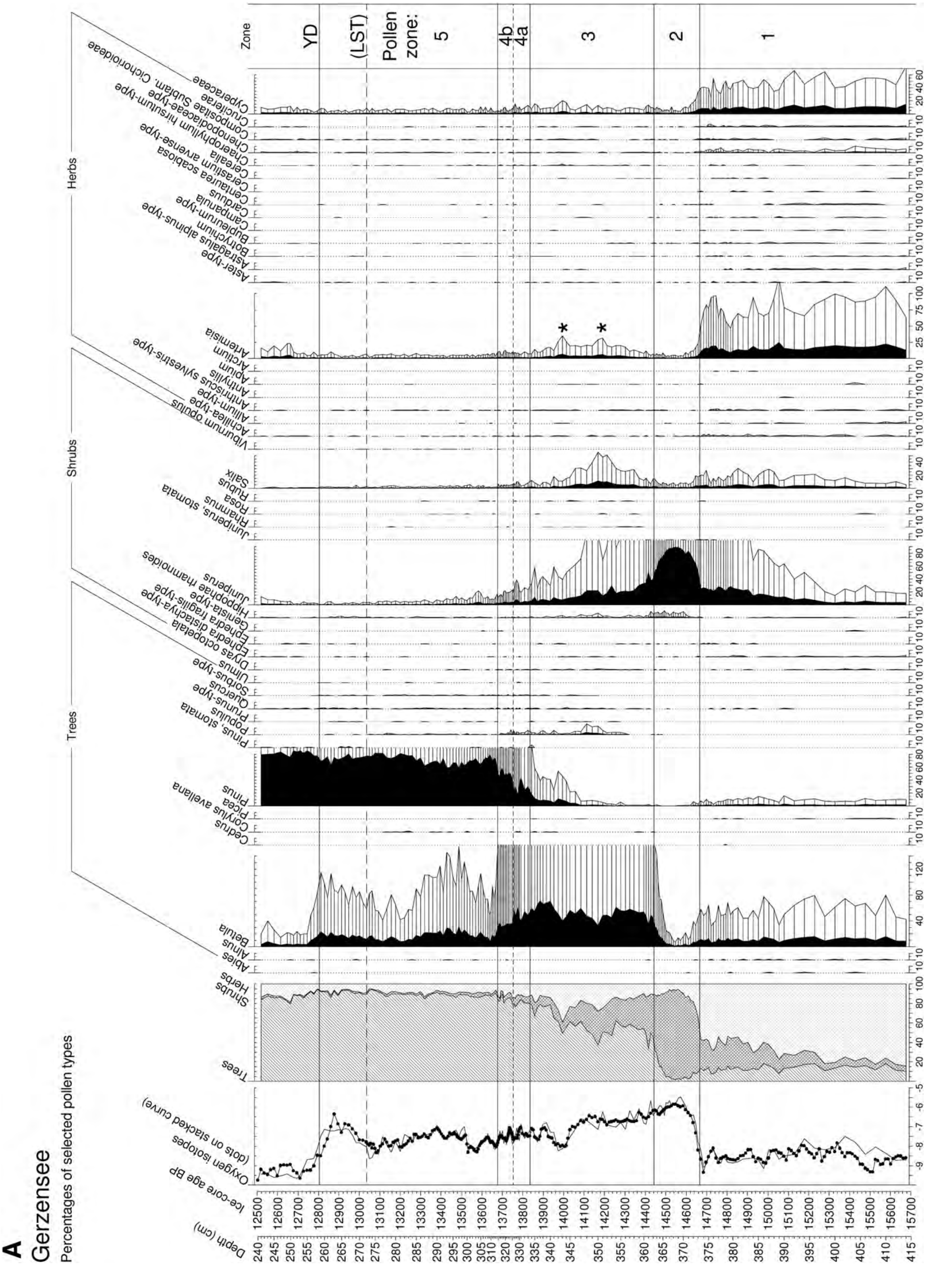
A
Gerzensee
Percentages of selected pollen types
Depth (cm)
Ice-core age BP
Oxygen isotopes (dots on stacked curve)
Trees
Shrubs
Herbs
Zone
YD
(LST)
Pollen zone:
5
4b
4a
3
2
1

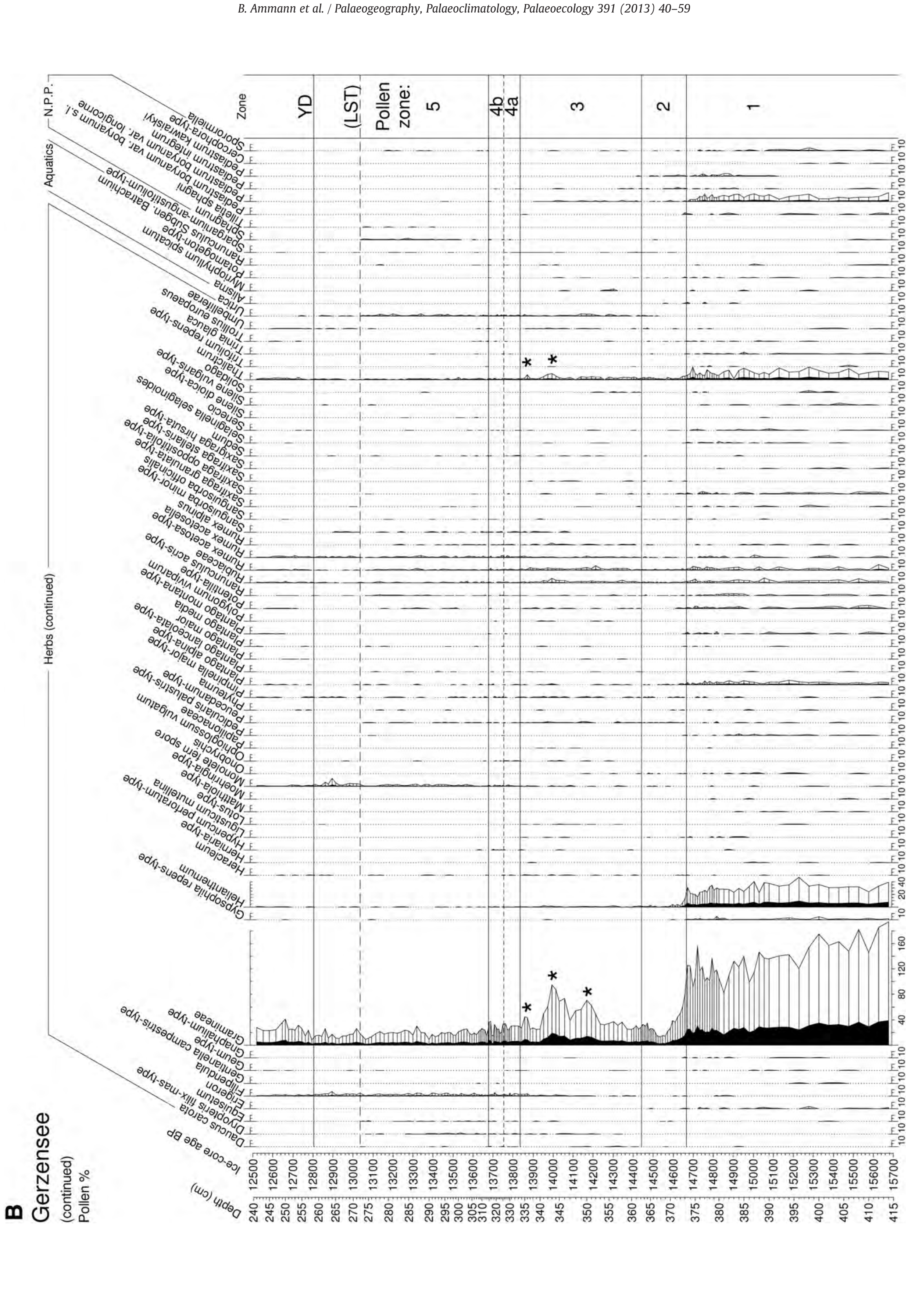

Fig. 2. Pollen diagram in percentages for Gerzensee: from the Oldest Dryas to the Lateglacial interstadial (Bølling and Allerød) and to the beginning of the Younger Dryas, selected pollen types only, on the time-scale of GICC-05 in BP (van Raden et al., this issue). Asterisks indicate minor peaks in non-arboreal pollen-types.

Primary Succession on a secular scale	**Oldest Dryas, last third, ca 15676–14665 cal BP**	**Early Bølling Ca14665–14443 cal BP**	**Late Bølling Ca14443–13835 cal BP**	**Allerød Ca14835–12710 cal BP**	**Younger Dryas Ca12710–11500 cal BP**
(A) Pollen zones Gerzensee	**GRZ_{pol}-1**	**GRZ_{pol}-2**	**GRZ_{pol}-3**	**GRZ_{pol}-4 and GRZ_{pol}-5**	**Wick 2000, Ammann et al. 2000**
Regional zones Western Swiss Plateau, Romandie (Gaillard 1984) 10 sites	***Artemisia–Betula nana***	***Juniperus–Hippophaë***	***Betula alba*–Gramineae**	***Betula–Pinus***	***Pinus*–Gramineae–*Artemisia***
Biozones (Welten 1982, Firbas 1952)	**Ia**	**Ib**		**II**	**III**
Regional biozones Swiss Plateau (Amman et al. 1996)	**CHb-1c**	**CHb-2**	**CHb-3**	**CHb-4a**	**CHb-4b**
Vegetation western and central Swiss Plateau	**Shrub tundra: *Artemisia,* Chenopods, *Salix* spp., *Betula nana***	**Juniper–birch forest, *B. alba-* type, *Hippophaë***	**Birch forests**	**Birch–pine forests, then pine–birch forests**	**More open pine–birch forests**
(B) Permafrost	**Probably important**	**Rapidly melting**	**Probably absent**	**Probably absent**	**?**
Potential effect on lake level		**Rise of lake level**			
Potential effect on soils	**Active layer thin**	**Active layer rapidly thickening**			
(C) Plant functional types	**Grasses, herbs, some legumes, shrubs**	**Trees and shrubs**	**Trees, some shrubs, herbs**	**Trees, some shrubs and herbs**	**Trees, some shrubs, more herbs**
Evapotranspiration	**Low**	**Rapidly increasing**	**increasing**	**Relatively high**	
Potential effects on lake level and soil humidity		**decreasing**	**decreasing**		
Potential effect on wind fetch	**Lakes exposed to wind**	**Lake sheltered between trees, wind fetch decreased, wind effects on lake and sedimentation decreased**			
(D) Soil development and the presence of N_2-fixers					
Pollen/Macros (Gaillard 1984) ***Dryas octopetala*** **Leguminosae** ***Hippophaë***	 + + +	 + + +++	 + + +	 + + +	 + + +
Soils on western and central Swiss Plateau (Gaillard 1984)	**Regosols or lithosols (patches of open ground and of vegetation)**	**Accumulation of organic matter ↑**	**Coexistence of dry and humid soils**	**Probably cambisols (Brown earths) of various types**	

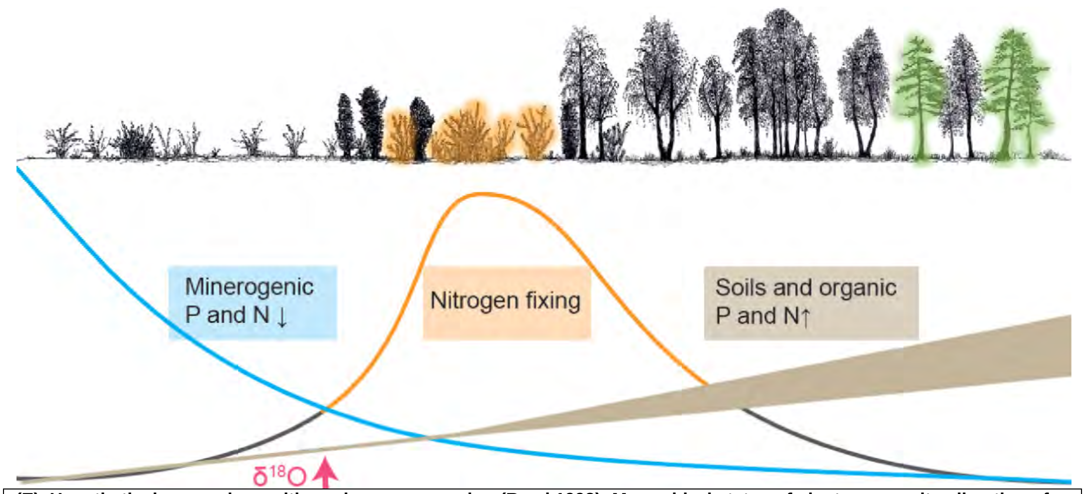

(E) Hypothetical comparison with a primary succession (Read 1993): Mycorrhizal status of plant community, direction of succession→→				
Plant–microbe mutualism	**Mineral P, N ↓, Cyanobacteria on raw soils; non-mycorrhizal ruderals, AM on grasses, Legumes fixing N_2**	**AM, and possibly maximum of N_2-fixation (e.g. *Hippophaë*)**	**Facultatively AM or ectomycorrhiza**	**Ecto-mycorrhiza increasing (on *Pinus*)**

Fig. 7. Primary succession, plant functional types, and nutrients during the transitions from the shrub-tundra to birch- and later pine forests as reflected in the pollen record. (A) Local and regional pollen zones. (B) Estimates of permafrost. (C) Changes in plant functional types and potential effects on evapotranspiration, lake levels, soil humidity, reduction of wind fetch. (D) Soil development: some selected taxa (recorded as pollen and plant macrofossils, the latter from neighbouring sites, Gaillard, 1984a,b) relevant for soil nutrients. (E) Comparison of potential N and P resources to the types of mycorrhiza in observed modern successions as proposed by Read, 1993. The red arrow near the bottom indicates time of the rapid increase of the d[18]O. At Gerzensee this coincides with the afforestation by juniper and tree-birches.

Contents lists available at ScienceDirect

Palaeogeography, Palaeoclimatology, Palaeoecology

journal homepage: www.elsevier.com/locate/palaeo

The effect of abrupt climatic warming on biogeochemical cycling and N_2O emissions in a terrestrial ecosystem

Mirjam Pfeiffer [a,*], Jacqueline van Leeuwen [b], Willem O. van der Knaap [b], Jed O. Kaplan [a]

[a] ARVE Group, Environmental Engineering Institute, Ecole Polytechnique Fédérale de Lausanne, 1015 Lausanne, Switzerland
[b] University of Bern, Institute of Plant Sciences, Altenbergrain 21, CH-3013 Bern, Switzerland

PPP 2013 391: 74-83

ARTICLE INFO

Article history:
Received 25 January 2012
Received in revised form 11 June 2012
Accepted 16 June 2012
Available online 30 June 2012

Keywords:
Rapid warming
Late Glacial
Hippophaë rhamnoides
N_2O emissions
Primary succession
Facilitation
Nitrogen fixation

ABSTRACT

The large, rapid increase in atmospheric N_2O concentrations that occurred concurrent with the abrupt warming at the end of the Last Glacial period might have been the result of a reorganization in global biogeochemical cycles. To explore the sensitivity of nitrogen cycling in terrestrial ecosystems to abrupt warming, we combined a scenario of climate and vegetation composition change based on multiproxy data for the Oldest Dryas–Bølling abrupt warming event at Gerzensee, Switzerland, with a biogeochemical model that simulates terrestrial N uptake and release, including N_2O emissions. As for many central European sites, the pollen record at the Gerzensee is remarkable for the abundant presence of the symbiotic nitrogen fixer *Hippophaë rhamnoides* (L.) during the abrupt warming that also marks the beginning of primary succession on immature glacial soils. Here we show that without additional nitrogen fixation, climate change results in a significant increase of N_2O emissions of approximately factor 3.4 (from 6.4 ± 1.9 to 21.6 ± 5.9 mg N_2O–N m^{-2} yr^{-1}). Each additional 1000 mg m^{-2} yr^{-1} of nitrogen added to the ecosystem through N-fixation results in additional N_2O emissions of 1.6 mg N_2O–N m^{-2} yr^{-1} for the time with maximum *H. rhamnoides* coverage. Our results suggest that local reactions of emissions to abrupt climate change could have been considerably faster than the overall atmospheric concentration changes observed in polar ice. Nitrogen enrichment of soils due to the presence of symbiotic N-fixers during early primary succession not only facilitates the establishment of vegetation on soils in their initial stage of development, but can also have considerable influence on biogeochemical cycles and the release of reactive nitrogen trace gases to the atmosphere.

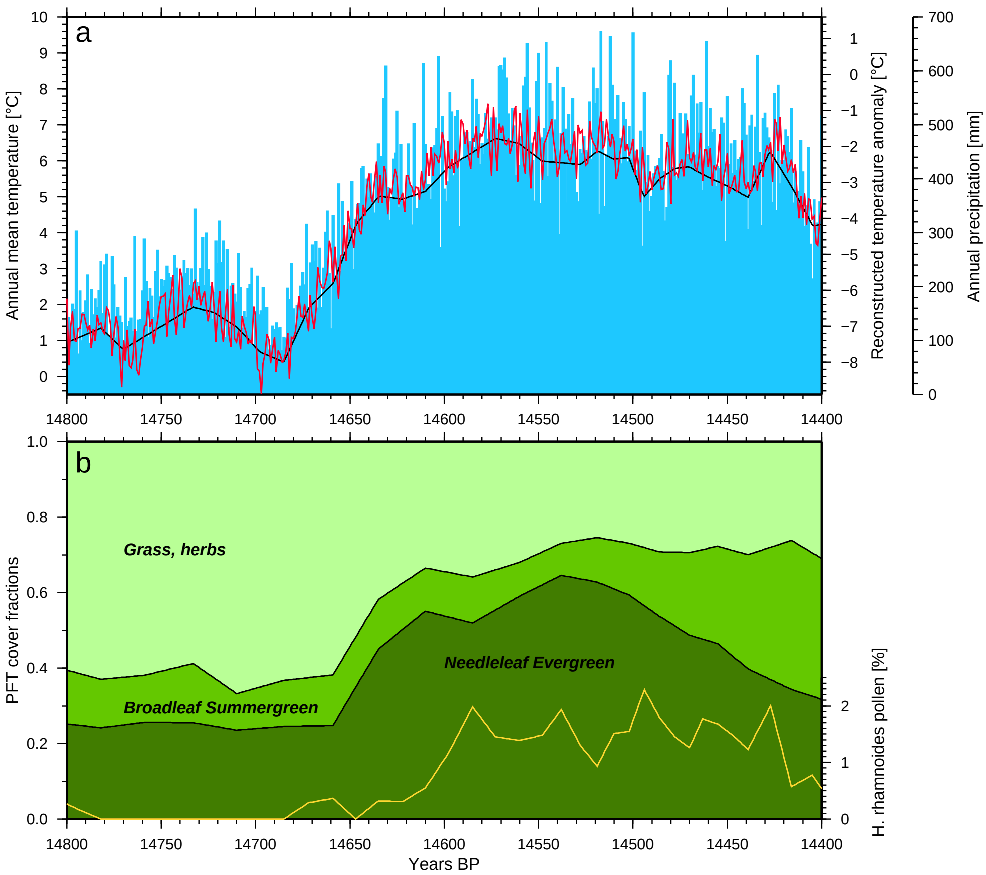

Fig. 2. a) Annual mean temperature (red curve) simulated with the weather generator, temperature anomalies reconstructed from $\delta^{18}O$ values from ostracod shells at Gerzensee, (black curve) and annual precipitation simulated with the weather generator. b) Left axis: cover of the three PFT types used by O-CN, based on the pollen record derived from the Gerzensee core samples. Fractional contribution of PFTs to the overall vegetation cover has been estimated based on the biomization method described by Prentice et al. (1996), and Peyron et al. (1998). Right axis: pollen percentage of *H. rhamnoides* (yellow curve).

Palaeogeography, Palaeoclimatology, Palaeoecology 391 (2013) 90–98

Contents lists available at ScienceDirect

Palaeogeography, Palaeoclimatology, Palaeoecology

journal homepage: www.elsevier.com/locate/palaeo

Response of chironomid assemblages to environmental change during the early Late-glacial at Gerzensee, Switzerland

Stephen J. Brooks [a,*], Oliver Heiri [b]

[a] Department of Entomology, Natural History Museum, Cromwell Road, London SW7 5BD, United Kingdom
[b] Institute of Plant Sciences and Oeschger Centre for Climate Change Research, University of Bern, Altenbergrain 21, CH-3013 Bern, Switzerland

ARTICLE INFO

Article history:
Received 8 February 2012
Received in revised form 18 October 2012
Accepted 23 October 2012
Available online 6 November 2012

Keywords:
Chironomidae
Switzerland
Late-glacial
Climatic change
Alps

ABSTRACT

Prior to ca. 14,660 yr BP, during the early Late-glacial (Oldest Dryas), larval assemblages of Chironomidae (Insecta: Diptera) in Gerzensee, Switzerland, were dominated by cold stenothermic taxa as well as by taxa typical of subalpine lakes today. This was the coldest period of the entire sequence. After ca. 14,660 yr BP, in the Late Glacial Interstadial (Bølling–Allerød), a temperature increase is recorded by a sharp rise in the oxygen-isotope ratio in lake marl and by an increase in the organic-matter content of the sediments. Changes in the chironomid fauna then are consistent with rising temperatures. This warming trend is interrupted between 14,070 and 13,940 yr BP, coinciding with the GI-1d cold oscillation, but the change in the chironomid assemblage is more consistent with a response to increasing lake depth and density of aquatic macrophytes than falling temperature. A rise in cold-adapted chironomid taxa between 13,840 and 13,710 yr BP suggests that summer air temperatures may have declined. Changes in the chironomid assemblage after 13,710 yr BP suggest a decline in submerged macrophytes coupled with a rise in lake productivity and summer temperature, although the latter is not reflected in the oxygen-isotope record. This suggests that there may have been increasing seasonality during this period when summer temperatures were rising, driven by rising summer insolation, and winters becoming cooler, which is largely reflected in the oxygen-isotope record. A decline in thermophilic chironomids and a rise in cold-adapted taxa after 13,180 yr BP suggest a response to cooling at the beginning of the Gerzensee Oscillation.

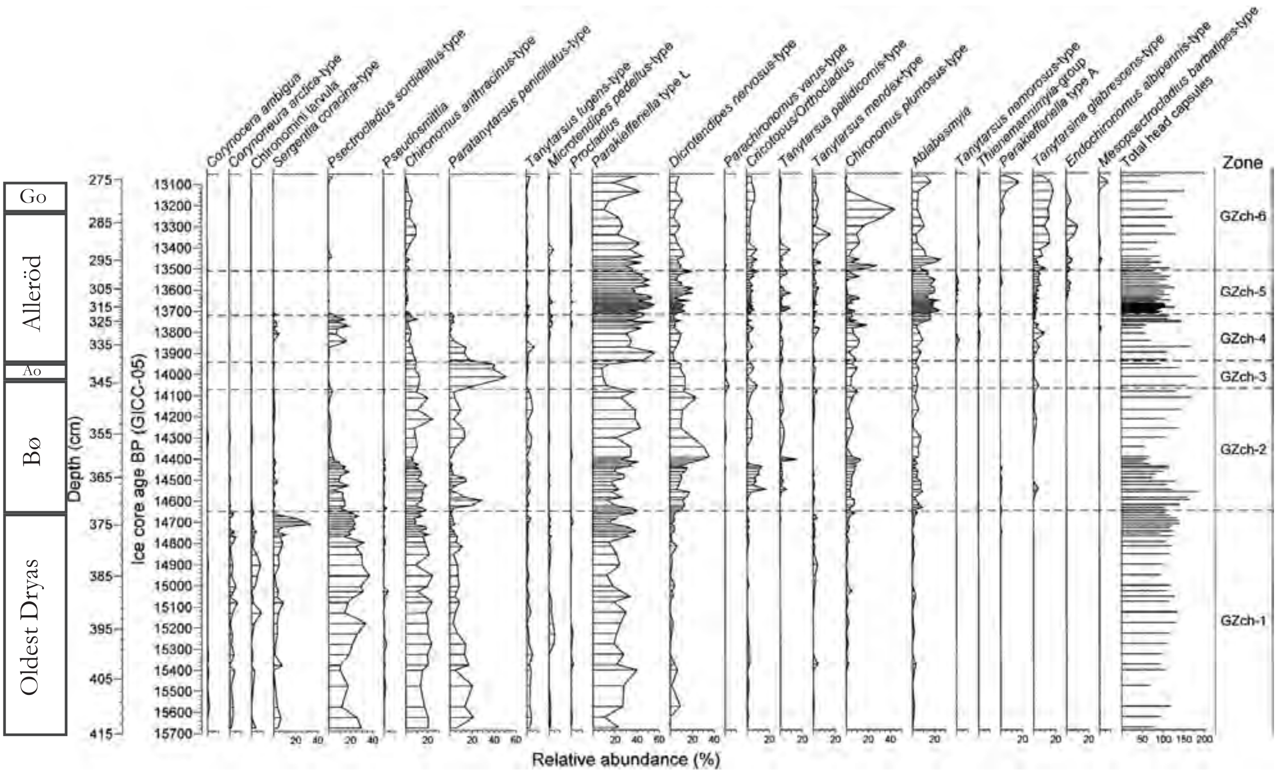

Fig. 2. Early Late-glacial chironomid sequence from Gerzensee, Switzerland (selected taxa only).

Response of the Lateglacial fauna to climatic change

Ebbe Nielsen *

University of Bern, Oeschger Centre for Climate Research, Institute of Plant Science, Altenbergrain 21, CH-3006 Bern, Switzerland

A R T I C L E I N F O

Article history:
Received 5 May 2012
Received in revised form 24 November 2012
Accepted 3 December 2012
Available online 10 January 2013

Keywords:

A B S T R A C T

This study deals with faunal finds from the Swiss Paleolithic, especially from the Late Glacial. Faunal assemblages from archeological sites as well as off-site finds dated by scientific means are included. In the middle of the Oldest Dryas the large glacial species – mammoth, rhinoceros, cave bear, musk ox – become extinct. During the Early Bølling the last arctic species disappear, and are succeeded by animals like red deer and elk, preferring a moderate climate. From the middle of the Allerød, species typical of a denser forest (roe deer and wild boar) are very frequent.

PPP 2013 391: 99-110

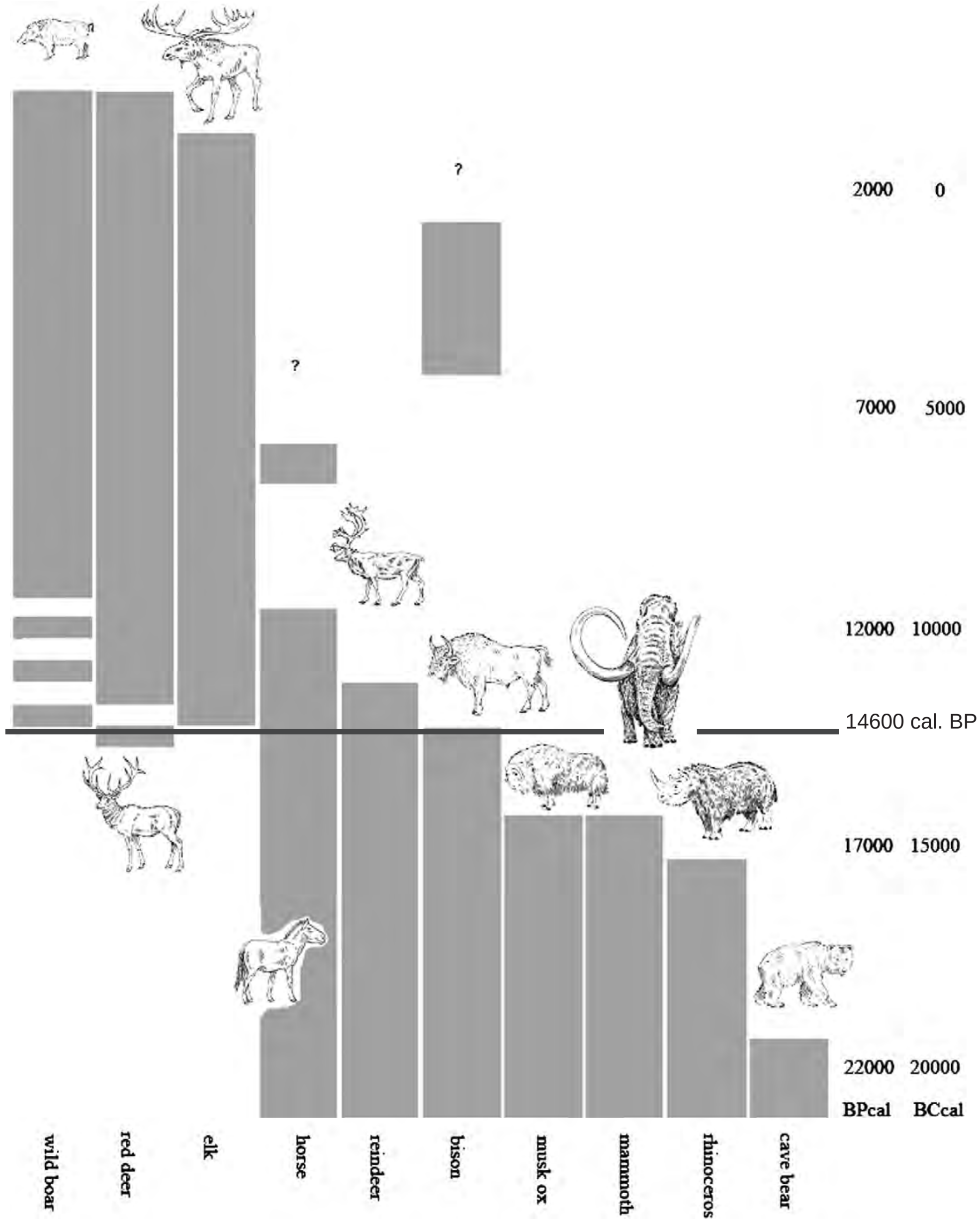

Fig. 9. Presence of important Glacial mammals.

Forest establishment/development (Melillo et al. 1993)			
	Tundra	Coniferous forest	Deciduous forest
Net annual biomass production g m^{-2} y^{-1}	100-200	200-600	600-1500
Carbon g m^{-2} y^{-1}	120	238	620
Kilocalories m^{-2} y^{-1}	600	3500	6000

Palaeogeography, Palaeoclimatology, Palaeoecology 391 (2013) 111–131

Contents lists available at ScienceDirect

Palaeogeography, Palaeoclimatology, Palaeoecology

journal homepage: www.elsevier.com/locate/palaeo

Responses to rapid warming at Termination 1a at Gerzensee (Central Europe): Primary succession, albedo, soils, lake development, and ecological interactions

Brigitta Ammann [a], Ulrike J. van Raden [b], Jakob Schwander [c], Ueli Eicher [c], Adrian Gilli [b], Stefano M. Bernasconi [b], Jacqueline F.N. van Leeuwen [a], Heike Lischke [d], Stephen J. Brooks [e], Oliver Heiri [a], Katařina Nováková [f], Maarten van Hardenbroek [a,g], Ulrich von Grafenstein [h], Soumaya Belmecheri [h,i], W.O. van der Knaap [a], Michel Magny [j], Werner Eugster [k], Daniele Colombaroli [a], Ebbe Nielsen [a,l], Willy Tinner [a], Herbert E. Wright [m]

[a] Institute of Plant Sciences and Oeschger Centre for Climate Change Research, University of Bern, Switzerland
[b] Geological Institute, ETH Zürich, Sonneggstrasse 5, 8092 Zürich, Switzerland
[c] University of Bern, Physics Institute, Switzerland
[d] Swiss Federal Research Institute WSL, Zürichstrasse 111, CH-8903 Birmensdorf, Switzerland
[e] Department of Entomology, Natural History Museum, Cromwell Road, London SW7 5BD, UK
[f] University of South Bohemia, Department of Botany, Branišovská 31, 370 05 České Budějovice, Czech Republic
[g] Geography and Environment, University of Southampton, University Road, Southampton SO17 1BJ, UK
[h] Laboratoire des Sciences du Climat et de l'Environnement (CNRS, CEA, UVSQ), Gif-sur-Yvette, France
[i] Institut de Paléontologie Humaine, Muséum National d'Histoires Naturelles, 1, Rue Panhard, Paris 75013, France
[j] Laboratoire de Chrono-Ecologie, Faculté des Sciences et Techniques, 16 route de Gray, 25 030 Besançon, France
[k] ETH Zurich, Institute of Plant Sciences, LFW C55.2, Universitaetsstrasse 2, CH-8092 Zurich, Switzerland
[l] Archaeological Survey Kanton Luzern, Libellenrain 15, 6002 Luzern, Switzerland
[m] Limnological Research Center, Dept. of Geology and Geophysics, University of Minnesota, Minneapolis, MN 55455, USA

ARTICLE INFO

Available online 21 November 2013

ABSTRACT

The transition from the Oldest Dryas to the Bølling around 14,685 cal yr BP was a period of extremely rapid climatic warming. From a single core of lake marl taken at Gerzensee (Switzerland) we studied the transition in stable isotopes of oxygen and carbon on bulk sediment and charophyte remains, as well as on monospecific samples of ostracods, after *Pisidium* a; in addition pollen, chironomids, and Cladocera were analyzed. The $\delta^{18}O$ record serves as an estimate of mean air temperature, and by correlation to the one from NGRIP in Greenland it provides a timescale.

The timing of responses: The statistically significant zone boundaries of the biostratigraphies are telescoped at the rapid increase of about 3‰ in $\delta^{18}O$ at the onset of Bølling. Biotic responses may have occurred within sampling resolution (8 to 16 years), although younger zone boundaries are less synchronous. Gradual and longer-lasting responses include complex processes such as primary or secular succession. During the late-glacial interstadial of Bølling and Allerød, two stronger and two weaker cool phases were found.

Biological processes involved in the responses occurred on levels of individuals (e.g. pollen productivity), of populations (increases or decreases, immigration, or extinction), and on the ecosystem level (species interactions such as facilitation or competition).

Abiotic and biotic interactions include pedogenesis, nitrogen-fixation, nutrient cycling, catchment hydrology, water chemistry of the lake and albedo (controlled by the transition from tundra to forest).

For the Swiss Plateau this major change in vegetation induced a change in the mammal fauna, which in turn led to changes in the tool-making by Paleolithic people.

E-mail addresses: Brigitta.Ammann@ips.unibe.ch (B. Ammann), ulrike.van.raden@alumni.ethz.ch (U.J. van Raden), schwander@climate.unibe.ch (J. Schwander), adrian.gilli@erdw.ethz.ch (A. Gilli), stefano.bernasconi@erdw.ethz.ch (S.M. Bernasconi), jacqueline.vanleeuwen@ips.unibe.ch (J.F.N. van Leeuwen), heike.lischke@wsl.ch (H. Lischke), S.Brooks@nhm.ac.uk (S.J. Brooks), Oliver.Heiri@ips.unibe.ch (O. Heiri), katkanovakova204@seznam.cz (K. Nováková), maarten.vanhardenbroek@ips.unibe.ch, vanhardenbroek@soton.ac.uk (M. van Hardenbroek), Ulrich.von-Grafenstein@lsce.ipsl.fr (U. von Grafenstein), belmecheri@mnhn.fr (S. Belmecheri), pim.vanderknaap@ips.unibe.ch (W.O. van der Knaap), michel.magny@univ-fcomte.fr (M. Magny), werner.eugster@ipw.agrl.ethz.ch (W. Eugster), daniele.colombaroli@ips.unibe.ch (D. Colombaroli), ebbe.nielsen@lu.ch (E. Nielsen), willy.tinner@ips.unibe.ch (W. Tinner), hew@umn.edu (H.E. Wright).

0031-0182/$ – see front matter © 2013 Elsevier B.V. All rights reserved.
http://dx.doi.org/10.1016/j.palaeo.2013.11.009

Table 1
Isotopic and biostratigraphic zone boundaries may summarize temporal aspects of biotic responses to climate change. In the isotope zones the first number for depth refers to the core GEJK, the second to the core GEM. All ages are given in stack ages yr BP (before 1959 AD) according to van Raden et al. (2013-in this issue). The asterisk at the zone levels of biostratigraphies indicates statistically significant zone boundaries. The highest coincidence of biostratigraphic zone boundaries coincides with the rapid increase in the oxygen-isotope ratio at the onset of the Bølling.

Regional PAZ	Isotope zones: North-GRIP	Isotope zones: Gerzensee, van Raden et al. (this issue): Depth	Age	Pollen zones, Ammann et al. (this issue): Depth	Age	Ostracod zones, von Grafenstein et al. (in prep.): Depth	Age	Chironomid zones, Brooks & Heiri (this issue): Depth	Age	Cladocera zones, Novákováet al. (this issue): Depth	Age
Transition YD		GRZi$_{bulk}$–12		Wick (2000)		von Grafenstein et al. (2000)		Brooks (2000)		Hofmann (2000)	
		262.75	12877								
Late Allerød	GI–1a	GRZi$_{bulk}$–11									
Limit		2 69.25	12989								
								271.0	13018		
Gerzensee Oscillation	1b	LST 272 cm, GRZi$_{bulk}$–10	13034 BP							273.0	13048
				GRZ$_{pol}$–5				GRZ$_{chi}$–6a		GRZ$_{cla}$–6	
Limit		285.0/ 282.75	13274								
										290.0*	13380*
Allerød	1c$_1$	GRZi$_{bulk}$–9									
								298.5*	13508*		
						GRZ$_{ost}$–11					
		299.0/ 293.25	13522								
	1c$_2$	GRZi$_{bulk}$–8								GRZ$_{cla}$–5	
		308.0/ 298.25	13624					GRZ$_{chi}$–5			
				314.5*	13677*						
	1c$_3$	GRZi$_{bulk}$–7		GRZ–po–4b				321.5*	13725*		
				325.5	13752						
				GRZ–po–4a		330.0*	13784*			327.0*	13763*
Limit		338.5/ 315.25	13908	333.5*	13835*			GRZ$_{chi}$–4			
						GRZ$_{ost}$–10					
Bio–Older Dryas, Aegelsee Oscillation	1d	GRZi$_{bulk}$–6						340.5*	13944*		
						344.5*	14022*	GRZ$_{chi}$–3		GRZ$_{cla}$–4	
				GRZ$_{pol}$–3				346.5*	14071*		
						GRZ$_{ost}$–9					
Limit		345.5/ 322.25	14044								
						354.5*/ 356.5*	14268*/ 14312*				
Bølling	1e$_1$	GRZi$_{bulk}$–5									
						GRZ$_{ost}$–7 & 8		GRZ$_{chi}$–2		355.0*	14279*
				362.5*	14447*	362.75	14443*				
		351.5/ 326.25	14183								
						GRZ$_{ost}$–6					
	1e$_2$	GRZi$_{bulk}$–4									
		361.5/ 336.25	14439			367.25*	14523*				
				GRZ$_{pol}$–2						GRZ$_{cla}$–3	
	1e$_3$	GRZi$_{bulk}$–3									
		369.5/ 341.75	14590								
						GRZ$_{ost}$–5					
	Transition	GRZi$_{bulk}$–2									
				373.25*	14665*	373.25*	14665*	372.75*	14653*	373.5*	14672*
Limit		374.0/ 345.25	14685			GRZ$_{ost}$–4					
				GRZ$_{pol}$–1		377.25*	14764*	GRZ$_{chi}$–1		GRZ$_{cla}$–2	
Oldest Dryas	GS2	GRZi$_{bulk}$–1				393.0*	15153*				
						409.0*	15552*			389.5*	15966*
						GRZ$_{ost}$–1				GRZ$_{cla}$–1	

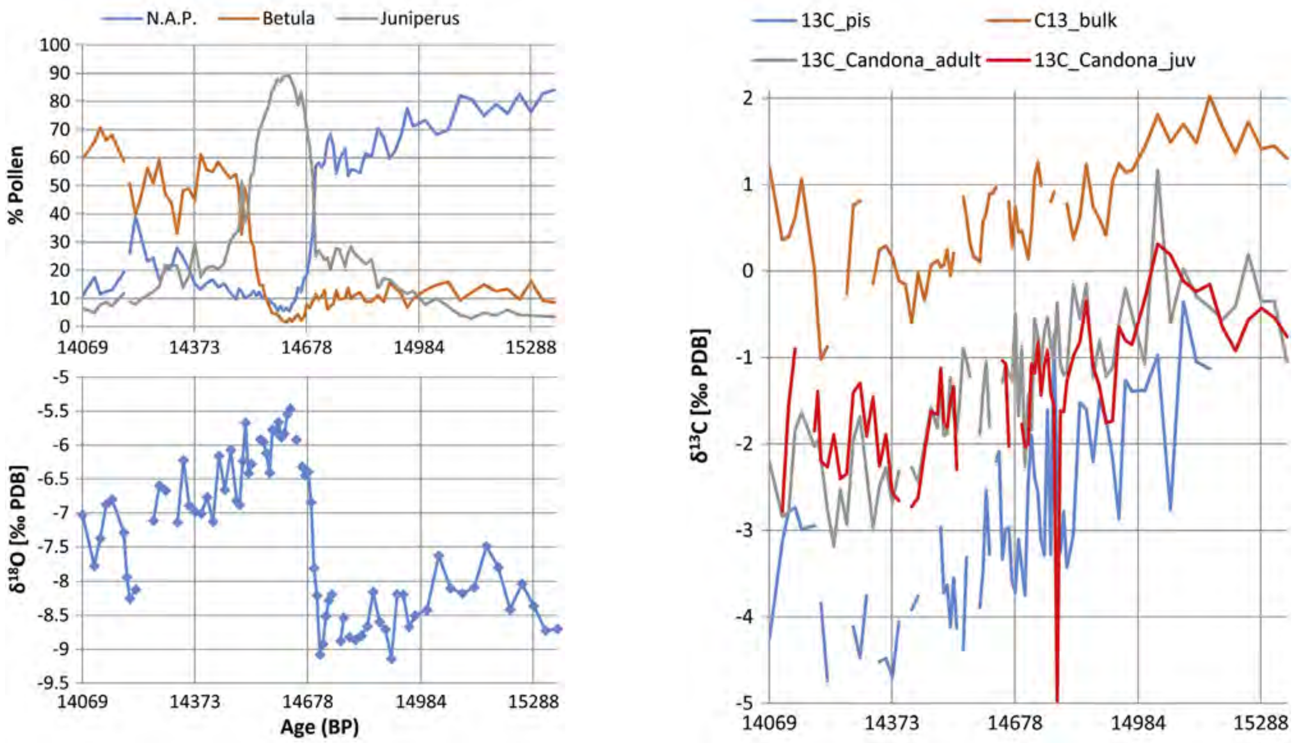

Fig. 4. The relationship between d^{13}C and vegetation visualizing pedogenesis across the major shift in d^{18}O at the transition from the Oldest Dryas to the Bølling (all data from same core GEJK): the top left panel shows the vegetation change from tundra to juniper and birch woodland (based on Ammann et al., 2013-in this issue-b); the right panel indicates the gradual decrease of d^{13}C as measured in the four types of samples (based on von Grafenstein et al., 2013-in this issue); the bottom left panel provides the reference to the shift in d^{18}O (based on van Raden et al., 2013-in this issue).

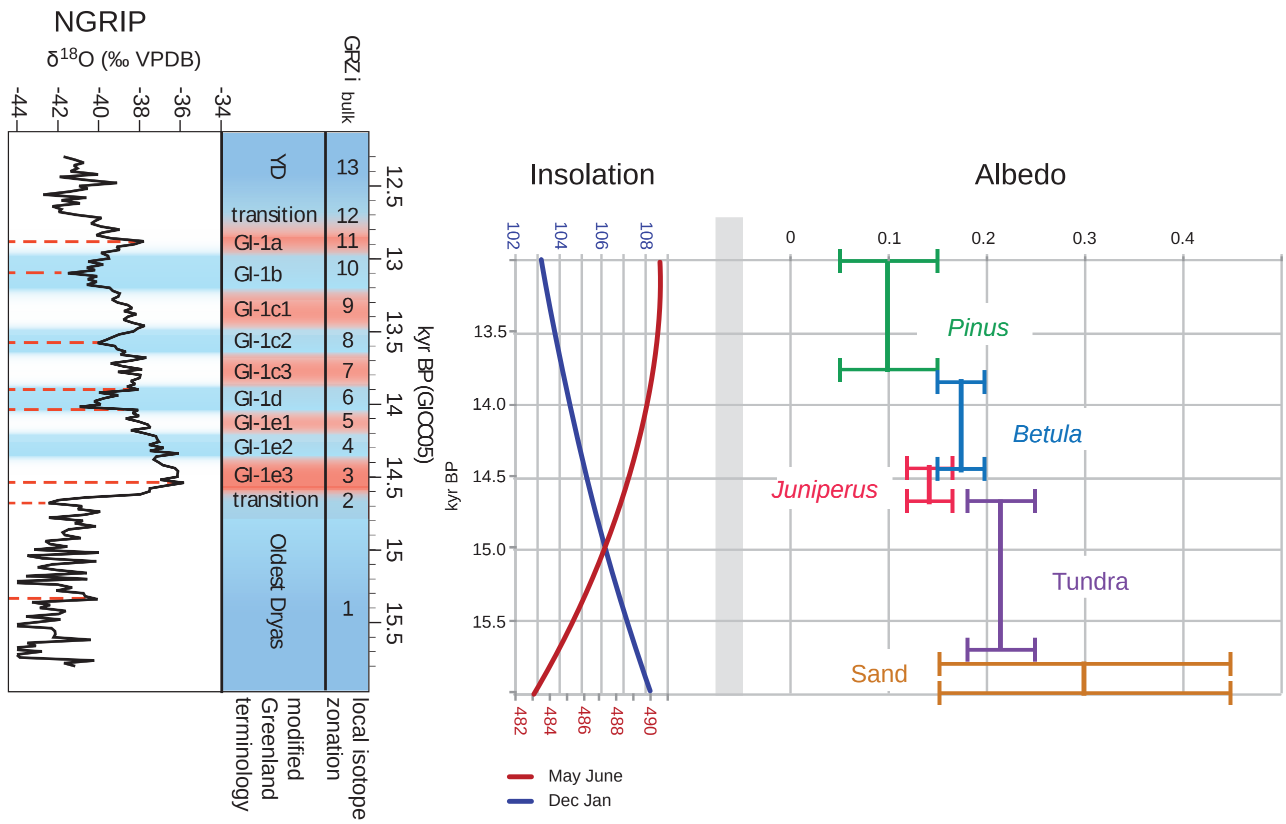

Fig. 5. Albedo decreased rapidly with afforestation by Juniperus. This shift is synchronous with the rapid increase in oxygen-isotope ratios around 14,650 yr BP. d^{18}O of NGRIP according to Rasmussen et al., 2006, isotope stratigraphy at Gerzensee according to van Raden et al., 2013-in this issue; Insolation at 47°N, according to .....; albedo values: sand =0.15–0.45, tundra = 0.18–0.25, Juniperus = 0.142 ± 0.024, deciduous forest (birch) = 0.15–0.20, coniferous forest (pine) = 0.05–0.15 (Eugster et al., 2000; http://doi.pangaea.de/10.1594/ PANGAEA.774715). Afforestation affected at least two surface characteristics, namely decreasing albedo and increasing surface roughness.

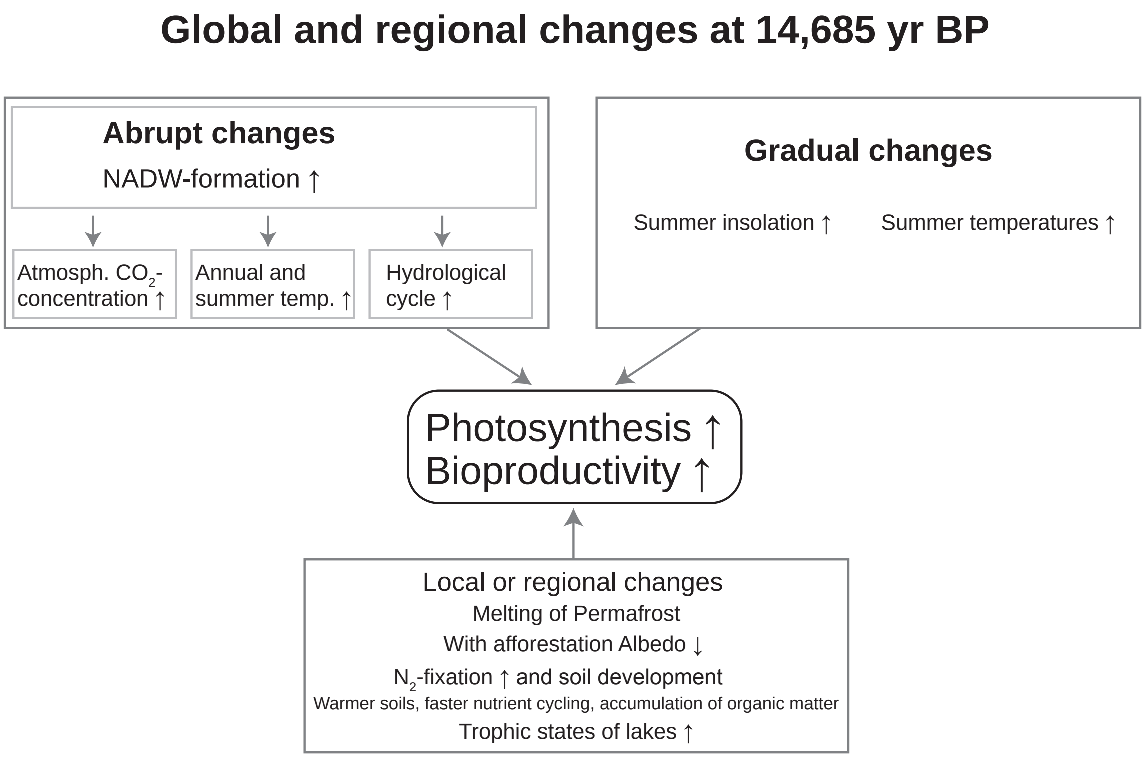

Fig. 6. Interacting processes in ecosystem changes during Termination 1a. Positive feedbacks on several spatial and temporal scales lead to an amplification of the biotic responses, e.g. through changes in albedo or faster hydrological and nutrient cycling in terrestrial and aquatic ecosystems.

- With atmospheric CO_2-concentration ↑ the stomata can be closed more often (stomatal conductance ↓), H_2O gets conserved, water-use efficiency ↑, soil moisture can ↑, surface runoff can ↑
- With enhanced hydrological cycle (see CH_4 in ice cores) and a warmer North Atlantic → higher precipitation and probably higher effective moisture (AE/PE= actual evapotranspiration/potential evapotr)
- With tundra → forest (Juniperus, Betula, Hippophaë, change in Plant Functional Types, PFT)
  * Albedo ↓
  * Bowen ratio ↓ (sensible heat/latent heat)
  * LAI ↑, higher evapotranspiration, can counteract higher water-use efficiency and higher soil moisture
  * pedogenesis ↑, nutrient cycling (see page 68)
  * changes in fauna (Mammals > changing techniques of Palaeoloithic hunters, see page 71)

Younger Dryas and Allerød summer temperatures at Gerzensee (Switzerland) inferred from fossil pollen and cladoceran assemblages

A.F. Lotter [a,b,*], H.J.B. Birks [c,d], U. Eicher [e], W. Hofmann [f], J. Schwander [e], L. Wick [a]

[a] *University of Bern, Geobotanical Institute, Altenbergrain 21, CH-3013 Bern, Switzerland*
[b] *Swiss Federal Institute of Environmental Science and Technology (EAWAG), CH-8600 Dübendorf, Switzerland*
[c] *University of Bergen, Botanical Institute, Allégaten 21, N-5007 Bergen, Norway*
[d] *University College London, Environmental Change Research Centre, 26 Bedford Way, London WC1H 0AP, UK*
[e] *University of Bern, Physical Institute, Sidlerstrasse 5, CH-3012 Bern, Switzerland*
[f] *Max-Planck-Institut für Limnologie, D-24302 Plön, Germany*

PPP 2000 159: 349-361

Abstract

Linear- and unimodal-based inference models for mean summer temperatures (partial least squares, weighted averaging, and weighted averaging partial least squares models) were applied to a high-resolution pollen and cladoceran stratigraphy from Gerzensee, Switzerland. The time-window of investigation included the Allerød, the Younger Dryas, and the Preboreal. Characteristic major and minor oscillations in the oxygen-isotope stratigraphy, such as the Gerzensee oscillation, the onset and end of the Younger Dryas stadial, and the Preboreal oscillation, were identified by isotope analysis of bulk-sediment carbonates of the same core and were used as independent indicators for hemispheric or global scale climatic change. In general, the pollen-inferred mean summer temperature reconstruction using all three inference models follows the oxygen-isotope curve more closely than the cladoceran curve. The cladoceran-inferred reconstruction suggests generally warmer summers than the pollen-based reconstructions, which may be an effect of terrestrial vegetation not being in equilibrium with climate due to migrational lags during the Late Glacial and early Holocene. Allerød summer temperatures range between 11 and 12°C based on pollen, whereas the cladoceran-inferred temperatures lie between 11 and 13°C. Pollen and cladocera-inferred reconstructions both suggest a drop to 9–10°C at the beginning of the Younger Dryas. Although the Allerød–Younger Dryas transition lasted 150–160 years in the oxygen-isotope stratigraphy, the pollen-inferred cooling took 180–190 years and the cladoceran-inferred cooling lasted 250–260 years. The pollen-inferred summer temperature rise to 11.5–12°C at the transition from the Younger Dryas to the Preboreal preceded the oxygen-isotope signal by several decades, whereas the cladoceran-inferred warming lagged. Major discrepancies between the pollen- and cladoceran-inference models are observed for the Preboreal, where the cladoceran-inference model suggests mean summer temperatures of up to 14–15°C. Both pollen- and cladoceran-inferred reconstructions suggest a cooling that may be related to the Gerzensee oscillation, but there is no evidence for a cooling synchronous with the Preboreal oscillation as recorded in the oxygen-isotope record. For the Gerzensee oscillation the inferred cooling was ca. 1 and 0.5°C based on pollen and cladocera, respectively, which lies well within the inherent prediction errors of the inference models.

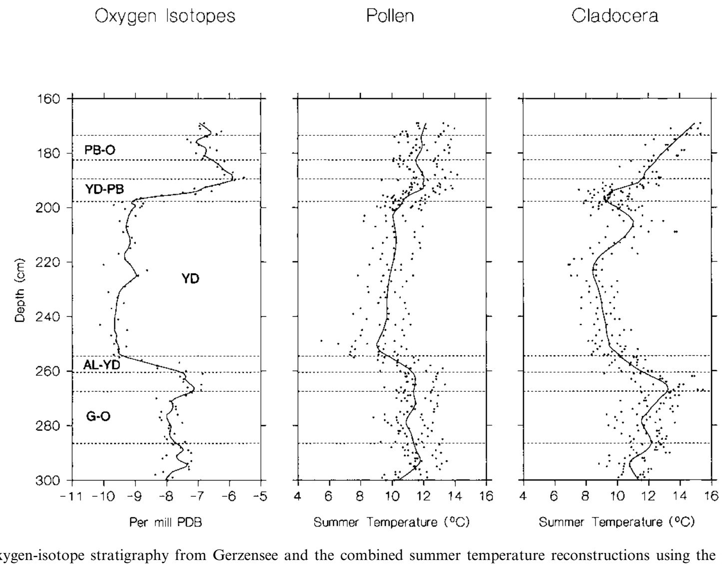

Fig. 3. Oxygen-isotope stratigraphy from Gerzensee and the combined summer temperature reconstructions using the pollen- and chydorid-inferred results of the PLS, WA, and WA-PLS models. The dots mark the sample-specific summer temperatures, whereas the solid lines represent LOWESS smoothed (span = 0.1) summer temperature reconstructions. PB-O: Preboreal oscillation; PB: Preboreal; YD: Younger Dryas cold phase; AL: Allerød; G-O: Gerzensee oscillation.

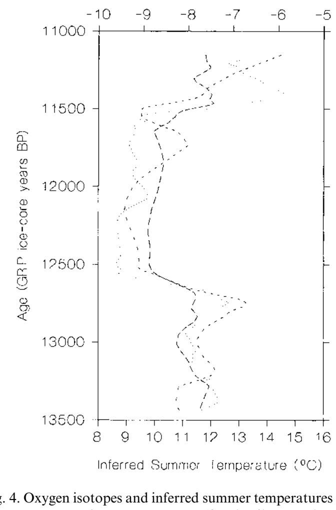

Fig. 4. Oxygen isotopes and inferred summer temperatures plotted versus GRIP ice-core ages B.P. (for details see Schwander et al., 2000). The top scale refers to the oxygen-isotope ratio (solid line) and is expressed in ‰ PDB. The inferred summer temperatures for pollen (dashed line) and chydorids (dotted line) are expressed as degrees Celsius (lower scale).

Oxygen isotopes of lake marl at Gerzensee and Leysin (Switzerland), covering the Younger Dryas and two minor oscillations, and their correlation to the GRIP ice core

Jakob Schwander [a,*], Ueli Eicher [a], Brigitta Ammann [b]

[a] *University of Bern, Physics Institute, Sidlerstrasse 5, CH-3012 Bern, Switzerland*
[b] *University of Bern, Geobotanical Institute, Altenbergrain 21, CH-3013 Bern, Switzerland*

PPP 2000 159: 203-214

Abstract

The ratio of oxygen isotopes is a temperature proxy both in precipitation and in the calcite of lacustrine sediments. The very similar oxygen-isotope records from Greenland ice cores and European lake sediments during the Last Glacial Termination suggest that the drastic climatic changes occurred quasi-simultaneously on an extra-regional, probably hemispheric scale. In order to study temporal relations of the different parameters recorded in lake sediments, for example biotic response times to rapid climatic changes, a precise chronology is required. In unlaminated lake sediments there is not yet available a method to provide a high-resolution chronology, especially for periods with radiocarbon plateaux. Alternatively, an indirect time scale can be constructed by linking the lake stratigraphy with other well-dated climate records. New oxygen-isotope records from Gerzensee and Leysin, with an estimated sampling resolution of between 15 and 40 years, match the Greenlandic isotope record in many details. Under the assumption that the main variations in temperature and thus in oxygen isotopes occurred about simultaneously in Greenland and Switzerland, we have assigned a time scale to the lake sediments of Gerzensee and Leysin by wiggle-matching their stable-isotope records with those of Greenland ice cores, which are among the best dated climatic archives. We estimate a precision of 20 to 100 years during the Last Glacial Termination.

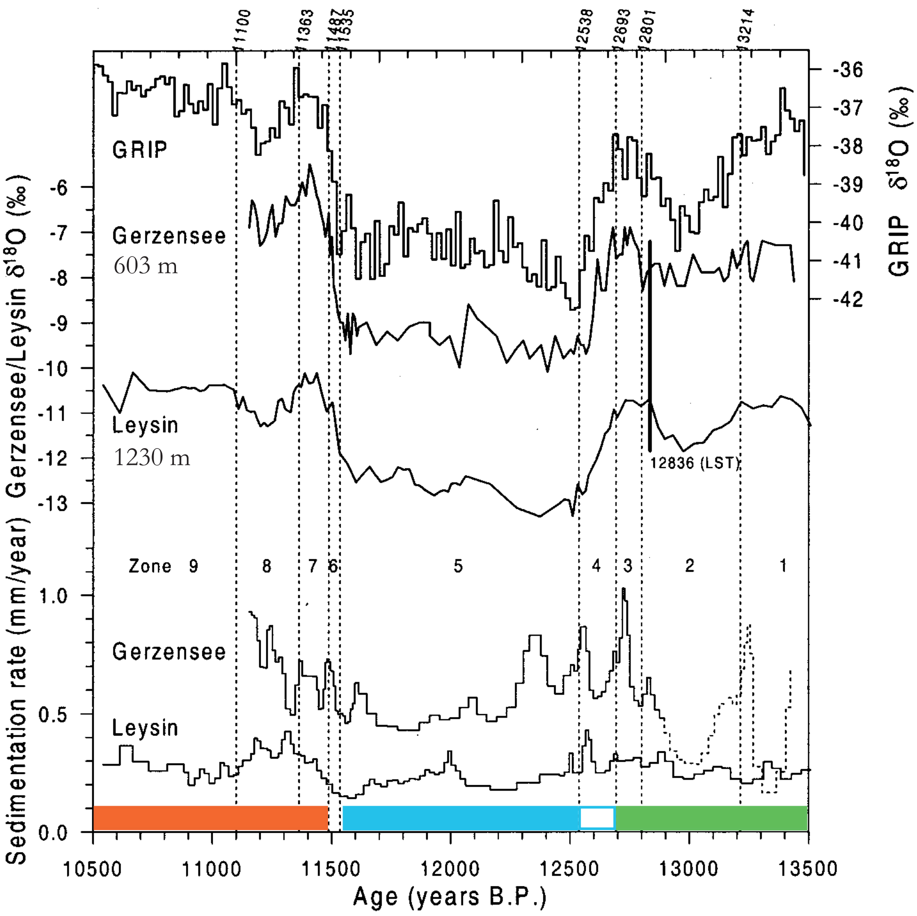

Fig. 4. Correlation between the $\delta^{18}O$ curves of Gerzensee, Leysin, and GRIP and inferred sedimentation rates for the lake cores. The age scale in calendar years before present (present is 1950 A.D.). Numbers indicated in the upper part of the figure are ages of isotopic zone boundaries. The dashed line in the Gerzensee sedimentation record indicates poor matching.

ELSEVIER

Palaeogeography, Palaeoclimatology, Palaeoecology 159 (2000) 215–229

PALAEO

www.elsevier.nl/locate/palaeo

Isotope signature of the Younger Dryas and two minor oscillations at Gerzensee (Switzerland): palaeoclimatic and palaeolimnologic interpretation based on bulk and biogenic carbonates

Ulrich von Grafenstein [a,*], Ueli Eicher [b], Helmut Erlenkeuser [c], Patrick Ruch [d,†], Jakob Schwander [e], Brigitta Ammann [f]

[a] *LSCE, CEA–CNRS, Avenue de la Terrasse, Domaine du CNRS, F-91198 Gif-sur-Yvette, France*
[b] *University of Bern, Physics Institute, Sidlerstrasse 5, CH-3012 Bern, Switzerland*
[c] *Leibniz-Labor für Altersbestimmung und Isotopenforschung der Universität Kiel, Max-Eyht-Straße 11, D-24111 Kiel, Germany*
[d] *Landeshydrologie, CH-3003, Buwal, Switzerland*
[e] *University of Bern, Physics Institute, Sidlerstrasse 5, CH-3012 Bern, Switzerland*
[f] *University of Bern, Geobotanical Institute, Altenbergrain 21, CH-3013 Bern, Switzerland*

Abstract

Oxygen- and carbon-isotope ratios in the carbonate of benthic ostracodes (*Pseudocandona marchica*) and molluscs (*Pisidium* ssp.) were measured across the transitions bordering the Younger Dryas chronozone in littoral lacustrine cores from Gerzensee (Switzerland). The specific biogenic carbonate records confirm the major shifts already visible in the continuous bulk-carbonate oxygen-isotope record ($\delta^{18}O_{Cc}$). If corrected for their vital offsets, oxygen-isotope ratios of *Pisidium* and juvenile *P. marchica*, both formed in summer, are almost identical to $\delta^{18}O_{Cc}$. This bulk carbonate is mainly composed of encrustations of benthic macrophythes (*Chara* ssp.), also mainly produced during summer. Adult *P. marchica*, which calcify in winter, show consistently higher $\delta^{18}O$, larger shifts across both transitions, and short positive excursions compared with the summer forms, especially during early Preboreal. Despite such complexity, the $\delta^{18}O$ of adult *P. marchica* probably reflects more accurately the variations of the $\delta^{18}O$ of former lake water because, during winter, calcification temperatures are less variable and the water column isotopically uniform. The difference between normalised $\delta^{18}O$ of calcite precipitated in winter to that formed in summer can be used to estimate the minimum difference between summer and winter water temperatures. In general, the results indicate warmer summers during the late Allerød and early Preboreal compared with the Younger Dryas. Altogether, the isotopic composition of lake water ($\delta^{18}O_L$) and of the dissolved inorganic carbonate ($\delta^{13}C_{DIC}$) reconstructed from adult *Pseudocandona marchica*, as well as the seasonal water temperature contrasts, indicate that the major shifts in the $\delta^{18}O$ of local precipitation at Gerzensee were augmented by changes of the lake's water balance, with relatively higher evaporative loss occurring during the Allerød compared with the Younger Dryas. It is possible that during the early Preboreal the lake might even have been hydrologically closed for a short period. We speculate that such hydrologic changes reflect a combination of varying evapotranspiration and a rearrangement of groundwater recharge during those climatic shifts.

Keywords: lake-level changes; ostracoda; palaeoclimate; palaeohydrology; stable isotopes

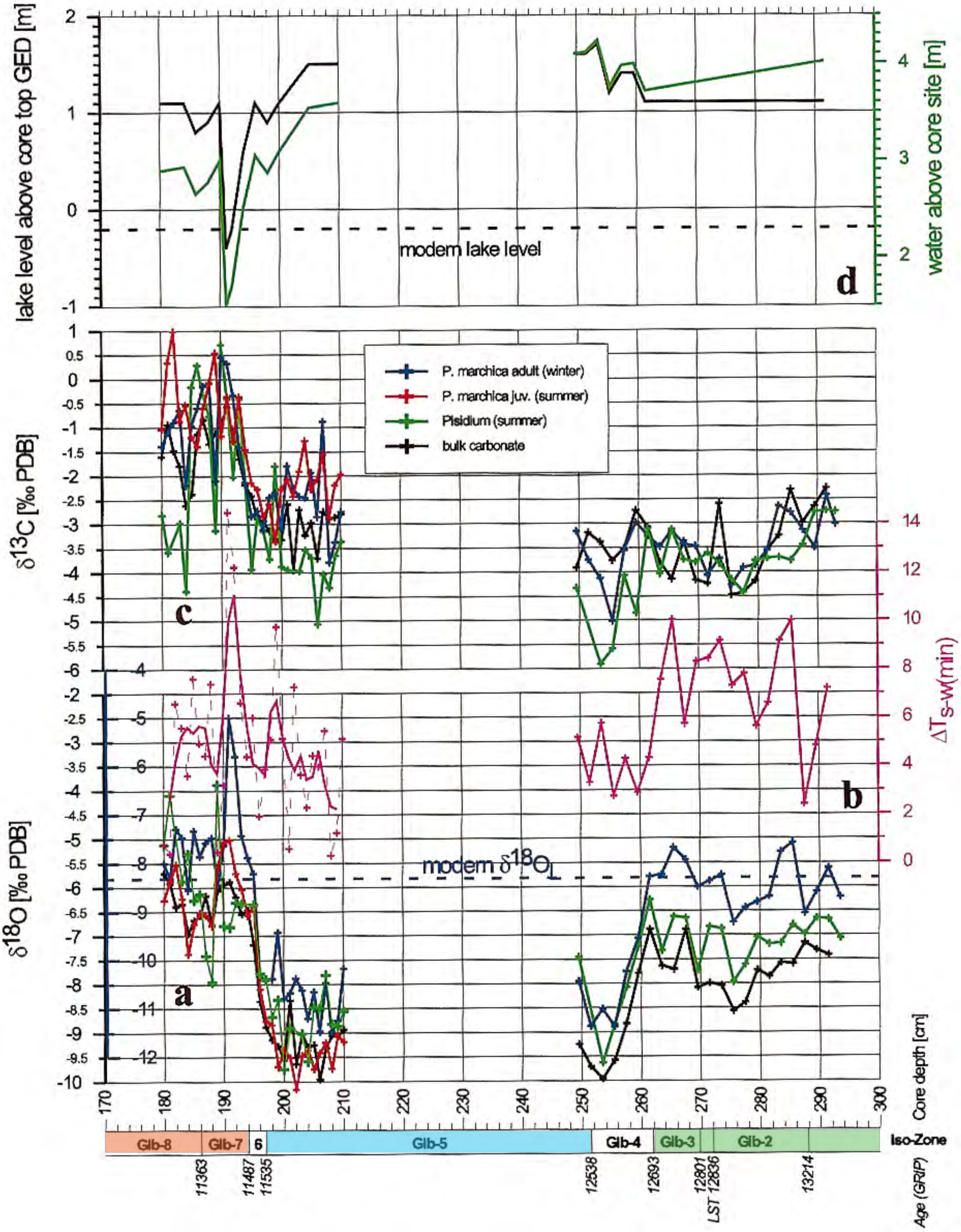

Fig. 3. (a) $\delta^{18}O$ of *Pseudocandona marchica* (adult: blue; juveniles: red), *Pisidium* (green), and bulk carbonate (black). Vital offsets are corrected for ostracods and molluscs (see text). The $\delta^{18}O$ of adult *P. marchica* is assumed to calcify at constant low winter water temperatures and to refer to $\delta^{18}O_L$ if scaled to the inner right-hand vertical axis (blue); the modern $\delta^{18}O_L$ of Gerzensee as a reference is given by the horizontal dashed blue line. The carbonate of juvenile *P. marchica* (instars A-4 and A-3), of *Pisidium*, and the bulk carbonate are mainly produced during summer. (b) Inferred minimal summer–winter water temperature differences [$\Delta t_{s-w(min)}$], calculated from the difference between $\delta^{18}O$ of adult *P. marchica* and $\delta^{18}O$ of juvenile *P. marchica* (for GEH) or *Pisidium* (for GED). (c) $\delta^{13}C$ of the same material as for $\delta^{18}O$ [colours as in (a)], normalised to reflect past DIC (see text). (d) Tentative lake-level reconstruction expressed as palaeo-water-depth (water above core site, green, left vertical scale) and as palaeo-lake-level above the core top of GED (black, right vertical scale). The reconstruction is constrained by an upper limit, equivalent to the elevation of the natural till dam before the outlet started to cut in (+1.7 m with respect to the modern lake level), and a lower limit (the sill depth of the modern outlet valley, +0.3 m). We let the palaeo-lake-level vary between these limits proportional to the different proxies, which indicate water balance and lake-level changes, with the exception of the positive spike in the early PB (191–192 cm), where we assume that the lake was closed.

Vegetational response to climatic changes recorded in Swiss Late Glacial lake sediments

Lucia Wick

Geobotanik, University of Bern, Altenbergrain 21, CH-3013 Bern, Switzerland

PPP 2000 159: 231-250

Abstract

High-resolution pollen analysis at five lakes on an altitudinal transect in Switzerland (Gerzensee, 603 m; Leysin, 1230 m; Regenmoos, 1260 m; Zeneggen, 1510 m; Hérémence, 2290 m) focused on the vegetational response to the rapid climatic changes at the end and beginning of the Younger Dryas and to the minor Gerzensee and Preboreal climatic oscillations. An absolute time scale transferred from the Greenland GRIP ice core to the Gerzensee and Leysin records by wiggle-matching the oxygen-isotope stratigraphies facilitates the estimation of pollen influx and rates of change. The climatic warming at the end of the Younger Dryas, indicated by increases in oxygen-isotope values and/or the beginning of organic sedimentation in the lakes, was immediately reflected in the vegetation at all the sites investigated. The time lags at sites situated above the timberline during the Younger Dryas are considered to be migrational lags. At the onset of the Younger Dryas a time lag of several decades occurred between the oxygen-isotope record of climatic cooling and the major response of the vegetation, whereas minor vegetation changes occurred with or without short time lags. *Betula* reacted earlier to the new environmental conditions (within about 40–50 yr at Gerzensee and within less than 36 yr at Leysin) than *Pinus* and *Artemisia* (about 170 yr), suggesting that time lags are due to the ecological requirements of the different taxa. For the Gerzensee and Preboreal oscillations little or no change can be observed in the pollen record from Gerzensee, whereas at Leysin both climatic oscillations produced a statistically significant vegetational response to both climatic oscillations. Generally the vegetation responses to climatic changes are more pronounced near vegetation ecotones at medium and higher altitudes than in the lowlands.

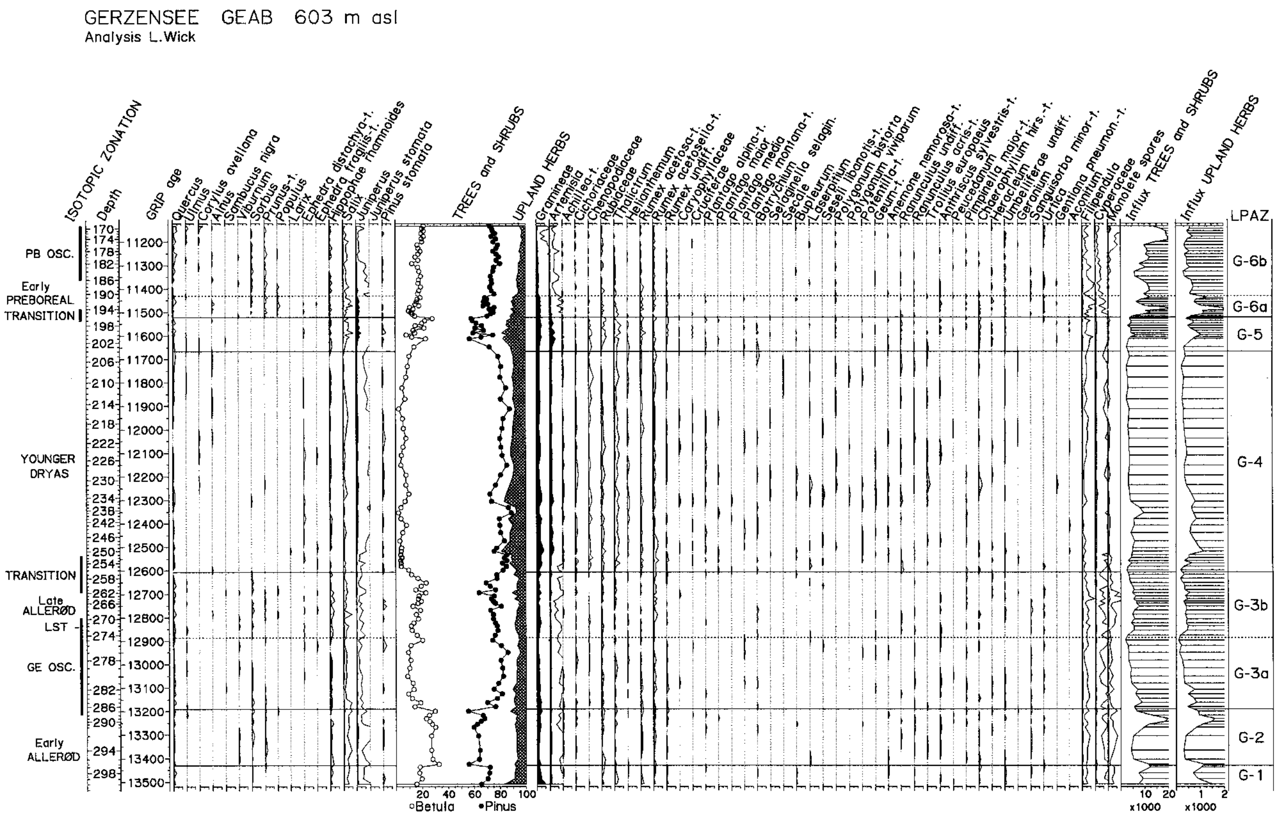

Fig. 1. Pollen percentage diagram of Gerzensee including the most important taxa. The time scale is given in GRIP yr B.P. (i.e. before A.D. 1950).

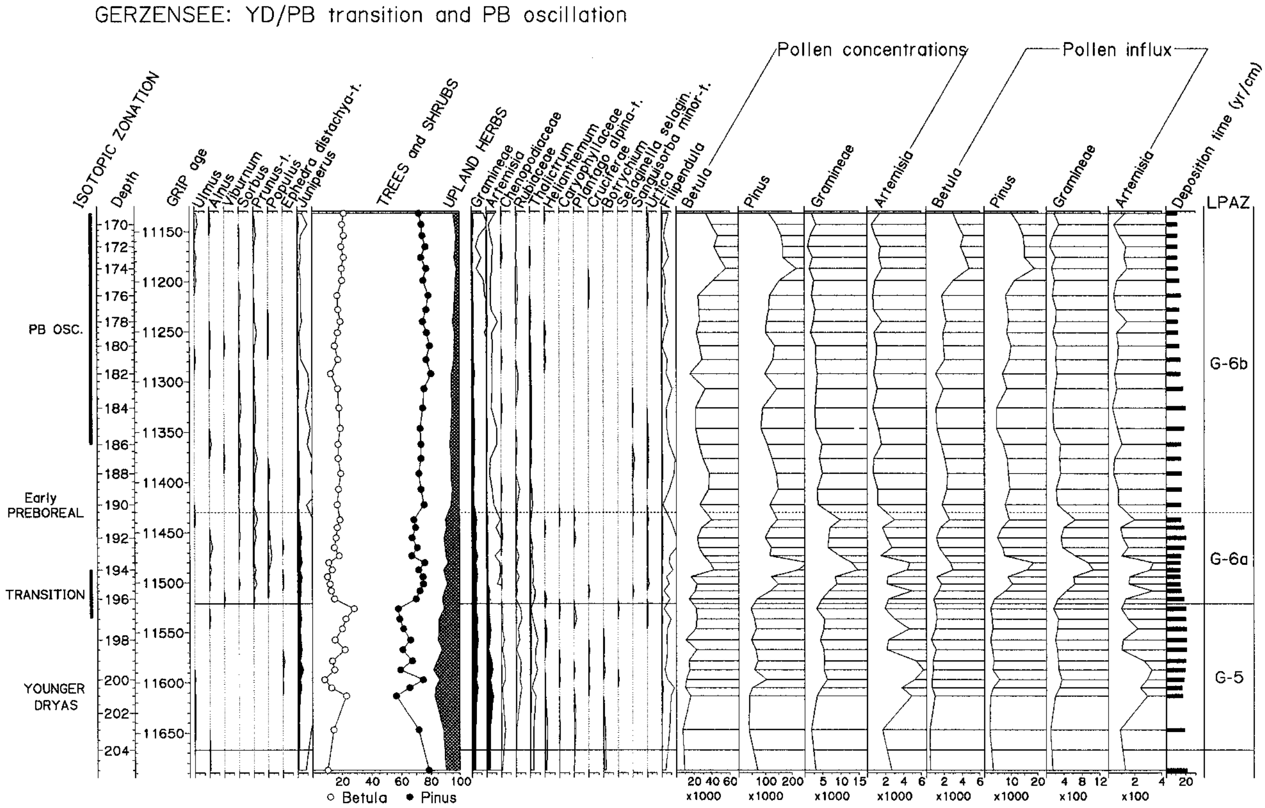

Fig. 2. Younger Dryas/Preboreal transition and Preboreal oscillation at Gerzensee: pollen percentages, concentrations, and influx of major taxa.

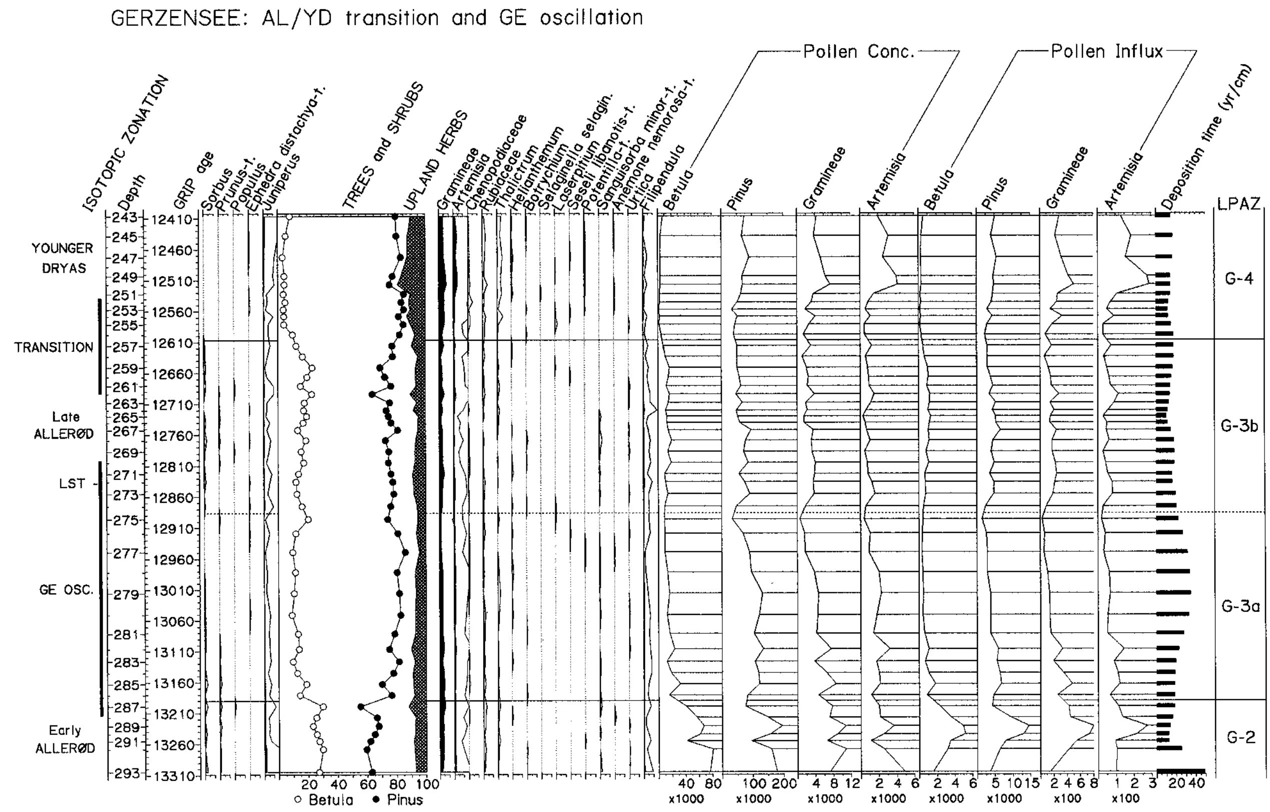

Fig. 8. Allerød/Younger Dryas transition and Gerzensee oscillation at Gerzensee: pollen percentages, concentrations, and influx of major taxa.

Macrofossils as records of plant responses to rapid Late Glacial climatic changes at three sites in the Swiss Alps

Kazimierz Tobolski [a], Brigitta Ammann [b,*]

[a] *Quaternary Research Institute, University Adam Mickiewicz, Fredry 10, PL-61-701 Poznan, Poland*
[b] *Geobotanical Institute, University of Bern, Altenbergrain 21, CH-3013 Bern, Switzerland*

PPP 2000 159: 251-260

Abstract

Plant macrofossils from the end of the Younger Dryas were analysed at three sites, Gerzensee (603 m asl), Leysin (1230 m asl), and Zeneggen (1510 m asl). For the first two sites an oxygen-isotope record is also available that was used to develop a time scale (Schwander et al., this volume); dates refer therefore to calibrated years according to the GRIP time scale. Around Gerzensee a pine forest with some tree birches grew during the Younger Dryas. With the onset of the isotopic shift initiating the rapid warming (about 11,535 cal. years before 1950), the pine forest became more productive and denser. At Leysin no trees except some juniper scrub grew during the Younger Dryas. Tree birches, pine, and poplar immigrated from lower altitudes and arrived after the end of the isotopic shift (about 11,487 B.P.), i.e., at the beginning of the Preboreal (at about 11,420 B.P.). Zeneggen is situated somewhat higher than Leysin, but single tree birches and pines survived the Younger Dryas at the site. At the beginning of the Preboreal their productivity and population densities increased. Simultaneously shifts from *Nitella* to *Chara* and from silt to gyttja are recorded, all indicating rapidly warming conditions and higher nutrient levels of the lake water (and probably of the soils in the catchment). At Gerzensee the beginning of the Younger Dryas was also analysed: the beginning of the isotopic shift correlates within one sample (about 15 years) to rapid decreases of macrofossils of pines and tree birches.

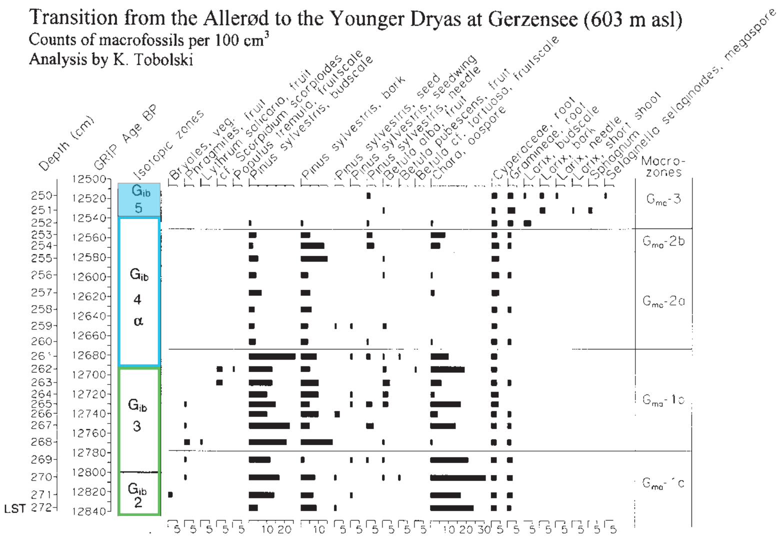

Fig. 1. Gerzensee. Plant macrofossils at the transition α from the Allerød (Gma-1) to the Younger Dryas (Gma-3, i.e., the isotopic low of the Younger Dryas). The rapid isotopic shift occurs in zone Gib-4 or transition a; in the plant-macrofossil zonation Gma-2 is closely related to it. Solid zone limits are statistically significant, dashed ones are not. The sediment is calcareous silt (lake marl) throughout, except for the level 272 cm where the Laacher See Tephra (LST) occurs.

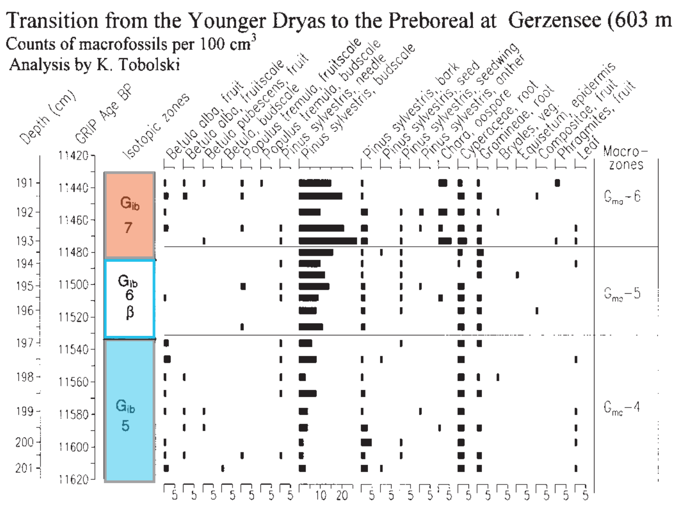

Fig. 2. Gerzensee. Plant macrofossils at the end of the Younger Dryas (transition β). Isotopically this transition corresponds to the zone Gib-6. The sediment is calcareous silt (lake marl) throughout the core section.

Late-glacial fossil midge stratigraphies (Insecta: Diptera: Chironomidae) from the Swiss Alps

Stephen J. Brooks *

Department of Entomology, Natural History Museum, Cromwell Road, London SW7 5BD, UK

PPP 2000 159: 261-279

Abstract

Chironomid midges (Insecta: Diptera: Chironomidae) are sensitive indicators of environmental change, but relatively few studies have been made of the response of European midge faunas to the high amplitude climatic oscillations of the late-glacial. In this study, late-glacial assemblages of chironomid midges from four Swiss lakes, or former lakes, [Gerzensee (603 m), Leysin (1230 m), Regenmoos (1260 m) and Hérémence (2300 m)] were compared and contrasted. The study focused on the response of chironomid assemblages to the beginning and end of the Younger Dryas cold interval (c. 12 690–11 485 cal. yr BP) and to minor cold climatic fluctuations (Gerzensee Oscillation, c.13200–12800 cal. yr BP, and Preboreal Oscillation, c. 113 65–11 100 cal. yr BP). The durations of these climatic fluctuations were defined climato-stratigraphically based on oxygen isotope boundaries and the chronology was derived by correlation with GRIP oxygen isotope records. Major differences in the composition of the four lakes' chironomid assemblages reflected differences in altitude and local environmental conditions. Nevertheless, each lake fauna showed a marked response to the major and minor climatic oscillations, demonstrating that large-scale temperature change had an overriding influence on the distribution of chironomid midges.

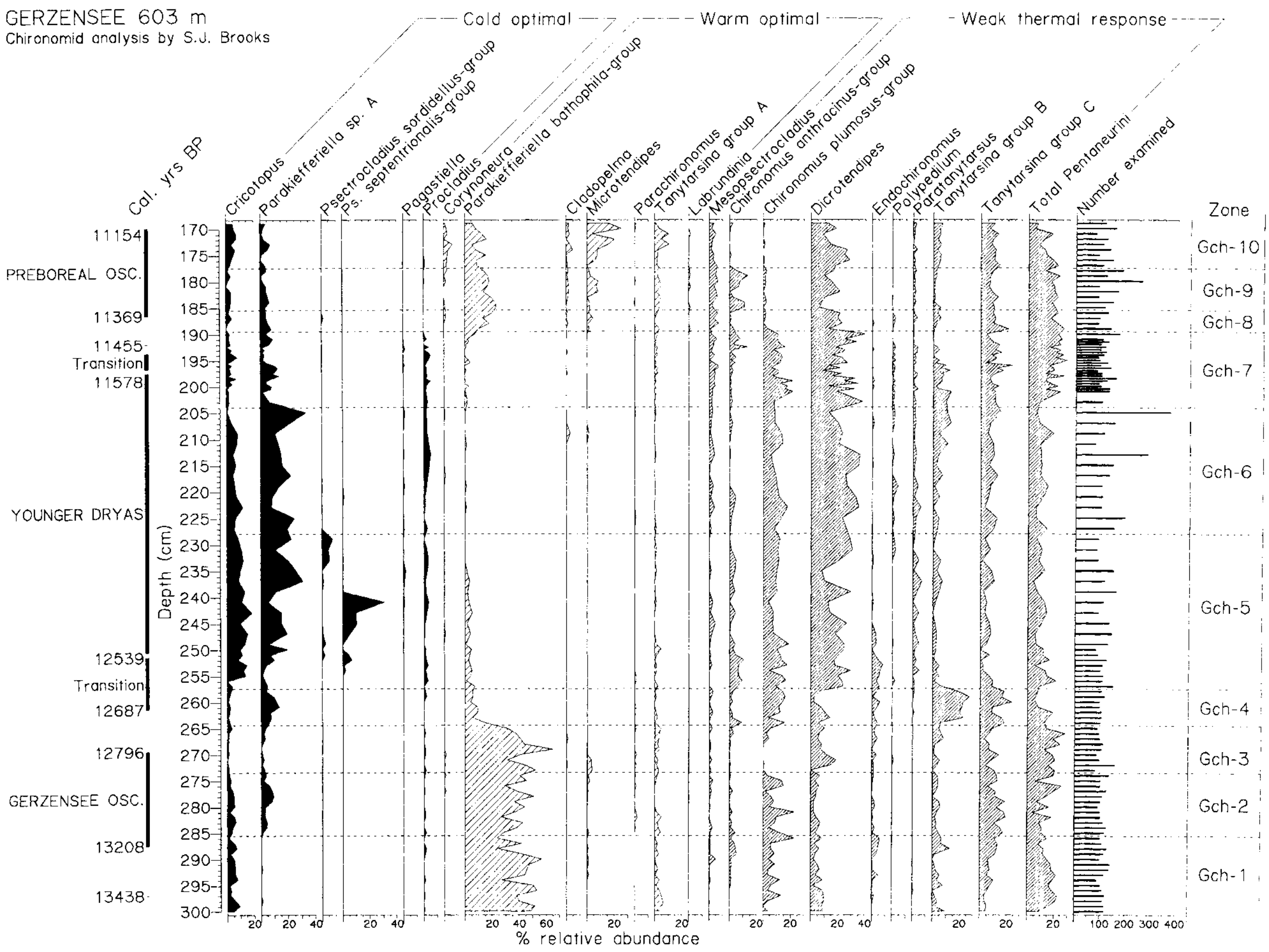

Fig. 1. Late-glacial percentage diagram of selected chironomid taxa from Gerzensee.

Quantification of biotic responses to rapid climatic changes around the Younger Dryas — a synthesis

Brigitta Ammann [a,*], H.J.B. Birks [b,c], Stephen J. Brooks [d], Ulrich Eicher [e], Ulrich von Grafenstein [f], Wolfgang Hofmann [g], Geoffrey Lemdahl [h], Jakob Schwander [e], Kazimierz Tobolski [i], Lucia Wick [a]

[a] *Geobotanical Institute, University of Bern, Altenbergrain 21, CH-3013 Bern, Switzerland*
[b] *Botanical Institute, University of Bergen, Allégaten 41, N-5007 Bergen, Norway*
[c] *Environmental Change Research Centre, University College London, 26 Bedford Way, London WC1H 0AP, UK*
[d] *Entomology Department, The Natural History Museum, Cromwell Road, London SW7 5BD, UK*
[e] *Physics Institute, University of Bern, Sidlerstarsse 5, CH-3012 Bern, Switzerland*
[f] *CFR, CEA-CNRS, Domaine du CNRS, Avenue de la Terrasse, F-91198 Gif-sur-Yvette, France*
[g] *Max-Planck Institute of Limnology, P.O. Box 165, D-24302 Plön, Germany*
[h] *Department of Engineering and Natural Sciences, University of Växjö, S-35195 Växjö, Sweden*
[i] *Quaternary Research Institute, University Adam Mickiewicz, Fredry 10, PL-61-701 Poznan, Poland*

PPP 2000 159: 313-347

Abstract

To assess the presence or absence of lags in biotic responses to rapid climatic changes, we: (1) assume that the $\delta^{18}O$ in biogenically precipitated carbonates record global or hemispheric climatic change at the beginning and at the end of the Younger Dryas without any lag at our two study sites of Gerzensee and Leysin, Switzerland; (2) derive a time scale by correlating the $\delta^{18}O$ record from these two sites with the $\delta^{18}O$ record of the GRIP ice core; (3) measure $\delta^{18}O$ records in ostracods and molluscs to check the record in the bulk samples and to detect possible hydrological changes; (4) analyse at Gerzensee and Leysin as well as at two additional sites (that lack carbonates and hence a $\delta^{18}O$ record) pollen, plant macrofossils, chironomids, beetles and other insects, and Cladocera; (5) estimate our sampling resolution using the GRIP time scale for the isotope stratigraphies and the biostratigraphies; and (6) summarise the major patterns of compositional change in the biostratigraphies by principal component analysis or correspondence analysis. We conclude that, at the major climatic shifts at the beginning and end of the Younger Dryas, hardly any biotic lags occur (within the sampling resolution of 8–30 years) and that upland vegetation responded as fast as aquatic invertebrates. We suggest that the minor climatic changes associated with the Gerzensee and Preboreal oscillations were weakly recorded in the biostratigraphies at the lowland site, but were more distinct at higher altitudes. Individualistic responses of plant and animal species to climatic change may reflect processes in individuals (e.g. productivity and phenology), in populations (e.g. population dynamics), in spatial distributions (e.g. migrations), and in ecosystems (e.g. trophic state). We suggest that biotic responses may be telescoped together into relatively short periods (50 to 150 years), perhaps disrupting functional interactions among species and thus destabilising ecosystems.

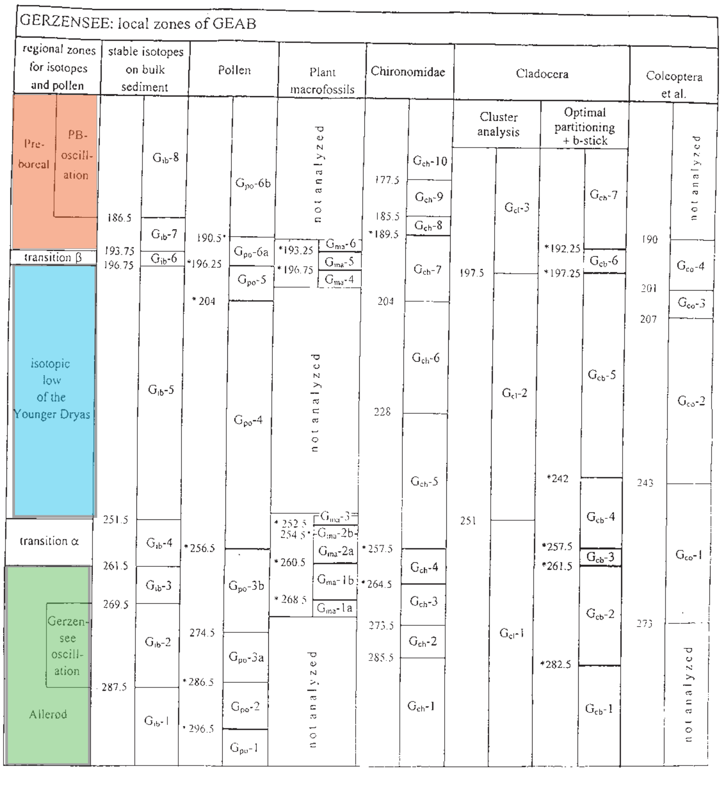

Fig. 1. Local zone boundaries at Gerzensee for isotope and biostratigraphies. The subscripts mean: ib, oxygen isotopes measured on bulk sediment; p, pollen; pm, plant macrofossils; ch, chironomids; cl, Cladocera (based on cluster analysis); cb, Cladocera (based on optimal partitioning and broken-stick model); co, Coleoptera. Zone boundaries with an asterisk and a heavy line are statistically significant after optimal partitioning (Birks and Gordon, 1985) and comparison with the broken-stick (b-stick) model (Bennett, 1996). Zone boundaries suggested by optimal partitioning, but not significant compared with the broken-stick model, have a black dot and thin lines. For plant macrofossils the statistical significance of zone boundaries is not directly comparable with the other biostratigraphies, because shorter core sections were analysed.

Transition from the Younger Dryas to the Preboreal
Gerzensee (603 m asl)

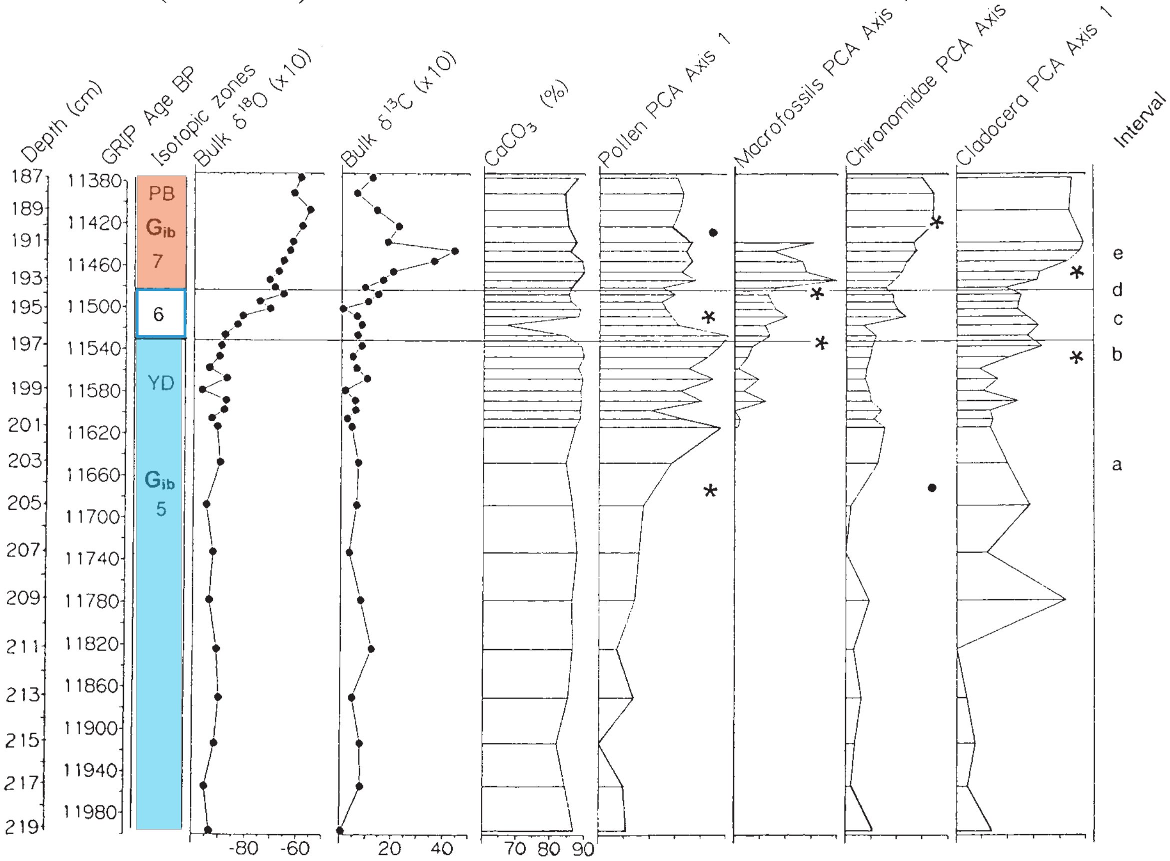

Fig. 5. The transition from the Younger Dryas to the Preboreal at Gerzensee: stable isotopes (as per mille PDB), carbonate content, and the scores of the first PCA axes for pollen, plant macrofossils, chironomids, and Cladocera. These scores give an estimate of the overall compositional change between two adjacent samples. The isotopic zone G_{ib}-6 corresponds to the transition β. The four intervals labelled b, c, d, e refer to the possible internal structure around this transition, see Table 5. For comparison the levels of zone boundaries proposed by optimal partitioning and assessed as 'statistically significant' (asterisk) or not significant (black dot) are indicated.

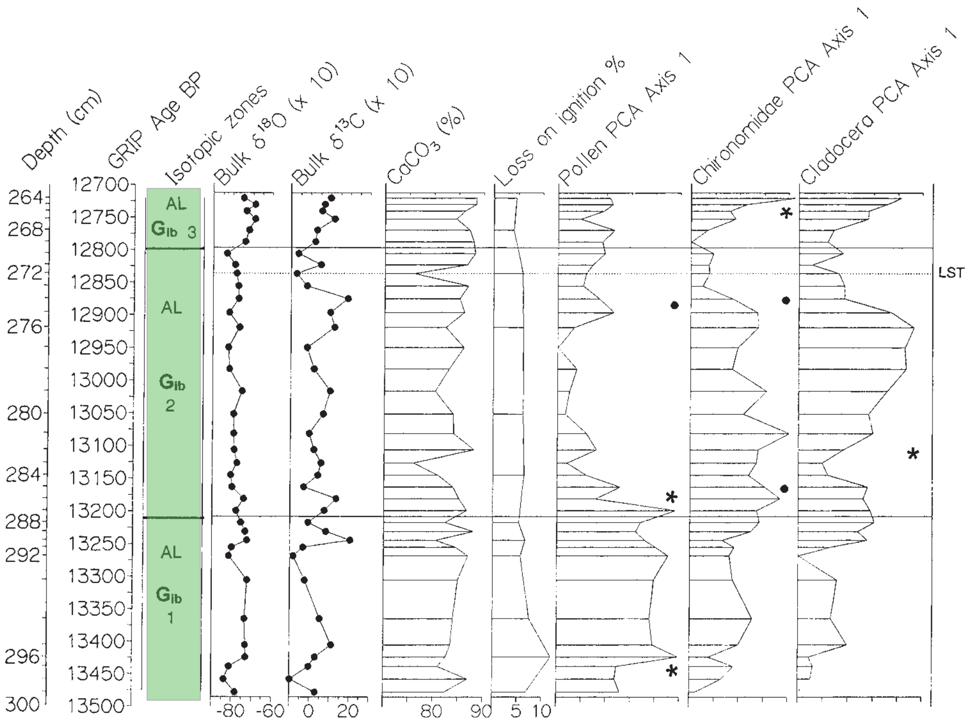

Fig. 11. The Gerzensee oscillation at Gerzensee: stable isotopes, carbonate content, loss on ignition, and the scores of the first PCA axes for pollen, chironomids, and cladocera. The isotopic zone G_{ib}-2 corresponds to the Gerzensee oscillation. At 272 cm (about 12,836 yrs B.P.) the Laacher See Tephra (LST) was found.

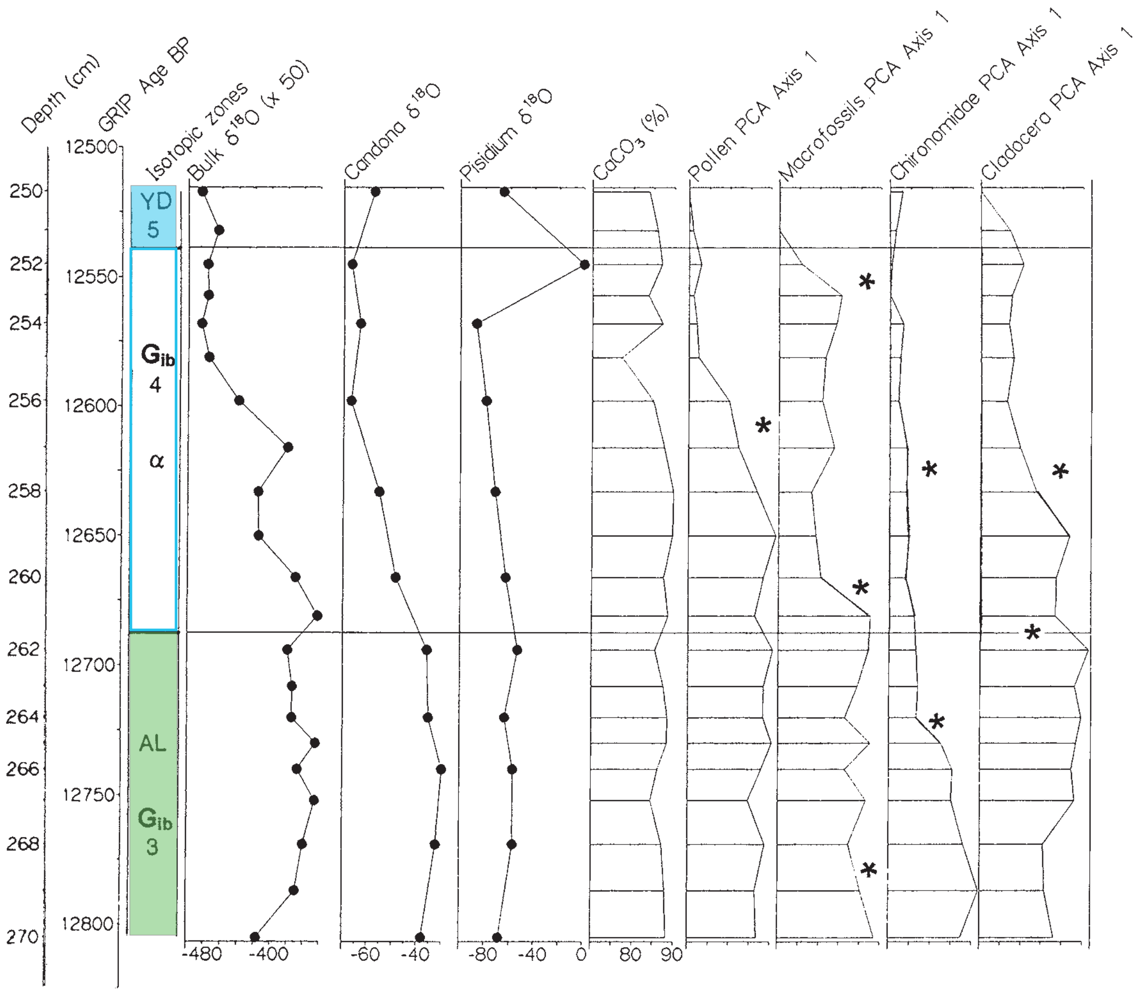

Fig. 9. The transition from the Allerød to the Younger Dryas at Gerzensee: stable isotopes of bulk samples (as per mille PDB), of *Candona* (short for *Pseudocandona marchica*), and *Pisidium*, carbonate content of the sediment, and the scores of the first PCA axes for pollen, plant macrofossils, chironomids, and cladocera. The isotopic zone G_{ib}-4 corresponds to the transition α.

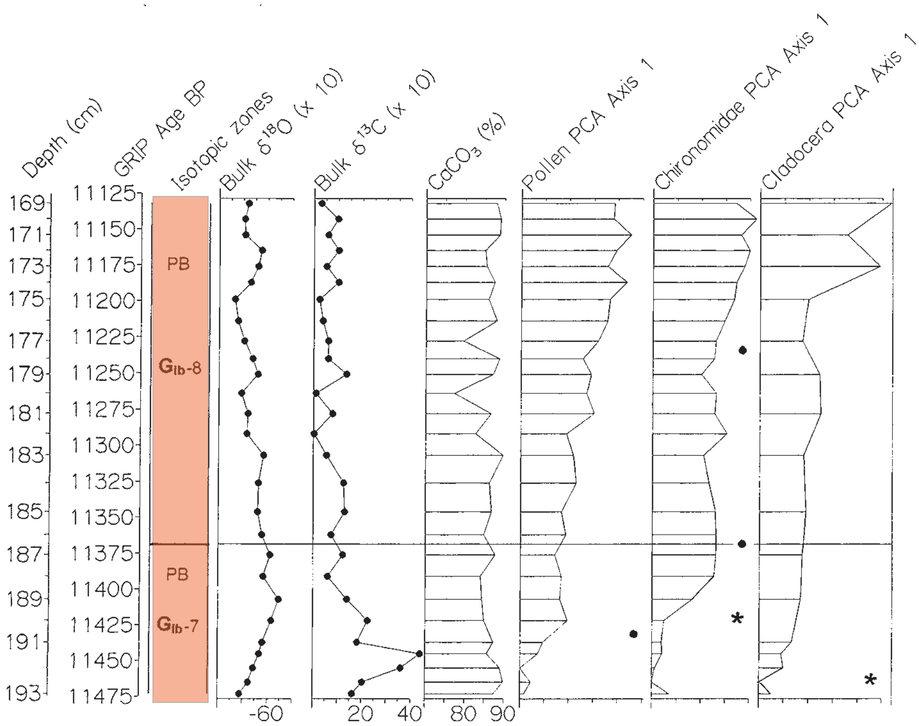

Fig. 13. The Preboreal oscillation at Gerzensee: stable isotopes, carbonate content, and the scores of the first PCA axes for pollen, chironomids, and cladocera. The isotopic zone G_{ib}-8 corresponds to the Preboreal oscillation; its end was not reached in this record.

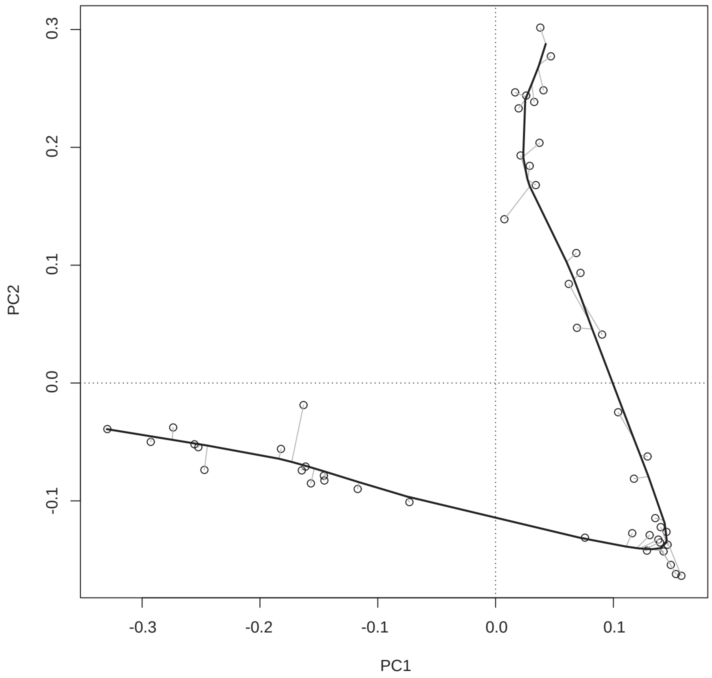

Fig. 9.23 Principal component analysis (PCA) plot of the Abernethy Forest late-glacial and early-Holocene pollen data with the fitted principal curve superimposed (*thick line*). The *thin, grey lines* join each observation with the point on the principal curve on which they project, and are the distances minimised during fitting. *PC* principal component. (Simpson & Birks 2012)

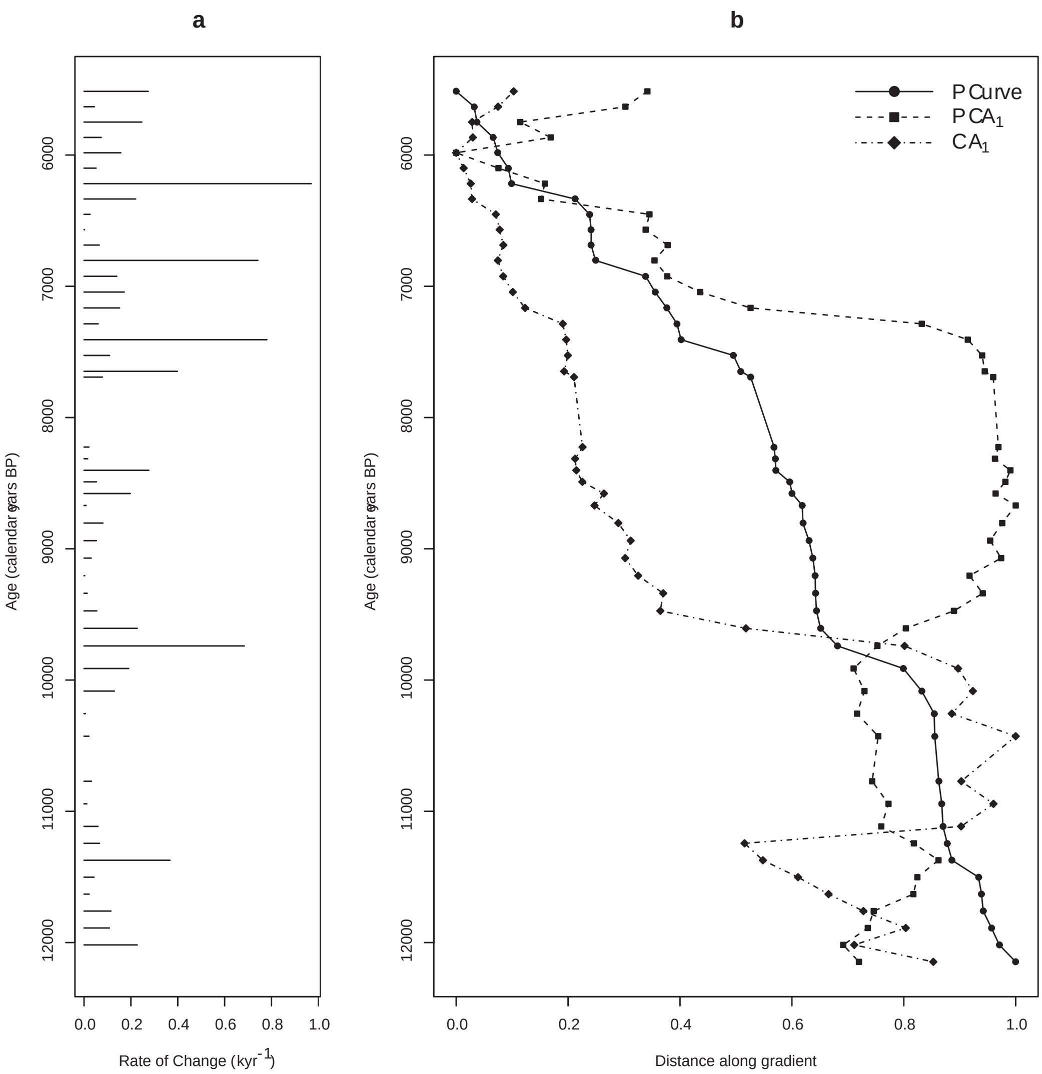

Fig. 9.24 (*left*) Distance along the principal curve expressed as a rate of change per kyr between samples for the Abernethy Forest pollen data-set. Several periods of rapid compositional change are detected. (*right*) Distance along the gradient expressed as a proportion of the total gradient for the fitted principal curve and the first ordination axes respectively of a principal component analysis (PCA) and a correspondence analysis (CA) fitted to the Abernethy Forest data. (Simpson & Birks 2012)

Chitinous invertebrate remains as indicators of past methane availability in lakes

Oliver Heiri, Institute of Plant Sciences and Oeschger Centre for Climate Change Research, University of Bern,
oliver.heiri@ips.unibe.ch

Figure 1. *Daphnia* ephippium (right), *Ceriodaphnia* ephippium (center), *Plumatella* statoblast (right). Photos: O. Heiri.

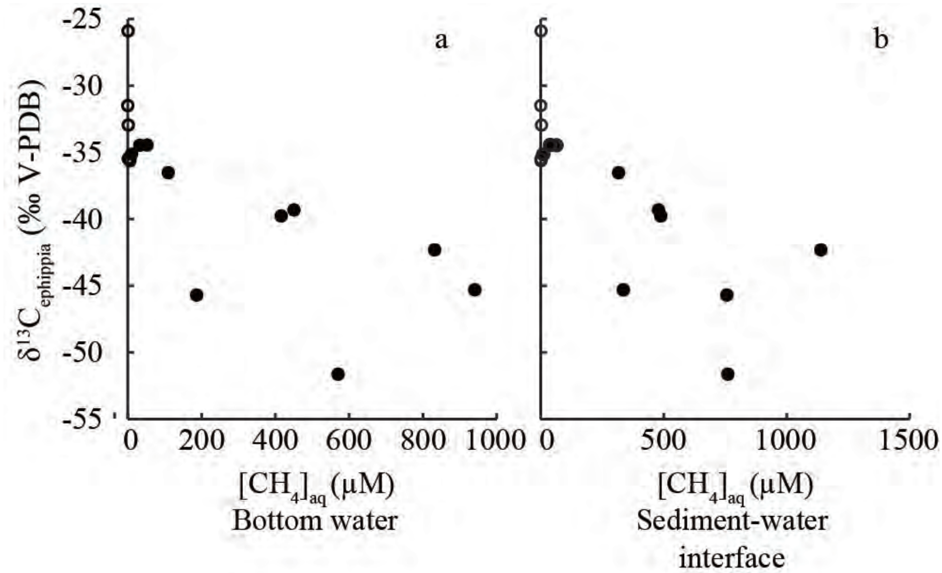

Figure 2. Relationship between $\delta^{13}C$ values of *Daphnia* ephippia in 15 small lakes in Finland, Sweden, Germany and Switzerland and methane concentrations (a) 1 m and (b) 10 cm above the sediment. From Schilder (2014) and Schilder et al. (2015).

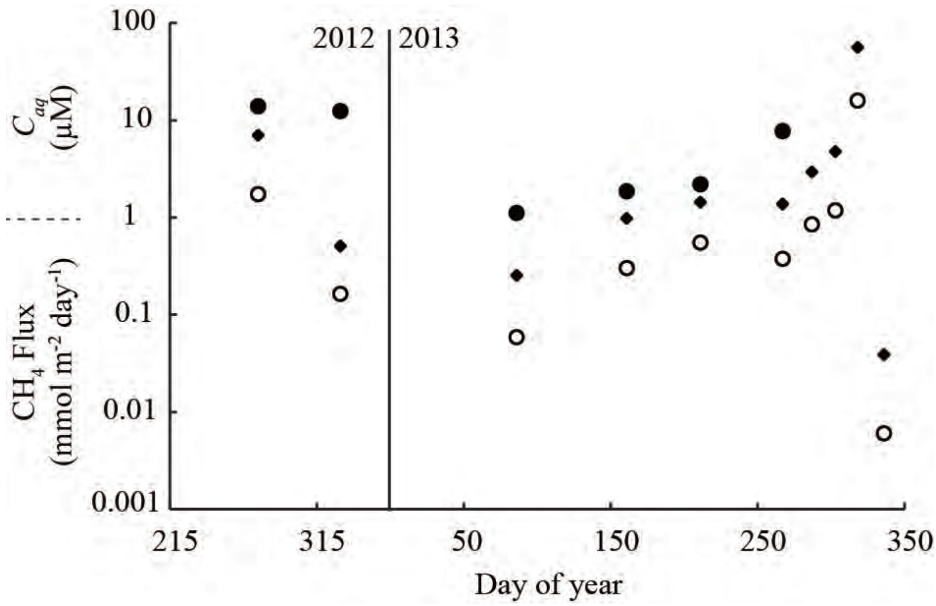

Figure 3. Average methane concentrations in the surface waters (diamonds) together with average diffusive flux (open circles) and total flux (filled circles) of methane measured for Lake Gerzensee in 2012/2013. From Schilder (2014) and Schilder et al. (2016).

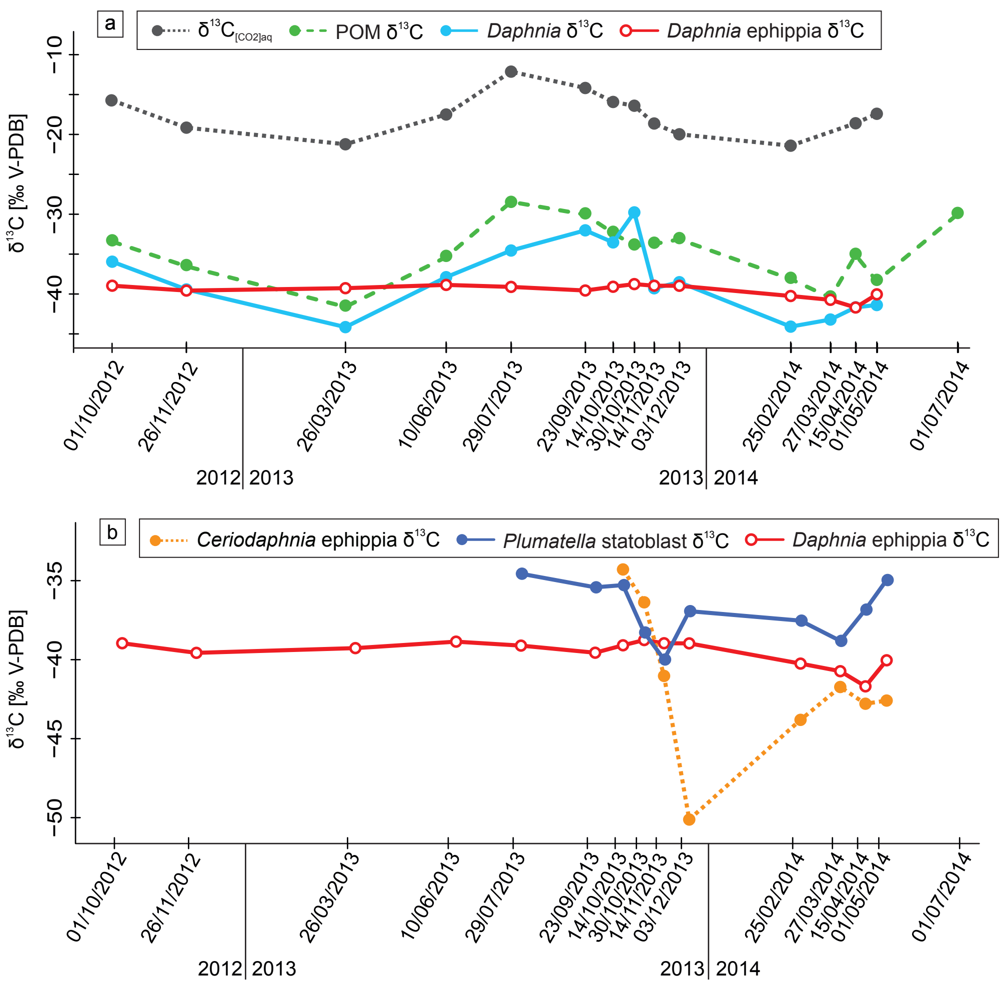

Figure 4. Isotopic composition of CO2 ($\delta^{13}C_{[CO2]aq}$), particulate organic matter (POM $\delta^{13}C$), *Daphnia*, *Daphnia* ephippia, *Ceriodaphnia* ephippia and *Plumatella* statoblasts in samples collected from Gerzensee in 2012-2014. From Morlock (2014) and Morlock et al. (submitted).

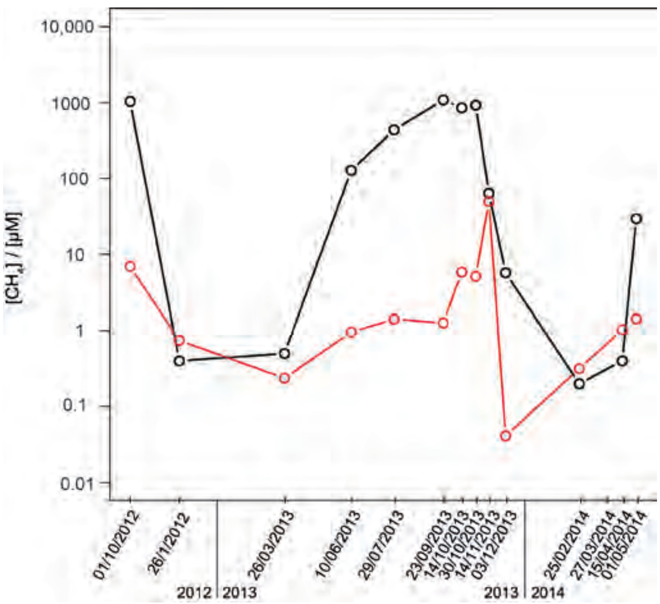

Figure 5. Methane concentrations in the lake centre of Gerzensee 2012-2014 measured 1 m above the sediment (black) and in the surface water (red). From Morlock (2014) and Morlock et al. (submitted).

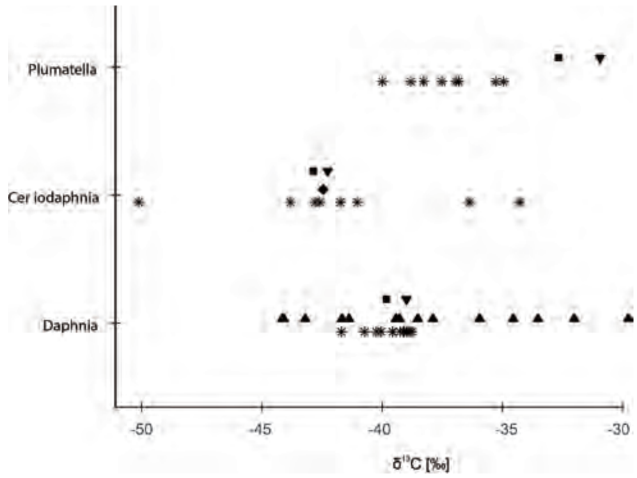

Figure 6. Ranges of $\delta^{13}C$ values measured for three groups of chitinous invertebrate remains in Gerzensee (*Daphnia* ephippia, *Ceriodaphnia* ephippia, *Plumatella* statoblasts). Stars represent $\delta^{13}C$ values of remains collected in the flotsam of the lake during fieldwork in 2012-2014, and triangles represent $\delta^{13}C$ values of living *Daphnia* collected during the same period. The diamond represents a measurement from the sediment trap exposed in the lake in 2012/13. Squares and inverse triangles represent measurements from two separate surface sediment samples. From Morlock (2014) and Morlock et al. (submitted).

References

Morlock, M. 2014. *Stable carbon isotopes of cladoceran and bryozoan remains in Lake Gerzensee: implications for their use to reconstruct past methane abundance*. MSc thesis, University of Bern.

Morlock, M., J. Schilder, M. van Hardenbroek, S. Szidat, M.J. Wooller, O. Heiri, submitted. Seasonality of cladoceran and bryozoan resting stage $\delta^{13}C$ values: Implications for their use as palaeolimnological indicators of lacustrine carbon cycle dynamics. *Journal of Paleolimnology.*

Schilder, J. 2014. *Methanogenic Carbon in Daphnia Tissue as an Indicator of Lacustrine Methane Budgets. Observations from the Field, Experiments and Fossil Records*. PhD thesis, University of Bern.

Schilder, J., D. Bastviken, M. van Hardenbroek, M. Leuenberger, P. Rinta, T. Stötter, O. Heiri, 2015. The stable carbon isotopic composition of Daphnia ephippia in small, temperate lakes reflects in-lake methane availability. *Limnology and Oceanography* 60: 1064–1075.

Schilder, J. D. Bastviken, M. van Hardenbroek, O. Heiri, 2016. Spatiotemporal patterns in methane flux and gas transfer velocity at low wind speeds: Implications for upscaling studies on small lakes. *Journal of Geophysical Research Biogeosciences*, in press.

Faulenseemoos: Threats to unique natural archives and restoration efforts, first influx calculations worldwide by Max Welten

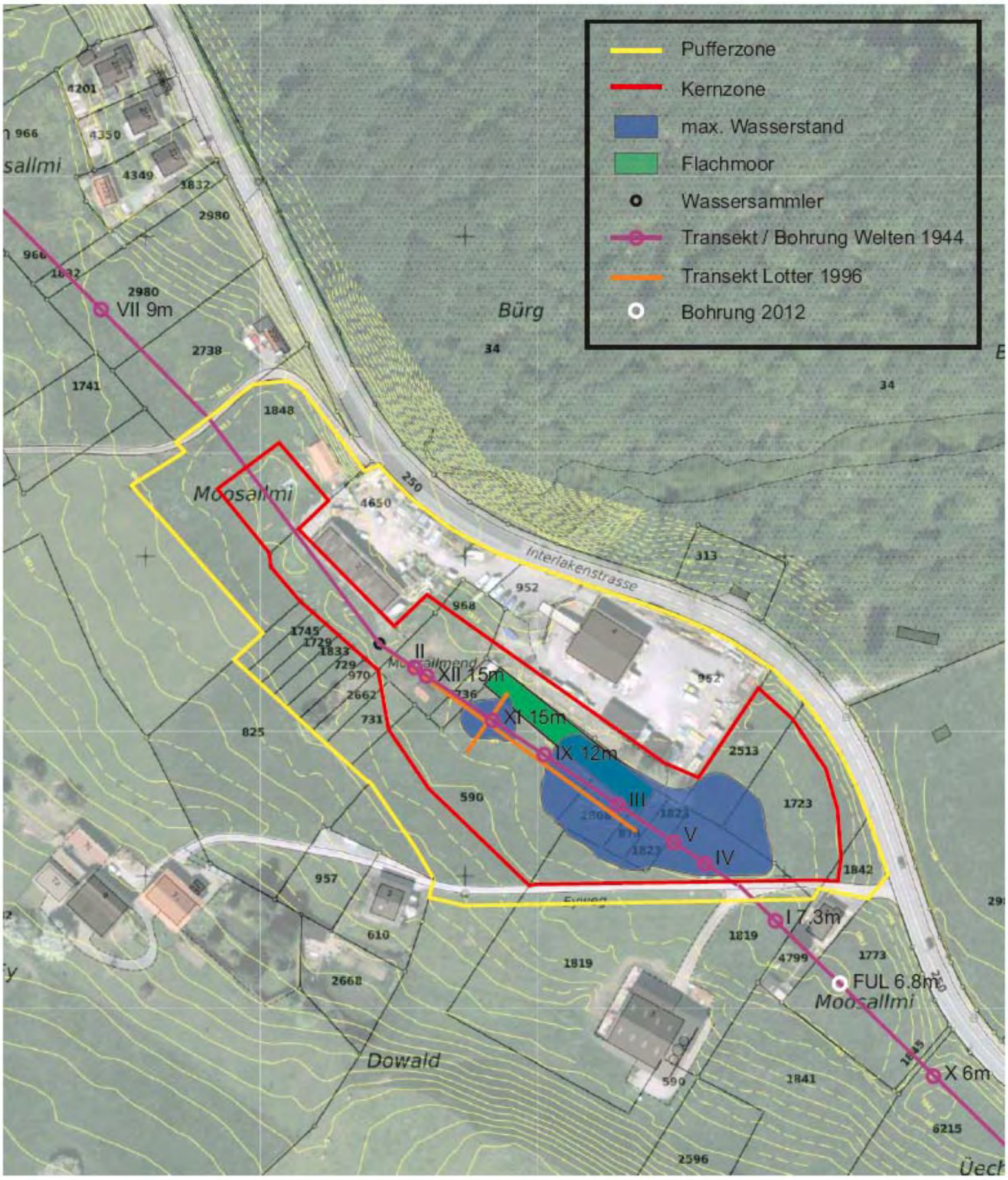

Perimeter Geotop Faulenseemoos (version November 2012)

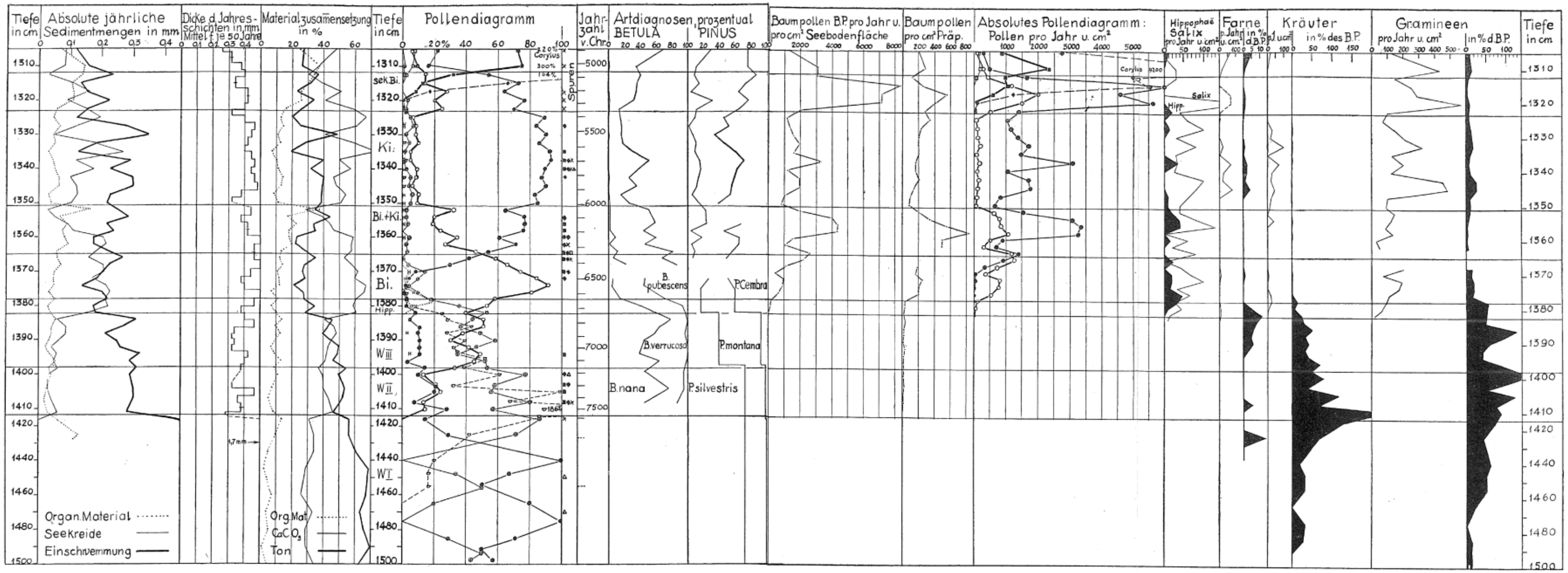

Abb. 16. Faulenseemoos. Pollen- und Sedimentdiagramm XII.

Fig. 1 Pollen and sediment-diagram of Faulenseemoos. The diagram shows (from left) annual sediment accululation rates (mm), varve thickness (mm), sediment composition (%), pollen percentages, influx and concentrations. (Welten 1944)

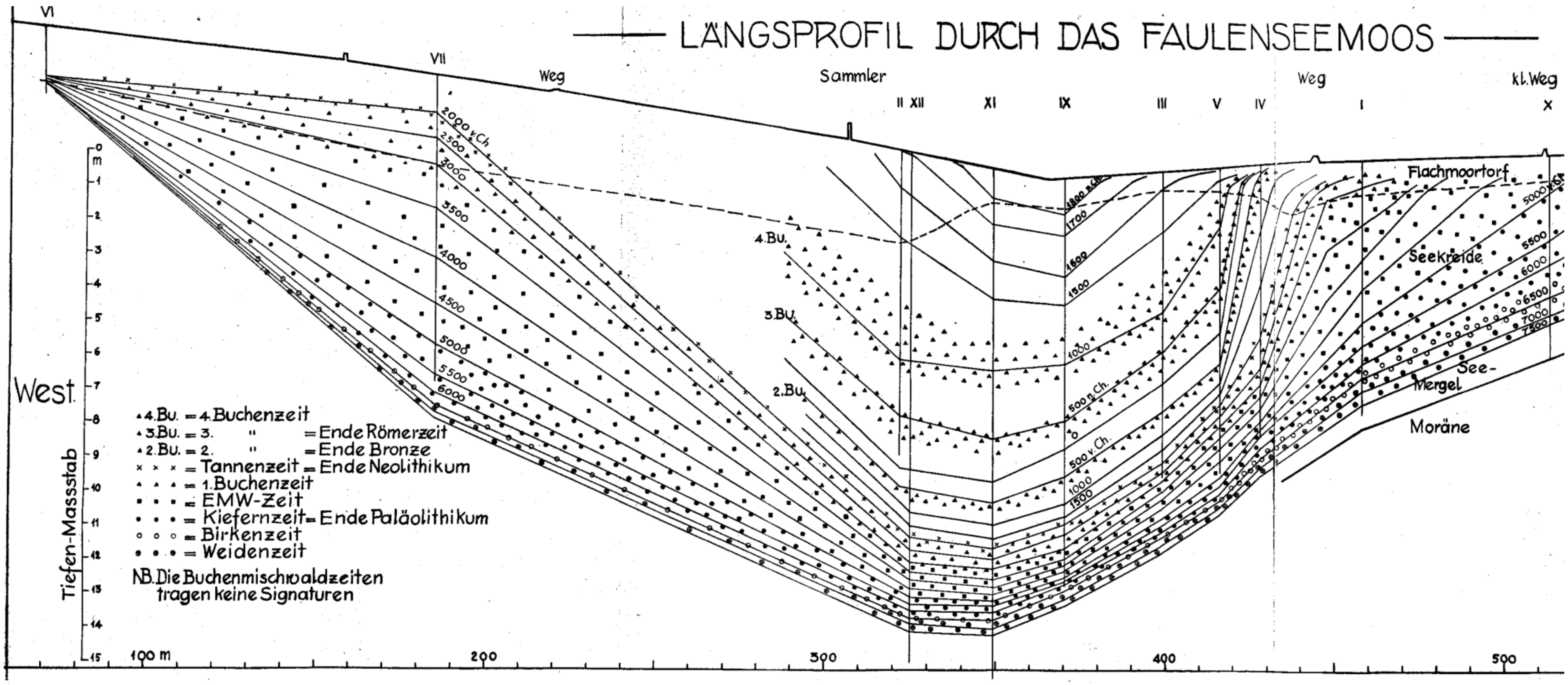

Abb. 26. Längsprofil des Faulenseemooses. Fünfhundertjahres-Zuwachskurven. Die römischen Ziffern bezeichnen die Lage der Bohrprofile

Fig. 2 Transect trhough the Faulenseemoos with ages given in 500 year steps. Roman numerals and vertical lines indicate coring sites. (Welten, 1944)

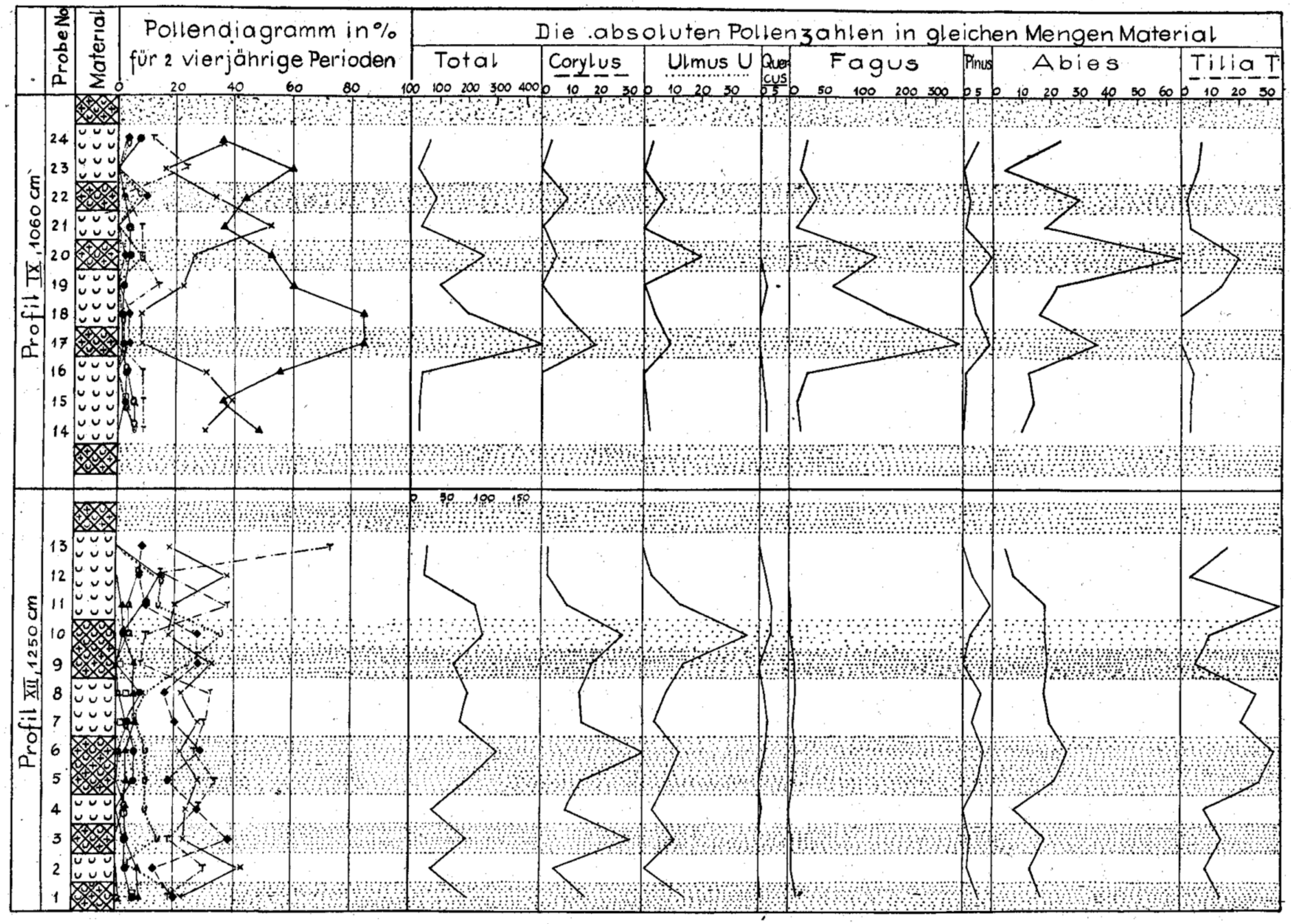

Fig. 3 Paleontological evidence of annual laminations. White: white laminae, summer. Dotted: brown laminae, autumn, winter, early spring. Pollen counts are presented in the usual way of a pollen diagram. (Welten, 1944)

Pact 50 - II.5 : André F. Lotter, Brigitta Ammann, Irena Hajdas, Michael Sturm
and Jacqueline van Leeuwen

Faulenseemoos Revisited : New Results from an Old Site

Because something is happening here
But you don't know what it is
R.A. Zimmerman, 1965, Ballad of a thin man

Abstract

The classical annually laminated site of Faulenseemoos, Switzerland, is currently being reinvestigated using various palaeoecological methods : pollen, magnetic susceptibility, geochemistry, microstratigraphy. The lithology of the sedimentary basin is described. Unfortunately the sediments did not provide the expected late-glacial laminated sediments. The research strategy for the study of Holocene dynamics in the pollen curve of beech is presented.

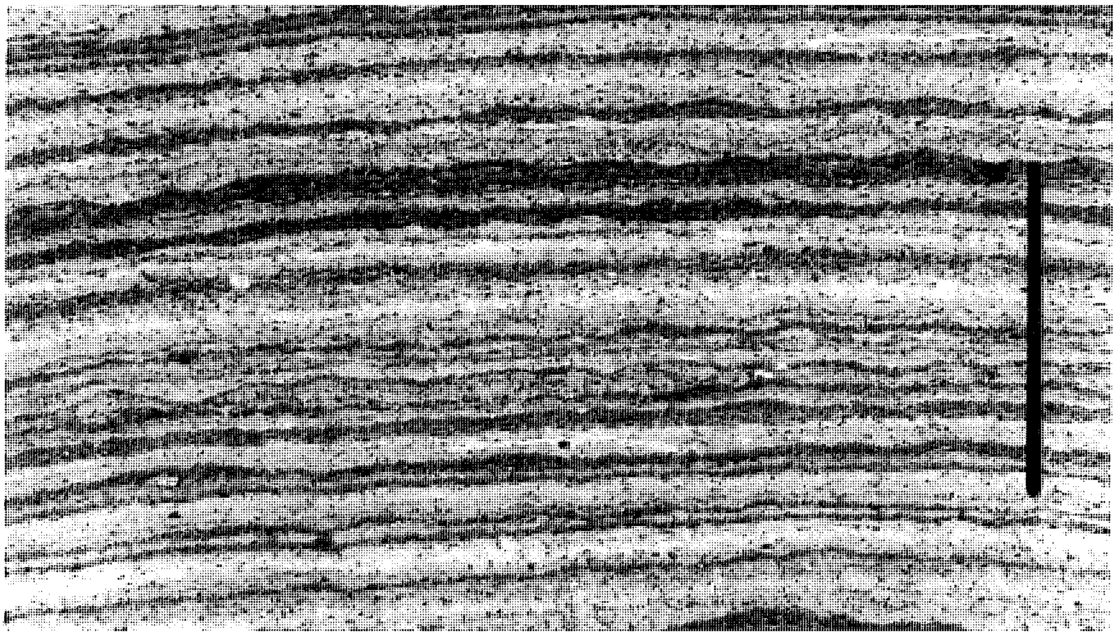

Fig. 3. Microstratigraphy of laminations. The sediment for this petrographic thin-section was taken in core FSM91-14 at a sediment depth of c. *1220 cm. Light layers consist of calcium carbonate (late spring and summer layer), whereas dark layers consist of organic detritus (autumn, winter, and early spring layer). Scale bar = 5 mm.*

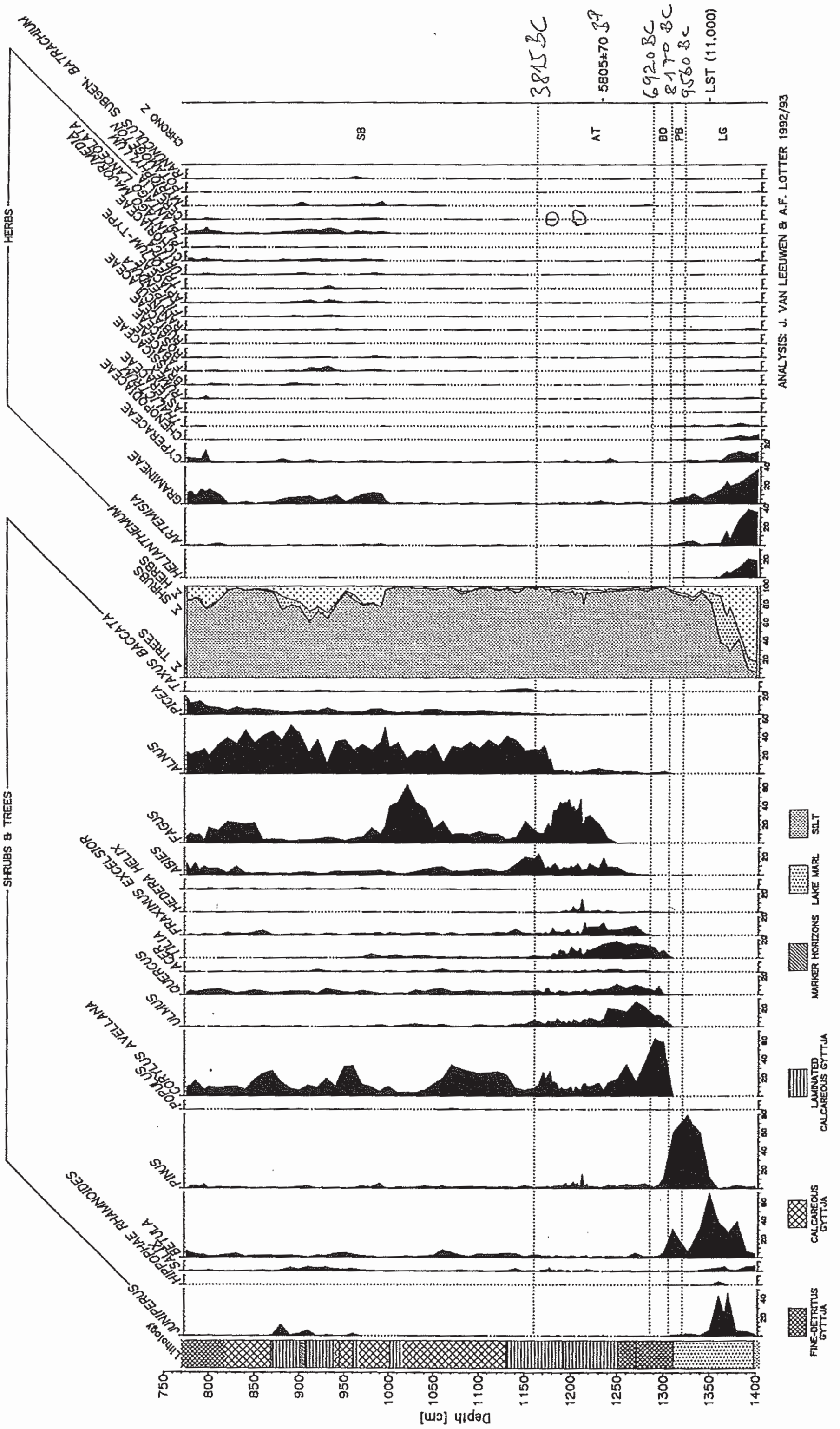

Fig. 5. Pollen diagram of Faulenseemoos core FSM91-14/15 including the sediment between the late-glacial (LG) and Subboreal (SB) chronozones. Only the most prominent taxa are shown. LST marks the Laacher See Tephra layer.

Thursday 08.09.2016

8:30 h	Departure to Lauenensee
9:30 h	**Lauenensee**: Vegetation and fire history of mountain environments, early human impact during the Neolithic and Bronze Age, high resolution series (Fabian Rey)
10:30 h	Chironomids as a proxy for temperature changes in the Alps (Oliver Heiri)
11 h	Departure to Gsteig
11:45 h	Cable car to Sénin and hike to Col du Sanetsch (2.5 hours). Alternative: Bus to Col du Sanetsch. Lunch en route.
14:45 h	**Col du Sanetsch**: Vegetation and fire history (Christoph Schwörer)
15:15 h	Past, present and future of treeline environments, the **Iffigsee** study (Christoph Schwörer)
16:15 h	Prehistory of pass environments, ice patch archaeology of Schnidejoch (Christoph Schwörer)
16:45 h	Frozen fire: Monte Rosa ice core palynology (Sandra Brügger)
17:30 h	Departure to Sion
18:30 h	Arrival at Hôtel Castel (Sion)
19:30 h	Dinner at Restaurant Cave de Tous-Vents (Sion)

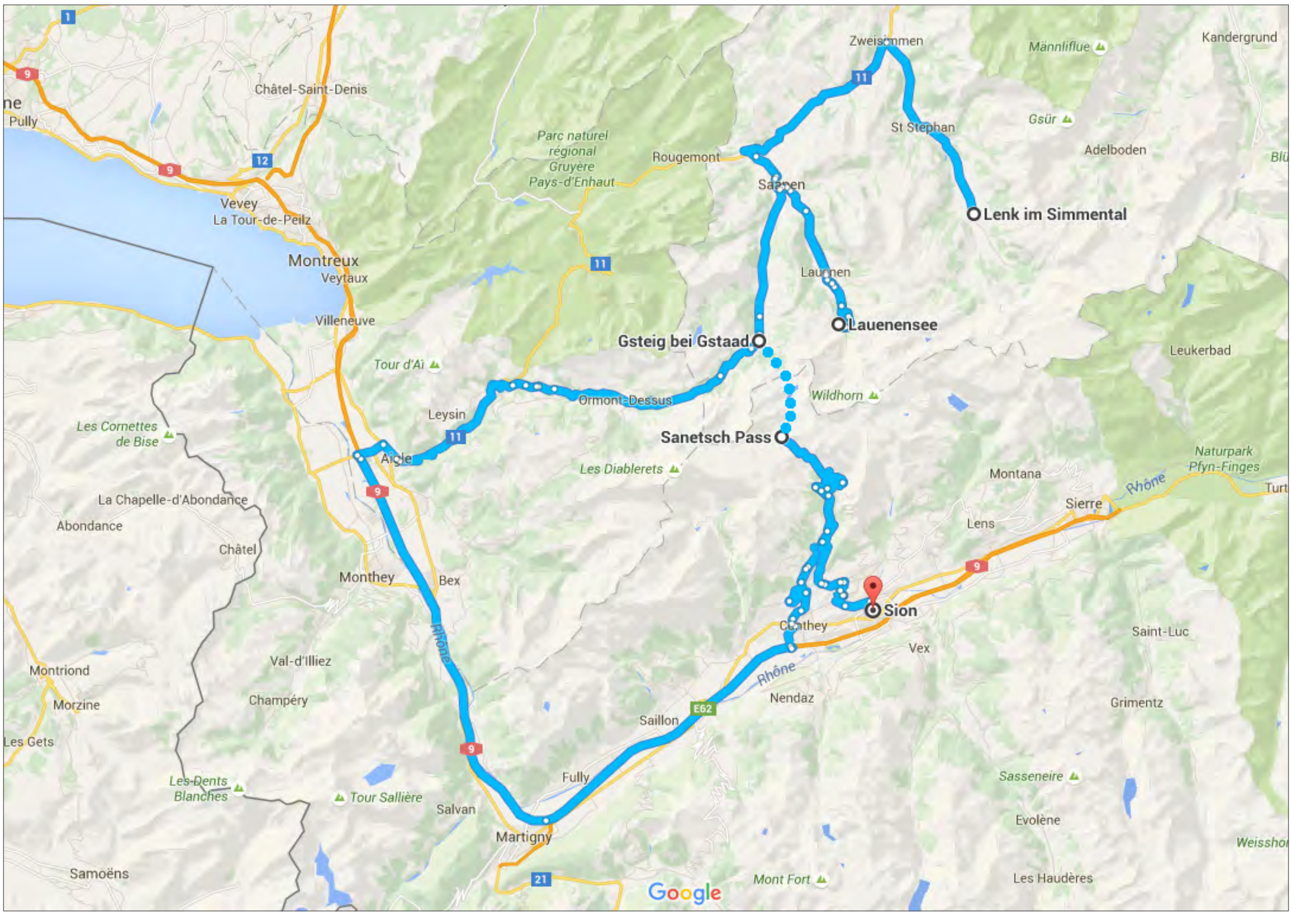

Research paper

Climatic and human impacts on mountain vegetation at Lauenensee (Bernese Alps, Switzerland) during the last 14,000 years

The Holocene
0(0) 1–13

Reprints and permissions:
sagepub.co.uk/journalsPermissions.nav
DOI: 10.1177/0959683613489585
hol.sagepub.com
SAGE

Fabian Rey, Christoph Schwörer, Erika Gobet, Daniele Colombaroli, Jacqueline FN van Leeuwen, Silke Schleiss and Willy Tinner

Abstract

Lake sediments from Lauenensee (1381 m a.s.l.), a small lake in the Bernese Alps, were analysed to reconstruct the vegetation and fire history. The chronology is based on 11 calibrated radiocarbon dates on terrestrial plant macrofossils suggesting a basal age of 14,200 cal. BP. Pollen and macrofossil data imply that treeline never reached the lake catchment during the Bølling–Allerød interstadial. Treeline north of the Alps was depressed by c. 300 altitudinal meters, if compared with southern locations. We attribute this difference to colder temperatures and to unbuffered cold air excursions from the ice masses in northern Europe. Afforestation started after the Younger Dryas at 11,600 cal. BP. Early-Holocene tree-*Betula* and *Pinus sylvestris* forests were replaced by *Abies alba* forests around 7500 cal. BP. Continuous high-resolution pollen and macrofossil series allow quantitative assessments of vegetation dynamics at 5900–5200 cal. BP (first expansion of *Picea abies*, decline of *Abies alba*) and 4100–2900 cal. BP (first collapse of *Abies alba*). The first signs of human activity became noticeable during the late Neolithic c. 5700–5200 cal. BP. Cross-correlation analysis shows that the expansion of *Alnus viridis* and the replacement of *Abies alba* by *Picea abies* after c. 5500 cal. BP was most likely a consequence of human disturbance. *Abies alba* responded very sensitively to a combination of fire and grazing disturbance. Our results imply that the current dominance of *Picea abies* in the upper montane and subalpine belts is a consequence of anthropogenic activities through the millennia.

Keywords

Bernese Alps, cross-correlation, human impact, *Picea abies* expansion, treeline, vegetation history

Received 16 January 2013; revised manuscript accepted 3 April 2013

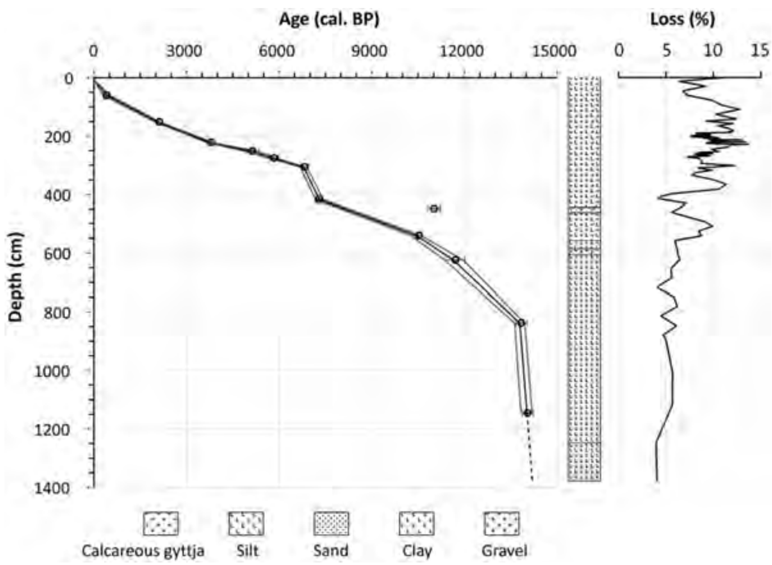

Figure 2. Age–depth model of Lauenensee, lithology column and loss-on-ignition at 550°C (from left to right). Circles in the age–depth model show the calibrated ages of terrestrial macrofossils. The black line is the calculated model with a 2σ envelope (grey lines) (*clam*, Blaauw, 2010).

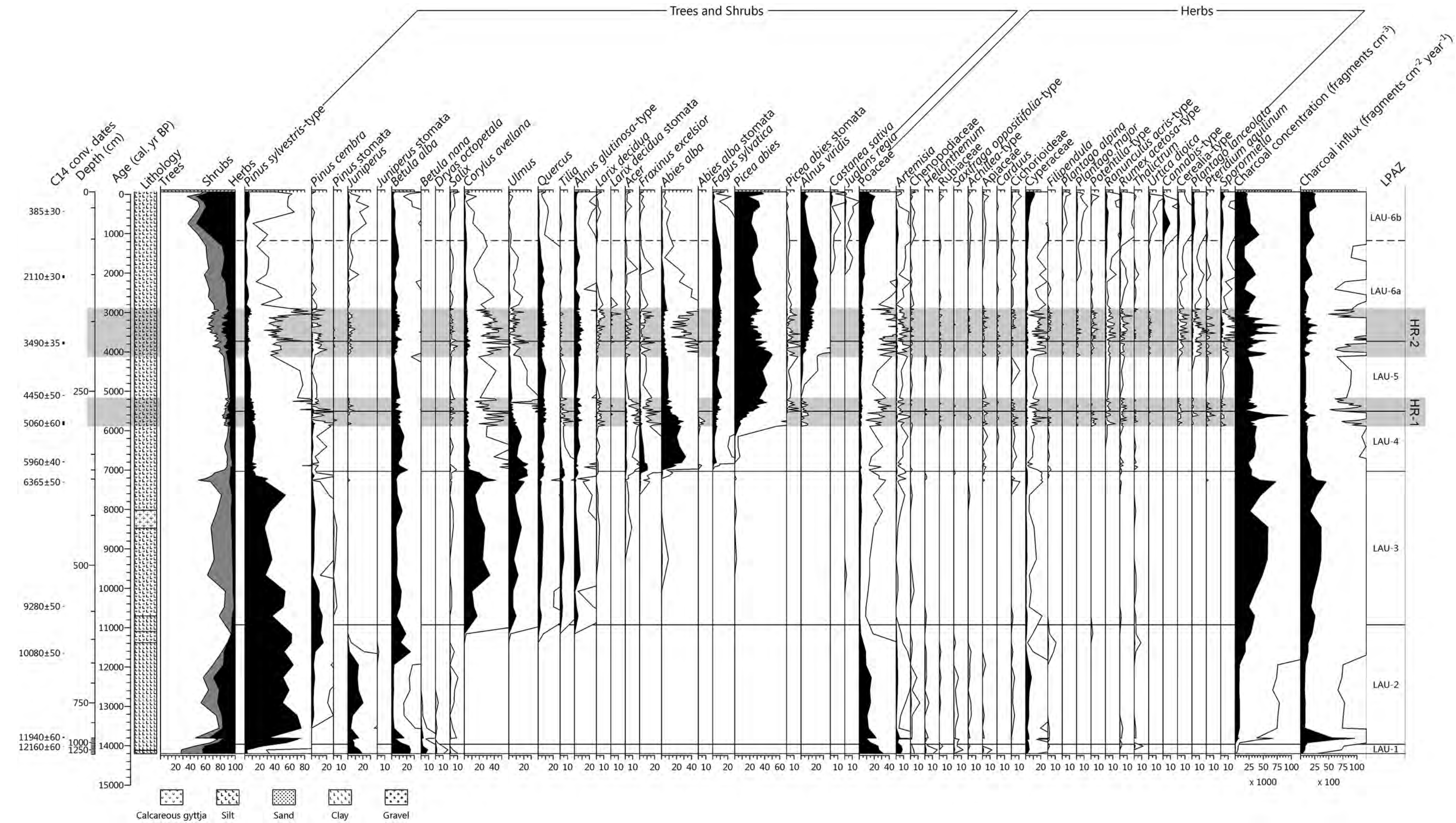

Figure 3. Pollen and stomata percentage and microscopic charcoal influx diagram of Lauenensee (selected taxa). The empty curves show the 10× exaggerations. The grey bands mark the position of the two high-resolution sequences HR 1 and HR 2 (Analysis: Fabian Rey).

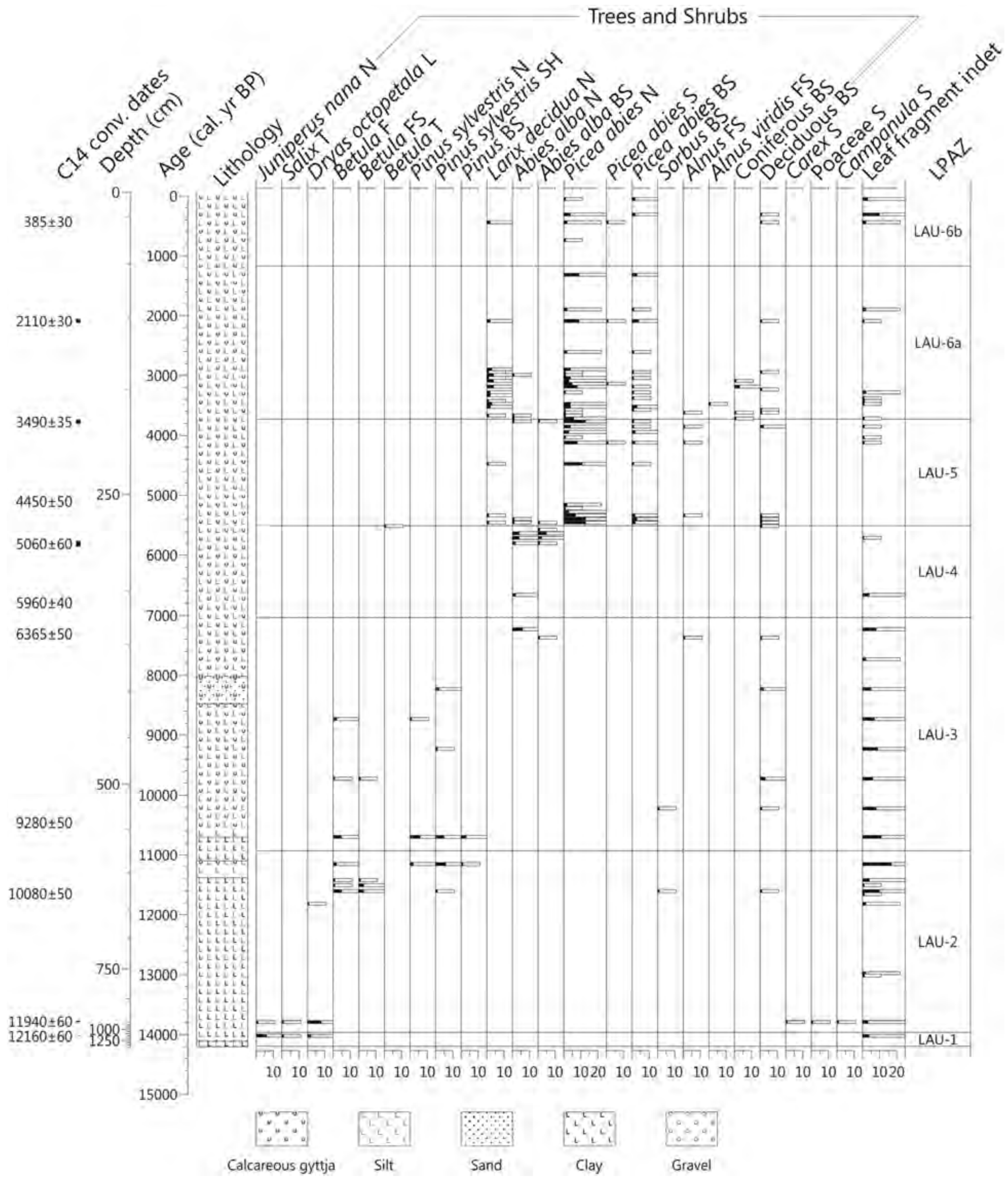

Figure 4. Macrofossil concentration diagram of Lauenensee (per 15.5 cm^3). The empty curves are the 10× exaggerations. BS: bud scales; F: fruits; FS: fruit scales; L: leaves; N: needles; SH: short shoots; T: twigs; S: seeds (Analysis: Fabian Rey and Silke Schleiss).

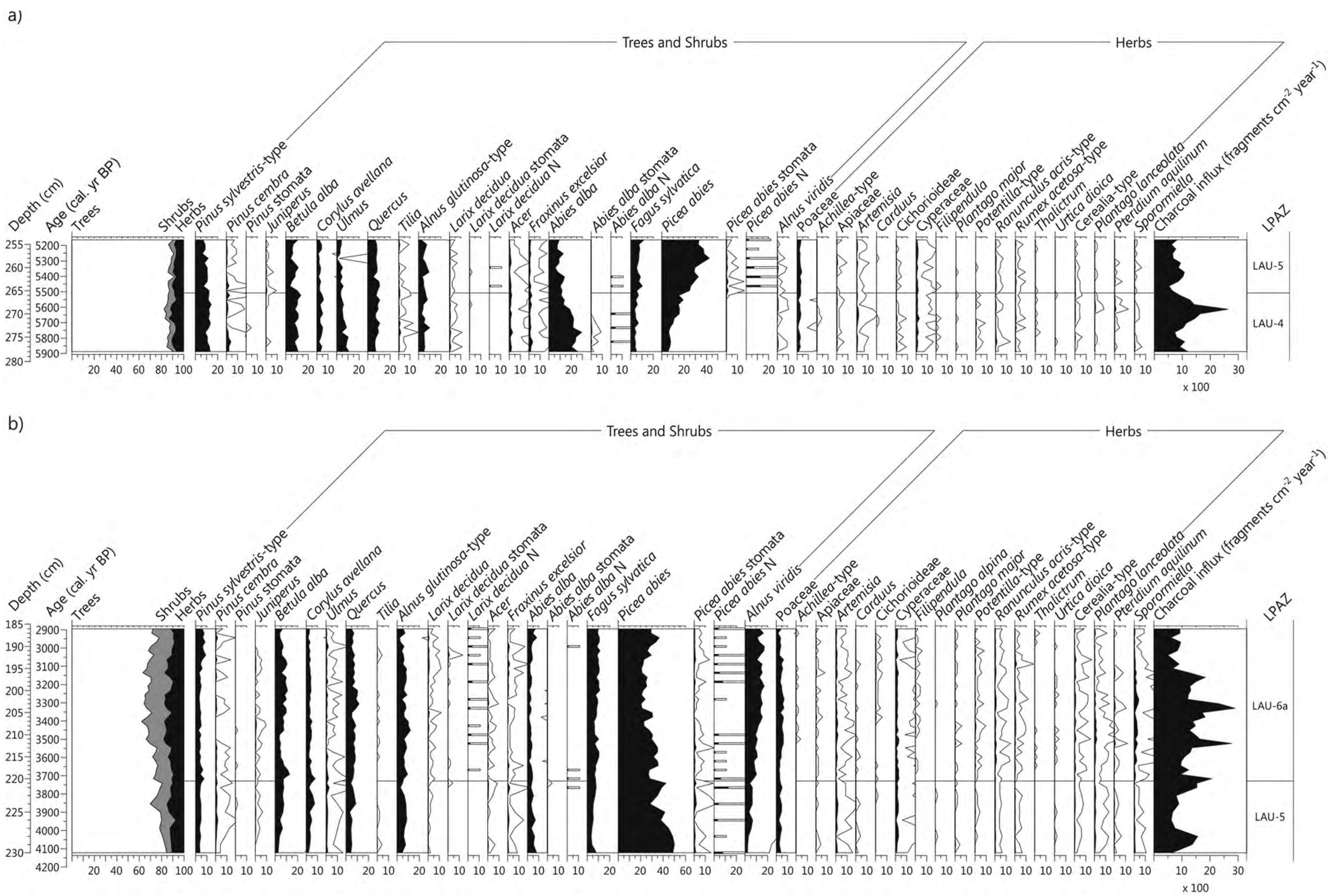

Figure 5. Pollen and stomata percentage diagram with macrofossil concentrations and microscopic charcoal influx (a: Neolithic sequence (HR 1), b: Bronze Age sequence (HR 2)). The empty curves are the 10×

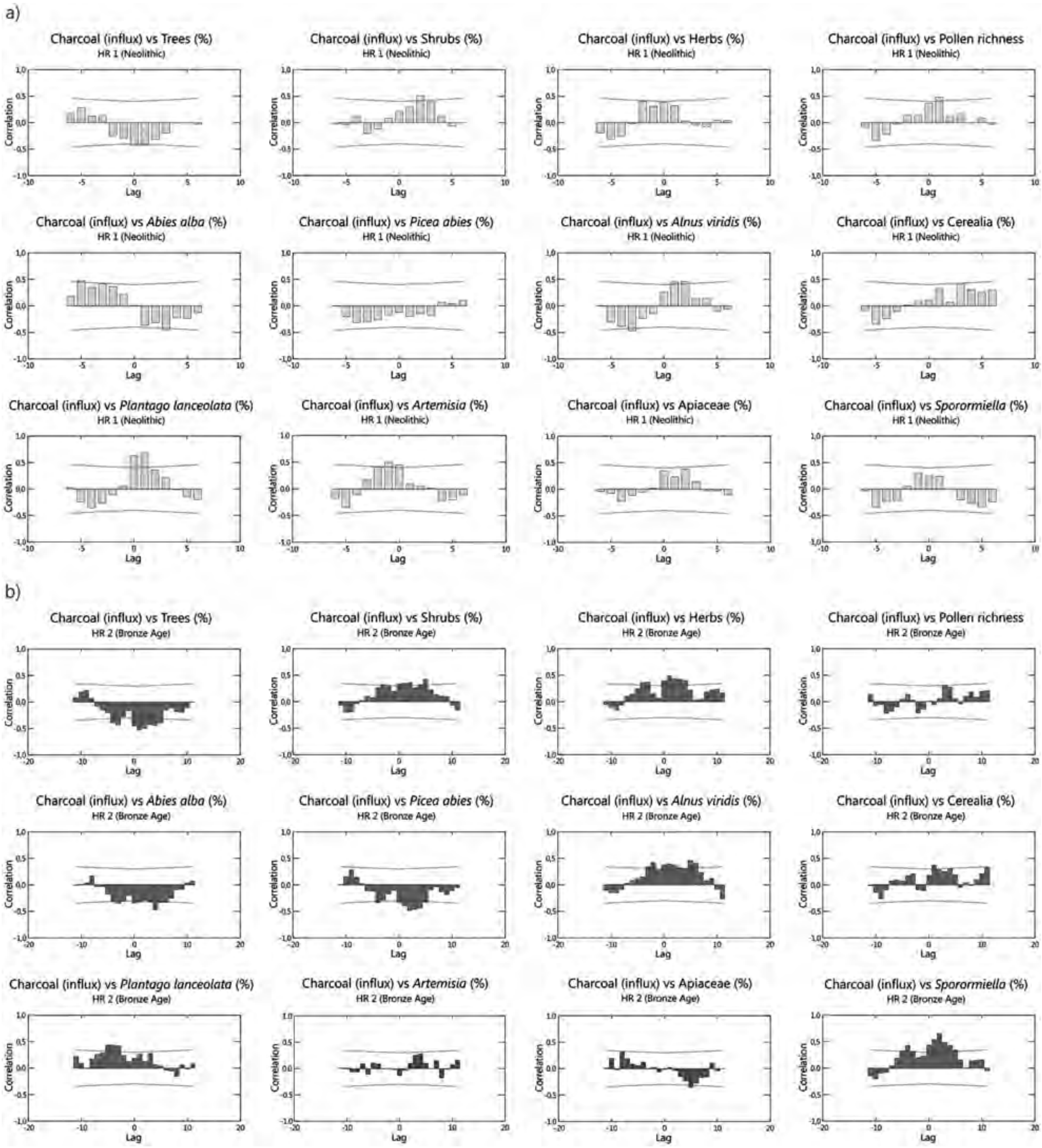

Figure 6. Selected cross-correlation plots 5700–5200 cal. BP, 3750–3250 cal. BC (a) Neolithic sequence, 1 lag = 30 years and 4100–2900 cal. BP, 2150–950 cal. BC (b) Bronze Age sequence, 1 lag = 28 years. The black lines mark the significance level.

Chironomids as palaeotemperature indicators in the Alps

Oliver Heiri, Institute of Plant Sciences and Oeschger Centre for Climate Change Research, University of Bern, oliver.heiri@ips.unibe.ch

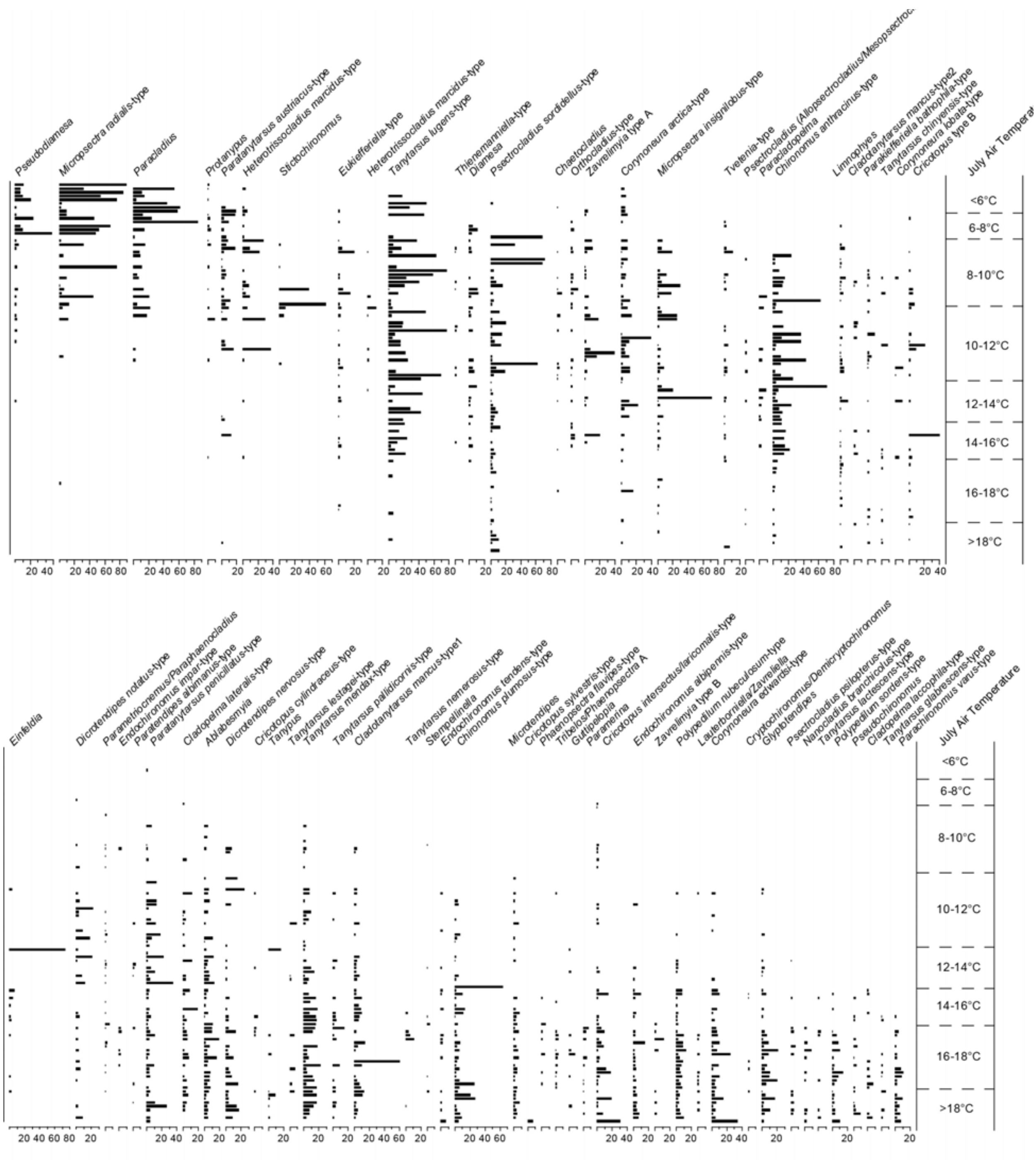

Figure 1. Distribution of chironomid assemblages in 114 lakes in the Swiss Alps. Chironomid abundances are plotted in percent and sites are arranged according to mean July air temperature (from Heiri and Lotter 2010).

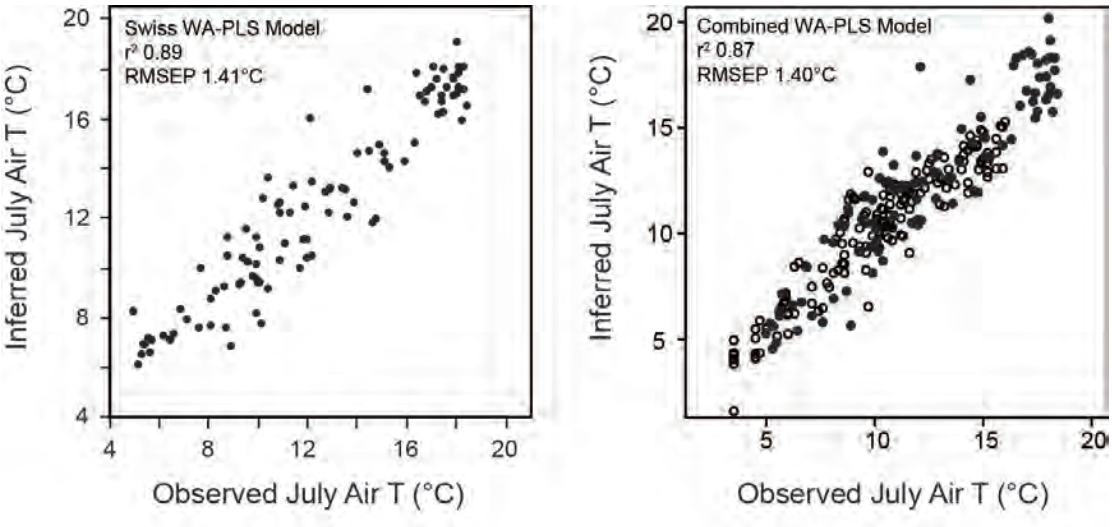

Figure 2. Performance of inference models (transfer functions) for estimating mean July air temperature based on chironomid assemblages in 100 lakes in Switzerland (left, Heiri and Lotter 2010) and 254 lakes in Switzerland, Norway and Svalbard (right, Heiri et al. 2011). The performance is evaluated by plotting chironomid-inferred mean July air temperatures (y-axes) against observed mean July air temperatures (x-axes). r^2 values and the root mean square errors of prediction are calculated using cross-validation (bootstrapping with 9999 cycles).

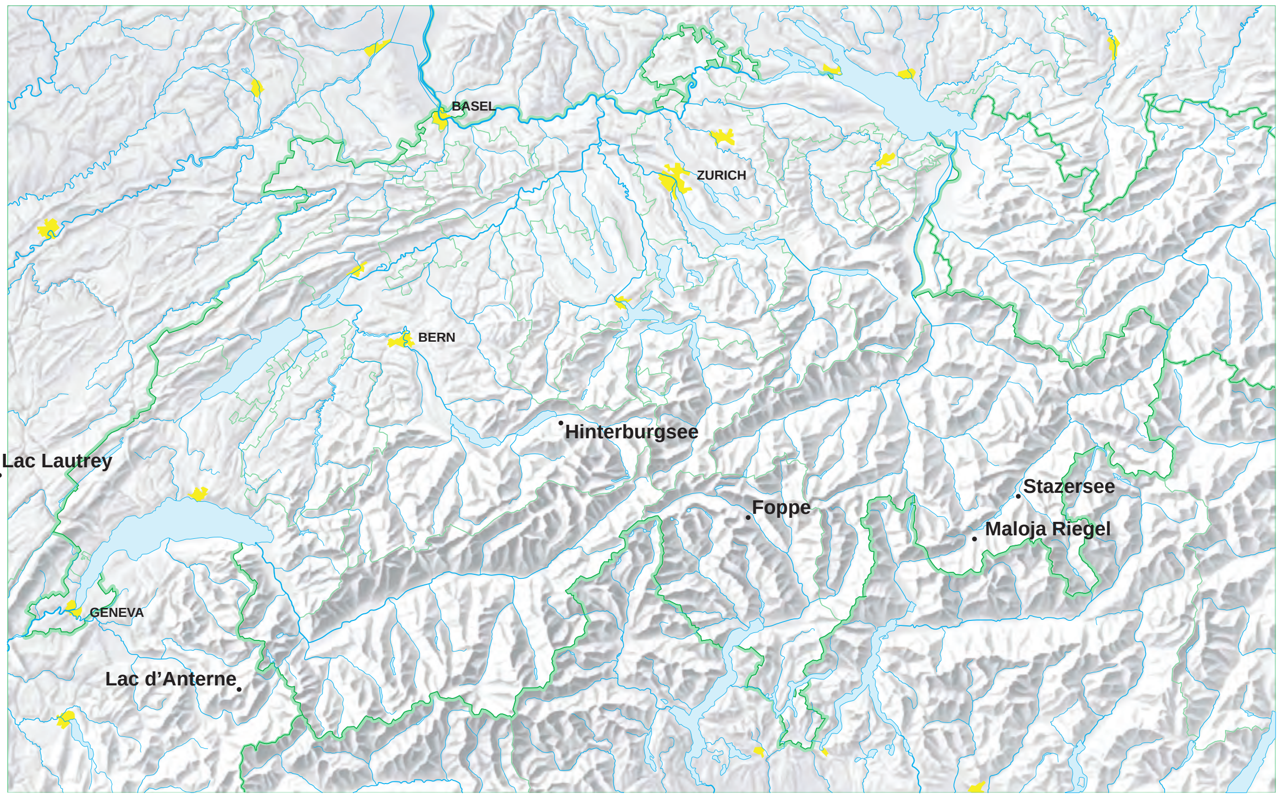

Figure 3. Location of chironomid records displayed in Figure 4. LAU Lac Lautrey (788 m a.s.l.), HIN Hinterburgsee (1515 m a.s.l.), STA Stazersee (1809 m a.s.l.), ANT Lac Anterne (2060 m a.s.l.), MAL Maloja Riegel (1865 m a.s.l.), FOP Foppe (1470 m a.s.l.).

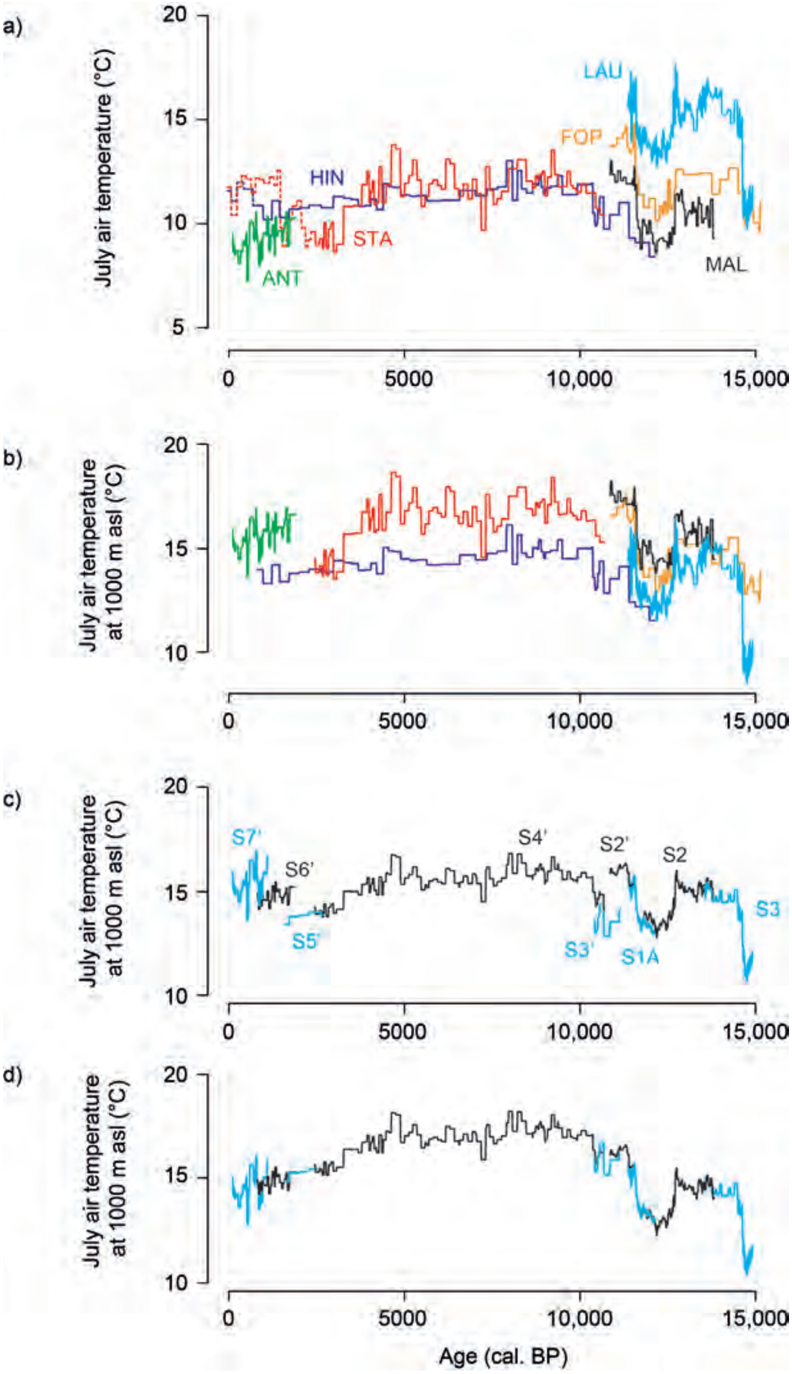

Figure 4. a) Chironomid-based temperature reconstructions from the Swiss Alps (HIN, STA, MAL, FOP), the French Jura mountains (LAU) and the French Alps (ANT). b) Reconstructions corrected to the same altitude using July air temperature lapse rates of 6° per 1000 m of altitude. c) Stacked (averaged) reconstructions based on the records in b, individual stacks were calculated for each interval with a particular group of records available. d) Spliced reconstruction based on the stacks in c, stacks are corrected for the offset between the stacked reconstructions and are spliced to the stacked record based on the largest number of chiromomid records (S1A). Dashed lines in a) indicate sections of the records that are affected by local human impact. From Heiri et al. (2015).

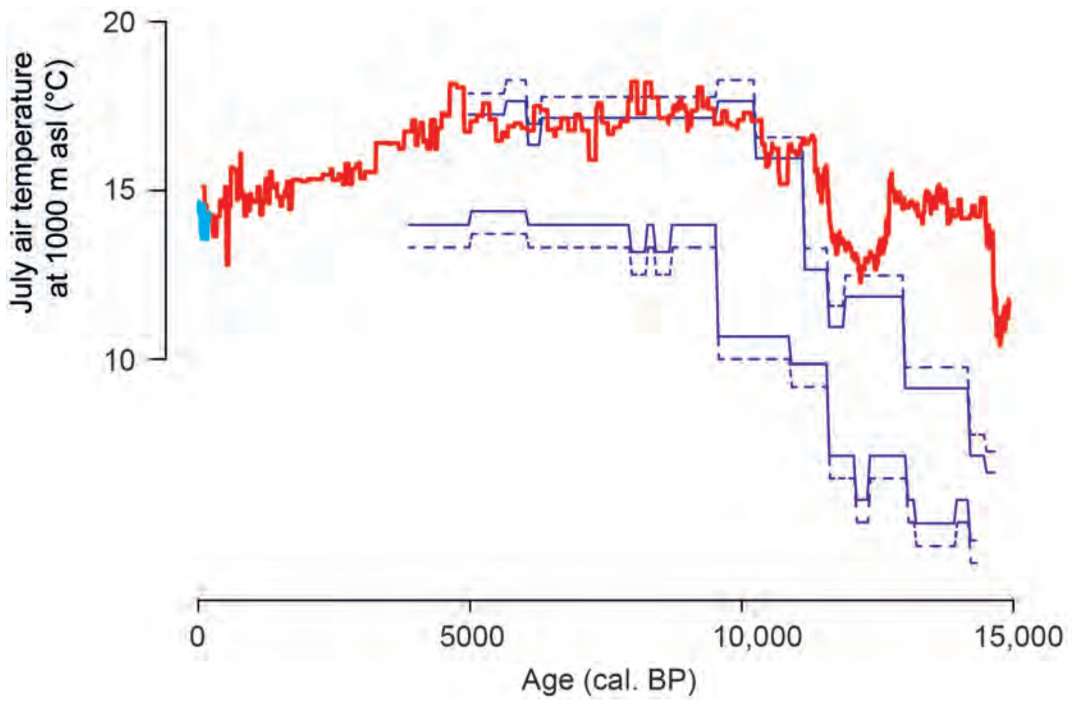

Figure 5. Comparison of the stacked and spliced temperature reconstruction from Figure 4d (red line, Heiri et al. 2015) with July air temperature estimates based on the past position of the Alpine treeline assuming minimum July temperatures for tree growth of 7.5-9.5 °C and that the position of the treeline is in equilibrium with climate (dark blue, Heiri et al. 2014a). Dashed lines indicate values taking into account an additional altitudinal uncertainty of 100 m when determining past treeline altitude. The light blue line indicates the instrumental July air temperature estimates from Basel Binningen 1755-1980 AD (smoothed within a 29-year moving window). All July air temperature estimates are corrected to an elevation of 1000 m a.s.l. with temperature lapse rates of 6°C per 1000 m of elevation.

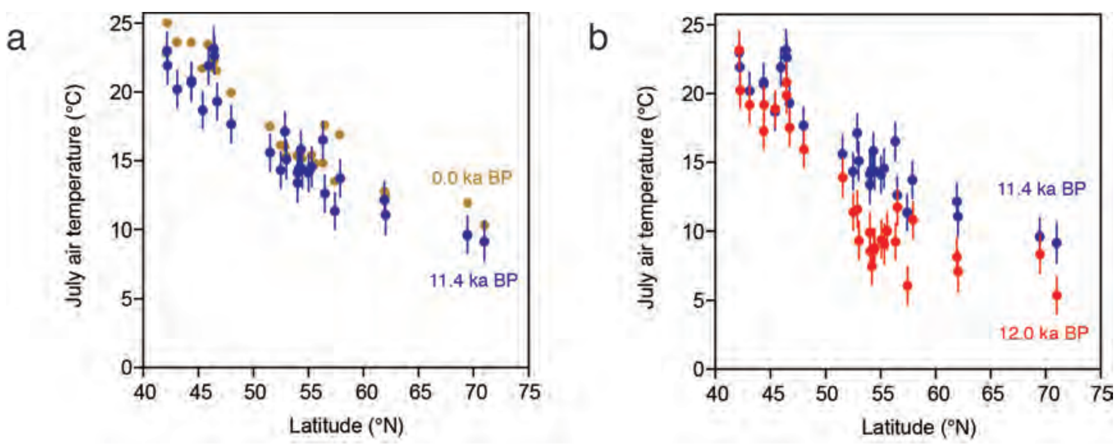

Figure 6. a) Chironomid-based July air temperature estimates for the early Holocene (ca. 11.4 ka cal. BP) across Europe compared with modern temperature estimates for the study sites. b) Chironomid-based July air temperature estimates for these sites for the early Holocene compared with temperatures inferred for the Younger Dryas (ca. 12.0 ka cal. BP). Temperatures are plotted versus latitude and corrected to an altitude of 0 m asl. From Heiri et al. (2014b).

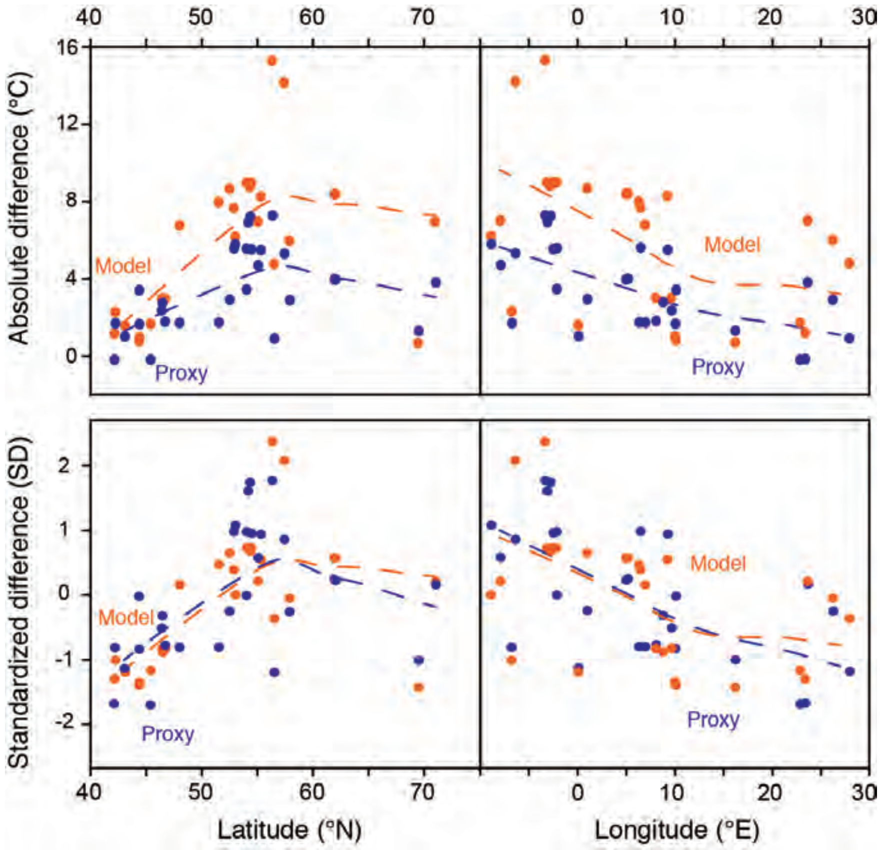

Figure 7. Warming at the Younger Dryas Holocene transition as inferred by chironomid records across Europe (blue) and the ECHAM4 climate model for the same locations (orange) plotted against latitude and longitude. The upper panel shows the absolute July air temperature increases, the lower panel standardized values. Dashed lines are fitted by locally weighted regression (LOESS). From Heiri et al. (2014b).

References

Heiri, O., A. F. Lotter, 2010. How does taxonomic resolution affect chironomid based temperature reconstruction? Journal of Paleolimnology 44:589-601.

Heiri, O., S. J. Brooks, H. J. B. Birks, A. F. Lotter, 2011. A 274-lake calibration data-set and inference model for chironomid-based summer air temperature reconstruction in Europe. Quaternary Science Reviews 30:3445-3456.

Heiri, O., S. J. Brooks, H. Renssen, A. Bedford, M. Hazekamp, B. Ilyashuk, E. S. Jeffers, B. Lang, E. Kirilova, S. Kuiper, L. Millet, S. Samartin, M. Toth, F. Verbruggen, J. E. Watson, N. v. Asch, E. Lammertsma, L. Amon, H. H. Birks, H. J. B. Birks, M. F. Mortensen, W. Z. Hoek, E. Magyari, C. M. Sobrino, H. Seppä, W. Tinner, S. Tonkov, S. Veski, A. F. Lotter, 2014b. Validation of climate model-inferred regional temperature change for late-glacial Europe. Nature Communications DOI: 10.1038/ncomms5914.

Heiri, O., K. A. Koinig, C. Spötl, S. Barrett, A. Brauer, R. Drescher-Schneider, D. Gaar, S. Ivy-Ochs, H. Kerschner, M. Luetscher, A. Moran, K. Nicolussi, F. Preusser, R. Schmidt, P. Schoeneich, C. Schwörer, T. Sprafke, B. Terhorst, W. Tinner, 2014a. Palaeoclimate records 60-8 ka in the Austrian and Swiss Alps and their forelands. Quaternary Science Reviews 106:186-205.

Heiri, O., B. Ilyashuk, L. Millet, S. Samartin, A. F. Lotter, 2015. Stacking of discontinuous regional palaeoclimate records: Chironomid-based summer temperatures from the Alpine region. The Holocene 25:137-149.

Review of Palaeobotany and Palynology 174 (2012) 91–100

Contents lists available at SciVerse ScienceDirect

Review of Palaeobotany and Palynology

journal homepage: www.elsevier.com/locate/revpalbo

Research paper

Impact of Holocene climate changes on alpine and treeline vegetation at Sanetsch Pass, Bernese Alps, Switzerland

Nadine Berthel, Christoph Schwörer *, Willy Tinner

Institute of Plant Sciences, University of Bern, Altenbergrain 21, CH-3013 Bern, Switzerland
Oeschger Centre for Climate Change Research, University of Bern, Zähringerstrasse 25, CH-3012 Bern, Switzerland

ARTICLE INFO

Article history:
Received 21 September 2011
Received in revised form 23 November 2011
Accepted 9 December 2011
Available online 19 December 2011

Keywords:
treeline
alpine vegetation
palaeoecology
climate change
human impact
upslope migration

ABSTRACT

In order to infer reactions of treeline and alpine vegetation to climatic change, past vegetation changes are reconstructed on the basis of pollen, macrofossil and charcoal analysis. The sampled sediment cores originate from the small pond Emines, located at the Sanetsch Pass (connecting the Valais and Bern, Switzerland) at an altitude of 2288 m a.s.l. Today's treeline is at ca. 2200 m a.s.l. in the area, though due to special pass (saddle) conditions it is locally depressed to ca. 2060 m a.s.l. Our results reveal that the area around Emines was covered by treeless alpine vegetation during most of the past 12,000 years. Single individuals of *Betula*, *Larix decidua* and possibly *Pinus cembra* occurred during the Holocene. Major centennial to millennial-scale responses of treeline vegetation to climatic changes are evident. However, alpine vegetation composition remained rather stable between 11,500 and 6000 cal. BP, showing that Holocene climatic changes of +/− 1 °C hardly influenced the local vegetation at Emines. The rapid warming of 3–4 °C at the Late Glacial/Holocene transition (11,600 cal. BP) caused significant altitudinal displacements of alpine species that were additionally affected by the rapid upward movement of trees and shrubs. Since the beginning of the Neolithic, vegetation changes at Sanetsch Pass resulted from a combination of climate change and human impact. Anthropogenic fire increase and land-use change combined with a natural change from subcontinental to more oceanic climate during the second half of the Holocene led to the disappearance of *P. cembra* in the study area, but favoured the occurrence of *Picea abies* and *Alnus viridis*. The mid- to late-Holocene decline of *Abies alba* was primarily a consequence of human impact, since this mesic species should have benefitted from a shift to more oceanic conditions. Future alpine vegetation changes will be a function of the amplitude and rapidity of global warming as well as human land use. Our results imply that alpine vegetation at our treeline pass site was never replaced by forests since the last ice-age. This may change in the future if anticipated climate change will induce upslope migration of trees. The results of this study emphasise the necessity of climate change mitigation in order to prevent biodiversity losses as a consequence of unprecedented community and species displacement in response to climatic change.

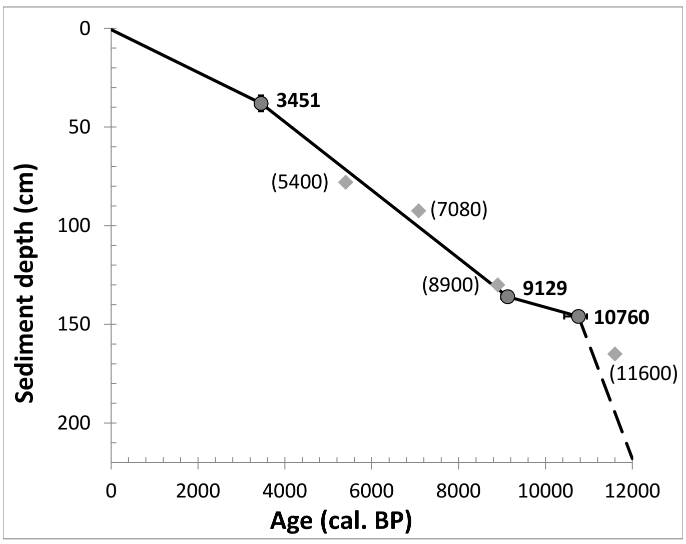

Fig. 2. Age-depth model based on linear interpolation between three radiocarbon dates. Grey circles indicate calibrated ^{14}C ages (based on terrestrial macrofossils). Grey diamonds indicate pollen-stratigraphical ages used only for verification. The error bars indicate 2σ ranges for the calibrated ^{14}C dates.

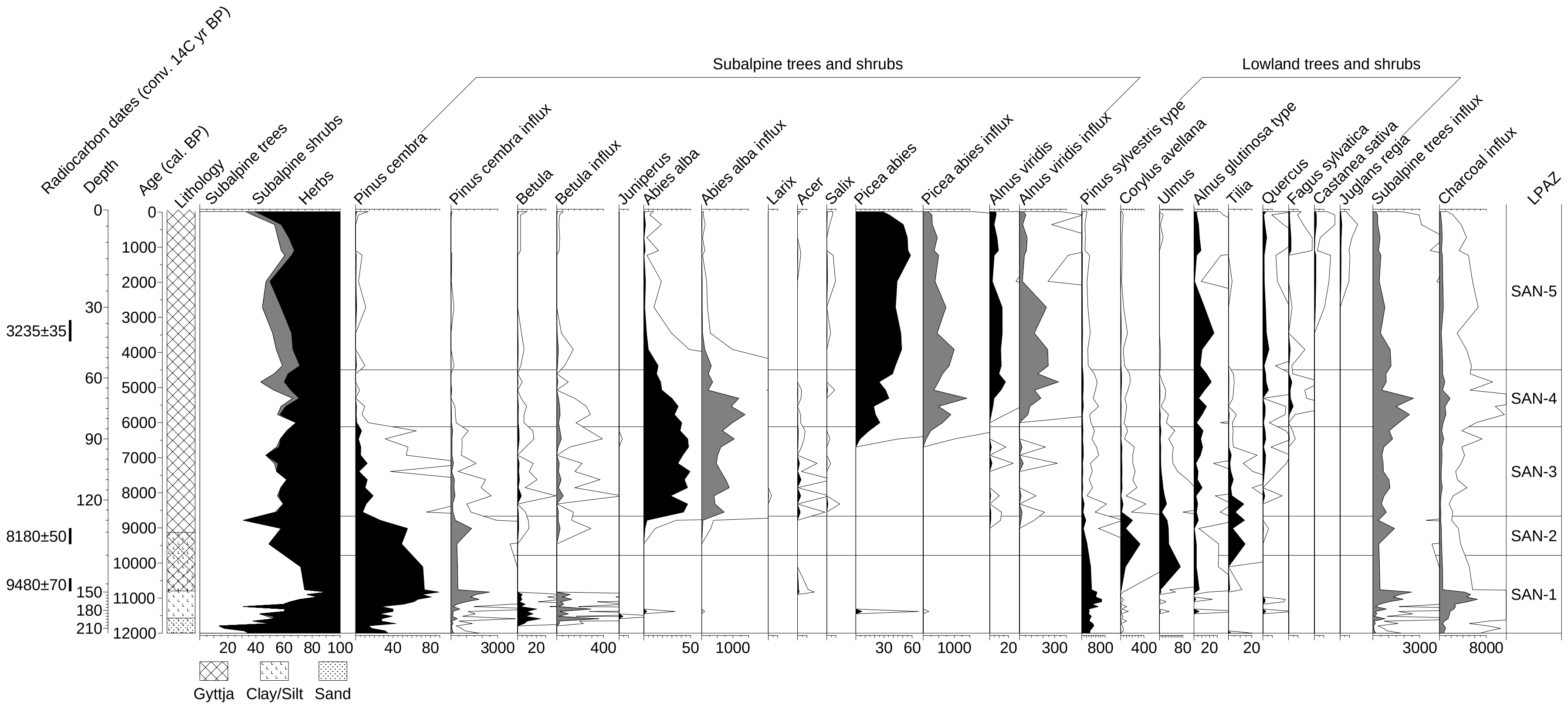

Fig. 3. Pollen percentage and influx diagram (selected taxa) showing arboreal pollen types. Lowland trees and shrubs as well as water plants and ferns are excluded from the pollen sum, which is used for percentage calculations. Influx values are given for selected subalpine tree and shrub taxa (grey curves). Empty curves show 10× exaggerations.

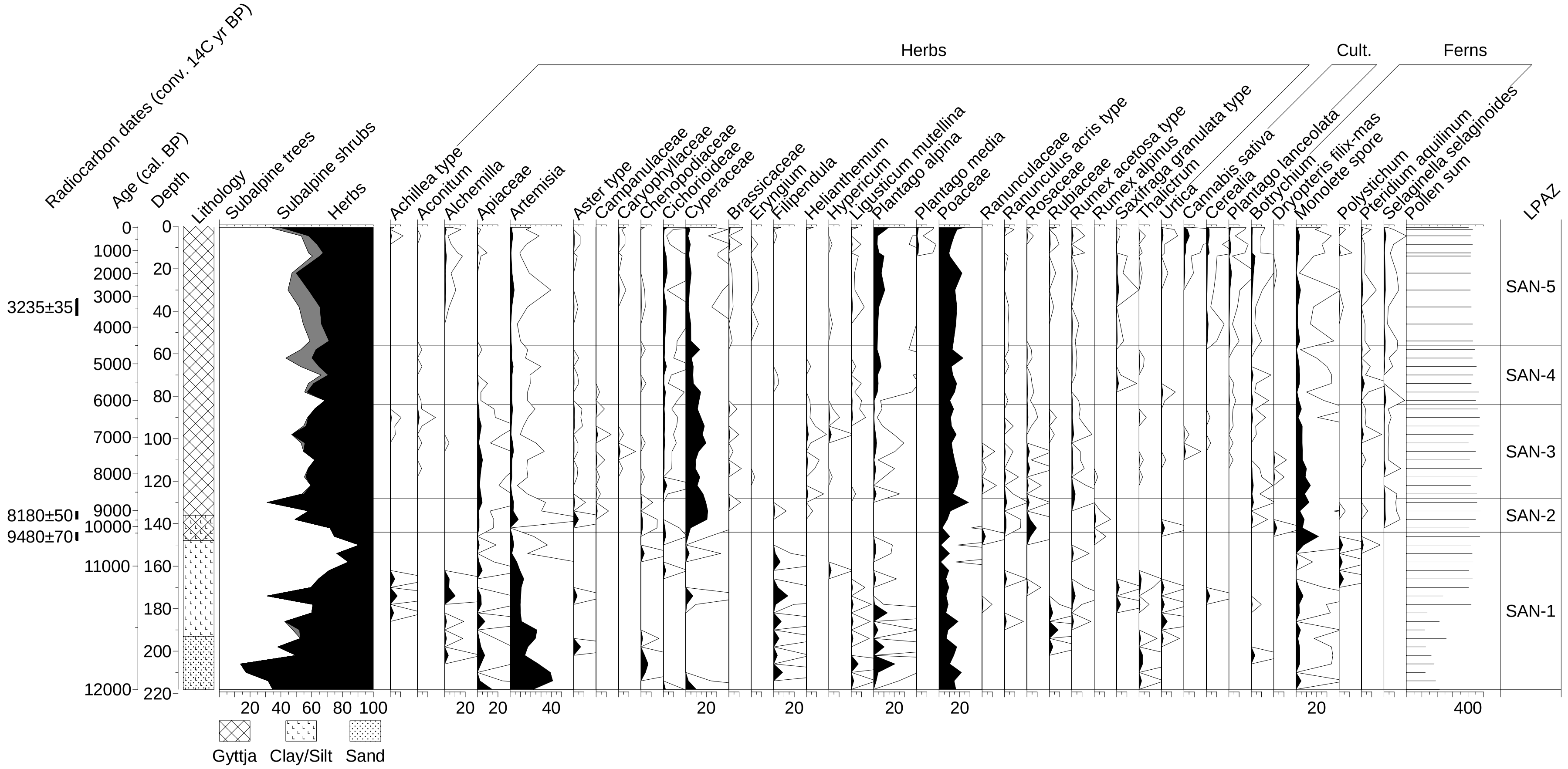

Fig. 4. Pollen percentage diagram (selected taxa) showing herbs and ferns. Lowland trees and shrubs as well as water plants and ferns are excluded from the pollen sum, which is used for percentage calculations. Empty curves show 10× exaggerations. Note the linear depth scale.

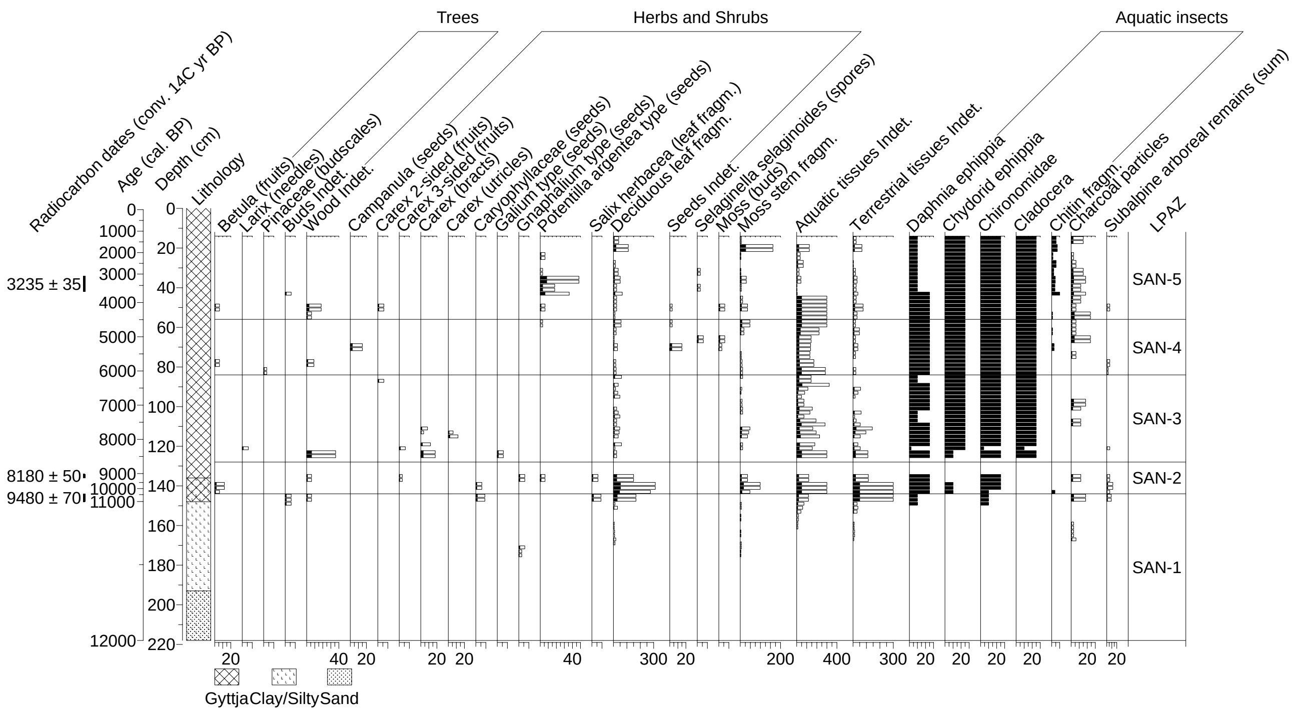

Fig. 5. Macrofossil concentrations per 44 cm^{-3}. Plant material is counted up to a number of 50 fragments. Insect numbers exceeding 10 are divided in classes ≥10 and ≥25. Empty curves show 5× exaggerations. Note the linear depth scale.

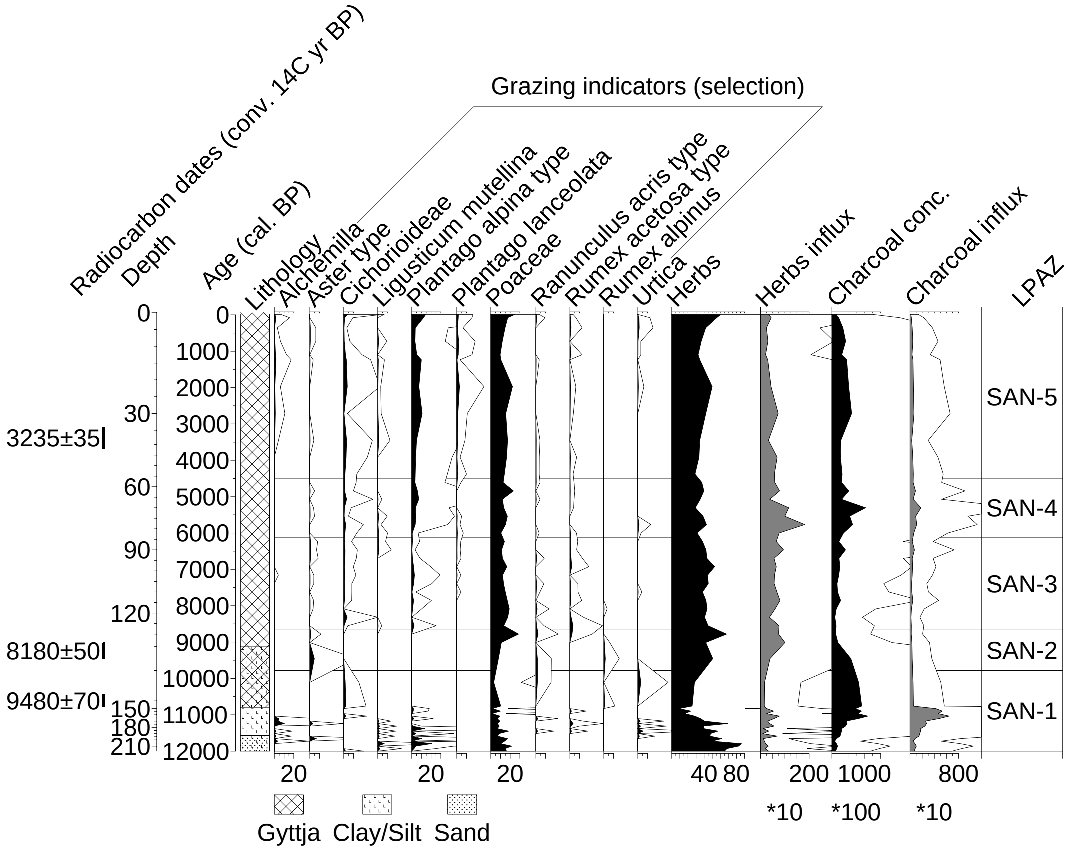

Fig. 6. Pollen percentage diagram showing selected grazing indicators. Lowland trees and shrubs as well as water plants and ferns are excluded from the pollen sum, which is used for percentage calculations. Grey pollen curves indicate influx values. Empty curves show 10× exaggerations.

Vertical mobility around the high-alpine Schnidejoch Pass. Indications of Neolithic and Bronze Age pastoralism in the Swiss Alps from paleoecological and archaeological sources.

Albert Hafner[1], Christoph Schwörer[2]

[1] University of Bern, Institute of Archaeological Sciences and Oeschger Centre for Climate Change Research (OCCR), Muesmattstrasse 27, 3012 Bern/Switzerland

albert.hafner@iaw.unibe.ch

[2] University of Bern, Institute of Plant Sciences and Oeschger Centre for Climate Change Research (OCCR), Altenbergrain 21, 3013 Bern

christoph.schwoerer@ips.unibe.ch

Abstract

Since 2003 a melting ice field on the Schnidejoch Pass (2756 m a.s.l.) has yielded several hundred objects from the Neolithic period, the Bronze and Iron Ages and from Roman and early medieval times. The oldest finds date from the beginning of the 5th millennium BC, whilst the most recent artefacts date from around AD 1000. Most of the objects date from the Neolithic period and the Bronze Age and are of organic origin. A series of over 70 radiocarbon dates confirm that the Schnidejoch Pass, which linked the Bernese Oberland with the Rhône Valley, was frequented from no later than 4800–4500 BC onwards. The pass was easily accessible when the glaciers descending from the nearby Wildhorn mountain range (summit at 3248 m a.s.l.) were in a retreating phase. On the other hand, the area was impassable during periods of glacial advances. A recent palaeoecological study of sediment cores from nearby Lake Iffigsee (2065 m a.s.l.) provides clear indications of early human impact in this Alpine area. Linking archaeological finds from the Schnidejoch Pass and the Rhône Valley with the palaeoecological data provides results that can be interpreted as early indications of Alpine pastoralism and transhumance. The combined archaeological and paleoecological research allows us to explain vertical mobility in the Swiss Alps.

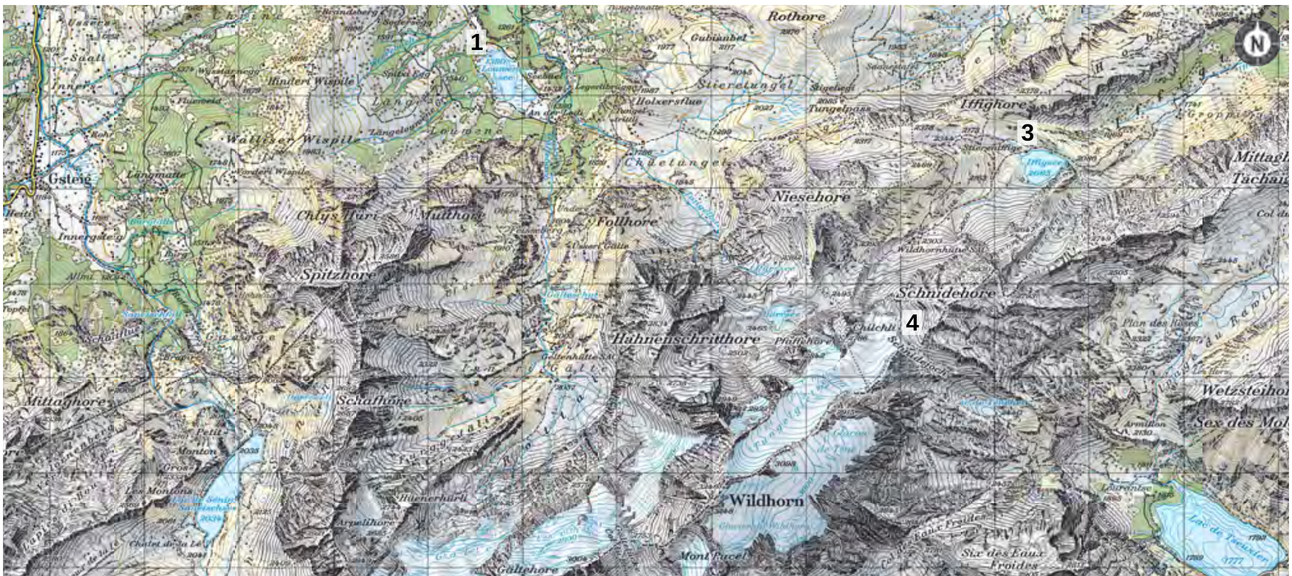

Fig. 1 Map of the Wildhorn region with the study sites (1) Lauenensee (1381 m a.s.l.), (2) Col du Sanetsch (2288 m a.s.l.), (3) Iffigsee (2065 m a.s.l.) and (4) Schnidejoch (2756 m a.s.l.)

Fig. 2: Above: View on the Schnidejoch Pass site in the foreground, the summit of the Wildhorn (3248 m a.s.l.) and its glaciers in the background. Below: Situation at the Schnidejoch Pass site in the autumn of 2005. Photos by Kathrin Glauser.

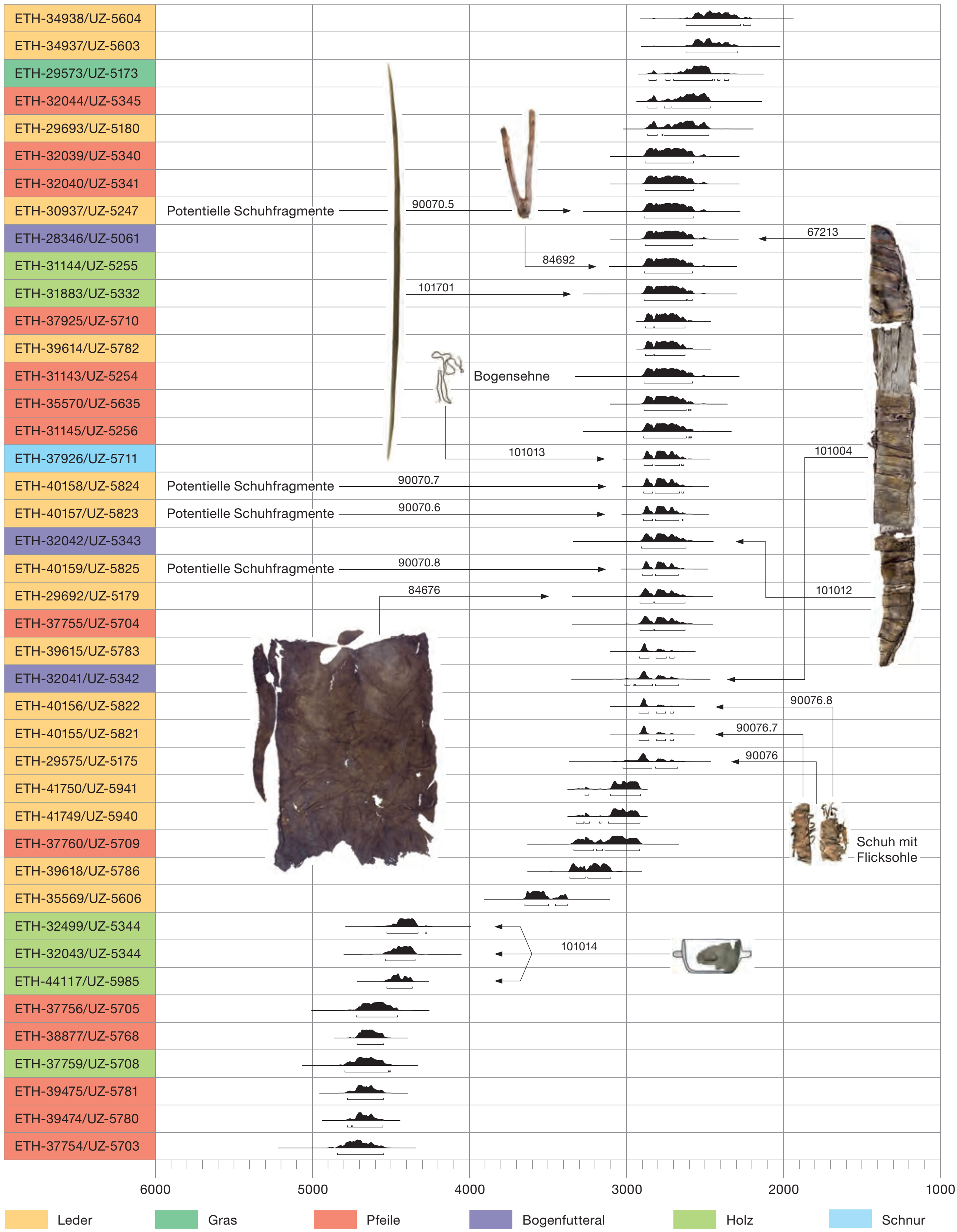

Fig. 4: Schnidejoch radiocarbon dates and specific archaeological finds from the Neolithic period, 4800–2200 calBC. Graphic by Daniel Marchand/Cornelia Schlup.

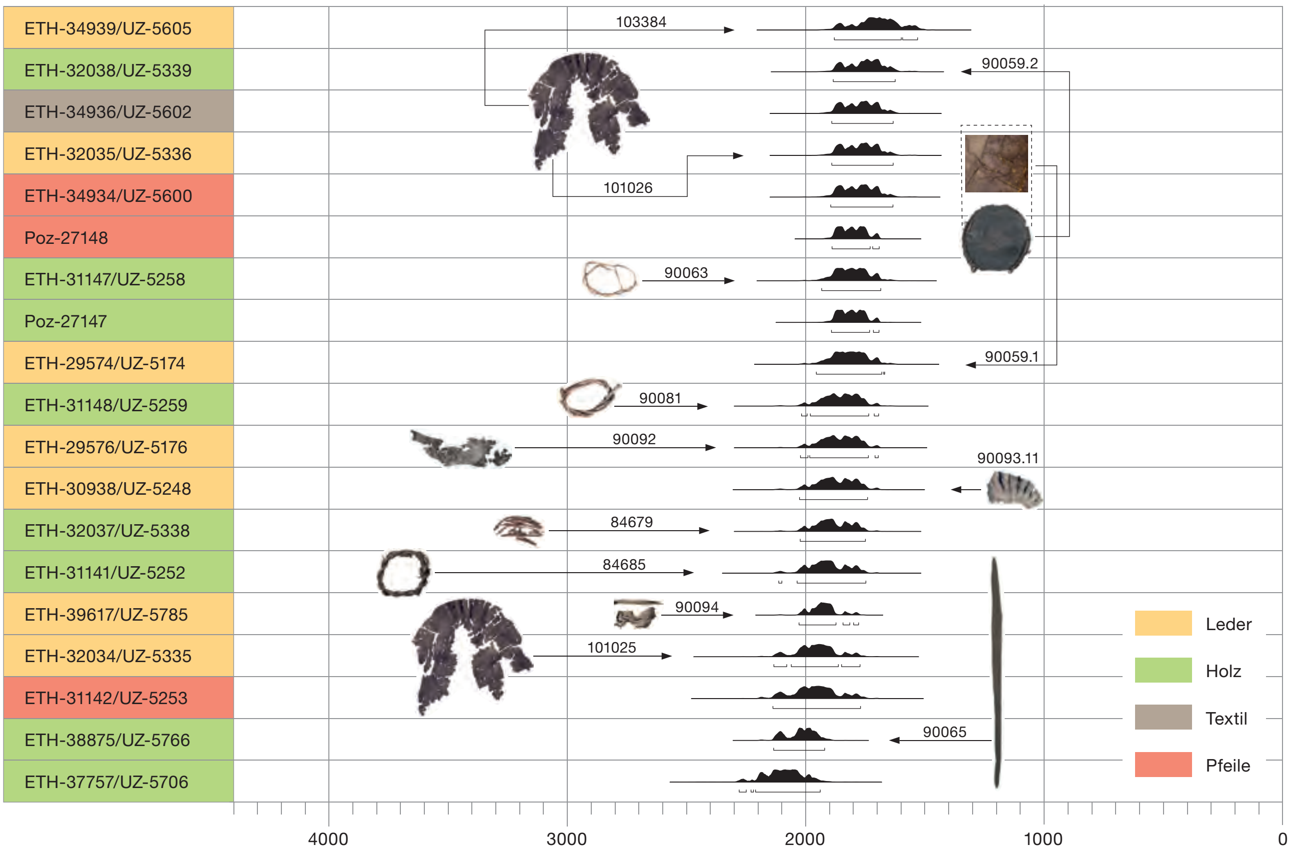

Fig. 5: Schnidejoch radiocarbon dates and specific archaeological finds from the Bronze Age, 2200 – 1600 BC. Graphic by Daniel Marchand/Cornelia Schlup.

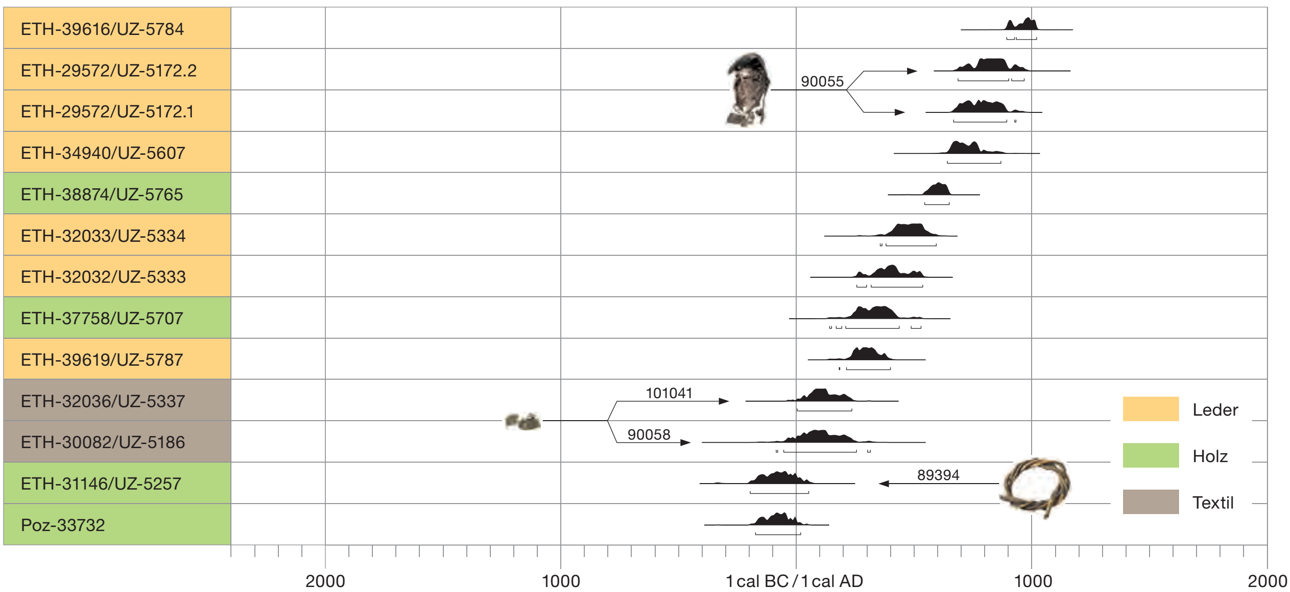

Fig. 6: Schnidejoch radiocarbon dates and specific archaeological finds from the Late Iron Age, Roman period and Early Middle Ages, 200 calBC – 1000 calAD. Graphic by Daniel Marchand/Cornelia Schlup.

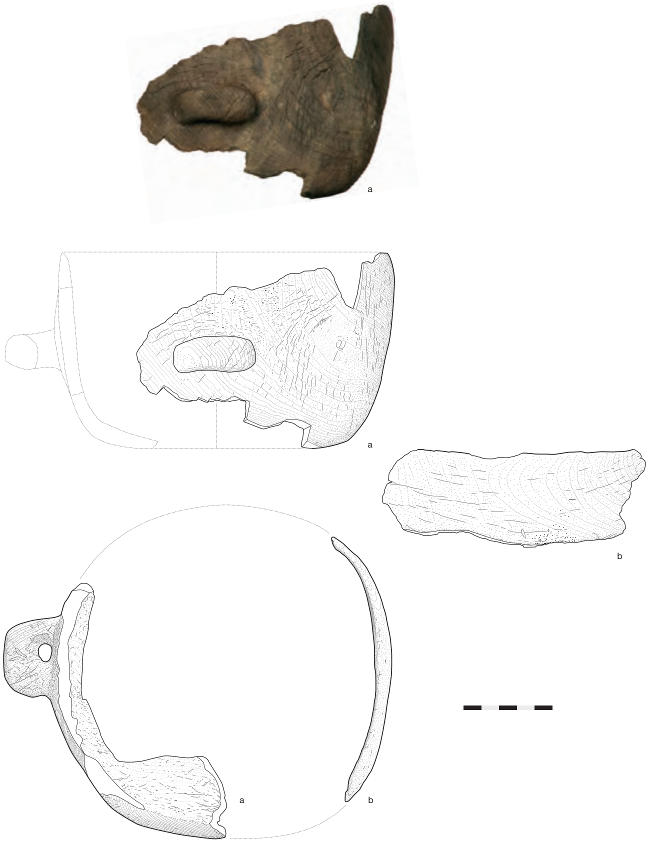

Fig. 7: Bowl, elm (*Ulmus*) wood, Neolithic period, dated to 4500 – 4300 calBC. Photo by Badri Redha.

Fig. 8: Vessel, stone pine (*Pinus cembra*) and willow (*Salix*) wood, Early Bronze Age period, dated to 2000-1600 calBC. Photo by Badri Redha.

Fig. 9: Rings made from plaited twigs, Early Bronze Age period. Left: birch (*Betula*) wood, dated to 2050-1750 calBC; middle: birch (*Betula*) wood, dated to 2000-1750 calBC; right: spruce (*Picea abies*) wood, dated to 1950-1700 calBC. Photo by Badri Redha.

Fig. 10: Historical ethnographic examples of a so-called Ringzaun or Schweiffelzaun from Teuffenthal near Thun, Canton of Bern. The man in the middle holds a ring made from plaited twigs, the man to the right keeps a whole bundle of rings. From Stuber et al. 2011.

Veget Hist Archaeobot (2014) 23:479–496
DOI 10.1007/s00334-013-0411-5

ORIGINAL ARTICLE

Holocene climate, fire and vegetation dynamics at the treeline in the Northwestern Swiss Alps

Christoph Schwörer · Petra Kaltenrieder · Lukas Glur · Matthias Berlinger · Julie Elbert · Stephanie Frei · Adrian Gilli · Albert Hafner · Flavio S. Anselmetti · Martin Grosjean · Willy Tinner

Received: 10 April 2013 / Accepted: 11 August 2013 / Published online: 31 August 2013

Abstract Treelines are expected to rise to higher elevations with climate warming; the rate and extent however are still largely unknown. Here we present the first multi-proxy palaeoecological study from the treeline in the Northwestern Swiss Alps that covers the entire Holocene. We reconstructed climate, fire and vegetation dynamics at Iffigsee, an alpine lake at 2,065 m a.s.l., by using seismic sedimentary surveys, loss on ignition, visible spectrum reflectance spectroscopy, pollen, spore, macrofossil and charcoal analyses. Afforestation with *Larix decidua* and tree *Betula* (probably *B. pendula*) started at ~9,800 cal. B.P., more than 1,000 years later than at similar elevations in the Central and Southern Alps, indicating cooler temperatures and/or a high seasonality. Highest biomass production and forest position of ~2,100–2,300 m a.s.l. are inferred during the Holocene Thermal Maximum from 7,000 to 5,000 cal. B.P. With the onset of pastoralism and transhumance at 6,800–6,500 cal. B.P., human impact became an important factor in the vegetation dynamics at Iffigsee. This early evidence of pastoralism is documented by the presence of grazing indicators (pollen, spores), as well as a wealth of archaeological finds at the nearby mountain pass of Schnidejoch. Human and fire impact during the Neolithic and Bronze Ages led to the establishment of pastures and facilitated the expansion of *Picea abies* and *Alnus viridis*. We expect that in mountain areas with land abandonment, the treeline will react quickly to future climate warming by shifting to higher elevations, causing drastic changes in species distribution and composition as well as severe biodiversity losses.

Keywords Palaeoecology · Treeline · Human impact · Vegetation history · Alps · Afforestation

Introduction

The treeline ecotone is the most conspicuous ecosystem boundary in mountain landscapes. It separates two ecosystems with different species pools, microclimates and ecosystem services: open alpine meadows and closed mountain forests (e.g. Körner 2003, 2012; Holtmeier 2009). The

Communicated by F. Bittmann.

C. Schwörer (✉) · P. Kaltenrieder · M. Berlinger · S. Frei · W. Tinner
Institute of Plant Sciences, University of Bern, Altenbergrain 21, 3013 Bern, Switzerland
e-mail: christoph.schwoerer@ips.unibe.ch

C. Schwörer · P. Kaltenrieder · J. Elbert · A. Hafner · F. S. Anselmetti · M. Grosjean · W. Tinner
Oeschger Centre for Climate Change Research, University of Bern, Zähringerstrasse 25, 3012 Bern, Switzerland

L. Glur · F. S. Anselmetti
Departement of Surface Waters – Sedimentology, Swiss Federal Institute of Aquatic Sciences, Eawag, Überlandstrasse 133, 8600 Dübendorf, Switzerland

J. Elbert · M. Grosjean
Institute of Geography, University of Bern, Erlachstrasse 9a, 3012 Bern, Switzerland

A. Gilli
Geological Institute, ETH Zurich, Sonneggstrasse 5, 8092 Zurich, Switzerland

A. Hafner
Department of Prehistory, Institute of Archaeological Sciences, University of Bern, Bernastrasse 15a, 3005 Bern, Switzerland

F. S. Anselmetti
Institute of Geological Sciences, University of Bern, Baltzerstrasse 1, 3012 Bern, Switzerland

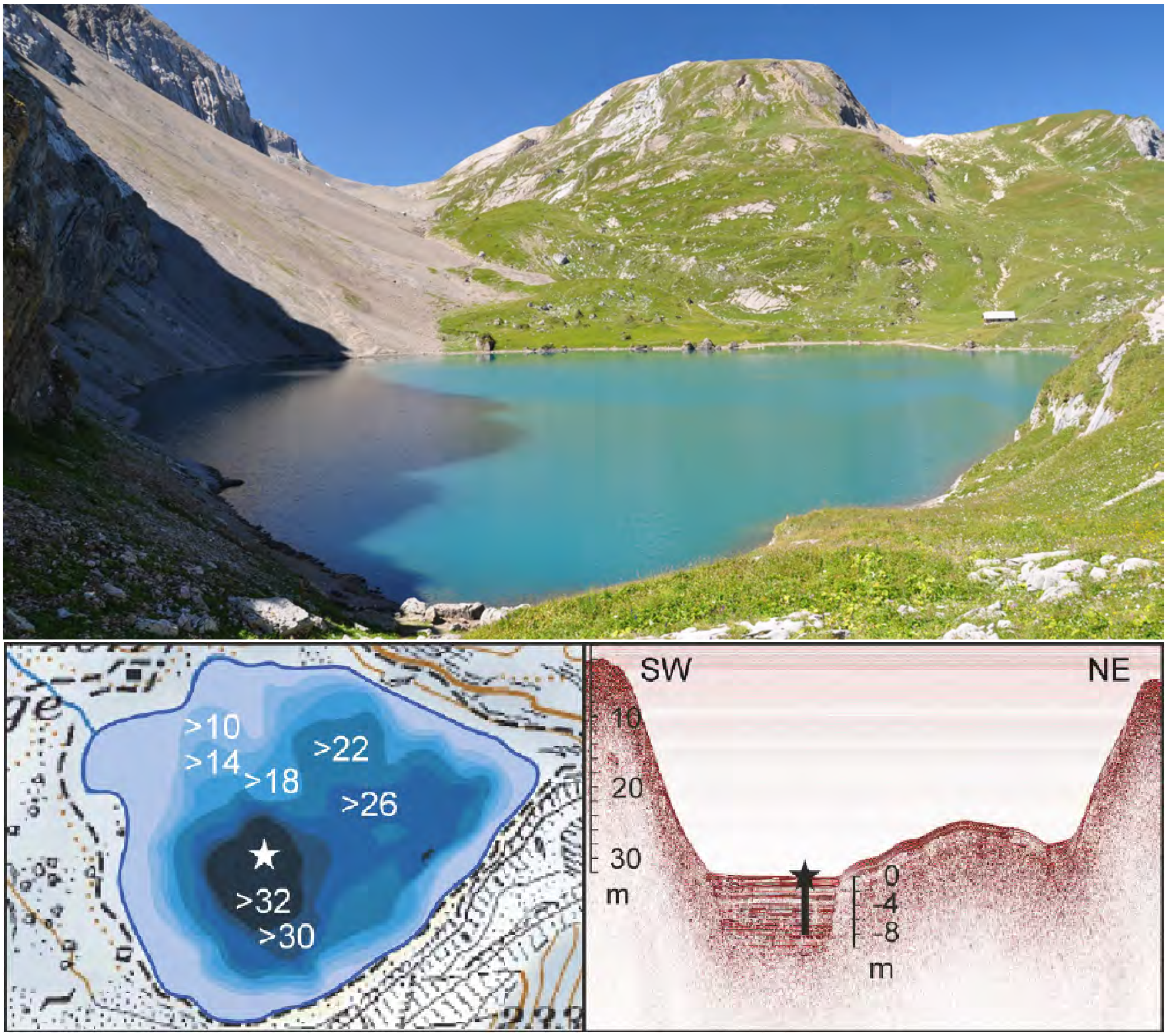

Fig. 1 Photo of Iffigsee (2065 m a.s.l.) and surrounding meadows (top) as well as a bathymetric map with the coring location (lower left), and the seismic profile (lower right)

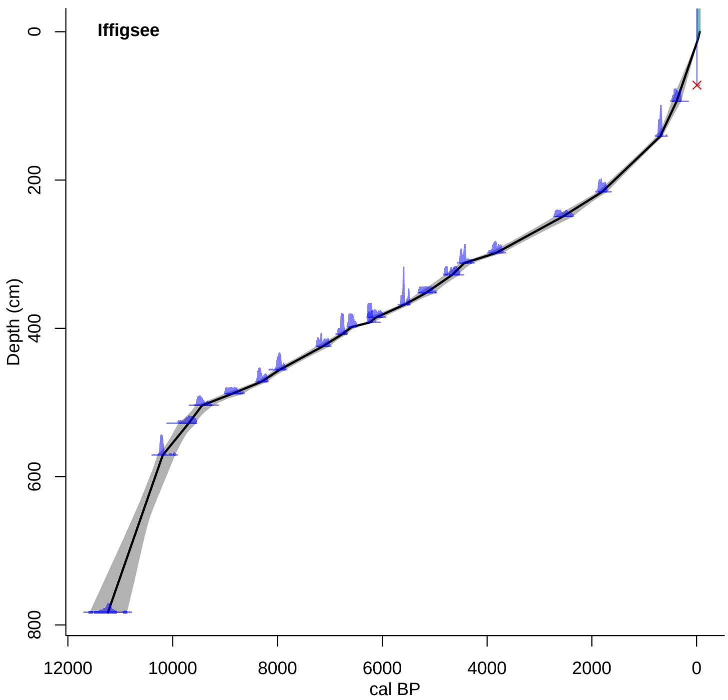

Fig. 2 Age-depth model of the sediment from Iffigsee based on Monte-Carlo sampling and linear interpolation (black line; Blaauw 2010). Blue curves show the probability distribution of the 22 radiocarbon dates and the grey area the 95 % confidence interval of the clam model run with 10000 iterations

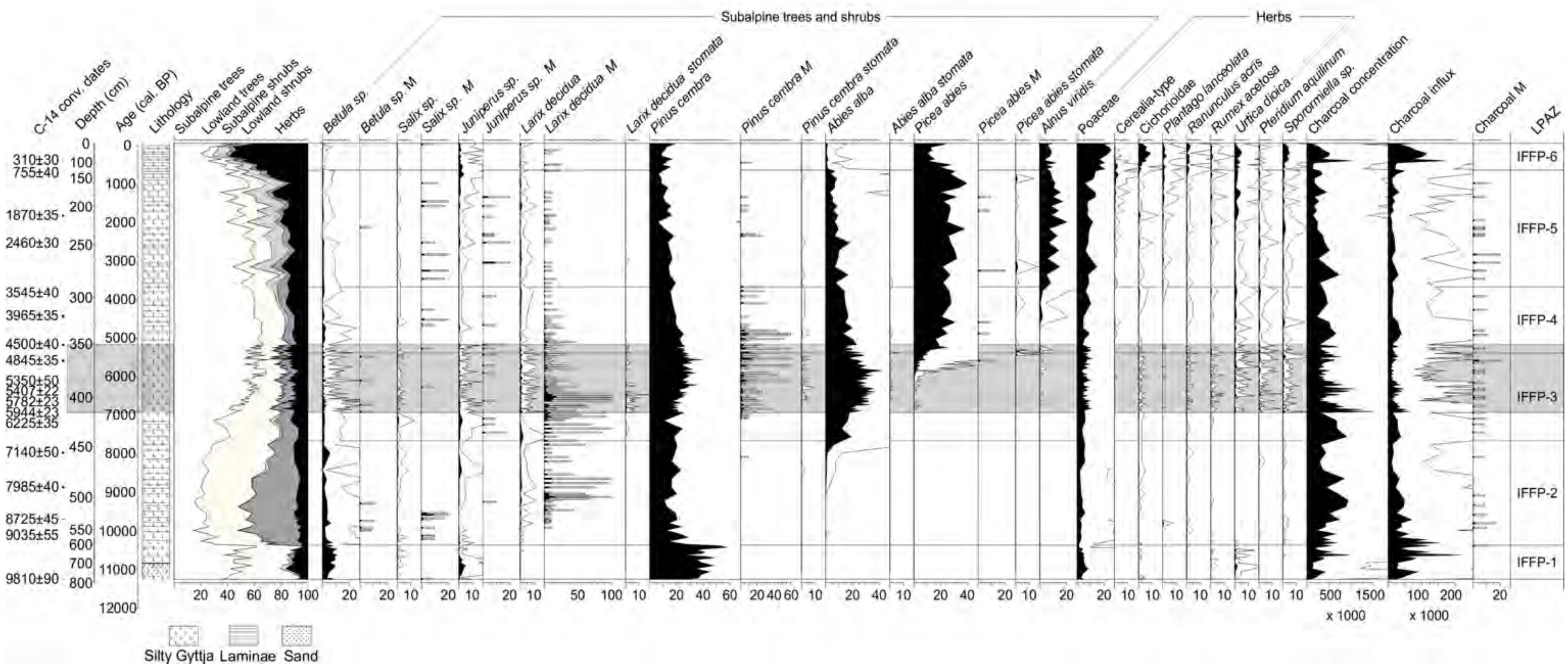

Fig. 3. Selected pollen, spore and stomata percentages of the entire Iffigsee record based on the terrestrial pollen sum as well as selected macrofossil concentrations (M), charcoal concentration and influx values and lithology. Empty curves and bars show 10x exaggeration. LPAZ = Local pollen assemblage zones. The grey area is the time period selected for high-resolution analysis. Analyst: Christoph Schwörer (pollen, spores, charcoal, macrofossils), Petra Kaltenrieder, Matthias Berlinger and Stephanie Frei (macrofossils).

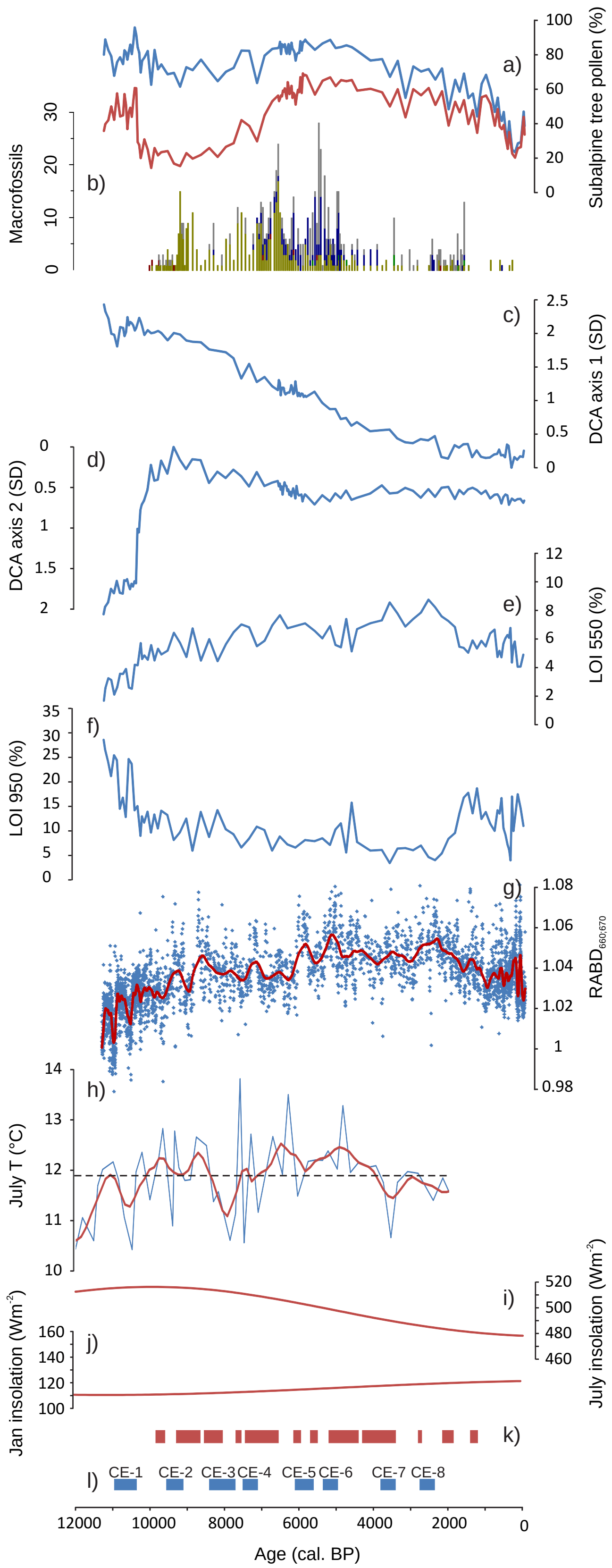

Fig. 4 Comparison of the main biotic and abiotic proxies of Iffigsee with different climate records. a) Percentage of subalpine tree pollen based on the total (red) and subalpine (blue) pollen sum. By calculating the pollen percentages based on the subalpine pollen sum (blue curve), the influence of lowland taxa is excluded. b) Stacked macrofossil record of subalpine tree macrofossils. Red: *Betula* sp., gold: *Larix decidua*, blue: *Pinus cembra*, green: *Picea abies*, grey: coniferous tree remains indet. c) DCA axis 1 and d) axis 2 of the Iffigsee pollen record. e) Percentage of Loss-On-Ignition (LOI) at 550 °C as a proxy for organic content of the sediment. f) Percentage of LOI at 950 °C as a proxy for carbonate content of the sediment. g) Relative absorbance band depth centred on the wavelengths 660/670 nm from visible light reflectance spectroscopy as a proxy for primary production in the lake. The red line is the LOESS smoothed data. h) July temperature reconstruction based on a chironomid transfer function from Hinterburgsee. The light blue line is the unsmoothed temperature reconstruction, the red line the LOESS smoothed data, the dashed horizontal line the current mean July T (Heiri et al. 2003a). i) July and j) January solar insolation (Laskar et al. 2004). k) Glacier recessions in the Swiss Alps indicating warm time periods (Joerin et al. 2006). l) Cold and wet phases identified from Central European pollen and macrofossil records (Haas et al. 1998)

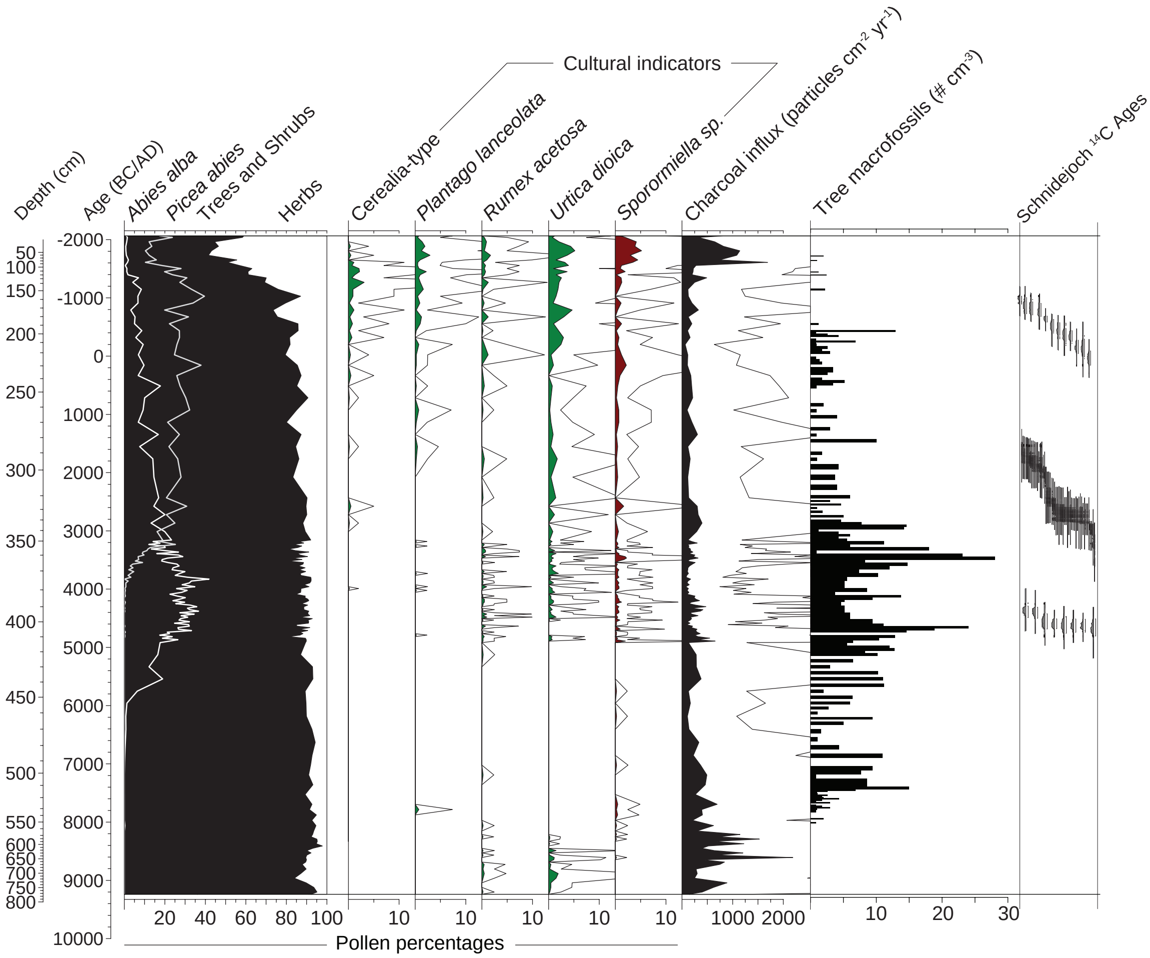

Fig. 12: Lake Iffigsee. Pollen diagram of select taxa, charcoal influx and arboreal macrofossils. Pollen percentages are based on the terrestrial pollen sum. Cultural indicators are pollen and spores indicative for anthropogenic activities. Charcoal influx is an indicator of regional fire activity. Empty curves are 10x exaggerations. Diagramm/graphic by Christoph Schwörer.

100 YEARS Journal of Ecology
British Ecological Society

Journal of Ecology 2015, **103**, 281–295 doi: 10.1111/1365-2745.12354

Early human impact (5000–3000 BC) affects mountain forest dynamics in the Alps

Christoph Schwörer[1,2]*, Daniele Colombaroli[1,2], Petra Kaltenrieder[1,2], Fabian Rey[1,2] and Willy Tinner[1,2]

[1]Institute of Plant Sciences, University of Bern, Altenbergrain 21, CH-3013, Bern, Switzerland; and [2]Oeschger Centre for Climate Change Research, University of Bern, Falkenplatz 16, CH-3012, Bern, Switzerland

Summary

1. The resilience, diversity and stability of mountain ecosystems are threatened by climatic as well as land-use changes, but the combined effects of these drivers are only poorly understood.
2. We combine two high-resolution sediment records from Iffigsee (2065 m a.s.l.) and Lauenensee (1382 m a.s.l.) at different elevations in the Northern Swiss Alps to provide a detailed history of vegetational changes during the period of first pastoralism (ca. 7000–5000 cal. BP, 5000–3000 BC) in order to understand ongoing and future changes in mountain ecosystems.
3. We use palaeoecological methods (fossil pollen, spore, microscopic charcoal and macrofossil analysis) as well as ecological ordination techniques and time-series analysis to quantify the impact of fire and grazing on natural mountain vegetation at Iffigsee.
4. Fire was used by Neolithic people to create pastures at timberline and clear forests for arable farming in the valley. This had a significant, long-term effect on the mountain vegetation and a negative impact on keystone forest species such as *Abies alba*, *Larix decidua* and *Pinus cembra*.
5. The mass expansion of *Picea abies* at ca. 5500 cal. BP (ca. 3500 BC) was facilitated by anthropogenic disturbance (fire, grazing and logging) causing an irreversible decline in *Abies alba*. Temperate *Abies alba* forests, which existed under warmer-than-today conditions, might be better adapted to projected climate change than today's drought-sensitive *Picea abies* forests, especially under low anthropogenic disturbance following land abandonment.
6. *Synthesis.* Human impact for millennia has shaped mountain vegetation in the Alps and still continues to have a large effect on today's species composition and distribution. Fire and traditional pastoralism have the potential to mitigate the effects of climate change, maintain species-rich high-alpine meadows and prevent biodiversity losses.

Key-words: biodiversity, climate change, conservation ecology, cross-correlations, fire, grazing, macrofossils, Neolithic, palaeoecology and land-use history, pollen

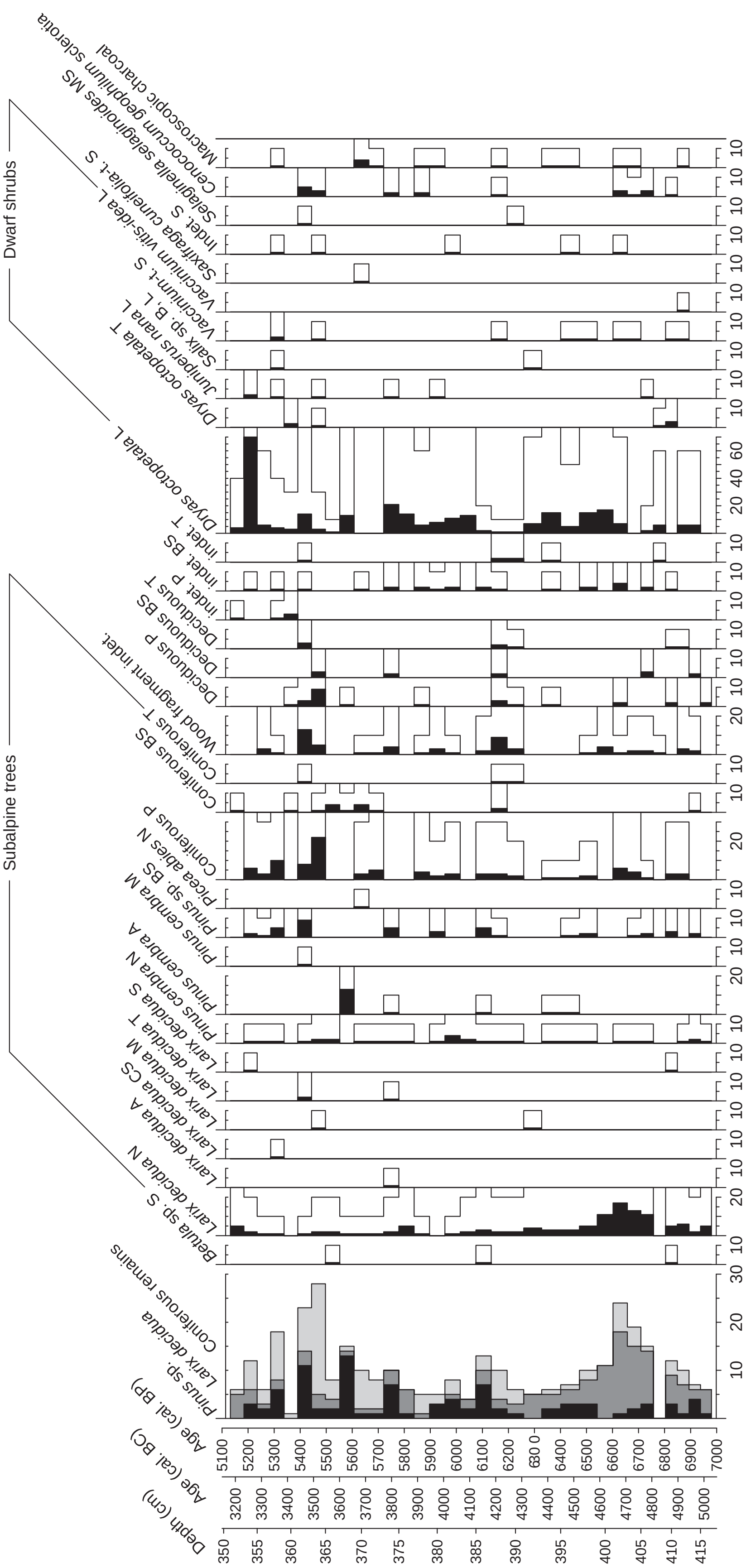

Fig. 3. Macrofossil diagram of the contiguous Iffigsee high-resolution sequence showing selected taxa only. S = seeds, N = needles, A = anthers, CS = conescales, M = mesoblasts, T = twigs, BS = budscales, P = periderm, L = leaves, B = buds, MS = macrospores. Empty bars show 10× exaggerations. Analysts: Petra Kaltenrieder and Stephanie Frei.

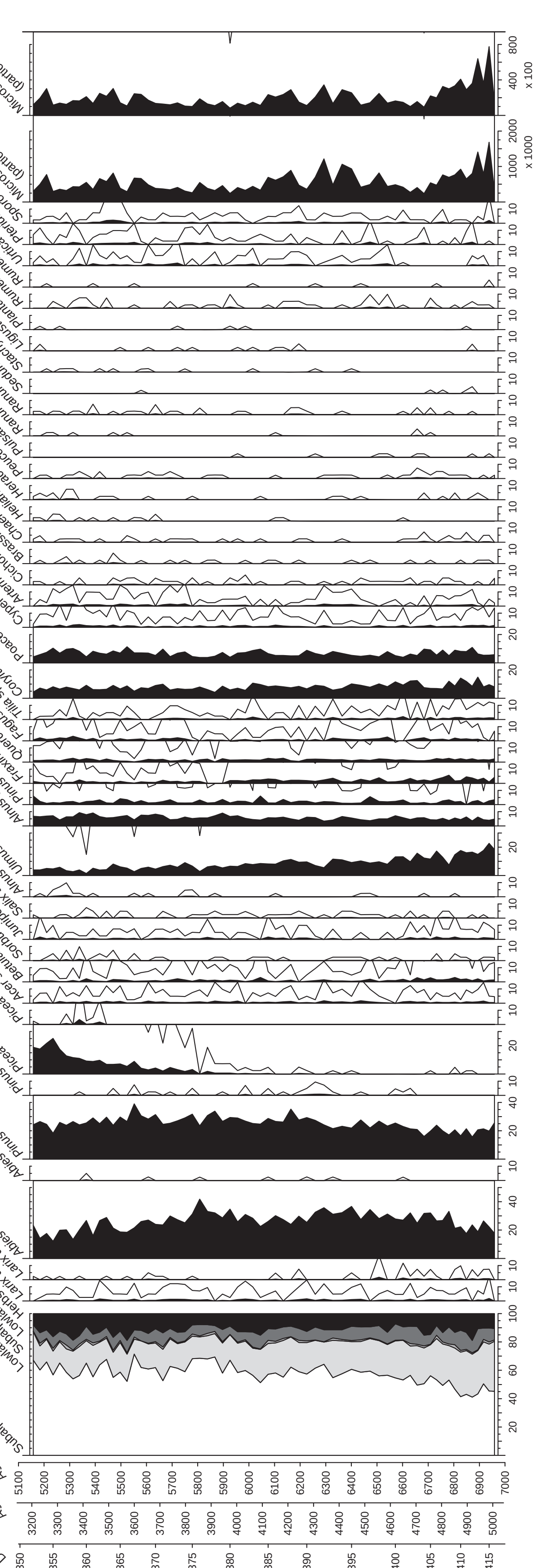

Fig. 4. Selected pollen, spore and stomata percentages as well as charcoal concentration and influx values of the contiguous Iffigsee high-resolution sequence. Empty curves show 10× exaggerations. Analyst: Christoph Schwörer.

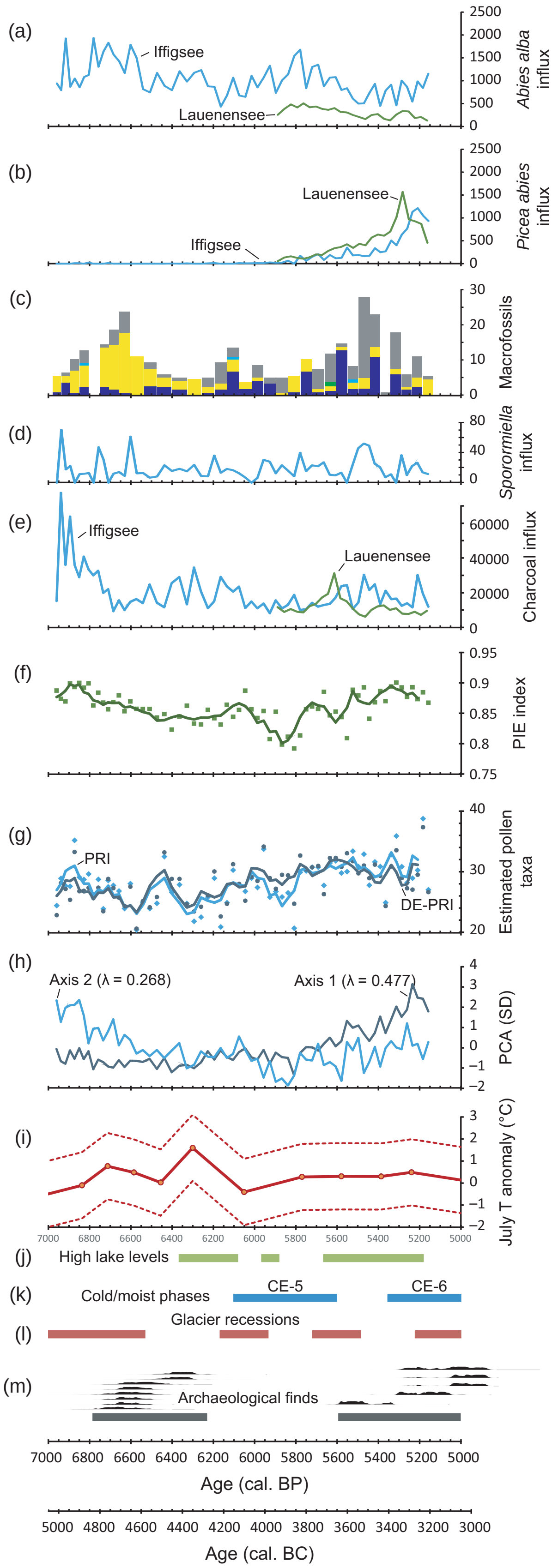

Fig. 5. a,b) Pollen influx values (# cm^{-2} yr^{-1}) of *Abies alba* and *Picea abies* at Iffigsee and Lauenensee respectively. c) Stacked macrofossil record of subalpine tree remains at Iffigsee. Blue = *Pinus cembra*, yellow = *Larix decidua*, green = *Picea abies*, light blue = *Betula* sp., grey = indet. coniferous. d) Sporormiella influx values at Iffigsee, e) microscopic charcoal influx at Iffigsee and Lauenensee. Note that the influx curve of Lauenensee is exaggerated by 10x for comparison. f) Palynological evenness (PIE) and g) palynological richness (PRI, light blue) as well as evenness-detrended palynological richness (DE-PRI, dark blue) as proxies for biodiversity. The smoothed lines are a three samples running mean. h) PCA-axis 1 and 2. i) July-temperature anomalies (solid line) from the chironomid-inferred Hinterburgsee temperature reconstruction including root mean square error of prediction (RMSEP; dotted lines) of 1.51°C (Heiri et al. 2003a). j) Periods of high lake levels in Central Europe after Magny (2004). k) Cold and wet phases identified from Central European pollen and macrofossil records after Haas et al. (1998). l) Glacier recessions in the Swiss Alps indicating warm time periods after Joerin et al. (2006). m) ^{14}C-Dates of archaeological finds from the Schnidejoch indicating human presence in the area (Hafner 2012).

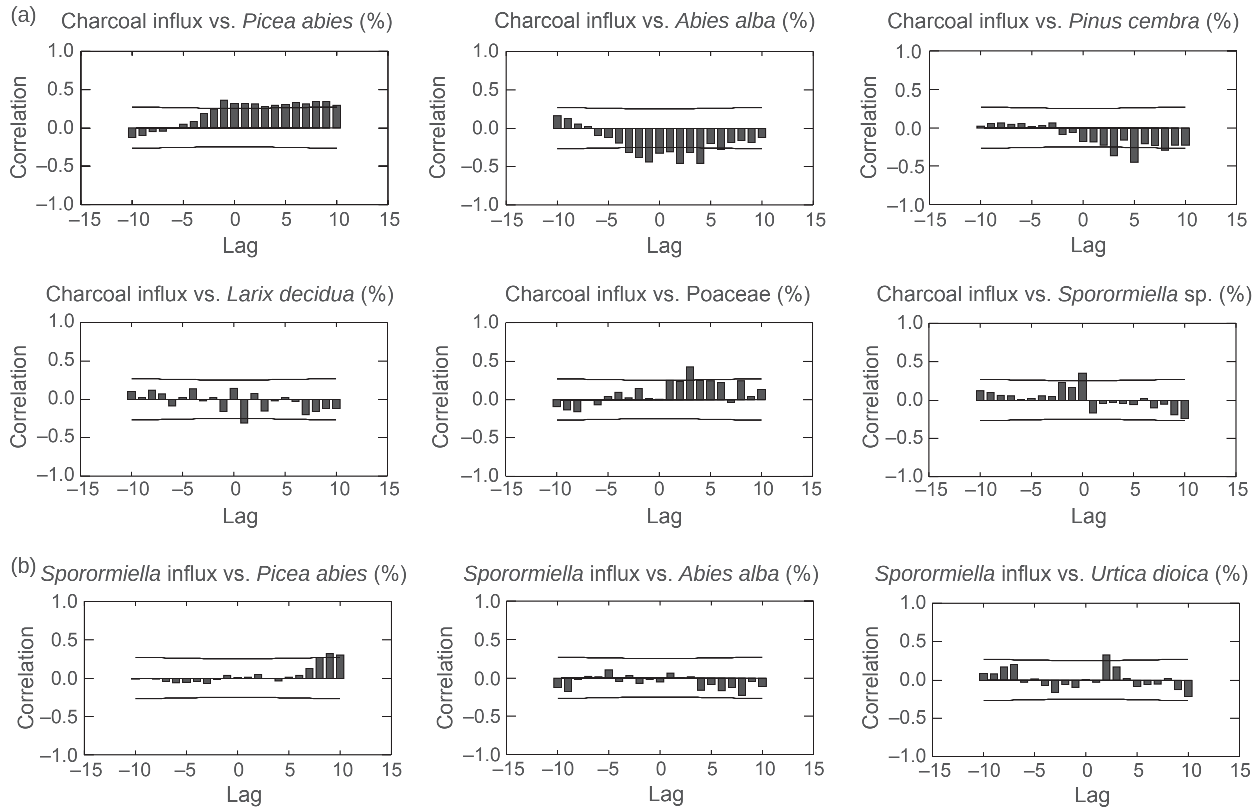

Fig. 7. Cross-correlation analysis of (a) microscopic charcoal influx and (b) *Sporormiella* influx vs. selected taxa from the high-resolution sequence (6960–5160 cal. BP). 1 lag = 29 ± 7.5 years. The solid black lines mark the significance level ($P < 0.05$). [Correction added on 12th February 2015, after first online publication: missing labels added to Figs 7 and 8]

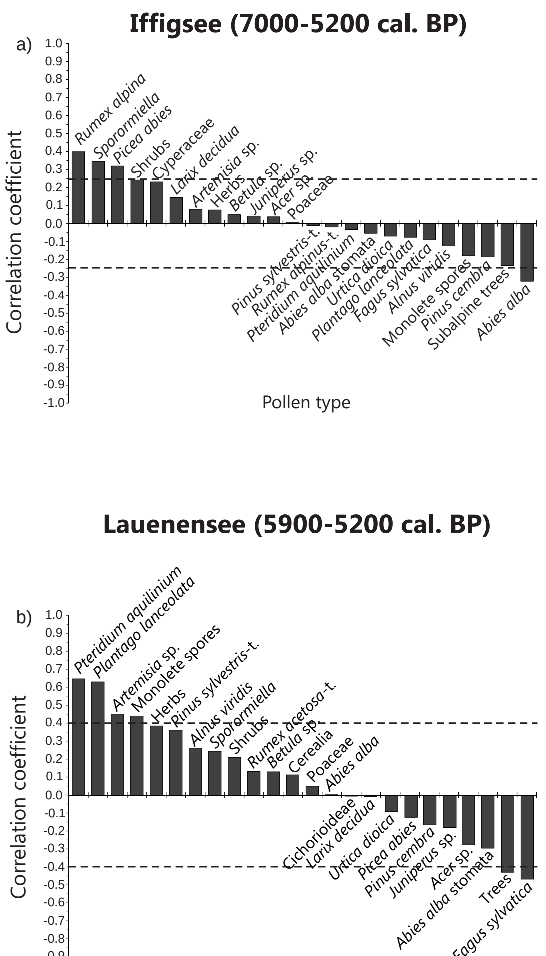

Fig. 8. Correlograms showing correlation coefficients between microscopic charcoal influx and selected pollen and spore types for a) Iffigsee and b) Lauenensee. The dashed lines mark the significance level ($P<0.05$).

Global Change Biology

Global Change Biology (2014) **20**, 1512–1526, doi: 10.1111/gcb.12456

A model-data comparison of Holocene timberline changes in the Swiss Alps reveals past and future drivers of mountain forest dynamics

CHRISTOPH SCHWÖRER*, PAUL D. HENNE*† and WILLY TINNER*†

*Paleoecology, Institute of Plant Sciences and Oeschger Centre for Climate Change Research, University of Bern, Altenbergrain 21, CH-3013 Bern, Switzerland, †Forest Ecology, Institute of Terrestrial Ecosystems, ETH Zürich, Universitätsstrasse 16, CH-8092 Zürich, Switzerland

Abstract

Mountain vegetation is strongly affected by temperature and is expected to shift upwards with climate change. Dynamic vegetation models are often used to assess the impact of climate on vegetation and model output can be compared with paleobotanical data as a reality check. Recent paleoecological studies have revealed regional variation in the upward shift of timberlines in the Northern and Central European Alps in response to rapid warming at the Younger Dryas/Preboreal transition ca. 11 700 years ago, probably caused by a climatic gradient across the Alps. This contrasts with previous studies that successfully simulated the early Holocene afforestation in the (warmer) Central Alps with a chironomid-inferred temperature reconstruction from the (colder) Northern Alps. We use LandClim, a dynamic landscape vegetation model to simulate mountain forests under different temperature, soil and precipitation scenarios around Iffigsee (2065 m a.s.l.) a lake in the Northwestern Swiss Alps, and compare the model output with the paleobotanical records. The model clearly overestimates the upward shift of timberline in a climate scenario that applies chironomid-inferred July-temperature anomalies to all months. However, forest establishment at 9800 cal. BP at Iffigsee is successfully simulated with lower moisture availability and monthly temperatures corrected for stronger seasonality during the early Holocene. The model-data comparison reveals a contraction in the realized niche of *Abies alba* due to the prominent role of anthropogenic disturbance after ca. 5000 cal. BP, which has important implications for species distribution models (SDMs) that rely on equilibrium with climate and niche stability. Under future climate projections, LandClim indicates a rapid upward shift of mountain vegetation belts by ca. 500 m and treeline positions of ca. 2500 m a.s.l. by the end of this century. Resulting biodiversity losses in the alpine vegetation belt might be mitigated with low-impact pastoralism to preserve species-rich alpine meadows.

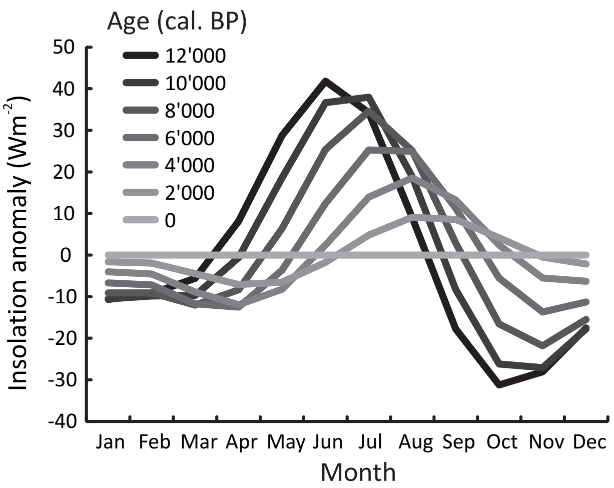

Fig. 2 Monthly insolation anomalies (relative to today) for different time periods in the Holocene (Laskar et al., 2004).

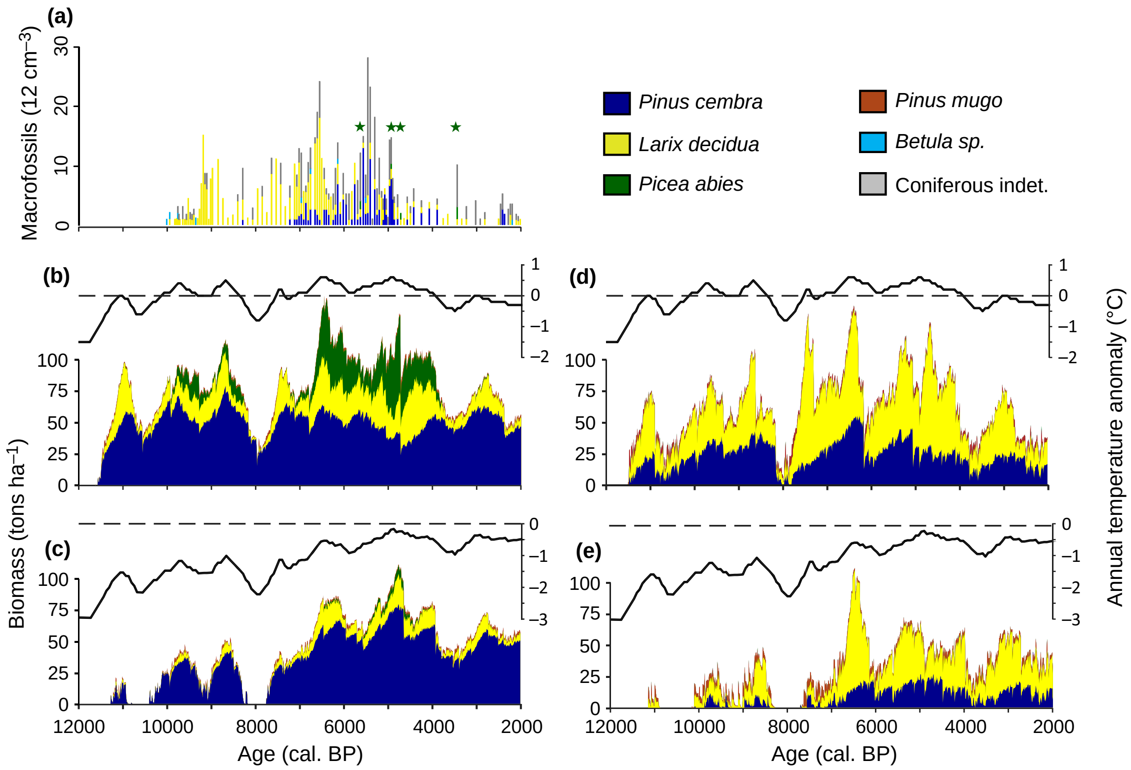

Fig. 3 Comparison of macrofossil data with different LandClim simulations (local scale). (a) Tree macrofossil concentrations (number of macrofossils cm^{-3} of sediment) at Iffigsee. The green stars highlight samples with spruce macrofossils. (b) Top, temperature input used in the model. Bottom, forest biomass simulated within a 50 m radius of Iffigsee with temperatures according to the Hinterburgsee July-temperature reconstruction (Heiri *et al.*, 2003), present soil, and precipitation (standard scenario). (c) Same as (b) but with monthly temperatures corrected for insolation (seasonality scenario). (d) Same as (b) but with maximum bucket size = 4 cm and precipitation set to 70% of present values (soil and precipitation scenario). (e) Same as (c) but with max bucket = 4 cm and precipitation = 70% (soil and precipitation scenario).

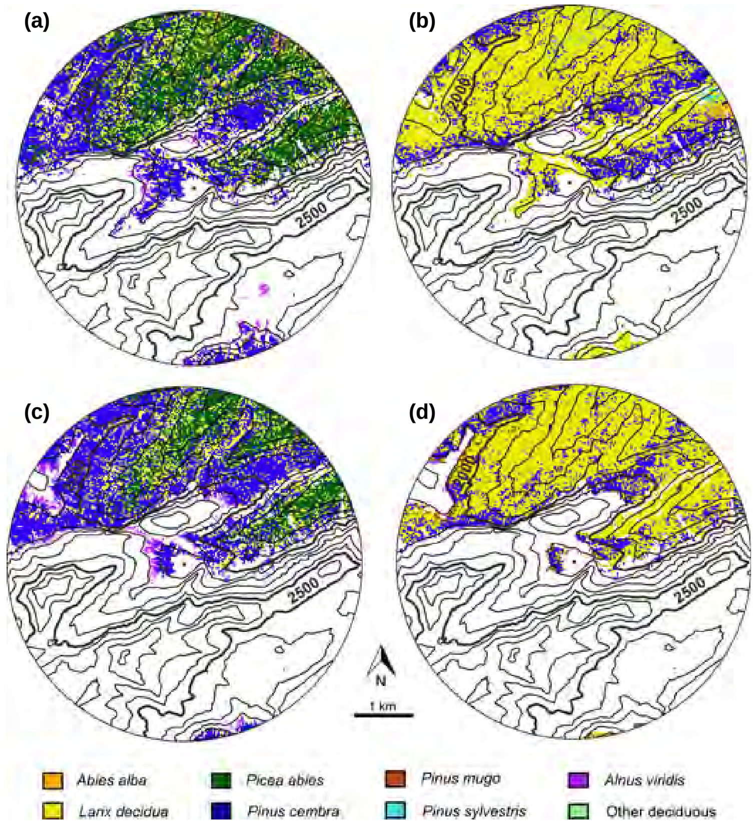

Fig. 5 Dominant tree species in every grid cell of the study landscape at 9800 cal. BP for different simulations. (a) Standard scenario with temperatures according to the Hinterburgsee July-temperature reconstruction (Heiri *et al.*, 2003), present soil and precipitation. (b) Same as (a) except maximum bucket size = 3 cm (soil scenario). (c) Same as (a) but with monthly temperatures corrected for solar insolation (seasonality scenario). (d) Same as (c) but with maximum bucket size = 4 cm and precipitation = 70% of present values (soil and precipitation scenario).

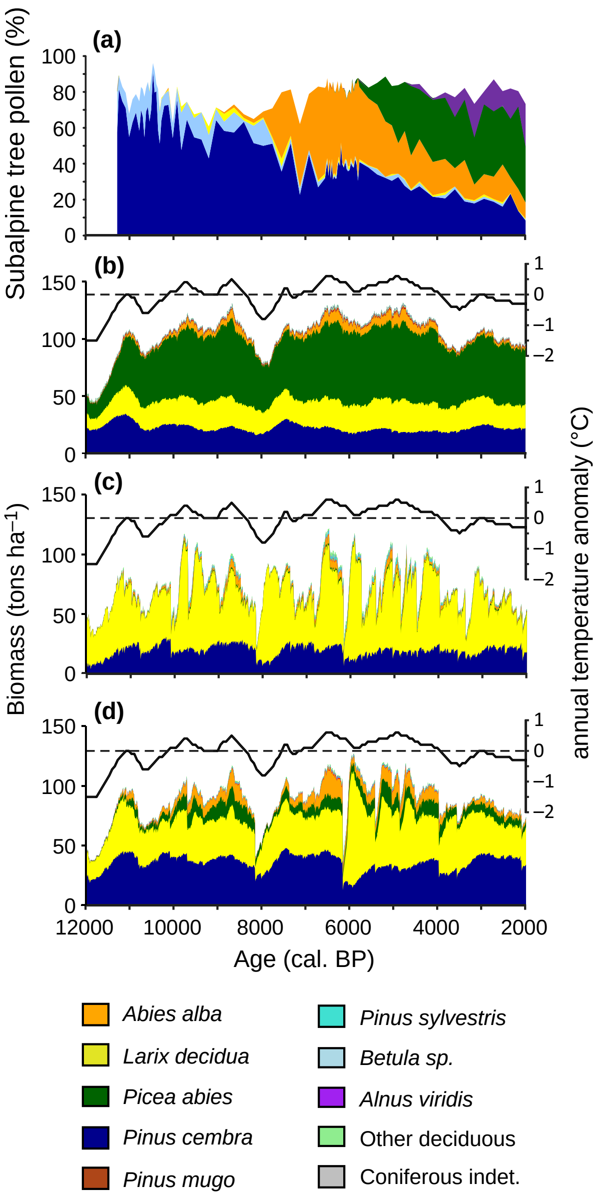

Fig. 4 Comparison of pollen data with different LandClim simulations (landscape scale). (a) Percentage of subalpine arboreal pollen at Iffigsee. (b) Top, temperature input used in the model. Bottom, forest biomass simulated within the study landscape with temperatures according to the Hinterburgsee July-temperature reconstruction (Heiri *et al.*, 2003), present soil, and precipitation (standard scenario). (c) Same as (b) except maximum bucket size = 3 cm (soil scenario). (d) Same as (b) except maximum bucket size = 4 cm and precipitation = 80% of present values (soil and precipitation scenario).

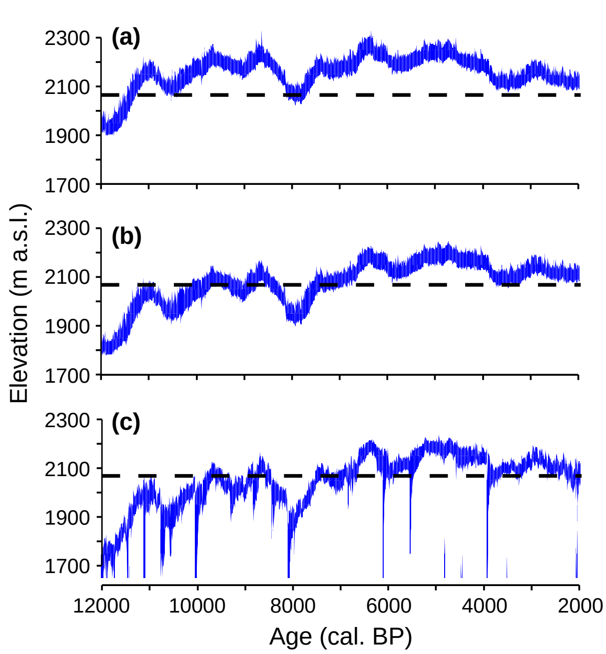

Fig. 6 Simulated changes in timberline elevation in the study landscape for different scenarios. Grid cells are defined as timberline if forest biomass is 25–50 t ha^{-1}. The elevation of Iffigsee (2065 m a.s.l.) is marked with a dashed line. (a) Standard scenario with temperatures according to the Hinterburgsee July-temperature reconstruction (Heiri *et al.*, 2003), present soil, and precipitation. (b) Same as (a) but with monthly temperatures corrected for solar insolation (seasonality scenario). (c) Same as (b) but with maximum bucket size = 4 cm and precipitation = 70% of present values (soil and precipitation scenario).

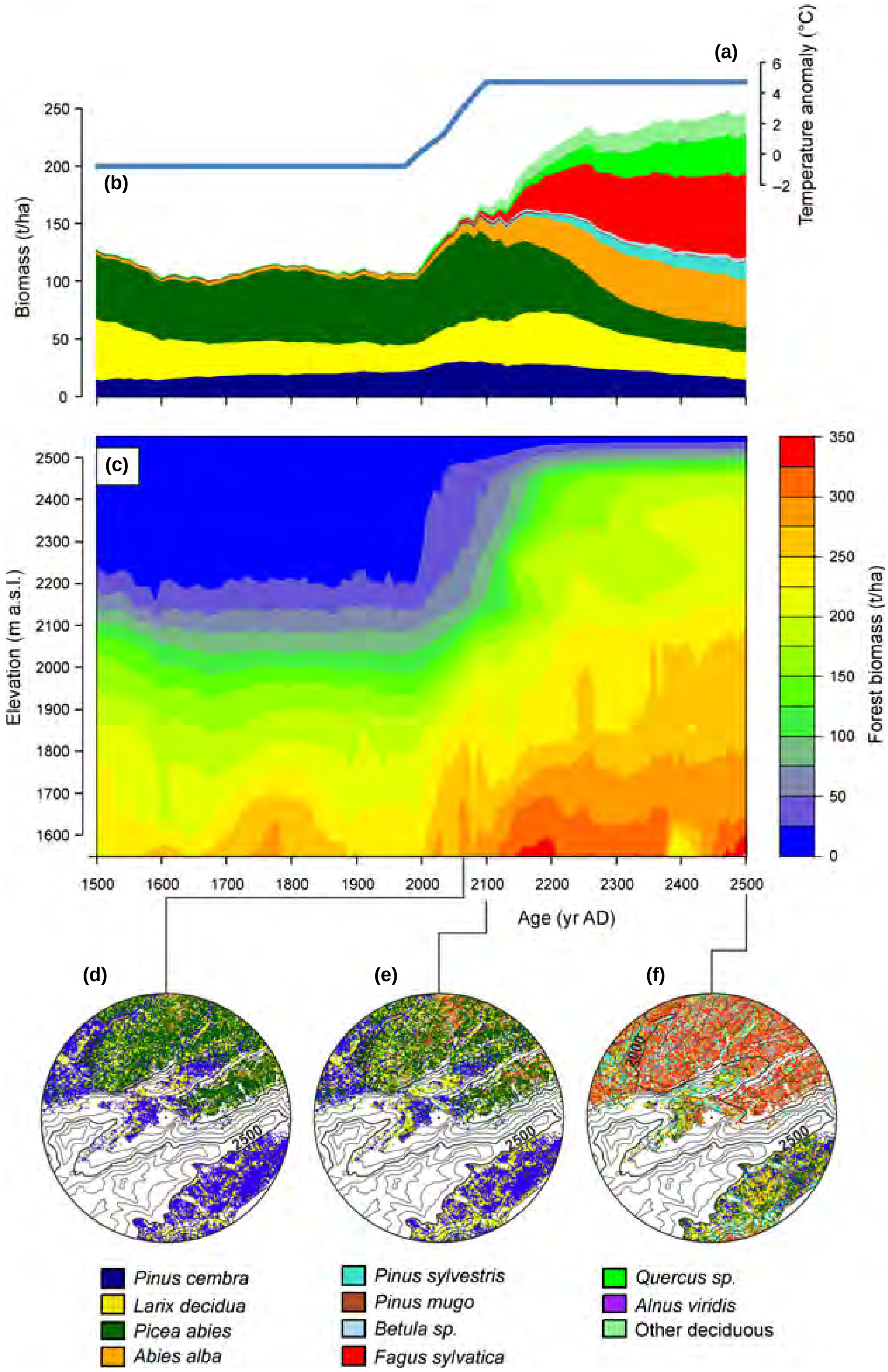

Fig. 7 Simulated changes in the vegetation in the study landscape under projected climate warming. (a) Temperature projections of the A1B scenario used to run the simulation. Note that temperatures were set to the values of 1960–1990 before 1975 and to the values of 2085–2115 after 2100. (b) Simulated forest biomass of all the tree species in the study landscape. (c) Simulated forest biomass at different elevations in the study landscape. (d) Dominant tree species in every grid cell of the study landscape at 2060 AD. (e) Same as (d) but at 2100 AD. (f) Same as (d) but at 2500 AD.

FrozenFire – a contribution to Paleo Fires, land use and vegetation dynamics from a high-alpine ice core over the last millennium

Sandra O. Brügger[1], Erika Gobet[1], Federica Schanz[1], Michael Sigl[2], Dimitri Osmont[2], Daniele Colombaroli[1], Margit Schwikowski[2], Willy Tinner[1]

[1] Institute of Plant Sciences & Oeschger Centre for Climate Change Research, University of Bern
[2] Laboratory of Environmental Chemistry, Paul Scherrer Institute, Villigen

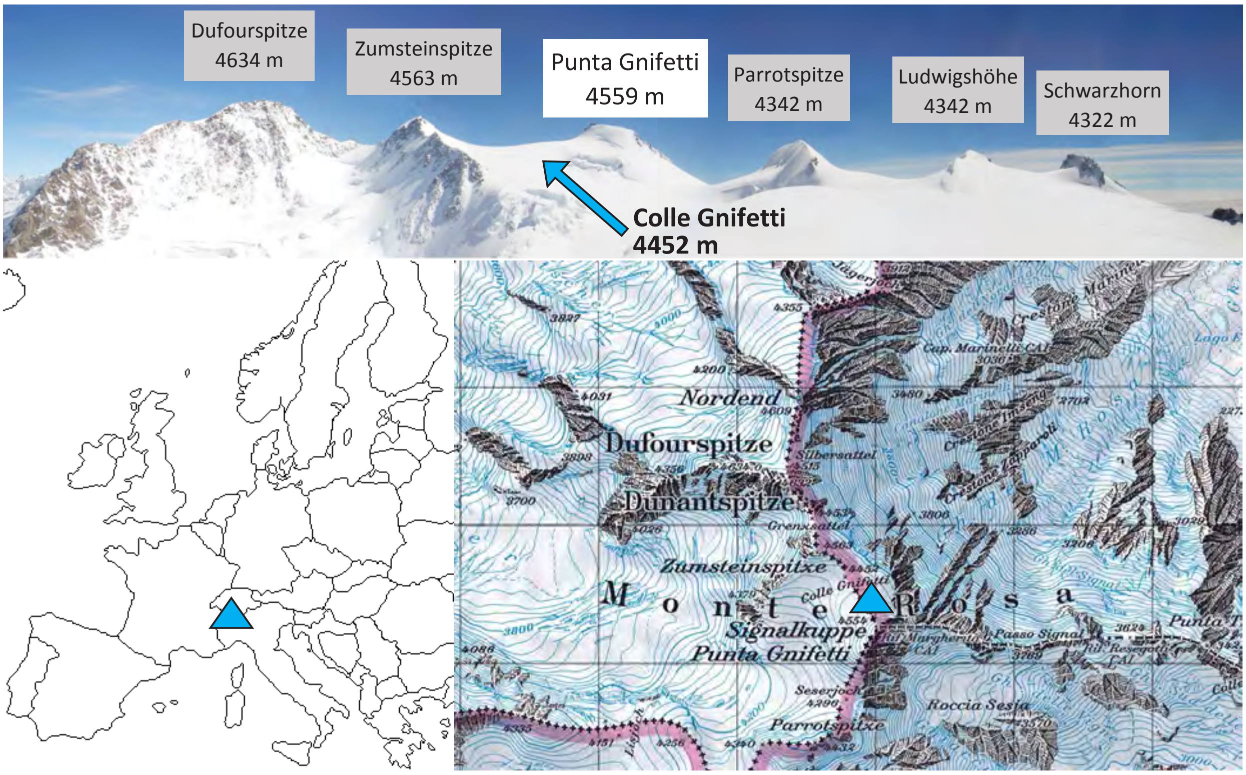

Figure 1 Panorama of the Monte Rosa massif (view from North) and a map showing the drilling location of the ice core on the Colle Gnifetti glacier (triangle).

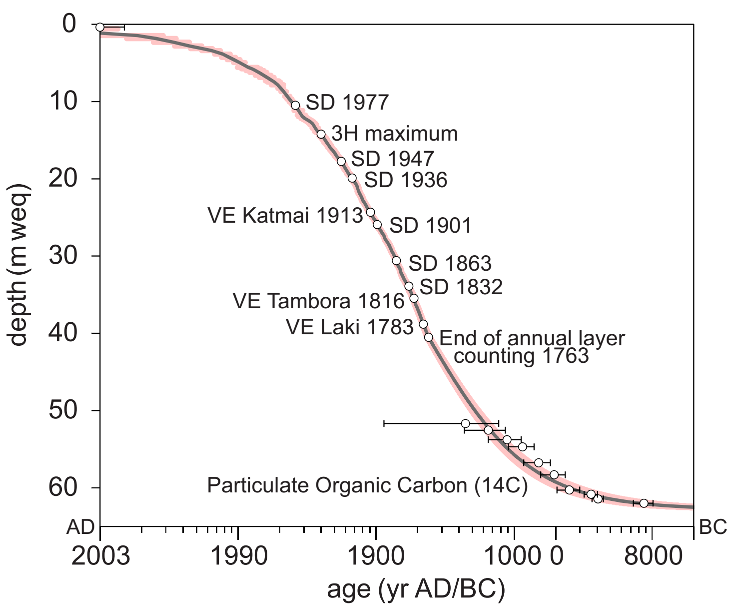

Figure 2 Two-parameter model derived depth-age relationship for the Colle Gnifetti ice core. The model is based on distinct Saharan dust events (SD), volcanic eruptions (VE), and the tritium signal from nuclear weapon tests (all indicated with calendar dates, AD), as well as calibrated ^{14}C ages $\pm1\sigma$ derived from the analysis of water-insoluble carbonaceous aerosols (i.e., OC) which were extracted from the ice. (Graph modified from Jenk et al. 2009, Sigl et al. 2009).

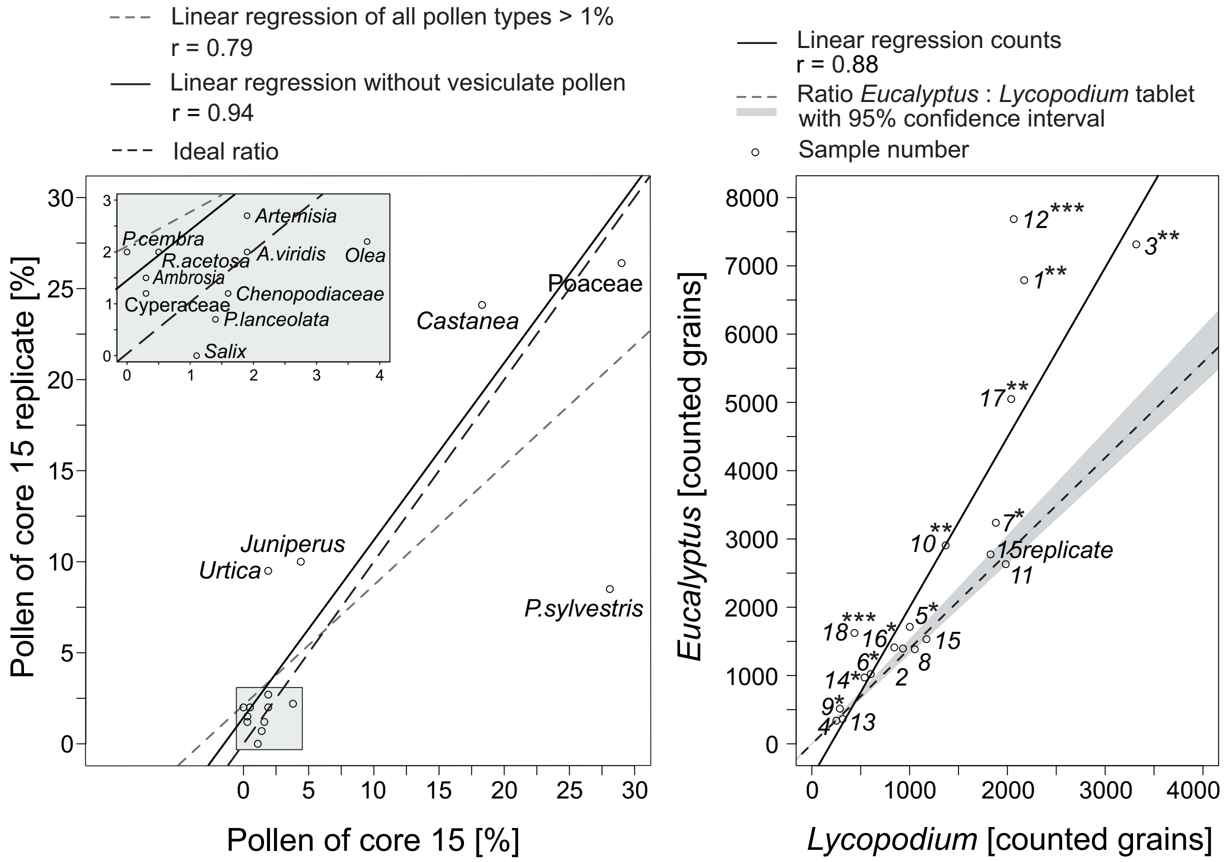

Figure 3 Left side: Comparison of a replicate pollen sample of the Colle Gnifetti record. All pollen types >1% in one of the samples shown. Linear regression of all pollen types >1% (continuous black line) and without vesiculate pollen types (dashed grey line). **Right side**: marker ratio of Eucalyptus (added before mounting in glycerine) and Lycopodium (added prior to sample treatment) for firn samples of Colle Gnifetti. Linear regression (continuous black line) and the ideal marker relationship (dashed line) with a confidence interval for the tablet uncertainty (grey). Sample loss was classified in " " = no loss, * = 0-33% loss, ** = 33-66% loss and *** = >66% loss of the sample during lab treatment.

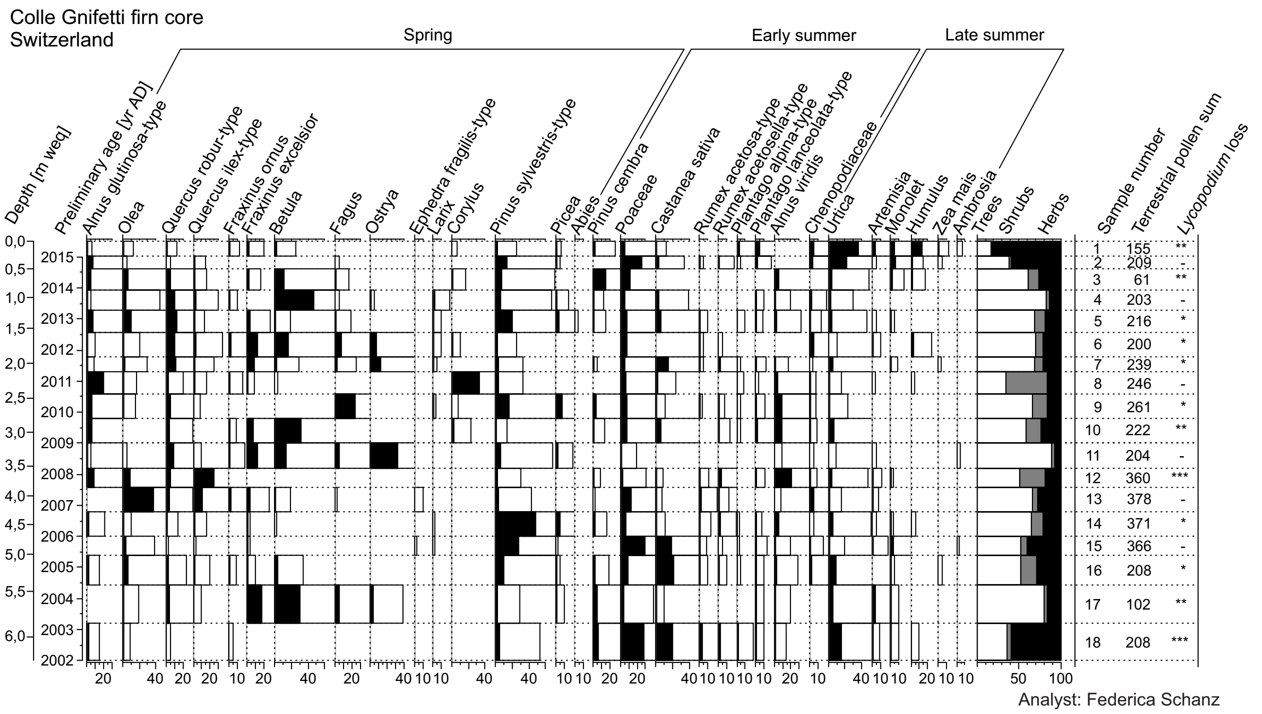

Figure 4 Pollen percentage diagram of a firn core from Colle Gnifetti cored in September 2015 with indication of sample loss during lab treatment (Sample loss was classified in " " = no loss, * = 0-33% loss, ** = 33-66% loss and *** = >66% loss of the total sample during lab treatment).

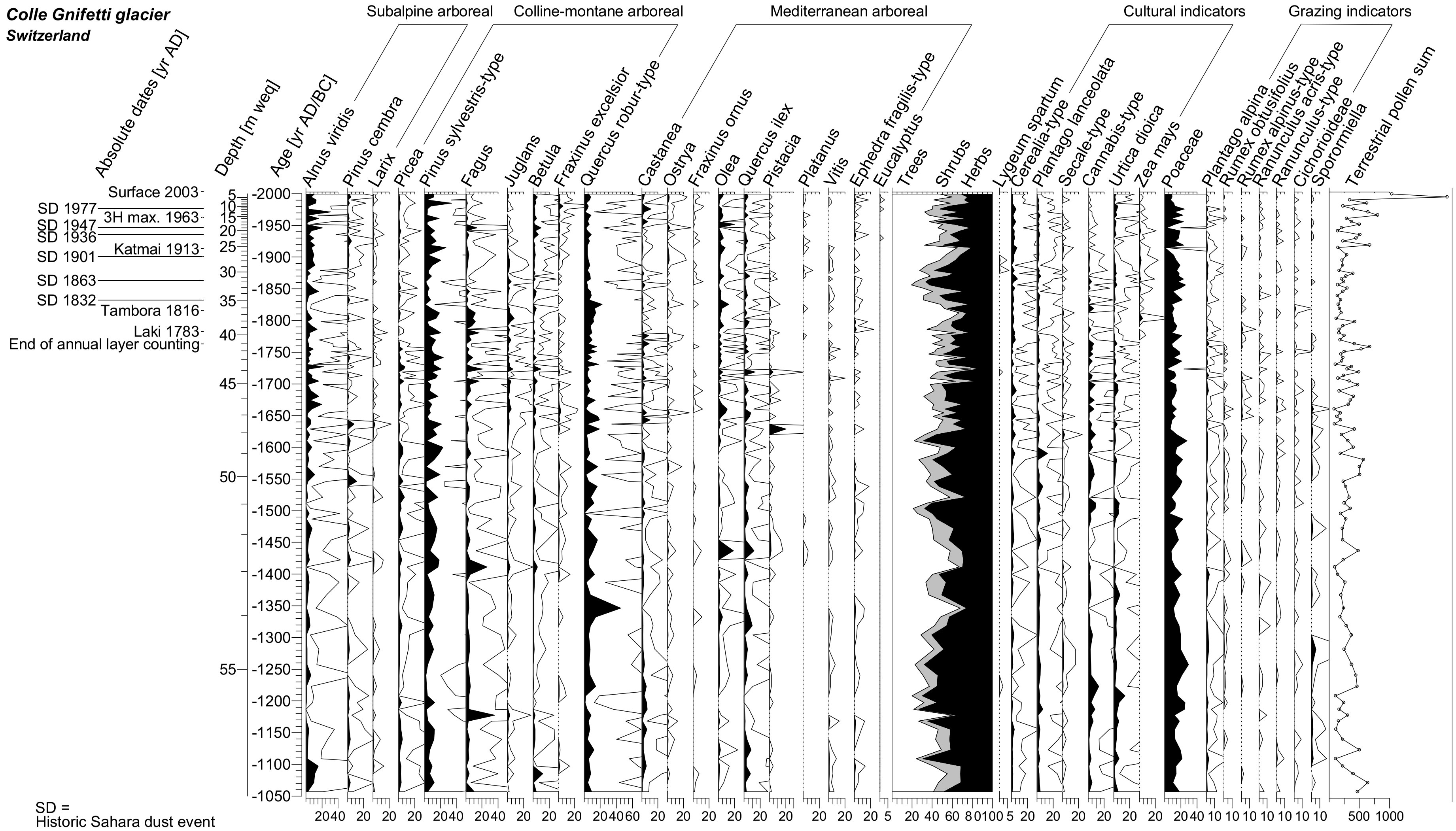

Figure 5 Pollen percentage diagram of Colle Gnifetti glacier with 10x exaggeration (white curves) based on the terrestrial pollen sum.

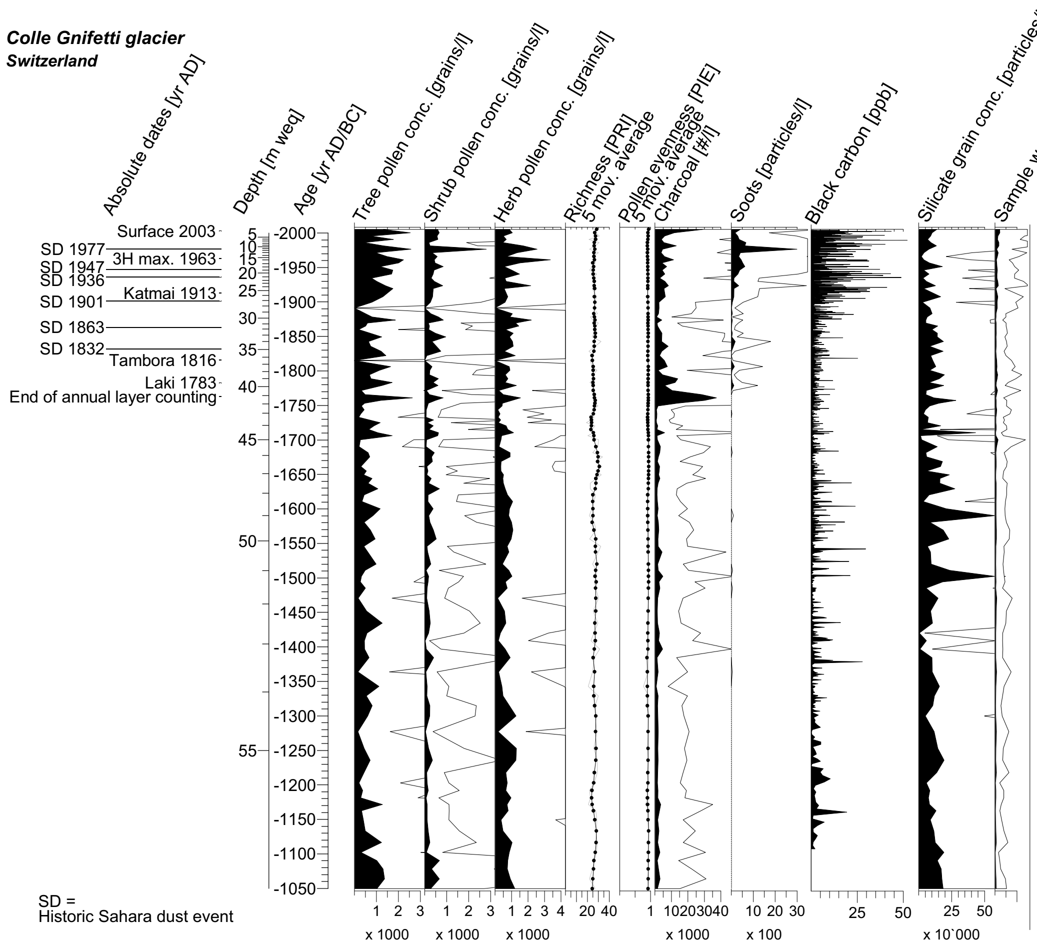

Figure 6 Summary curves of pollen, charcoal, soot and silicate concentrations, palynological richness (PRI), pollen evenness (PIE), (all curves showing a maximum resolution of 5 years, optical analysis in pollen samples: S. Brugger), high resolution black carbon concentration (measurements: M. Sigl, Paul Scherrer Institute Villigen) and absolute dates (taken from Jenk et al. 2009, Sigl et al. 2009).

References:

M. Sigl, T.M. Jenk, T. Kellerhals, M. Ruff, S. Szidat, H.W. Gäggeler, L. Wacker, H.-A. Synal, C. Boutron, C. Barbante, M. Schwikowski (2009). Towards radiocarbon dating of ice cores. Journal of Glaciology, 55(194), 985-996.

T.M. Jenk, S. Szidat, D. Bolius, M. Sigl, H.W. Gäggeler, L. Wacker, M. Ruff, C. Barbante, C.F. Boutron, M. Schwikowski (2009). A novel radiocarbon dating technique applied to an ice core from the Alps indicating late Pleistocene ages. Journal of Geophysical Research: Atmospheres, 114(D14).

Friday 09.09.2016

8:30 h	Walk to the Valais Museum of History
9:00 h	Archaeology of Central Alpine environments (Philippe Curdy)
10:00 h	Departure to Lac du Mont d'Orge
10:30 h	**Lac du Mont d'Orge**: 16'000 years of vegetation history, the Welten record. Human impact and diversity dynamics at the Mesolithic/Neolithic transition (Daniele Colombaroli)
11:30 h	Charcoal and pollen trap measurements: remote-sensing based fire and biodiversity estimates (Carole Adolf)
12:00 h	Ancient viticulture (Lucia Wick)
12:30 h	Lunch
13:30 h	Departure to Villars-sur-Ollon
15 h	Train to Col de Bretaye
15:45 h	**Lac de Bretaye**: vegetation, land use and fire history, extinct boreo-nemoral forests in the Alps (Lena Thöle and Christoph Schwörer)
17:30 h	Train back to Villars-sur-Ollon (last train!)
18 h	Departure to Gruyères
19 h	Arrival at Hôtel de Gruyères (Gruyères)
20 h	Farewell dinner at Chalet de Gruyères (Gruyères)

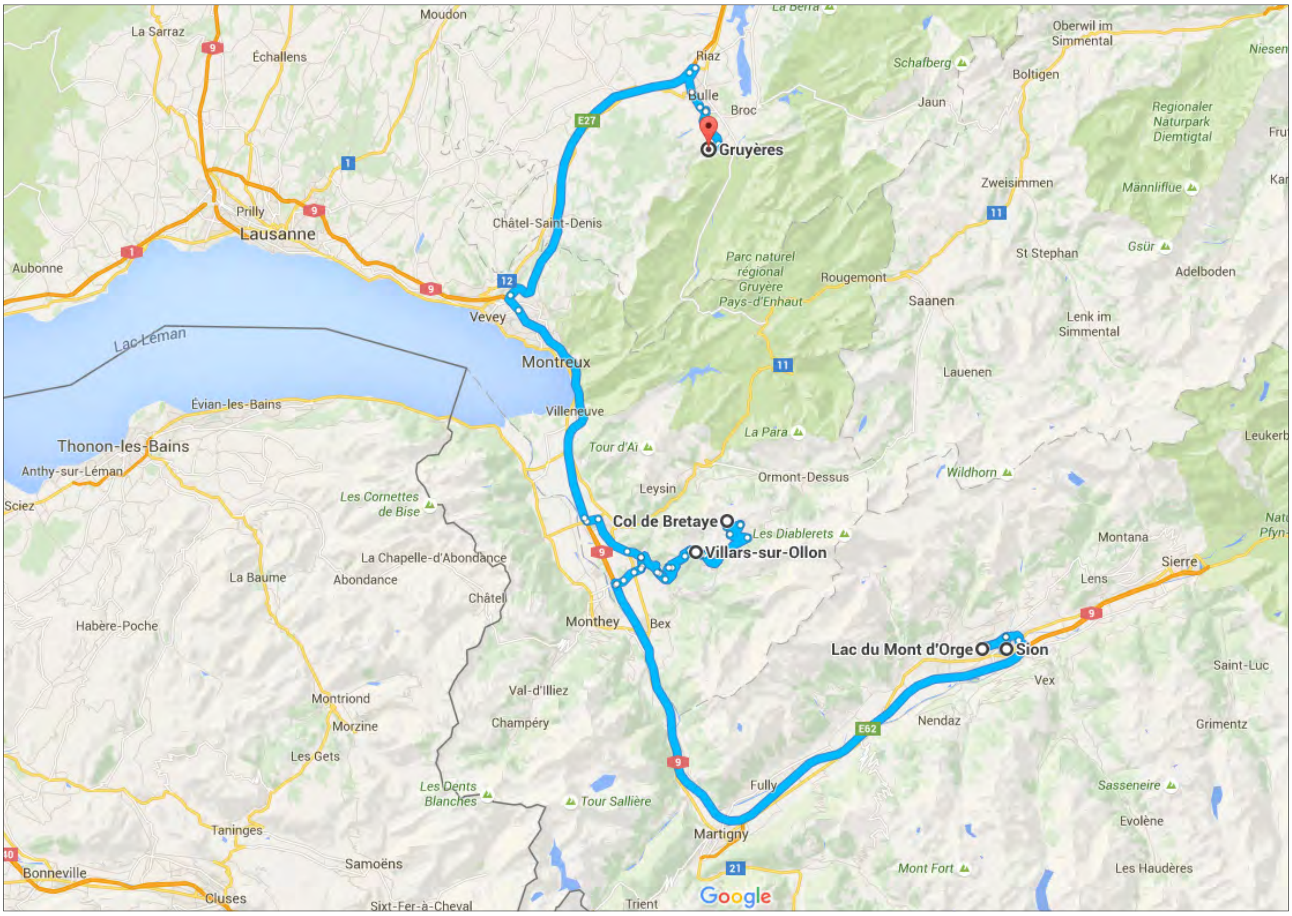

Prehistoric settlement evolution in the Upper Rhone valley: ca 9'000 BC – 15 BC.

Philippe Curdy

Musée d'Histoire du Valais, Canton du Valais, Rue des Châteaux 14, 1950 Sion, Switzerland
philippe.curdy@admin.vs.ch

During the 20th century, the evolution of prehistoric settlements in the Upper Rhone Valley, from the source of the Rhone River to the Lake of Geneva's eastern banks (Switzerland), became evident as a result of numerous excavations and research projects. In 1983, the first theoretical model for the Mesolithic, Neolithic and Early Bronze Age periods was published by A. Gallay. At the end of the 1990's, this model was developed to include all of prehistoric time (ca 9,500-15 BC).
From the year 2000 to 2012, small surveys and excavations confirmed the hypothesis of a gradual colonisation of vegetation belts from the plain (collinean belt) to the alpine zones over 2,000 m in relation to the evolution of agro-pastoral practices. After the end of the last Ice Age, Mesolithic hunter-gatherers seemed to have colonized the Rhone Valley in a south-north direction, over the mountain passes connecting northern Italy to the Rhone Valley and a western route by Lake Geneva and Swiss Midlands. It is presumed that early Neolithic culture spread to Valais following these south-north journeys. The Bronze Age reveals a strong demographic development. Later on, mountain passes seem to have played a more important role and the alpine communities profited from their location between south and north-alpine Europe.
The economic management of the production zones can be seen as an attempt to control the differing altitude levels over time, cumulating in the Iron Age, with the first graveyards and permanent settlements in middle altitude. At the Roman Period the indigenous settlement seems to follow the same organisation. This was understood to indicate an economic organisation of the region which generally remained the same until recent times, at least in certain regions of the Rhone Valley.

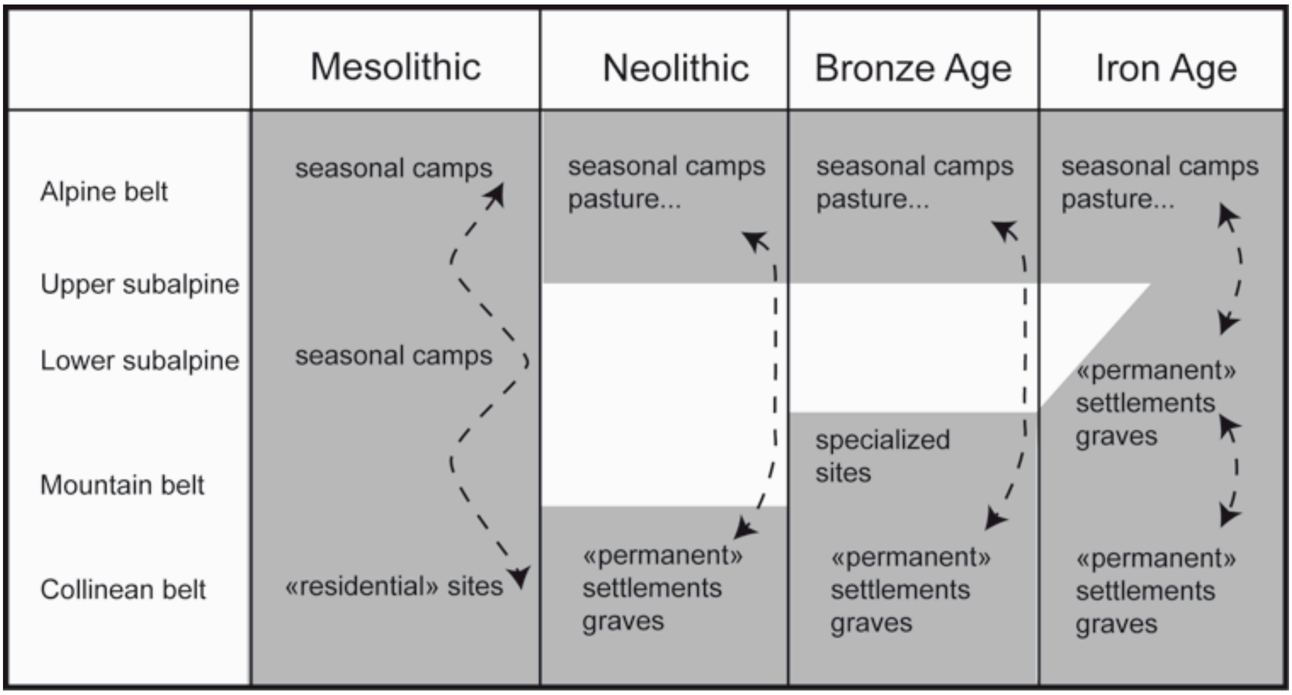

Upper Rhone valley (Valais). Model of the evolution of the main economic territories in prehistoric times. After Curdy 2015.

Bibliography

Curdy 2015, Philippe Curdy, Prehistoric settlement evolution in the Upper Rhone Valley (Western Swiss Alps): an upgraded vision, in: Giovanna Pizziolo Lucia Sarti (eds), Predicting Prehistory, Predictive models and field research methods for detecting prehistoric contexts. Milleni, studi di archeologia preistorica, 11, 2015, 85-96.

Curdy/Chaix 2009, Philippe Curdy et Louis Chaix, Les premiers pasteurs du Valais. Le Globe, 149, 2009, 93-116.

Gallay (ed.) 2008, Alain Gallay (ed.), Des Alpes au Léman. Images de la préhistoire. Gollion 2008.

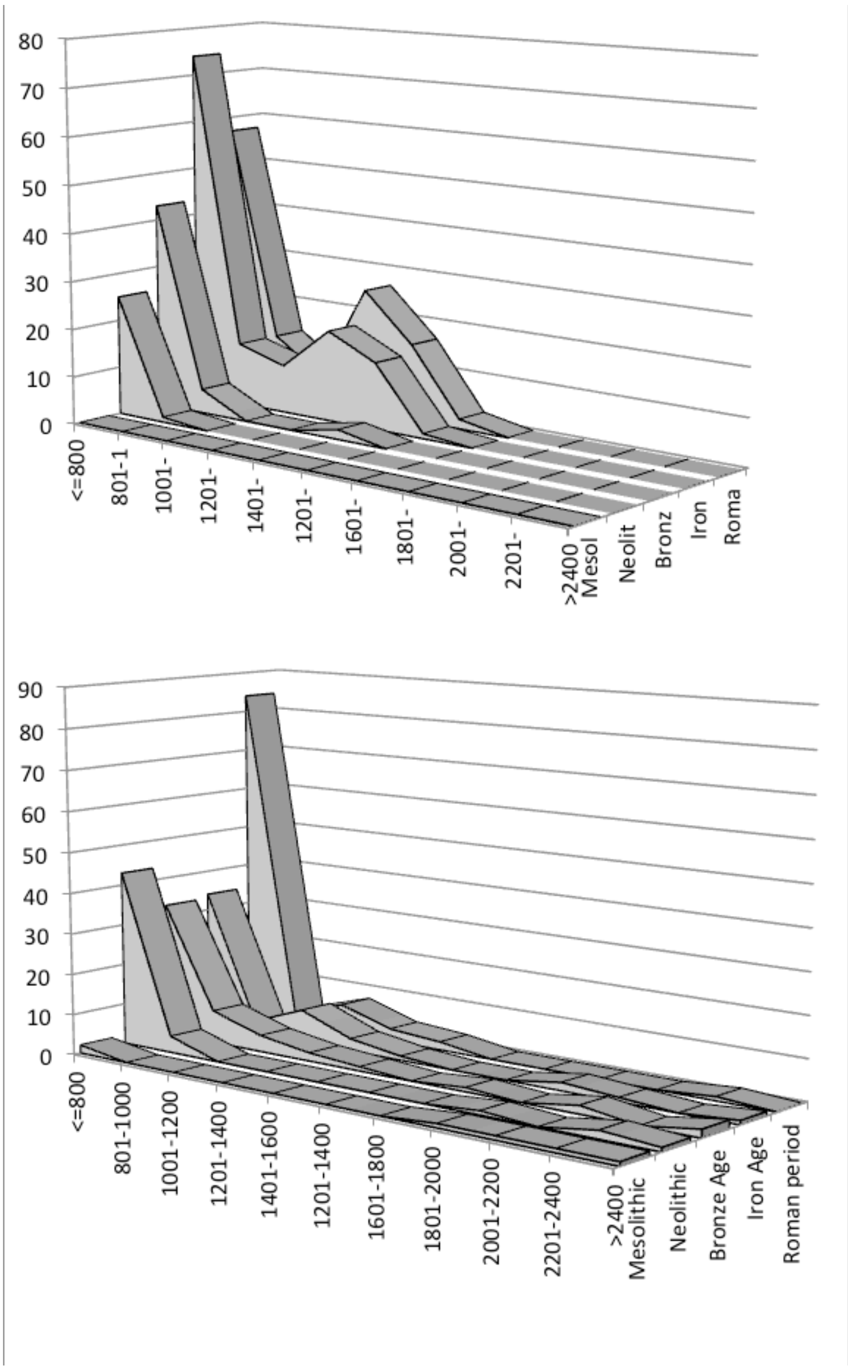

Upper Rhone valley (Valais). Distribution of settlements (below) and graves (above) by period and height range (state of knowledge 2012). After Curdy 2015.

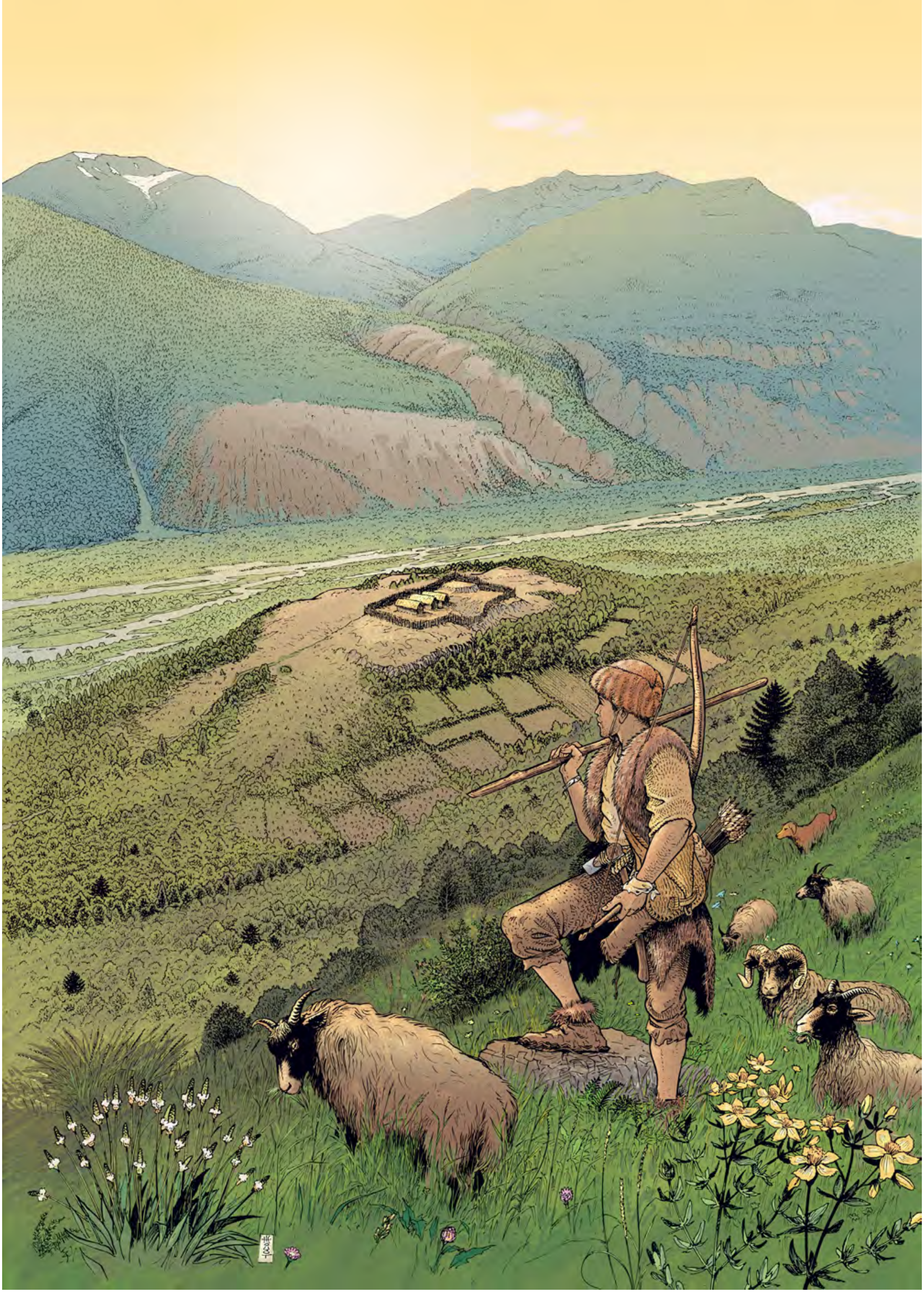

Neolithic herdsman overlooking the valais (Gallay, 2008)

The region of Sion around 13 000 B.C.: The retreat of the Rhône glacier

In the central Valais, the glacier retreated around 13 000 B.C., at the end of the Older Dryas. In this recreation, the tongue of the glacier is visible in the foreground, around the Val d'Hérens. The valley slopes are dominated by steppe vegetation, consisting of herbaceous meadows, shrubs and a few pines. Birch is present in alluvial zones partially inundated by glacial meltwater. The upper elevational limit of the vegetation lies at 1000 to 1200 m a.s.l. (Université de Geneve, Institut Forel, Laboratoire d'archéologie préhistorique et anthropologie)

The region of Sion around 12 000 B.C.: the landscape during the afforestation

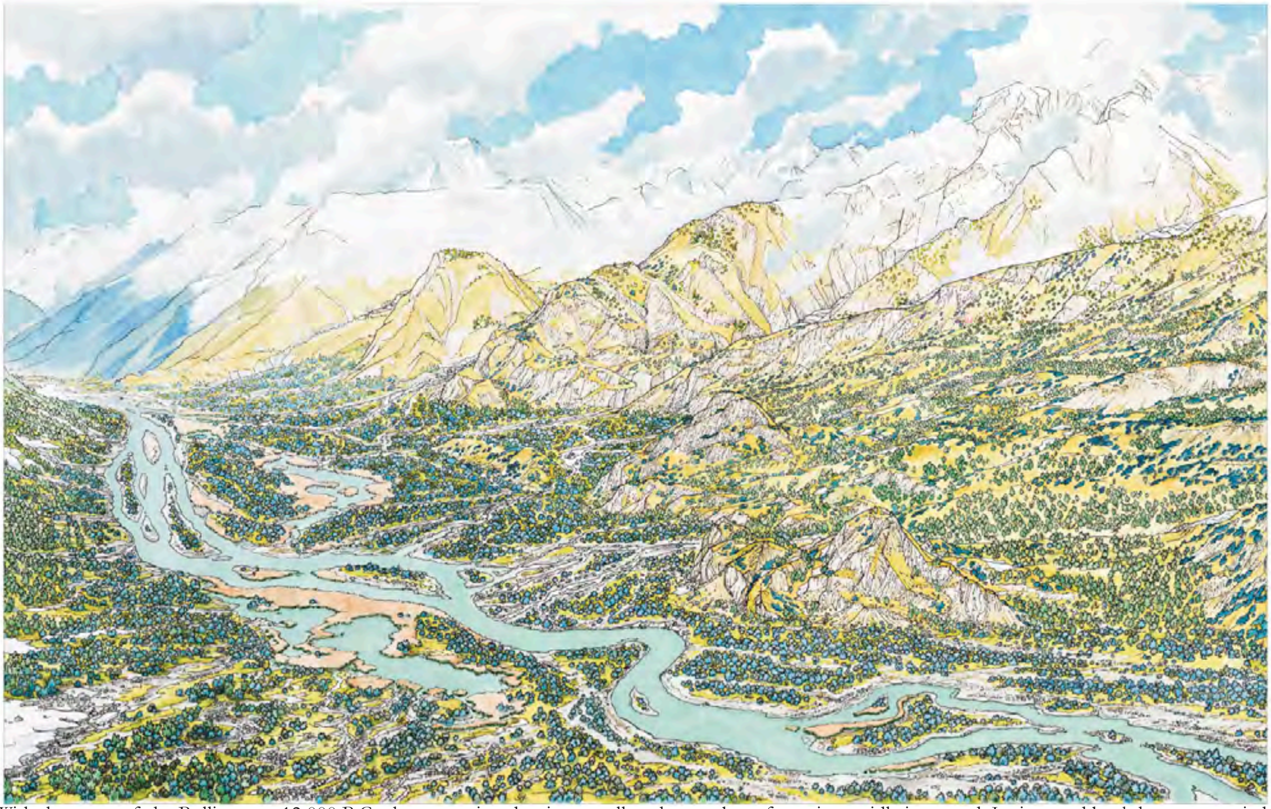

With the onset of the Bølling at c. 12 000 B.C., the vegetation density as well as the number of species rapidly increased. Juniper and buckthorne occupied bare soils whereas birch progressively invaded areas previously dominated by pine and juniper. The alluvial plains are dominated by willow and alder. The upper elevational limit of the vegetation already reached up to 2000 m a.s.l. (Université de Geneve, Institut Forel, Laboratoire d'archéologie préhistorique et anthropologie)

The region of Sion around 4000 B.C.: the landscape during the maximum extent of the vegetation

During the Middle Neolithic, the vegetation reached its maximum extent in the central Valais. The forest was dominated by oak, lime, hazel and fir. Spruce was present above 1500 m a.s.l. where it competed with fir, while larch and stonepine occupied areas above 2000 m a.s.l. The alluvial zones are still dominated by alder and willow. Ash, elm and maple colonized exposed slopes not higher than 800 m a.s.l. Human occupation is localized on loess hills, on the edge of the Rhône valley or on alluvial terraces such as at La Sonne near Sion and La Lienne near Saint-Léonard. (Université de Geneve, Institut Forel, Laboratoire d'archéologie préhistorique et anthropologie)

The region of Sion around 1000 B.C.: the landscape during the end of the Bronze Age

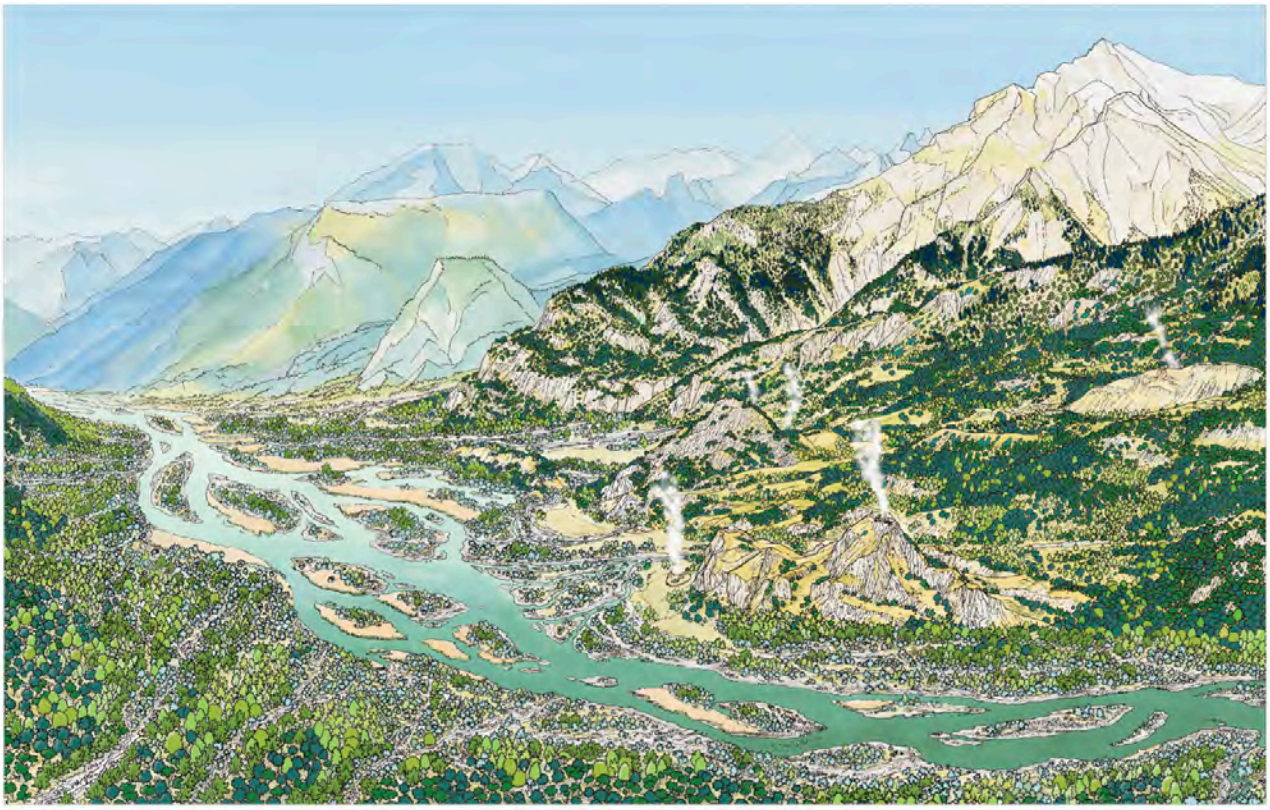

Around 1000 B.C., lower elevations are still dominated by oak whereas spruce and Scots pine are present at intermediate and larch and stonepine at higher elevations. Human impact leads to the expansion of spruce and green alder, especially at higher elevations where forests are cleared with fire to expand pastures. Human settlements are frequent at intermediate elevation around 1000 m a.s.l. (Université de Geneve, Institut Forel, Laboratoire d'archéologie préhistorique et anthropologie)

Diversity and Distributions, (Diversity Distrib.) (2012) 1–14

BIODIVERSITY RESEARCH

Changes in biodiversity and vegetation composition in the central Swiss Alps during the transition from pristine forest to first farming

Daniele Colombaroli[1]*, Madlena Beckmann[1,2], Willem O. van der Knaap[1], Philippe Curdy[3] and Willy Tinner[1]

[1]*Institute of Plant Sciences & Oeschger Centre for Climate Change Research, University of Bern, Altenbergrain 21, CH-3013, Bern, Switzerland,* [2]*The Wooden House, 4 Breanish, HS2 9HB, Uig, Isle of Lewis, Outer Hebrides, UK,* [3]*Department of Archeology, History Museum of Valais, Rue des Châteaux 14, CH-1950, Sion, Switzerland*

*Correspondence: Daniele Colombaroli Institute of Plant Sciences & Oeschger Centre for Climate Change Research, University of Bern, Altenbergrain 21, CH-3013 Bern, Switzerland.
E-mail: daniele.colombaroli@ips.unibe.ch

ABSTRACT

Aim We investigate the response of vegetation composition and plant diversity to increasing land clearance, burning and agriculture at the Mesolithic–Neolithic transition (*c.* 6400–5000 BC) when first farming was introduced.

Location The Valais, a dry alpine valley in Switzerland.

Methods We combine high-resolution pollen, microscopic charcoal and sedimentological data to reconstruct past vegetation, fire and land use. Pollen evenness, rarefaction-based and accumulation-based palynological richness analyses were used to reconstruct past trends in plant diversity.

Results Our results show that from *c.* 5500 cal. yr BC, slash-and-burn activities created a more open landscape for agriculture, at the expense of *Pinus* and *Betula* forests. Land clearance by slash-and-burn promoted diverse grassland ecosystems, while on the long term it reduced woodland and forest diversity, affecting important tree species such as *Ulmus* and *Tilia*.

Main conclusions Understanding the resilience of Alpine ecosystems to past disturbance variability is relevant for future nature conservation plans. Our study suggests that forecasted land abandonment in the Alps will lead to pre-Neolithic conditions, with significant biodiversity losses in abandoned grassland ecosystems. Thus, management measures for biodiversity, such as ecological compensation areas, are needed in agricultural landscapes with a millennial history of human impact, such as the non-boreal European lowlands. Our study supports the hypothesis that species coexistence is maximized at an intermediate level of disturbances. For instance, species richness decreased when fire exceeded the quasi-natural variability observed during the Mesolithic times. Under a more natural disturbance regime, rather closed *Pinus sylvestris* and mixed oak forests would prevail.

Keywords
Alps, beta-diversity, conservation biogeography, human impact, intermediate disturbance hypothesis, Neolithic, palynological richness.

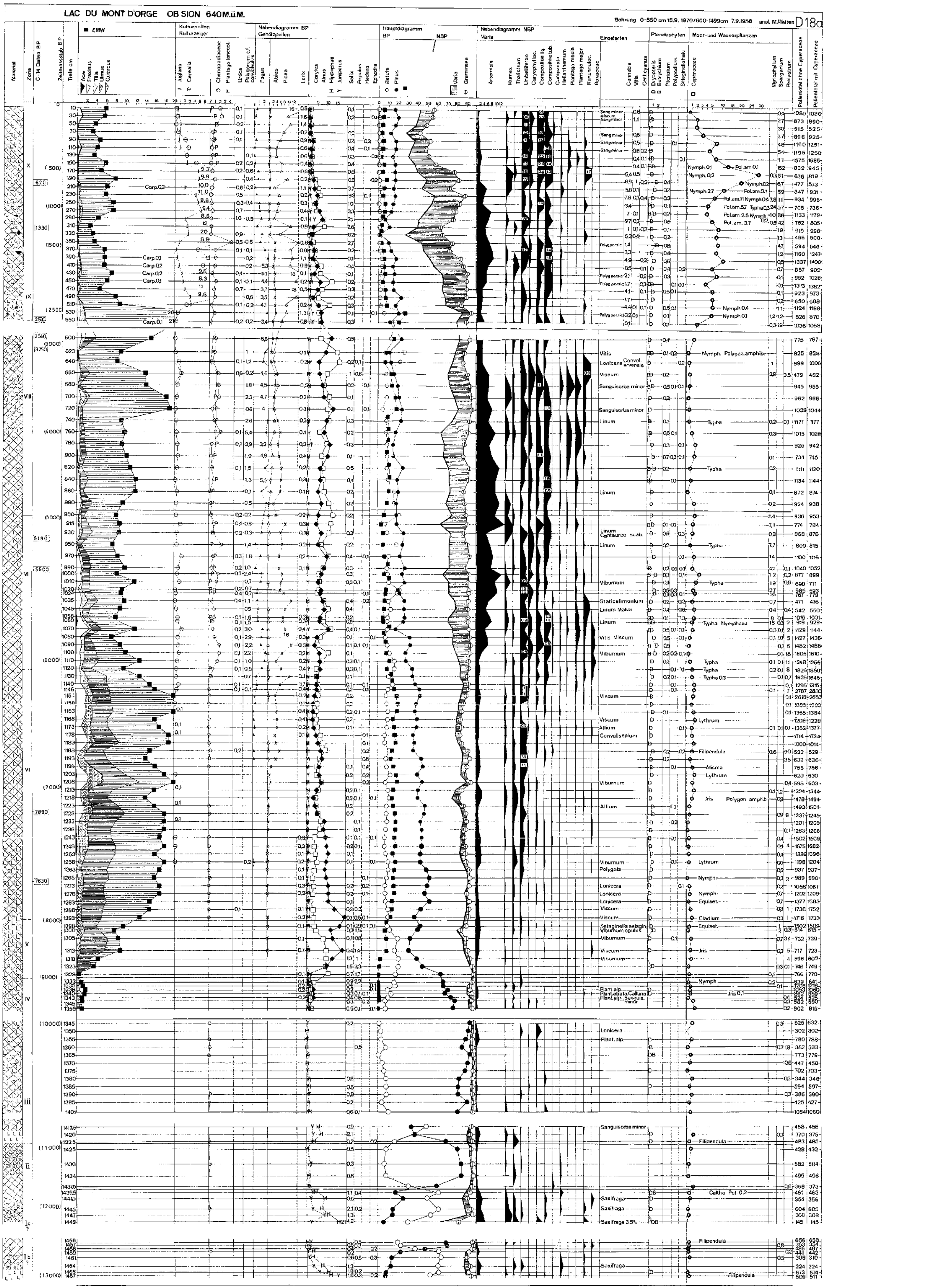
LAC DU MONT D'ORGE OB SION 640M.ü.M.
D18a
Hauptdiagramm
Nebendiagramm NBP
Moor- und Wasserpflanzen
Pteridophyten
Einzelfunde

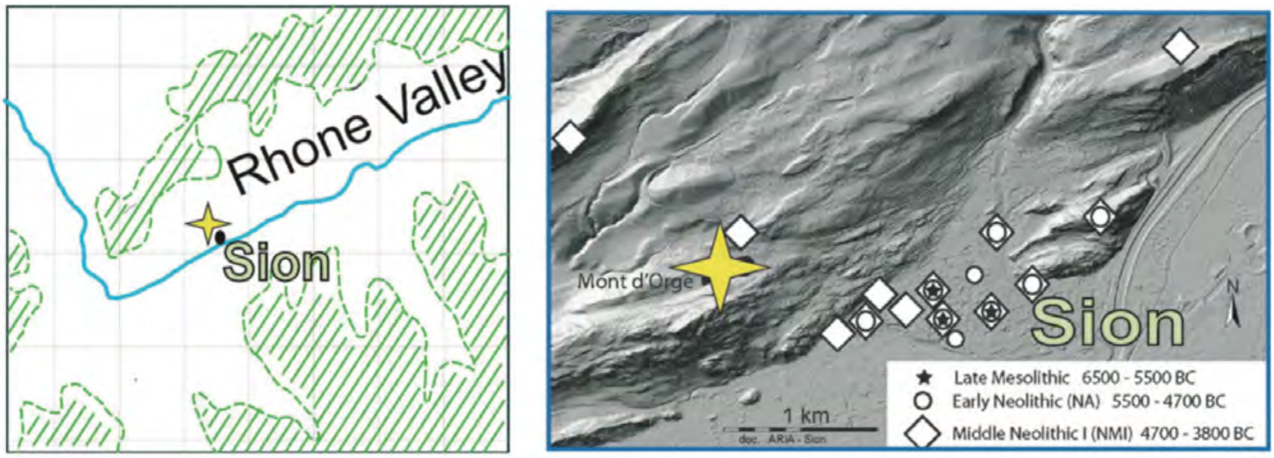

Figure 1 Lac du Mont d'Orge in the valley of the upper Rhone river, near the town of Sion, south-western Swiss Alps; (left) hatched areas delimit pastures above the present timberline (c. 2100 m a.s.l.); (right) distribution of late Mesolithic and Neolithic settlements in and around Sion between 5500 and 3800 cal. yr BC. Early Neolithic = NA (Néolithique ancien); Middle Neolithic I = NMI (Néolithique moyen I). Modified from (Moinat et al., 2007). Settlements around Mont d'Orge (200 m from the lake) are from 4700 cal. yr BC.

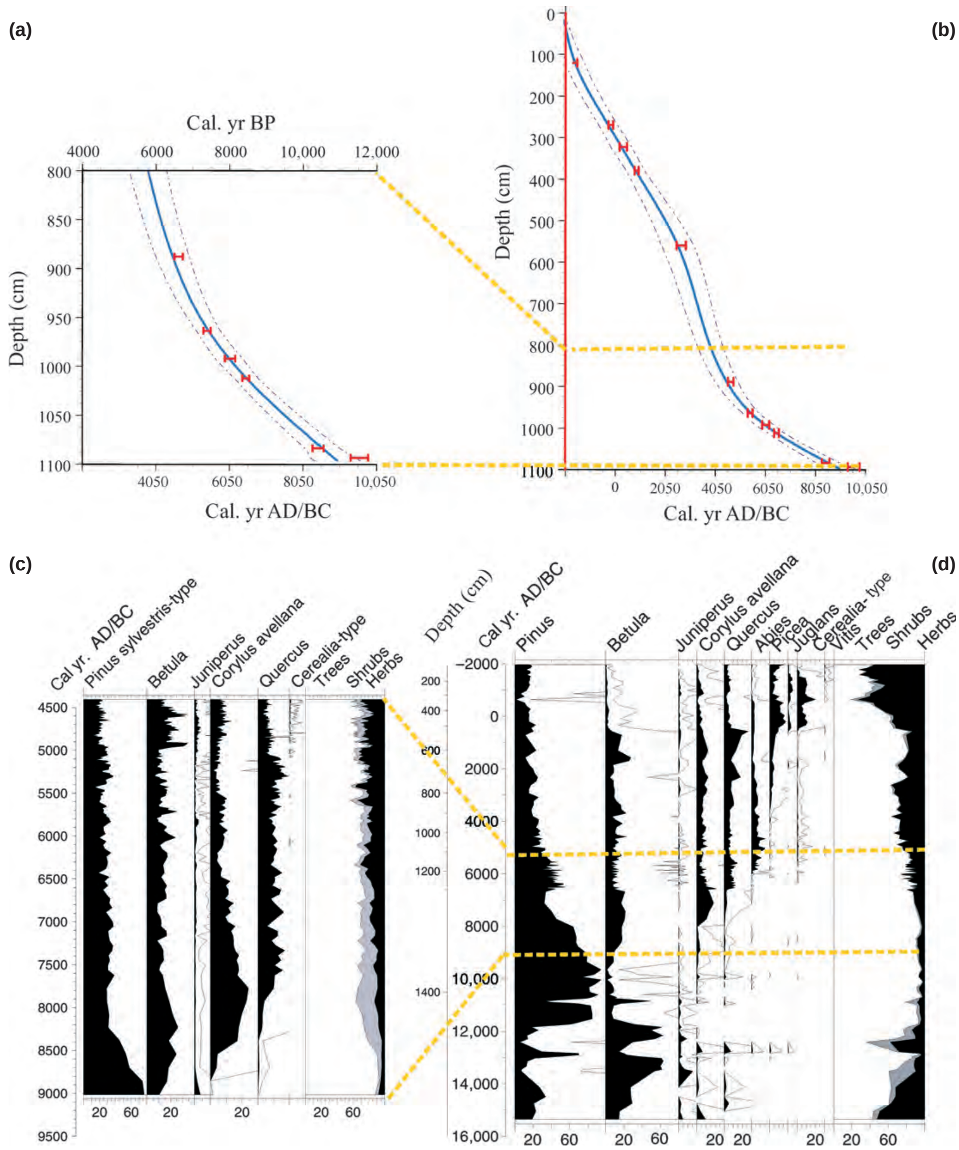

Figure 2 (a) and (b) depth–age model (close-up and whole sequence) based on a generalized mixed-effect regression model (Heegaard *et al.*, 2005), with confidence intervals (bracketing envelope). Error bars indicate the error range of the calibrated radiocarbon ages (two sigma); (c) the high-resolution pollen diagram is compared with (d) the former diagram from Welten (total of 109 pollen samples and 113 pollen types, see Welten, 1982) plotted on the chronology proposed by van der Knaap & Ammann (1997). The presence of *Quercus* and *Corylus* grains before the Holocene (i.e. 11,500 cal. yr BP) was interpreted by Welten (1982) as reworked material from older layers.

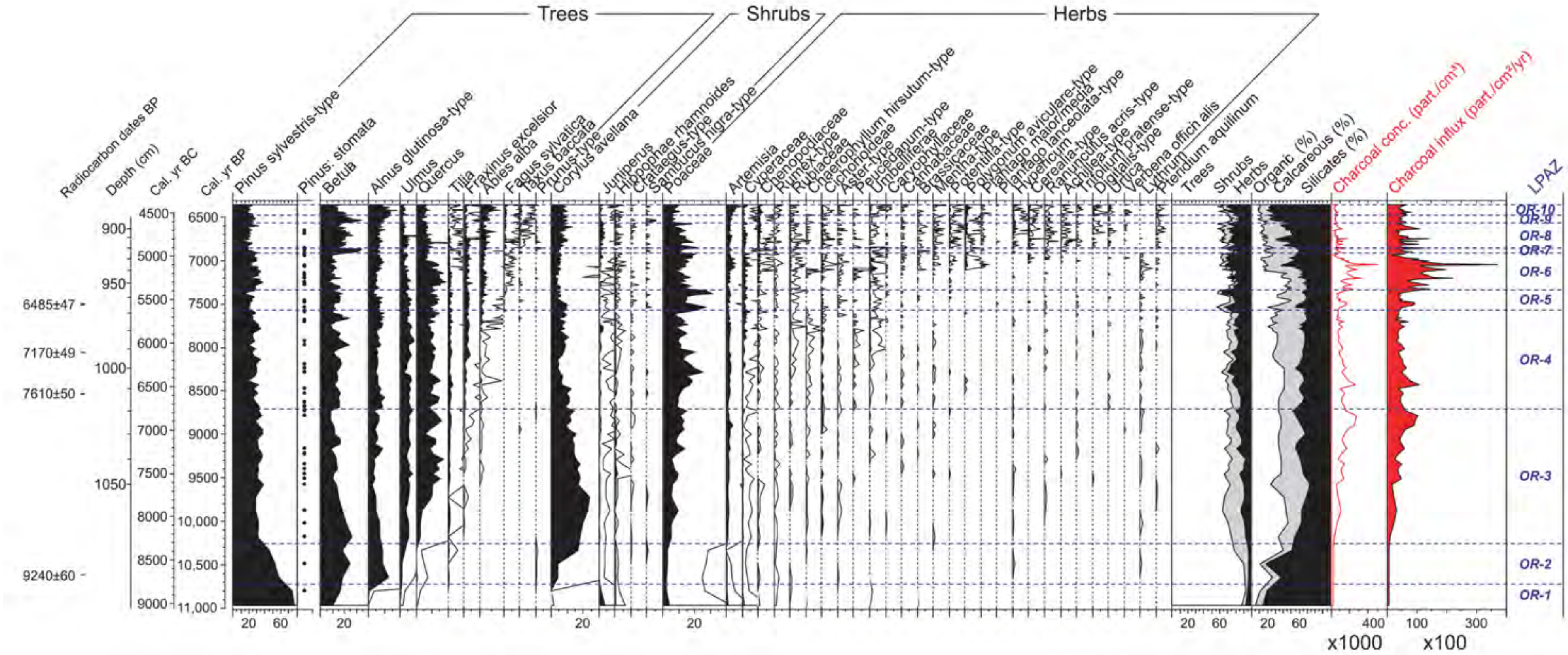

Figure 3 High-resolution pollen diagram with selected pollen and spore percentages, LOI, charcoal concentrations and charcoal influx. A total of 183 pollen types were identified. The intensification of agriculture (continuous Cerealia-type curve) is attested from c. 5050 cal. yr BC (zone Or-6).

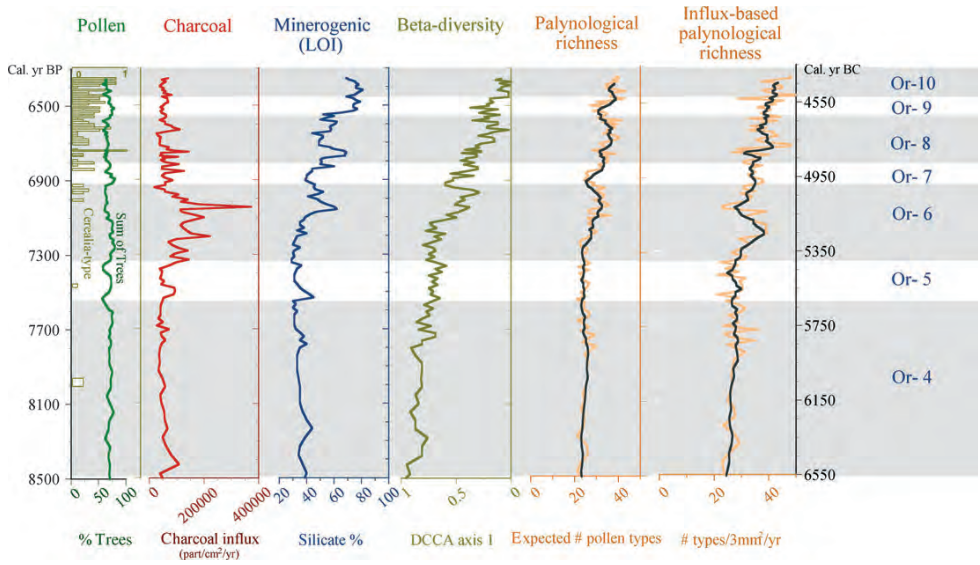

Figure 5 Comparison among pollen (Cerealia-type and % sum of trees), microscopic charcoal influx, LOI-inferred minerogenic input, rates of palynological change, Detrended Canonical Correspondence Analysis axis 1 and accumulation-based palynological richness (raw data and moving average, with $n = 5$). Note the exaggerated x-axis scale for Cerealia-type pollen.

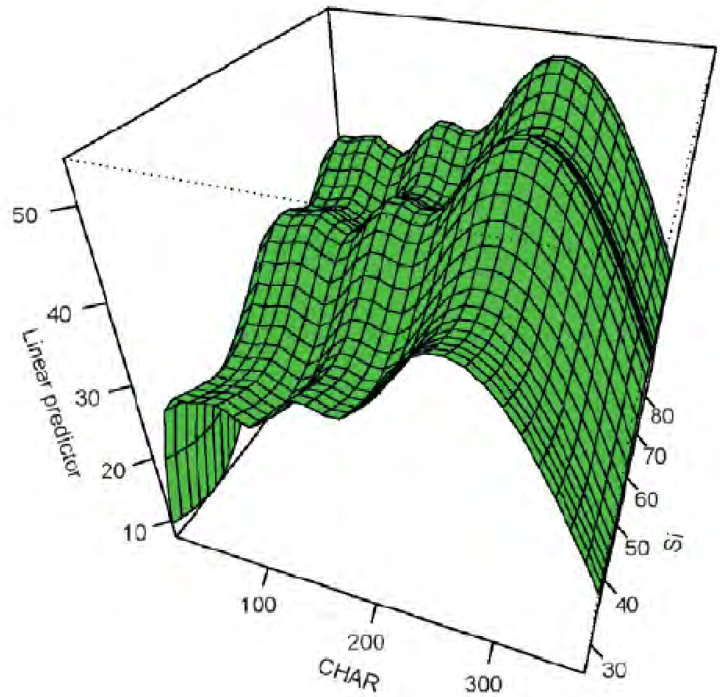

Figure 6 Generalized additive model response surfaces of accumulation-based palynological richness to charcoal influx (CHAR, 91000) and silica %. Our estimated index for biodiversity exhibits a linear response to increasing fire and land use, with a sharp decrease over the threshold value of 200,000 charcoal particles cm^2 year^{-1}.

Lac du Mont d'Orge

Pollen percentages of selected taxa

Analysis L.Wick, 2010

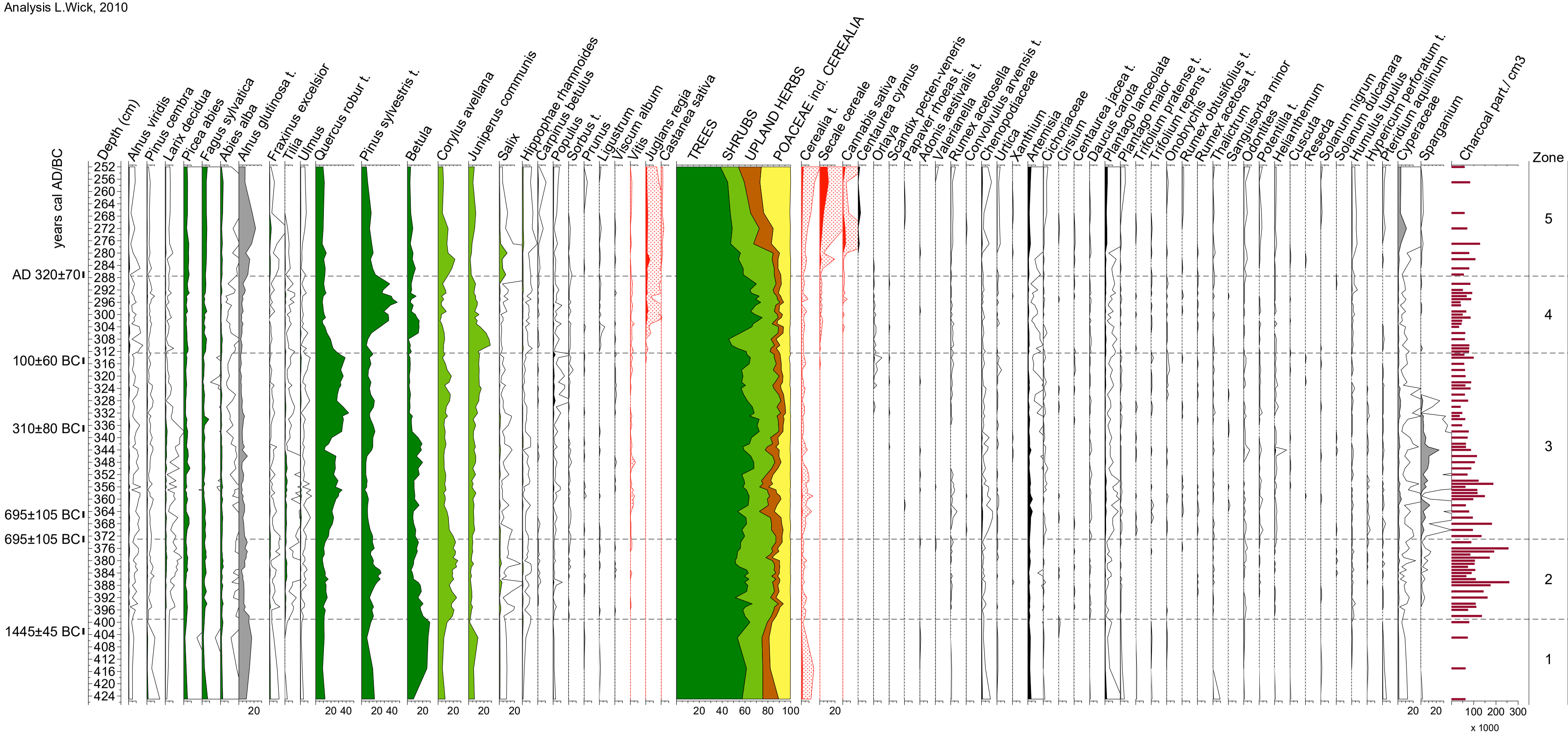

Calibration of lake sediment charcoal particle fluxes with remote sensing data for a quantitative reconstruction of past fire activity

Carole Adolf[1], Stefan Wunderle[2], Willy Tinner[1]

[1]Institute of Plant Sciences and Oeschger Centre for Climate Change Research, Universtiy of Bern, Switzerland
[2]Geographical Institute and Oeschger Centre for Climate Change Research, University of Bern, Switzerland

Abstract

Lake-sediment charcoal records are a valuable source of information on the long-term causes and consequences of changing fire activity. However, quantitative reconstructions are badly needed to develop an understanding of the long-term dynamics among climate, land use, and vegetation, as well as for the development of fire management and mitigation strategies in the future.
We present a new approach combining chronologically well constrained sediments from sediment traps and annually laminated lakes with remote sensing techniques to acquire present-day data about fires. With these datasets the amount of micro – and macroscopic charcoal found within the sediments is calibrated with the fire number (FN), burned area (BA), intensity (Fire radiative power, FRP) and distance of fires registered by MODIS sensors. This relationship will be used to calculate regression models to be applied to Holocene charcoal records with the aim of quantitatively reconstructing important fire parameters (size, number, intensity and distance to archive).
The study area is made up of two transects across Europe, one from North to South and the second from West to East, including a total of 38 study lakes. Covering as many ecosystems as possible, the "calibration-in-space" approach is followed. The sediment traps were emptied once a year during the time period of three years (2012-2015) to allow for the calculation of annual fluxes. Additional freeze- and surface cores from 5 annually laminated lakes extend our time series further back in time.
Our results imply that remote-sensing calibrated sedimentary charcoal has the potential to deliver new quantitative insights in past fire regime parameters.

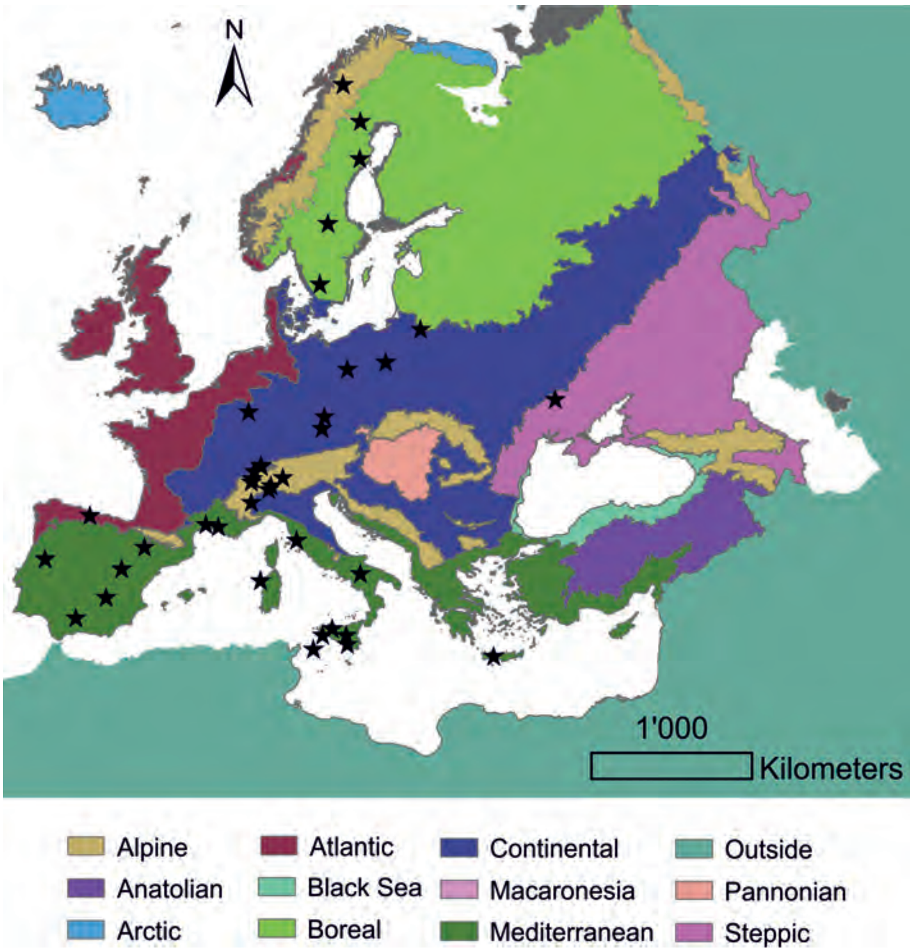

Figure 1: Location of study lakes within biogeographical regions of Europe.

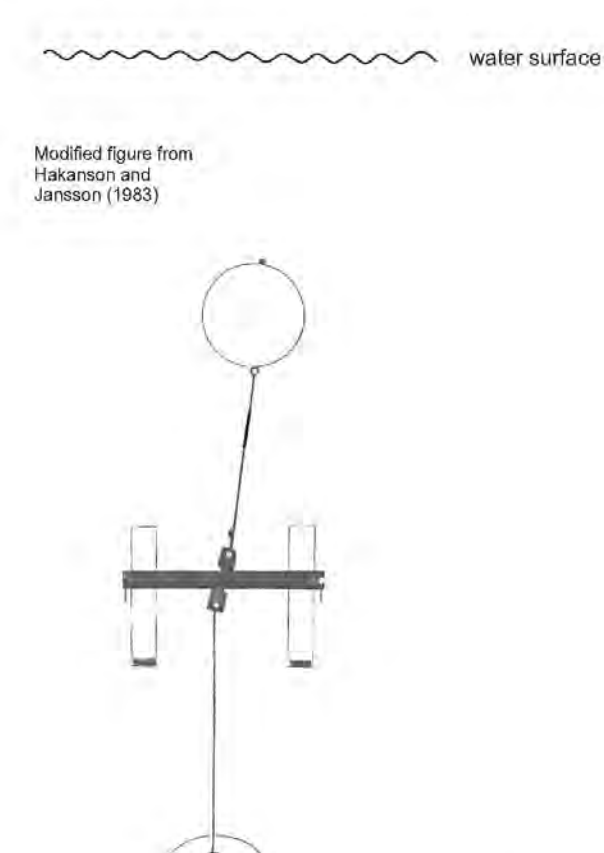

Figure 2: Schematic view of sediment trap within lake.

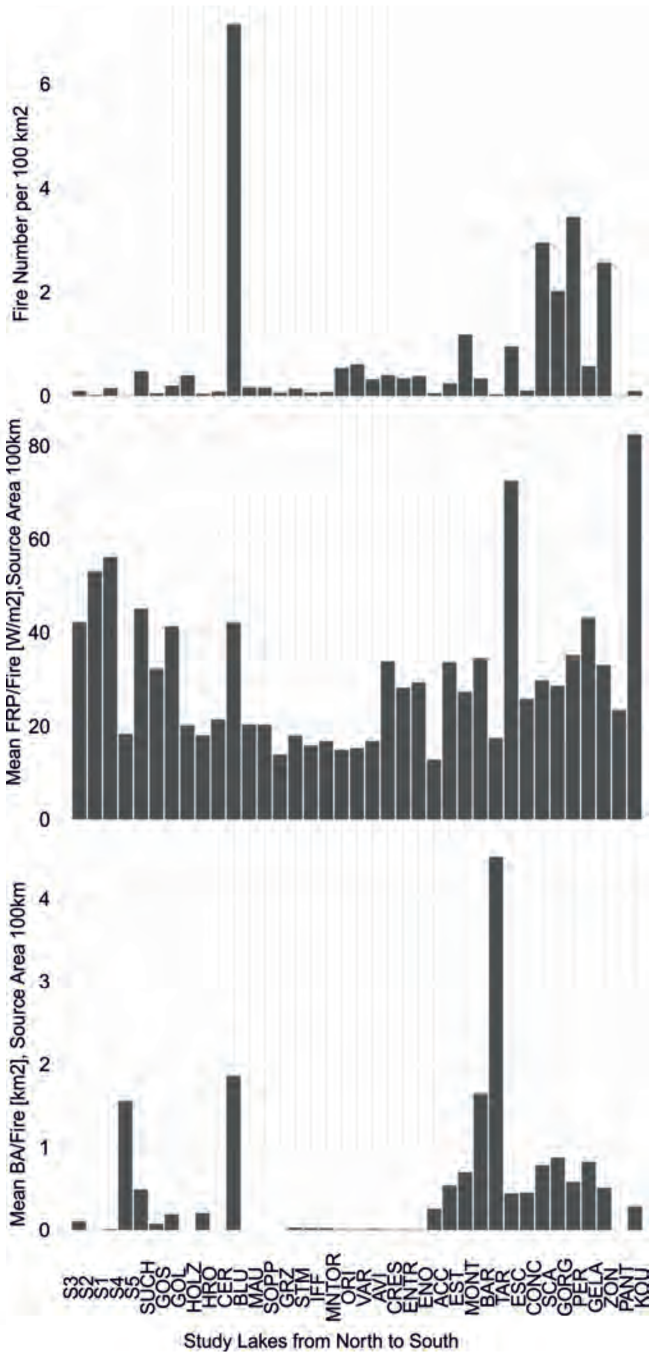

Figure 3: Fire parameters FN (Fire Number), FRP (Fire Radiative Power) and BA (Burned Area) around each study site (source area of 100 km radius).

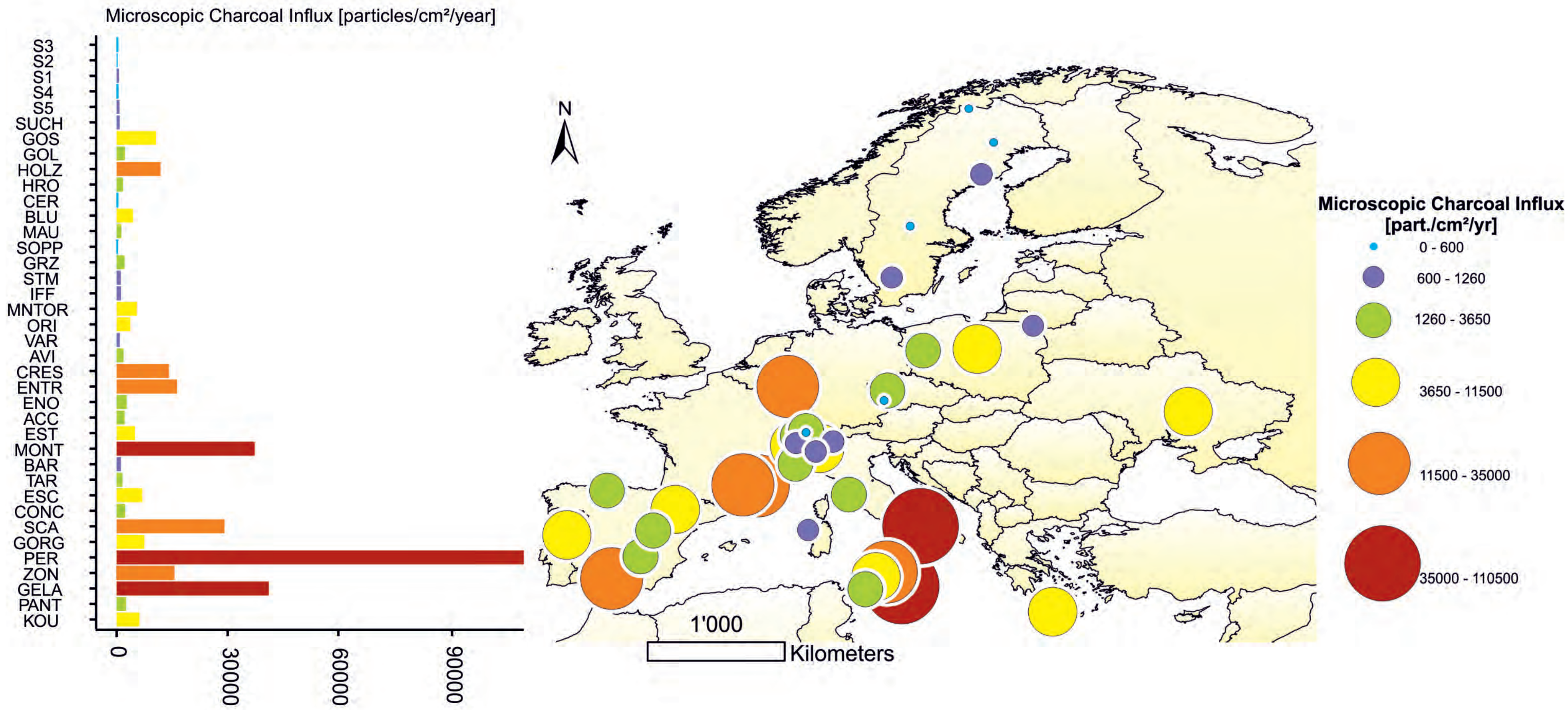

Figure 4: Influx of microscopic charcoal per site ordered along latitude.

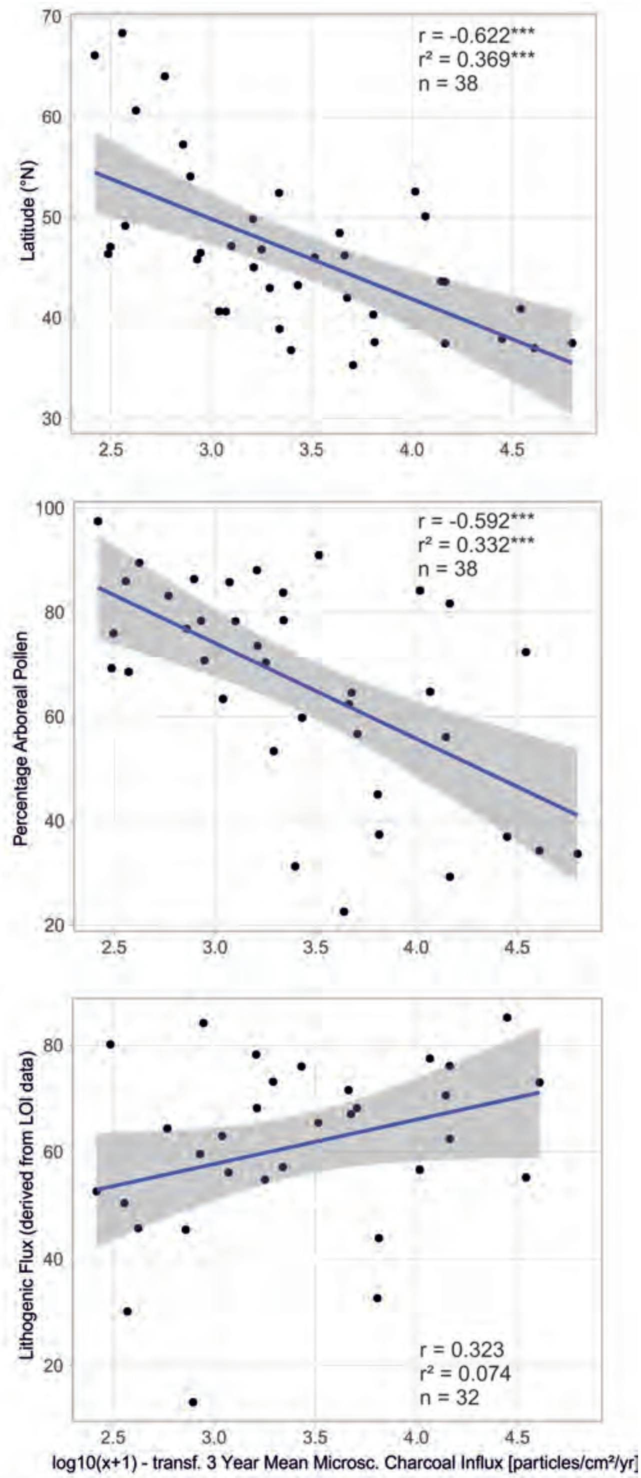

Figure 5: Correlations and regressions between latitude, % of Arboreal Pollen from each site and lithogenic flux (dry weight after burning sample at 950°C divided by dry weight of sample before Loss on Ignition procedure) with microscopic charcoal influx.

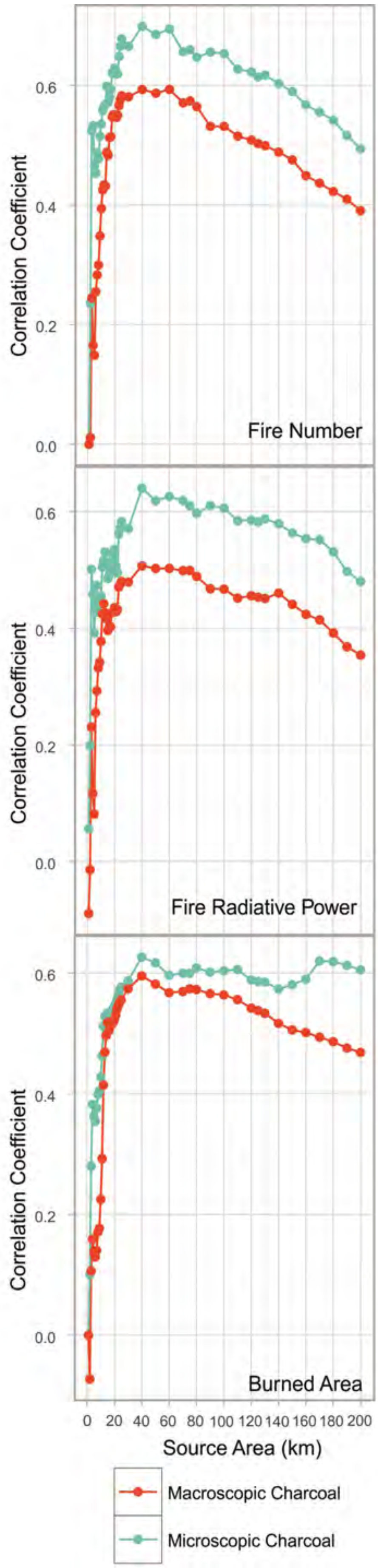

Figure 6: Correlations of FN, FRP and BA with micro- and macroscopic charcoal in dependence of source area (radius in km around each study lake).

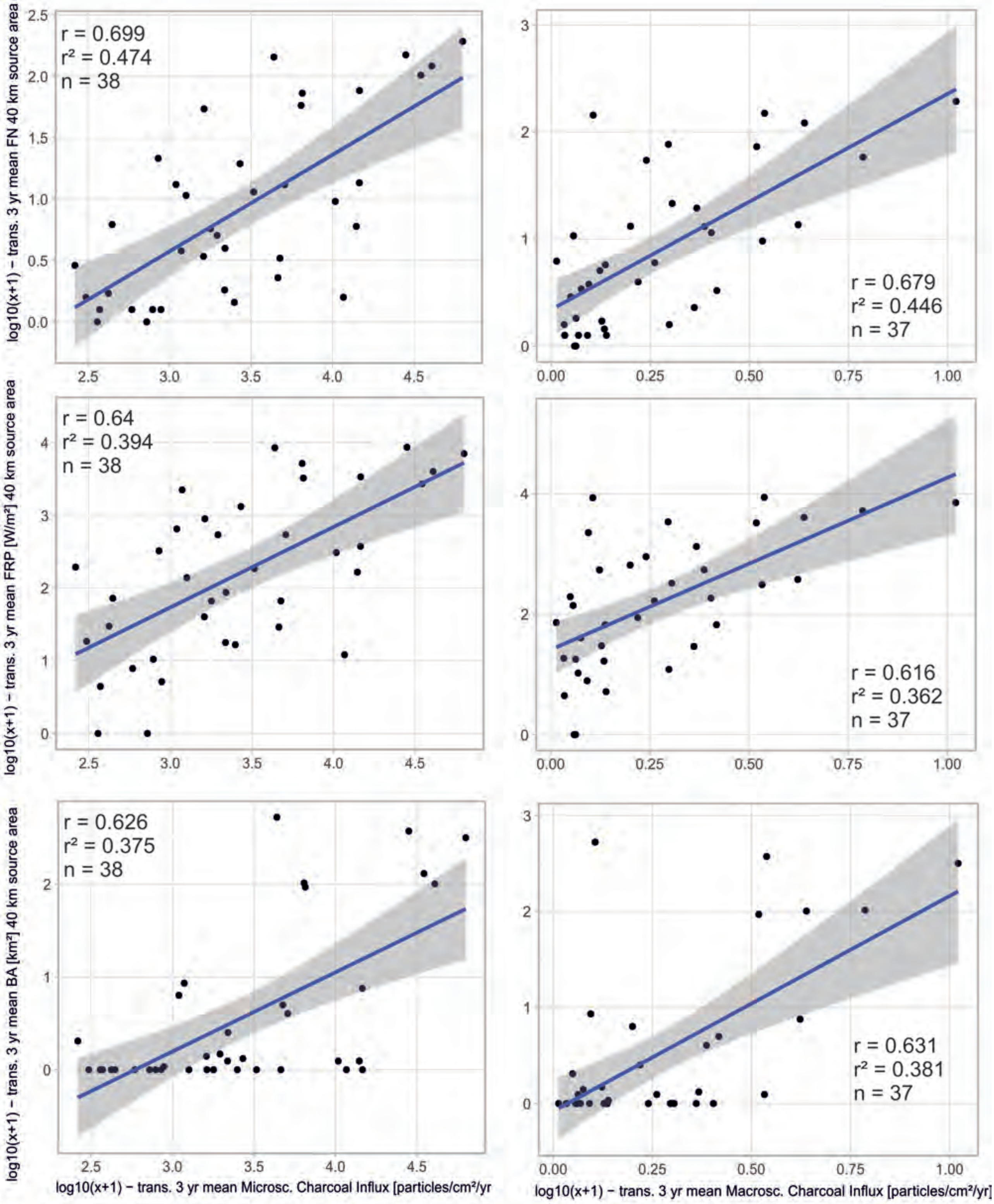

Figure 7: Regression diagrams between FN, FRP, BA with micro- and macroscopic charcoal with source area of 40 km. All regressions are highly significant ($p<0.001$).

Research paper

Reconstruction of Holocene vegetation dynamics at Lac de Bretaye, a high-mountain lake in the Swiss Alps

The Holocene
2016, Vol. 26(3) 380–396

DOI: 10.1177/0959683615609746
hol.sagepub.com
SAGE

Lena Thöle,[1,2] Christoph Schwörer,[1] Daniele Colombaroli,[1] Erika Gobet,[1] Petra Kaltenrieder,[1] Jacqueline van Leeuwen[1] and Willy Tinner[1]

Abstract

A deeper understanding of past vegetation dynamics is required to better assess future vegetation responses to global warming in the Alps. Lake sediments from Lac de Bretaye, a small subalpine lake in the Northern Swiss Alps (1780 m a.s.l.), were analysed to reconstruct past vegetation dynamics for the entire Holocene, using pollen, macrofossil and charcoal analyses as main proxies. The results show that timberline reached the lake's catchment area at around 10,300 cal. BP, supporting the hypothesis of a delayed postglacial afforestation in the Northern Alps. At the same time, thermophilous trees such as *Ulmus, Tilia* and *Acer* established in the lowlands and expanded to the altitude of the lake, forming distinctive boreo-nemoral forests with *Betula, Pinus cembra* and *Larix decidua*. From about 5000 to 3500 cal. BP, thermophilous trees declined because of increasing human land use, mainly driven by the mass expansion of *Picea abies* and severe anthropogenic fire activity. From the Bronze Age onwards (*c.* 4200–2800 cal. BP), grazing indicators and high values for charcoal concentration and influx attest an intensifying human impact, fostering the expansion of *Alnus viridis* and *Picea abies*. Hence, biodiversity in alpine meadows increased, whereas forest diversity declined, as can be seen in other regional records. We argue that the anticipated climate change and decreasing human impact in the Alps today will not only lead to an upward movement of timberline with consequent loss of area for grasslands, but also to a disruption of *Picea abies* forests, which may allow the re-expansion of thermophilous tree species.

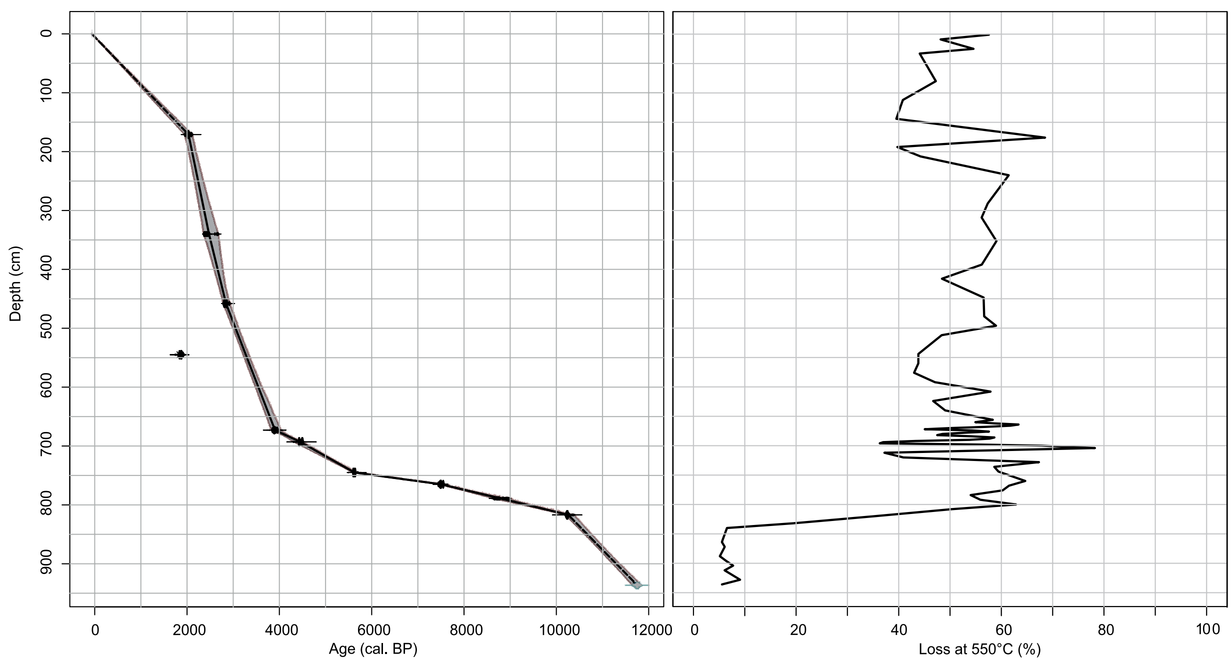

Figure 2. Left: Age–depth model of the sediment calculated with clam 2.2 (Blaauw, 2010) from Lac de Bretaye with the calibrated ages and linear interpolation (black line) and 95% confidence intervals (grey areas). Dashed lines are estimated ages and not based on radiocarbon dates. Right: Loss on ignition at 550°C as a proxy for sedimentary organic content.

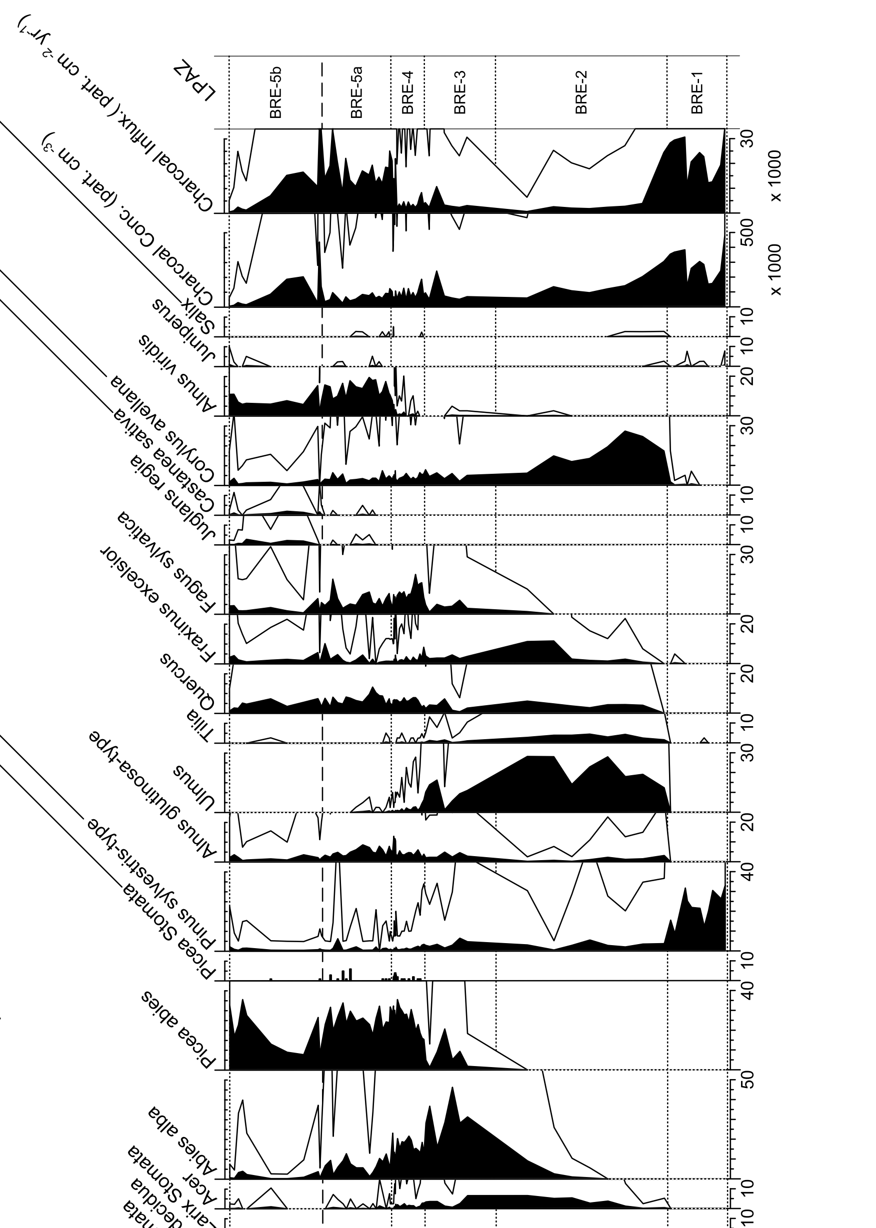

Figure 3. (Continued)

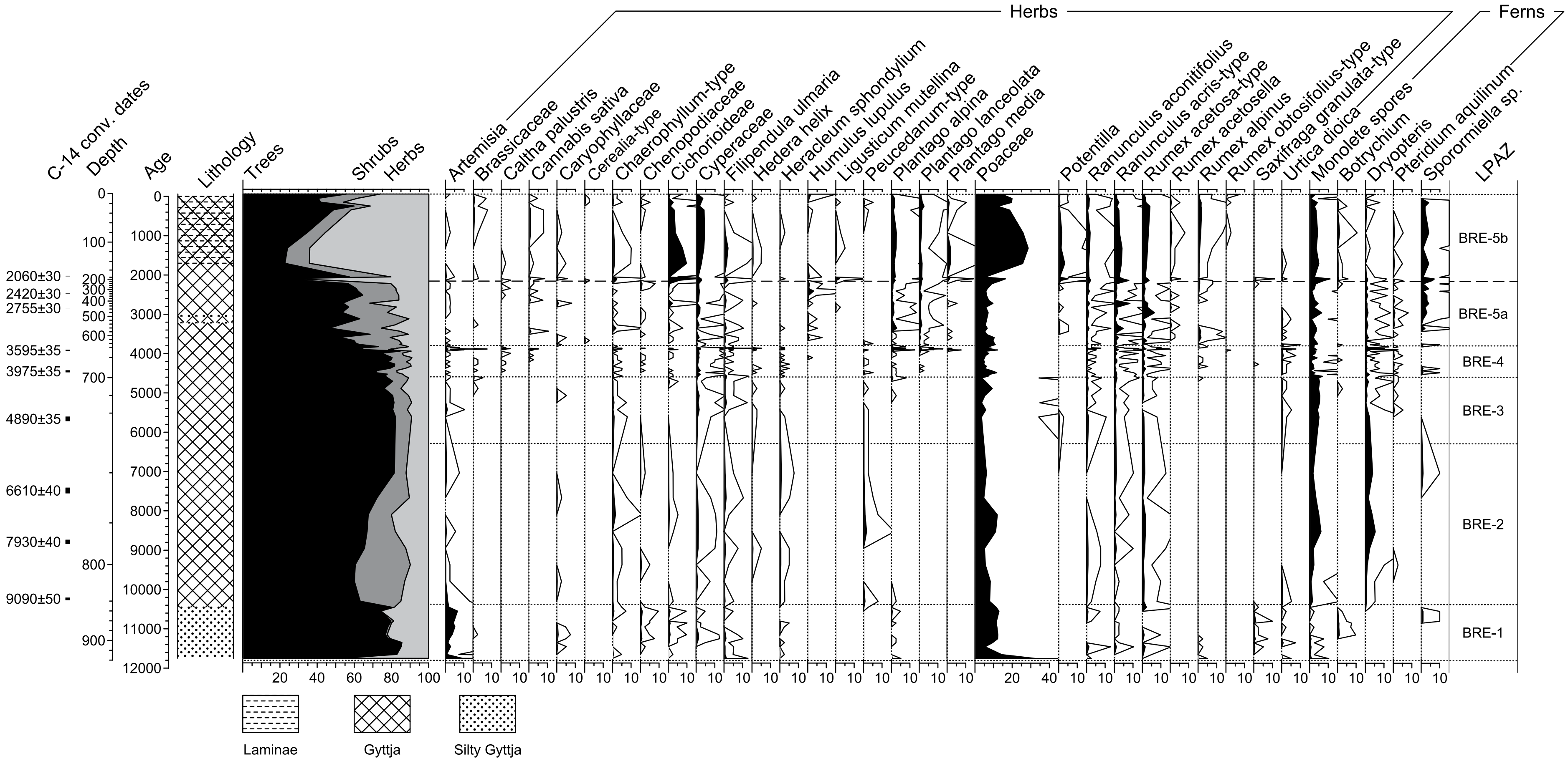

Figure 3. Selected pollen, spores and stomata percentages as well as lithology, microscopic charcoal concentrations and influx diagrams of Lac de Bretaye. Empty curves show 10× exaggeration. Analyst: Lena Thöle. LPAZ: local pollen assemblage zones.

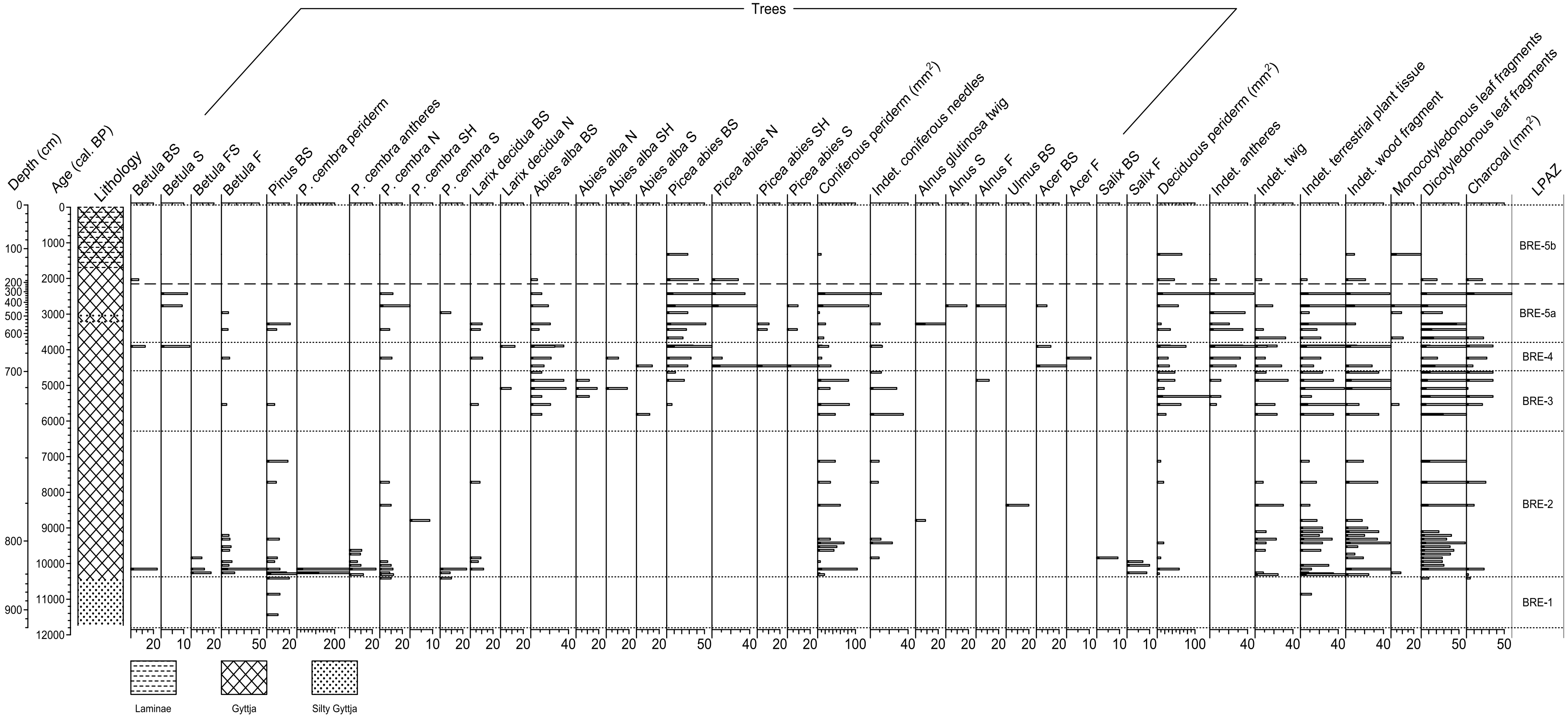

Figure 4. Macrofossil diagram of Lac de Bretaye. All values are standardized to 14 cm³ of volume. Indet. antheres had no pollen and could not be identified. Analyst: Lena Thöle.
F: fruits; N: needles; S: seeds; BS: bud scales; FS: fruit scales; SH: short shoots; LPAZ: local pollen assemblage zones.

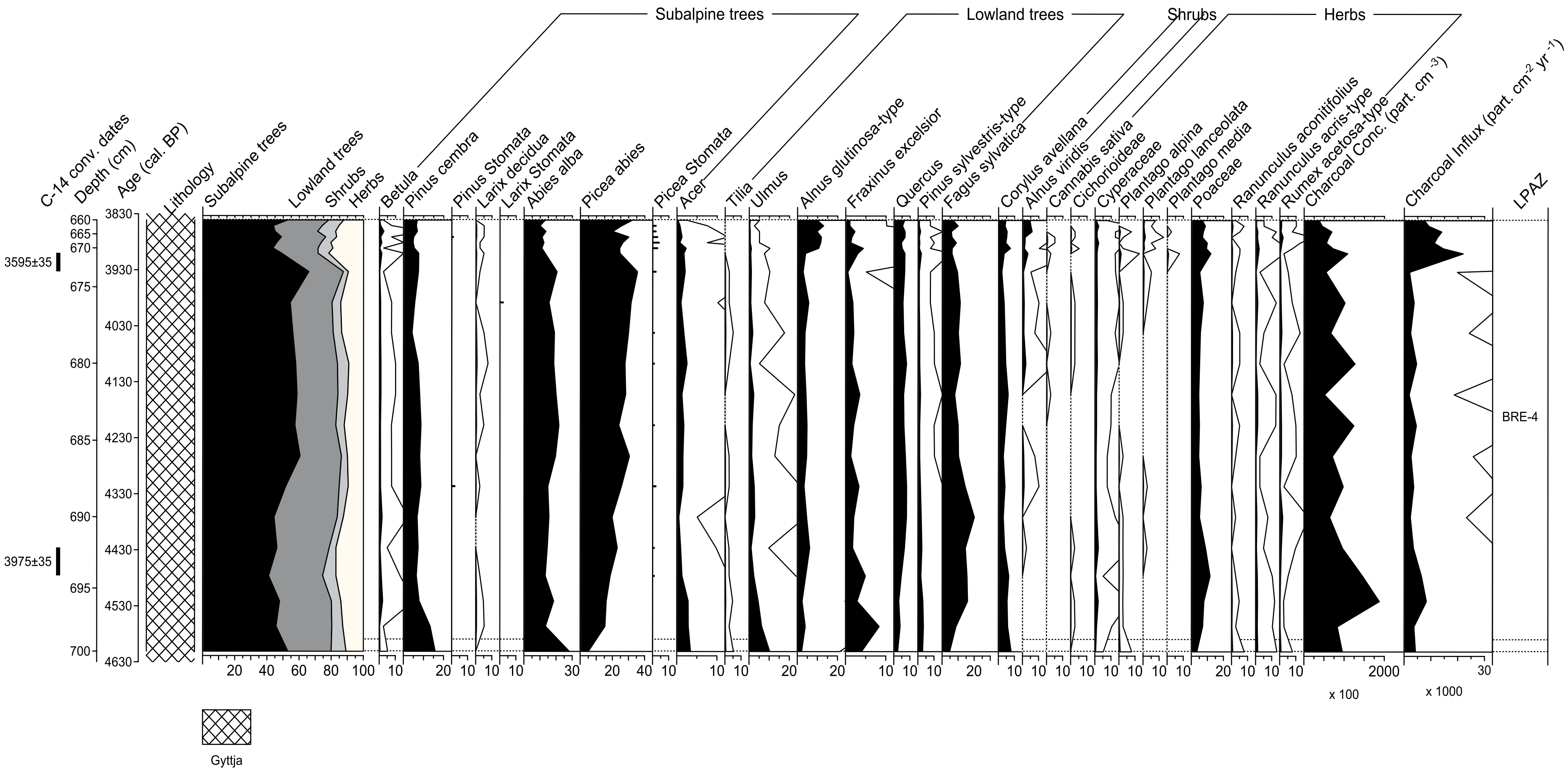

Figure 5. Pollen and stomata percentages as well as lithology, microscopic charcoal concentrations and influx values for the high-resolution sequence (4600–3850 cal. BP). Empty curves show 10× exaggeration.

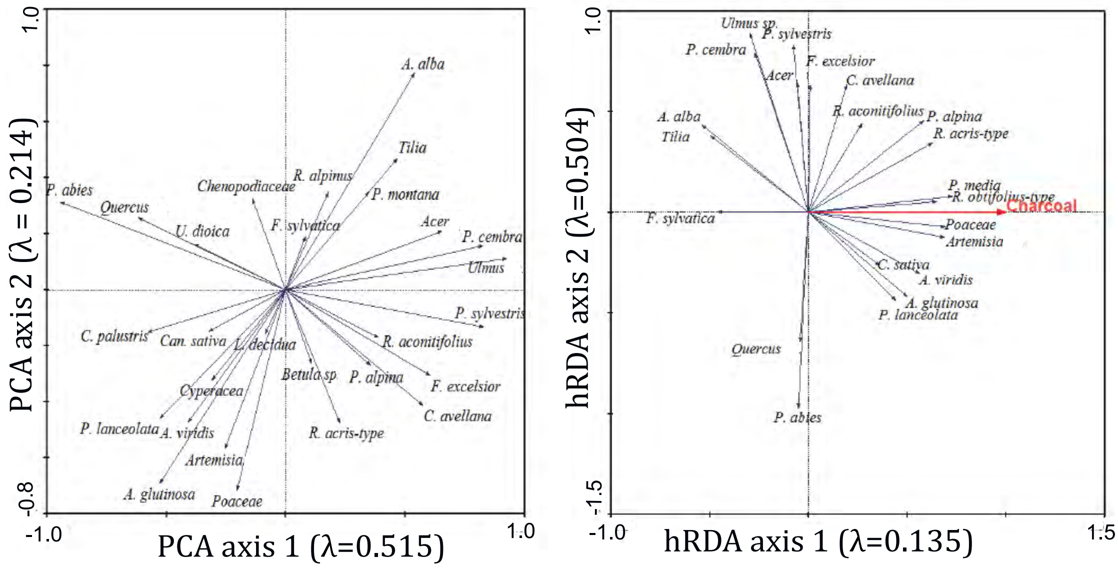

Figure 7. Left: Principal component analysis (PCA) scatterplot of species for the high-resolution sequence (LPAZ 4, 4600–3850 cal. BP). The first axis explains 51.5% of the variance in the data set and the second axis 21.4%. Right: hRDA-biplot of selected species and microscopic charcoal influx as a proxy for fire as explanatory variable. Axis 2 of the hRDA represents the residual variation not explained by fire.

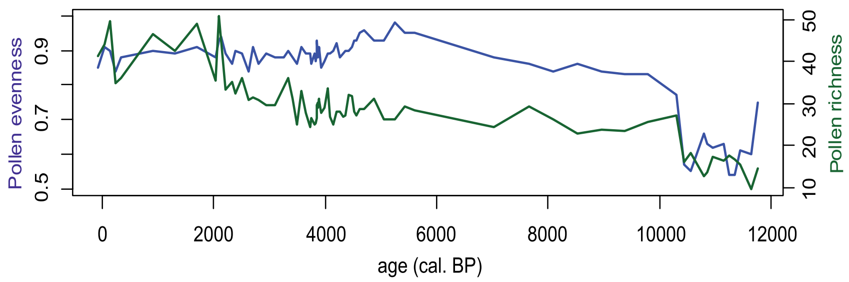

Figure 8. Comparison of palynological evenness (PIE, blue line) and richness (PRI, green line) estimated on a constant sum of 356 pollen grains.

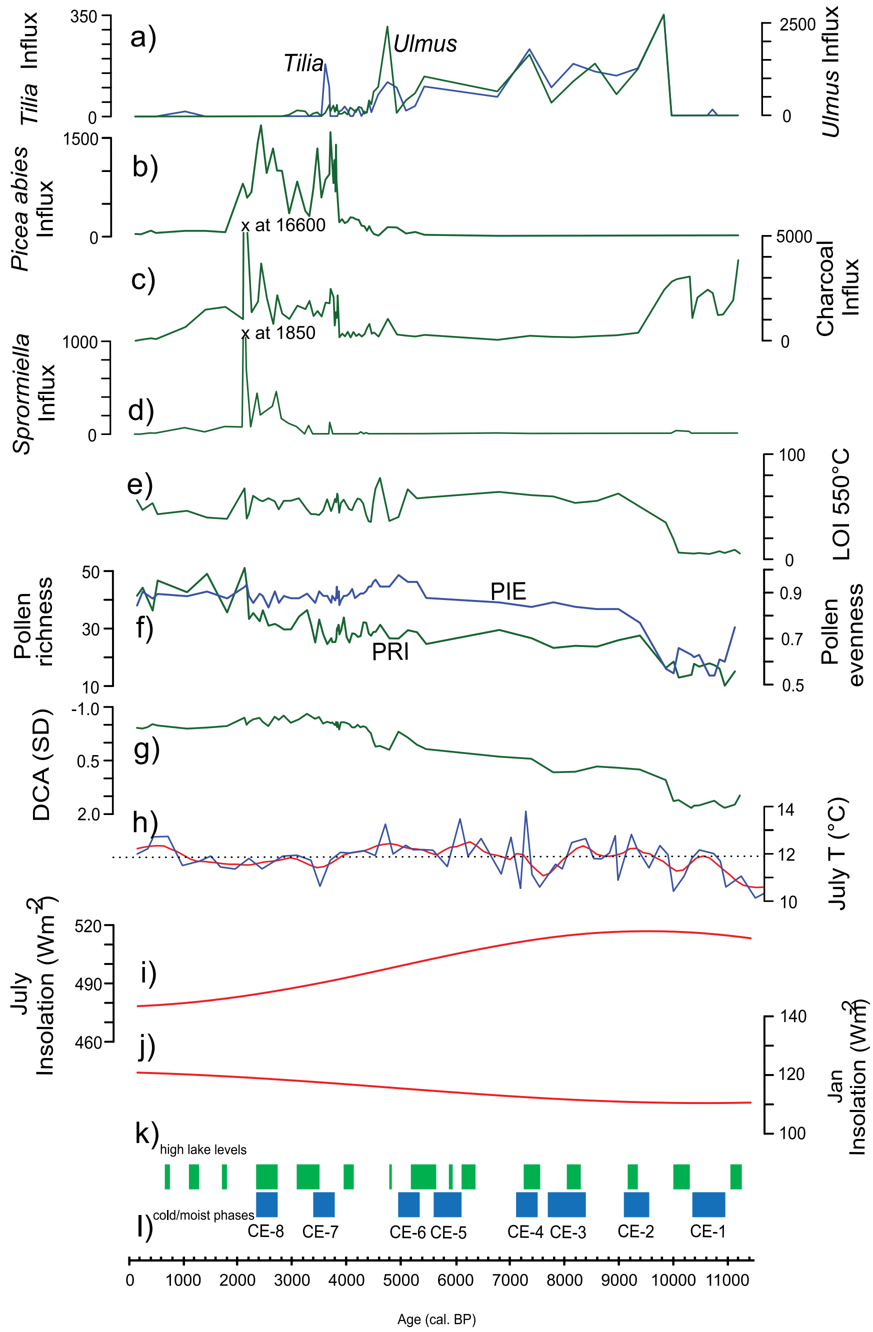

Figure 9. Comparison of biotic and abiotic proxies of Lac de Bretaye with different climate records: (a) pollen influx of *Ulmus* (green) and *Tilia* (blue); (b) pollen influx of *Picea abies*; (c) influx of microscopic charcoal; (d) influx of *Sporormiella*; (e) percentage of loss on ignition (LOI) at 550°C as a proxy for organic content of the sediment; (f) palynological richness (PRI, green) and pollen evenness (PIE, blue) as proxies for species diversity; (g) detrended correspondence analysis (DCA) axis 1 sample scores; (h) July temperature reconstruction based on a chironomid transfer function from Hinterburgseeli (the blue line is the unsmoothed temperature reconstruction, the red line the LOESS smoothed data, the dashed horizontal line the current mean July T (Heiri et al., 2003b)); (i) July and (j) January solar insolation (Laskar et al., 2004); (k) periods of high lake levels after Magny (2004); and (l) cold and wet phases identified from Central European pollen and macrofossil records (Haas et al., 1998).

Saturday 10.09.2016

8:30	Departure to Bern
9:30-10 h	Arrival at the Institute of Plant Sciences (Bern)

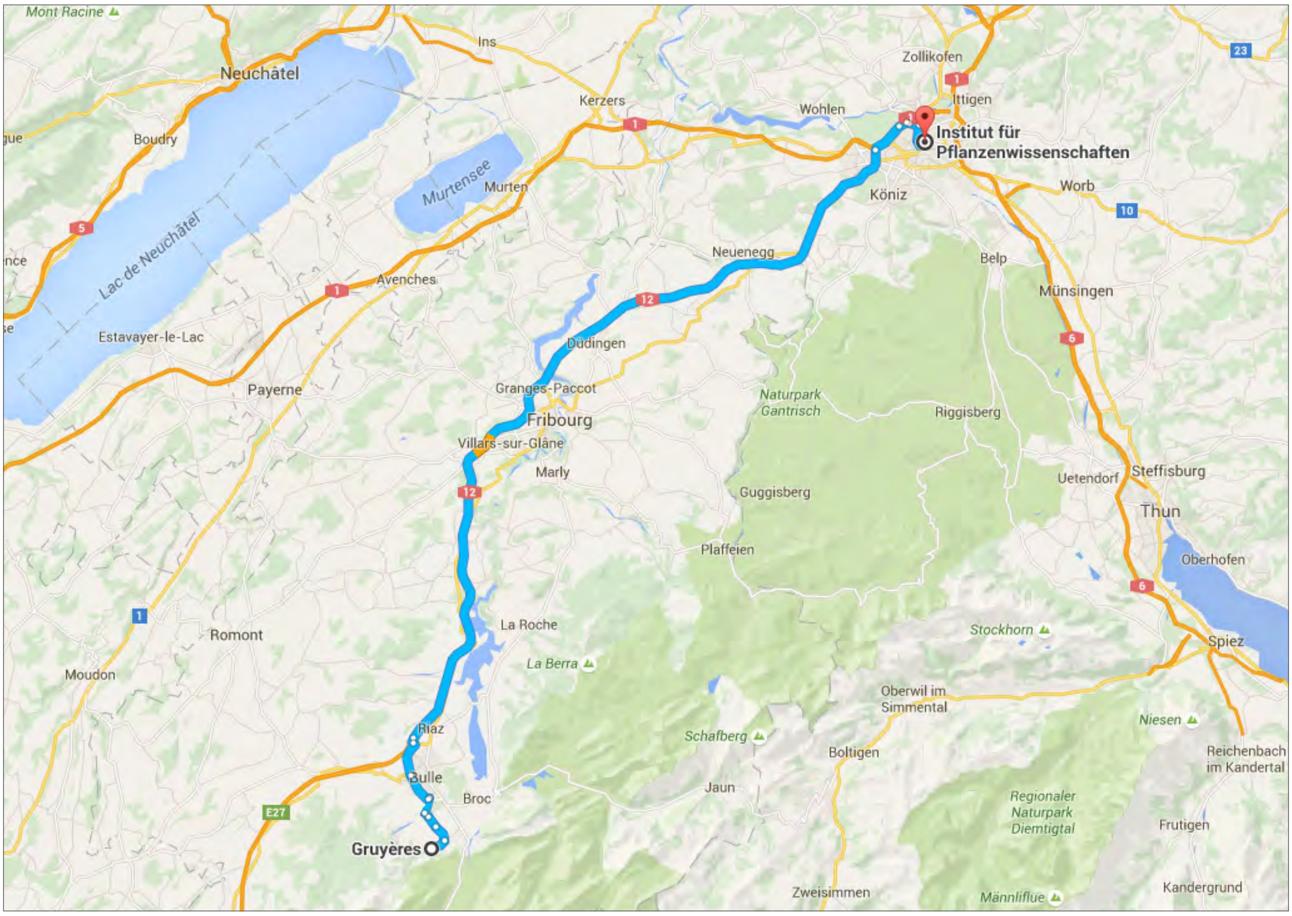

References

Ammann B., Birks H.J.B., Brooks S.J., Eicher U., Grafenstein U. von, Hofmann W., Lemdahl G., Schwander J., Tobolski K., & Wick L. (2000) Quantification of biotic responses to rapid climatic changes around the Younger Dryas -- a synthesis. Palaeogeography, Palaeoclimatology, Palaeoecology, 159, 313–347.

Ammann B., van Leeuwen J.F.N., van der Knaap W.O., Lischke H., Heiri O., & Tinner W. (2013a) Vegetation responses to rapid warming and to minor climatic fluctuations during the Late-Glacial Interstadial (GI-1) at Gerzensee (Switzerland). Palaeogeography, Palaeoclimatology, Palaeoecology, 391, Part B, 40–59.

Ammann B., van Raden U.J., Schwander J., Eicher U., Gilli A., Bernasconi S.M., van Leeuwen J.F.N., Lischke H., Brooks S.J., Heiri O., Nováková K., van Hardenbroek M., von Grafenstein U., Belmecheri S., van der Knaap W.O., Magny M., Eugster W., Colombaroli D., Nielsen E., Tinner W., & Wright H.E. (2013b) Responses to rapid warming at Termination 1a at Gerzensee (Central Europe): Primary succession, albedo, soils, lake development, and ecological interactions. Palaeogeography, Palaeoclimatology, Palaeoecology, 391, Part B, 111–131.

Auer M., Meister R., & Stoffel A. (2007) Mean Snow Depths 1983 - 2002. Hydrologischer Atlas der Schweiz : Atlas hydrologique de la Suisse = Atlante idrologico della Svizzera (ed. by M. Spreafico, R. Weingartner, and Leibundgut), Bundesamt für Landestopographie, Bern.

Berthel N., Schwörer C., & Tinner W. (2012) Impact of Holocene climate changes on alpine and treeline vegetation at Sanetsch Pass, Bernese Alps, Switzerland. Review of Palaeobotany and Palynology, 174, 91–100.

Bini A., Schlüchter C., Burkhalter R., Buoncristiani J.-F., Couterrand S., Ellwanger D., Felber M., Florineth D., Graf H.R., Keller O., Kelly M., & Schoeneich P. (2009) Die Schweiz während des letzteiszeitlichen Maximums (LGM): Switzerland during the last glacial maximum. Federal Office of Topography swisstopo, Wabern.

Brooks S.J. (2000) Late-glacial fossil midge stratigraphies (Insecta: Diptera: Chironomidae) from the Swiss Alps. Palaeogeography, Palaeoclimatology, Palaeoecology, 159, 261–279.

Brooks S.J. & Heiri O. (2013) Response of chironomid assemblages to environmental change during the early Late-glacial at Gerzensee, Switzerland. Palaeogeography, Palaeoclimatology, Palaeoecology, 391, Part B, 90–98.

Burga C.A., Perret R., & Vonarburg C. (1998) Vegetation und Klima der Schweiz seit dem jüngeren Eiszeitalter: Vegetation and climate history in Switzerland during the later Pleistocene and Holocene. Ott, Thun.

Colombaroli D., Beckmann M., van der Knaap W.O., Curdy P., & Tinner W. (2013) Changes in biodiversity and vegetation composition in the central Swiss Alps during the transition from pristine forest to first farming. Diversity and Distributions, 19, 157–170.

Gnägi C. & Labhart T.P. (2015) Geologie der Schweiz. Ott, Bern.

Gobet E., Vescovi E., & Tinner W. (2010) Ein paläoökologischer Beitrag zum besseren Verständnis der natürlichen Vegetation der Schweiz. Botanica Helvetica, 120, 105–115.

von Grafenstein U., Belmecheri S., Eicher U., van Raden U.J., Erlenkeuser H., Andersen N., & Ammann B. (2013) The oxygen and carbon isotopic signatures of biogenic carbonates in Gerzensee, Switzerland, during the rapid warming around 14,685 years BP and the following interstadial. Palaeogeography, Palaeoclimatology, Palaeoecology, 391, Part B, 25–32.

von Grafenstein U., Eicher U., Erlenkeuser H., Ruch P., Schwander J., & Ammann B. (2000) Isotope signature of the Younger Dryas and two minor oscillations at Gerzensee (Switzerland): palaeoclimatic and palaeolimnologic interpretation based on bulk and biogenic carbonates. Palaeogeography, Palaeoclimatology, Palaeoecology, 159, 215–229.

Hegg O., Béguin C., & Zoller H. (1993) Atlas schutzwürdiger Vegetationstypen. Eidg. Drucksachen- und Materialzentrale (EDMZ), Bern.

Hurni L. (2014) Schweizer Weltatlas. Lehrmittelverlag des Kantons Zürich, Zürich.

Kirchhofer W. (2000) Klimaatlas der Schweiz. Federal Office of Topography swisstopo, Wabern..

Landolt E. (2003) Unsere Alpenflora. SAC-Verlag, Bern.

Lotter A.F., Ammann B., Hajdas I., Sturm M., & Van Leeuwen J. (1996) Faulenseemoos revisited : New results from an old site. PACT, 133–144.

Lotter A.F., Birks H.J.B., Eicher U., Hofmann W., Schwander J., & Wick L. (2000) Younger Dryas and Allerød summer temperatures at Gerzensee (Switzerland) inferred from fossil pollen and cladoceran assemblages. Palaeogeography, Palaeoclimatology, Palaeoecology, 159, 349–361.

Lotter A.F., Heiri O., Brooks S., van Leeuwen J.F.N., Eicher U., & Ammann B. (2012) Rapid summer temperature changes during Termination 1a: high-resolution multi-proxy climate reconstructions from Gerzensee (Switzerland). Quaternary Science Reviews, 36, 103–113.

Magny M. (2013) Climatic and environmental changes reflected by lake-level fluctuations at Gerzensee from 14,850 to 13,050 yr BP. Palaeogeography, Palaeoclimatology, Palaeoecology, 391, Part B, 33–39.

Nielsen E. (2013) Response of the Lateglacial fauna to climatic change. Palaeogeography, Palaeoclimatology, Palaeoecology, 391, Part B, 99–110.

van Raden U.J., Colombaroli D., Gilli A., Schwander J., Bernasconi S.M., van Leeuwen J., Leuenberger M., & Eicher U. (2013) High-resolution late-glacial chronology for the Gerzensee lake record (Switzerland): δ18O correlation between a Gerzensee-stack and NGRIP. Palaeogeography, Palaeoclimatology, Palaeoecology, 391, Part B, 13–24.

Rey F., Schwörer C., Gobet E., Colombaroli D., van Leeuwen J.F., Schleiss S., & Tinner W. (2013) Climatic and human impacts on mountain vegetation at Lauenensee (Bernese Alps, Switzerland) during the last 14,000 years. The Holocene, 23, 1415–1427.

Schwander J., Eicher U., & Ammann B. (2000) Oxygen isotopes of lake marl at Gerzensee and Leysin (Switzerland), covering the Younger Dryas and two minor oscillations, and their correlation to the GRIP ice core. Palaeogeography, Palaeoclimatology, Palaeoecology, 159, 203–214.

Schwörer C., Colombaroli D., Kaltenrieder P., Rey F., & Tinner W. (2015) Early human impact (5000–3000 BC) affects mountain forest dynamics in the Alps. Journal of Ecology, 103, 281–295.

Schwörer C., Henne P.D., & Tinner W. (2014a) A model-data comparison of Holocene timberline changes in the Swiss Alps reveals past and future drivers of mountain forest dynamics. Global Change Biology, 20, 1512–1526.

Schwörer C., Kaltenrieder P., Glur L., Berlinger M., Elbert J., Frei S., Gilli A., Hafner A., Anselmetti F., Grosjean M., & Tinner W. (2014b) Holocene climate, fire and vegetation dynamics at the treeline in the Northwestern Swiss Alps. Vegetation History and Archaeobotany, 23, 479–496.

Simpson G.L. & Birks H.J.B. (2012) Statistical Learning in Palaeolimnology. Tracking Environmental Change Using Lake Sediments (ed. by H.J.B. Birks, A.F. Lotter, S. Juggins, and J.P. Smol), pp. 249–327. Springer Netherlands,

Thöle L., Schwörer C., Colombaroli D., Gobet E., Kaltenrieder P., van Leeuwen J., & Tinner W. (2016) Reconstruction of Holocene vegetation dynamics at Lac de Bretaye, a high-mountain lake in the Swiss Alps. Holocene, 26, 380–396.

Tobolski K. & Ammann B. (2000) Macrofossils as records of plant responses to rapid Late Glacial climatic changes at three sites in the Swiss Alps. Palaeogeography, Palaeoclimatology, Palaeoecology, 159, 251–259.

Welten M. (1944) Pollenanalytische, stratigraphische und geochronologische Untersuchungen aus dem Faulenseemoos bei Spiez. Verlag H. Huber,

Wick L. (2000) Vegetational response to climatic changes recorded in Swiss Late Glacial lake sediments. Palaeogeography, Palaeoclimatology, Palaeoecology, 159, 231–250.